

UNIVERSIDADE FEDERAL DE MINAS GERAIS
Instituto de Ciências Biológicas
Programa de Pós-Graduação em Microbiologia

Isabella Luiza Martins de Aquino

VÍRUS GIGANTES DE AMEBAS: Análise estrutural e funcional de fibrilas de superfície e investigação de mecanismos envolvidos no bloqueio da superinfecção

Belo Horizonte

2024

Isabella Luiza Martins de Aquino

VÍRUS GIGANTES DE AMEBAS: Análise estrutural e funcional de fibrilas de superfície e investigação de mecanismos envolvidos no bloqueio da superinfecção

Tese de Doutorado apresentada ao Programa de Pós-Graduação em Microbiologia do Instituto de Ciências Biológicas da Universidade Federal de Minas Gerais, como requisito parcial à obtenção do título de Doutora em Microbiologia.

Orientador: Prof. Jônatas Santos Abrahão

Belo Horizonte

2024

043

Aquino, Isabella Luiza Martins de.

Vírus gigantes de amebas: análise estrutural e funcional de fibrilas de superfície e investigação de mecanismos envolvidos no bloqueio da superinfecção [manuscrito] / Isabella Luiza Martins de Aquino. – 2024. 156 f. : il. ; 29,5 cm.

Orientador: Prof. Jônatas Santos Abrahão.

Tese (doutorado) – Universidade Federal de Minas Gerais, Instituto de Ciências Biológicas. Programa de Pós-Graduação em Microbiologia.

1. Microbiologia. 2. Mimiviridae. 3. Vírus Gigantes. 4. Fagocitose. 5. Interações entre Hospedeiro e Microrganismos. I. Abrahão, Jônatas Santos. II. Universidade Federal de Minas Gerais. Instituto de Ciências Biológicas. III. Título.

CDU: 579



UNIVERSIDADE FEDERAL DE MINAS GERAIS
INSTITUTO DE CIÊNCIAS BIOLÓGICAS
PÓS-GRADUAÇÃO EM MICROBIOLOGIA

ATA DE DEFESA DE TESE

ATA DA DEFESA DE TESE DE **ISABELLA LUIZA MARTINS DE AQUINO**

Nº REGISTRO: 2021695837

Às 14:00 horas do dia **09 de agosto de 2024**, reuniu-se, por via remota, a Comissão Examinadora composta pelos Drs. Jordana Graziela Alves Coelho dos Reis (Departamento de Microbiologia/ICB/UFMG), Rodrigo Araújo Lima Rodrigues (Departamento de Microbiologia/ICB/UFMG), Jaqueline Germano de Oliveira (Fundação Oswaldo Cruz, Centro de Pesquisas René Rachou), Juliana Reis Cortines (Universidade Federal do Rio de Janeiro) e o Prof. Dr. Jônatas Santos Abrahão (Orientador) para julgar o trabalho final "**Vírus gigantes de amebas: análise estrutural e funcional de fibrilas de superfície e investigação de mecanismos envolvidos no bloqueio da superinfecção**" da aluna **Isabella Luiza Martins de Aquino**, requisito final para a obtenção do Grau de **DOUTORA EM CIÊNCIAS BIOLÓGICAS: MICROBIOLOGIA**. Abrindo a sessão, o Presidente da Comissão, Prof. Dr. Jônatas Santos Abrahão, após dar a conhecer aos presentes o teor das Normas Regulamentares do Trabalho Final, passou a palavra à candidata, para a apresentação de seu trabalho. Seguiu-se a arguição pelos Examinadores, com a respectiva defesa da candidata. Logo após, a Comissão se reuniu, sem a presença da candidata e do público, para julgamento e expedição de resultado final. A candidata foi considerada **APROVADA**. O resultado final foi comunicado publicamente à candidata pelo Presidente da Comissão. Nada mais havendo a tratar, o Presidente encerrou a reunião e lavrou a presente ata, que será assinada por todos os membros participantes da Comissão Examinadora. A candidata tem 60 (sessenta) dias, a partir desta data, para entregar a versão final da tese ao Programa de Pós-graduação em Microbiologia da UFMG e requerer seu diploma.

Belo Horizonte, 09 de agosto de 2024

Membros da Banca:

Profa. Dra. Jordana Graziela Alves Coelho dos Reis

Prof. Dr. Rodrigo Araújo Lima Rodrigues

Dra. Jaqueline Germano de Oliveira

Profa. Dra. Juliana Reis Cortines

De acordo:

Prof. Dr. Jônatas Santos Abrahão

(Orientador)

Prof. Dr. Daniel de Assis Santos
(Coordenador do Programa de Pós-graduação
em Microbiologia)



Documento assinado eletronicamente por **Daniel de Assis Santos, Coordenador(a) de curso de pós-graduação**, em 12/08/2024, às 08:32, conforme horário oficial de Brasília, com fundamento no art. 5º do [Decreto nº 10.543, de 13 de novembro de 2020](#).



Documento assinado eletronicamente por **Jonatas Santos Abrahao, Professor do Magistério Superior**, em 12/08/2024, às 09:22, conforme horário oficial de Brasília, com fundamento no art. 5º do [Decreto nº 10.543, de 13 de novembro de 2020](#).



Documento assinado eletronicamente por **Jordana Graziela Alves Coelho dos Reis, Membro de comitê**, em 12/08/2024, às 09:38, conforme horário oficial de Brasília, com fundamento no art. 5º do [Decreto nº 10.543, de 13 de novembro de 2020](#).



Documento assinado eletronicamente por **Rodrigo Araújo Lima Rodrigues, Professor do Magistério Superior**, em 12/08/2024, às 09:44, conforme horário oficial de Brasília, com fundamento no art. 5º do [Decreto nº 10.543, de 13 de novembro de 2020](#).



Documento assinado eletronicamente por **Juliana Reis Cortines, Usuário Externo**, em 12/08/2024, às 16:26, conforme horário oficial de Brasília, com fundamento no art. 5º do [Decreto nº 10.543, de 13 de novembro de 2020](#).



Documento assinado eletronicamente por **Jaquelline Germano de Oliveira, Usuário Externo**, em 12/08/2024, às 16:35, conforme horário oficial de Brasília, com fundamento no art. 5º do [Decreto nº 10.543, de 13 de novembro de 2020](#).



A autenticidade deste documento pode ser conferida no site https://sei.ufmg.br/sei/controlador_externo.php?acao=documento_conferir&id_orgao_acesso_externo=0, informando o código verificador **3427280** e o código CRC **25889C5E**.

*Aos meus pais, que me deram e criaram todas
as ferramentas e oportunidades para chegar
até aqui, além de amor e um lar.*

AGRADECIMENTOS

Foi uma longa e árdua caminhada até aqui, e uma linha de chegada que por muitas vezes parecia distante, finalmente se aproximou. E é preciso agradecer, pois não cheguei até aqui sozinha.

Agradeço a Deus por nunca me abandonar, mesmo quando eu me distanciei.

Agradeço à minha mãe, Eriene, por ser meu maior exemplo na vida. Minha mãe sacrificou muito em nome de seus filhos, enfrentou dificuldades inimagináveis, mas nunca teve sua força abalada. É impossível mensurar o amor e admiração que sinto por ela. Eu jamais seria capaz de escolher uma mãe tão bem.

Ao meu pai, Jussel, por todos os lugares onde me levou e experiências que me proporcionou. Muitos dos caminhos profissionais que escolhi seguir, vem da forma como meu pai me ensinou a amar e respeitar a natureza, a ter curiosidade e os pés no chão. De preferência, na grama ou na terra. Sinto sua falta e penso em você todos os dias da minha vida.

Sou grata ao meu noivo, Rubens, por me admirar, me respeitar e ser meu companheiro. Você me ensinou que o amor pode ser tranquilo e jamais me abandonou, mesmo nos meus dias mais difíceis. “Somos nós contra todos”.

À minha família, avós, tios e tias, primos e ao meu irmão. É um privilégio e uma raridade ter uma família unida e que torce por cada um de seus membros, que celebra cada conquista e que permanece unida após as perdas e fracassos.

Aos meus sobrinhos, Miguel, Victor, Pedro e Laura. Vocês encheram nossas vidas de alegria e propósito. Sou muito feliz por ser a tia Bel de vocês.

À minha segunda família, que meu noivo trouxe para a minha vida e que me acolheram desde o primeiro dia como parte do “seu povo”. Tenho muita sorte por isso!

Às minhas amigas Beatriz, Bruna, Isabela, Talita, Jussara e Ana Paula. Não existem palavras para agradecer por todos esses anos, para explicar nossa conexão e parceria. Vocês salvaram minha vida diversas vezes e me deram muita força para seguir em frente sempre. Eu admiro e amo cada uma de vocês e as tenho como um exemplo!

Aos amigos Ana Gabriela, Thaís, Karol, Natalinha, Iago, Matheus e Mateus. Quando eu me senti sozinha no laboratório, vocês me acolheram com muita compreensão e daí surgiu uma linda amizade, cheia de memes, musiquinhas e torcida pelo meu sucesso. Obrigada por me ampararem tantas vezes e por tantas memórias que tornam minha partida do laboratório ainda mais difícil.

Ao meu orientador, Jônatas, pelo seu brilhantismo e pela sua paixão pelos vírus gigantes, que me inspiraram durante esses 7 anos e ainda me inspiram. Obrigada por todos esses anos de conversas honestas, orientação, confiança, paciência e coletas em lugares incríveis!

Aos professores do Labvírus, Erna, Cláudio, Betânia, Giliane e Rodrigo. Obrigada por todo o aprendizado, discussões e oportunidades de aprimoramento em reuniões, pelas comemorações e por se preocuparem em criar um ambiente de trabalho em equipe e parceria.

Aos meus colegas do Labvírus e do Gepvig, por todo aprendizado, troca e companheirismo nos últimos anos. É um privilégio fazer parte dessa história. Agradeço em especial á Rafaella, pela oportunidade de coorientação e por toda a ajuda para tornar esse trabalho possível.

Ao PPG Micro e seus professores e funcionários, por todo o empenho e dedicação em criar um programa de excelência e mantê-la por tantos anos, formando cientistas notáveis.

À UFMG, o meu sonho de universidade que se tornou realidade em 2012 e me abriu tantas portas, me permitindo viver muitas experiências que me tornaram a mulher que sou hoje. Para além da minha educação, a UFMG mudou a minha vida.

Ao centro de Microscopia da UFMG, que foi nosso grande parceiro na obtenção das imagens e resultados aqui apresentados, mas também desde os primórdios da caça por vírus gigantes.

À banca avaliadora por aceitar nosso convite e pela disponibilidade em colaborar para a melhoria deste trabalho.

Às agências de fomento, por tornarem possível fazer ciência de qualidade em um país com tanta desigualdade social, mas com tanto potencial e sede por desenvolvimento.

RESUMO

A descoberta dos vírus gigantes de amebas surpreendeu e impulsionou a comunidade científica a buscar por novos isolados após a descrição do mimivírus. Desde então, vários outros isolados de mimivírus foram descobertos, descritos e classificados, exibindo diferenças genômicas claras que os subdivide em três principais gêneros atualmente: *Mimivirus*, *Moumouvirus* e *Megavirus*. Durante nossos esforços para isolar e caracterizar novos vírus gigantes, um novo vírus foi isolado de amostras de água coletadas da Lagoa da Pampulha em Belo Horizonte. Por meio de sequenciamento completo de seu genoma e de análise filogenética baseada no gene que codifica a DNA polimerase de subtipo B, identificamos o isolado como um megavírus, e o nomeamos de megavirus caiporensis. Ao analisarmos o isolado por microscopia eletrônica de transmissão, foi observado que as fibrilas desses vírus se organizam de forma diferente, formando grumos. Também foi observado durante a multiplicação viral que o ciclo do novo isolado parecia ser mais lento quando comparado a outros mimivírus. Desse ponto adiante, a análise da morfologia da partícula, com ênfase nas fibrilas, o estudo do ciclo e análises de possíveis genes ligados às fibrilas desses vírus, se tornaram o objetivo desse trabalho. Adicionalmente, escolhemos um representante dos gêneros *Mimivirus* e *Moumouvirus* para realizar comparações entre nossos resultados. Por meio de microscopias eletrônicas, descrevemos pela primeira vez que mimivírus podem apresentar pelo menos três padrões distintos de organização de suas fibrilas, ligados aos gêneros/linhagens aos quais são proximamente relacionados. Foi mostrado que os padrões diferentes são intrínsecos à partícula viral, e não artefatos produto de preparações para as microscopias. O estudo do ciclo do m. caiporensis se mostrou similar ao de outros megavírus e em estágios tardios do ciclo, observamos vírions recém-formados dentro de vesículas. Estudamos a possibilidade de uma liberação por exocitose, como é observado para outros vírus gigantes, como os cedratvírus e os pandoravírus. Nossas análises combinando ensaios de infecções e titulações virais, microscopias eletrônicas e de imunofluorescência, mostraram que esses vírus não são liberados por exocitose, mas sim que ocorre uma incorporação contínua de partículas pela ameba infectada pelo megavirus caiporensis, um fenômeno conhecido como superinfecção. Análises comparativas demonstraram que o megavírus não é capaz de bloquear a superinfecção em *Acanthamoeba*, diferente de mimivírus e moumouvírus, e que esse processo pode ser revertido com a inibição química da fagocitose. Descrevemos aqui pela primeira vez, a superinfecção e sua inibição por vírus gigantes que infectam amebas. Este trabalho contribui com informações acerca da morfologia, genômica, filogenia, ecologia e evolução dos mimivírus. Além disso, contribui para a compreensão da superinfecção e sua inibição em mimivírus, moumouvírus e megavírus, demonstrando que apesar de seu parentesco evolutivo, esses vírus apresentam diferenças profundas em suas interações com seus hospedeiros.

Palavras-chave: mimivírus; moumouvírus; megavírus; fibrilas; fagocitose; relação vírus-hospedeiro.

ABSTRACT

The discovery of giant viruses of amoeba surprised and prompted the scientific community to search for new isolates after the description of mimivirus. Since then, several other mimivirus isolates have been discovered, described and classified, exhibiting clear genomic differences that currently subdivide them into three main genera: *Mimivirus*, *Moumouvirus* and *Megavirus*. During our efforts to isolate and characterize new giant viruses, a new virus was isolated from water samples collected from Pampulha Lagoon in Belo Horizonte. Through complete sequencing of its genome and phylogenetic analysis based on the gene encoding DNA polymerase subtype B, we identified the isolate as a megavirus and named it megavirus caiporensis. When analyzing the isolate by transmission electron microscopy, it was observed that the fibrils of these viruses are organized differently, forming clumps. It was also observed that during viral multiplication the cycle of the new isolate seemed to be slower when compared to other mimiviruses. From this point onwards, the analysis of the particle morphology, with emphasis on the fibrils, the study of the cycle and analysis of possible genes linked to these viruses' fibrils, became the objective of this work. Additionally, we chose a representative of the genera *Mimivirus* and *Moumouvirus* to perform comparisons among our results. Through electron microscopy, we described for the first time that mimiviruses can present at least three distinct patterns of organization of their fibrils, linked to the genera/lineages to which they are closely related. It was showed that the different patterns are intrinsic to the viral particle, and not artifacts produced by preparations for microscopy. The study of the cycle of m. caiporensis was similar to that of other megaviruses and in late stages of the cycle, we observed newly formed virions inside vesicles. We studied the possibility of release by exocytosis, as is observed for other giant viruses, such as cedratviruses and pandoraviruses. Our analyses, combining viral infection and titration assays, electron microscopy, and immunofluorescence, showed that these viruses are not released by exocytosis, but rather that there is a continuous incorporation of particles by the amoeba infected by megavirus caiporensis, a phenomenon known as superinfection. Comparative analyses demonstrated that megavirus is not able to block superinfection in *Acanthamoeba*, unlike mimivirus and moumouvirus, and this process can be reversed by chemical inhibition of phagocytosis. Here, we describe for the first time superinfection and its inhibition by giant viruses that infect amoebas. This work contributes with information about the morphology, genomics, phylogeny, ecology, and evolution of mimiviruses. In addition, it contributes to the understanding of superinfection and its inhibition in mimiviruses, moumouviruses, and megaviruses, demonstrating that despite their evolutionary kinship, these viruses present profound differences in their interactions with their hosts.

Keywords: mimivirus; moumouvirus; megavirus; fibrils; phagocytosis; virus-host relationship.

SUMÁRIO

1- INTRODUÇÃO	11
2- JUSTIFICATIVA.....	18
3- OBJETIVOS.....	19
3.1 Objetivos gerais	19
3.2 Objetivos específicos	19
4. RESULTADOS	20
4.1 Artigo 1- Diversity of Surface Fibril Patterns in Mimivirus Isolates	20
4.2 Artigo 2- Surface fibrils on the particles of nucleocytoviruses: A review	36
4.3 Artigo 3- Giant viruses inhibit superinfection by downregulating phagocytosis in <i>Acanthamoeba</i>	45
5- DISCUSSÃO.....	63
6- CONCLUSÕES	67
7- PERSPECTIVAS	69
REFERÊNCIAS	70
EVENTOS CIENTÍFICOS E PRODUÇÕES.....	75
Participações em eventos científicos	75
Formação complementar.....	75
Atividades de extensão	76
Atividades didáticas	76
Coorientação	76
Participação em bancas	77
Artigos científicos publicados	77
ANEXOS- OUTROS ARTIGOS PUBLICADOS DURANTE O DOUTORADO	80

1- INTRODUÇÃO

Por muito tempo, os vírus foram definidos com base em características como entidades ultramicroscópicas, sendo filtráveis em filtros contendo poros de 0,2 μm e apresentarem genomas pequenos que codificam poucas proteínas (Lwoff, 1957). Porém, a descoberta de vírus que apresentam características que vão de encontro a essas, por exemplo, aqueles que se agrupam dentro do filo *Nucleocyotoviricota*, têm mostrado que os vírus são muito mais diversos e complexos.

A classificação taxonômica dos vírus gigantes (VGs) que infectam amebas como um todo é um terreno da virologia em constante debate e construção. Por se tratar de vírus descritos, em sua maioria, há menos de duas décadas, estão sempre recebendo novos exemplares que expandem este grupo e novas informações acerca de sua biologia, filogenia e genética, o que consiste em um desafio para a classificação. Dessa forma, várias famílias foram sugeridas ao longo dos anos, com o aumento da diversidade de novos isolados. Recentemente, muitos destes vírus passaram por uma reclassificação pelo órgão responsável, o Comitê Internacional em Taxonomia de Vírus (do inglês *International Committee on Taxonomy of Viruses* -ICTV), e os mimivírus são um deles. Atualmente, os mimivírus são classificados taxonomicamente dentro do domínio *Varidnaviria*, reino *Bamfordvirae*, filo *Nucleocyotoviricota*, classe *Megaviricetes*, ordem *Imitervirales*, família *Mimiviridae* e subfamília *Megamimivirinae*. Dentro desta subfamília, encontramos cinco gêneros: *Cotonvirus*, *Megavirus*, *Mimivirus*, *Moumouvirus* e *Tupanvirus*. Antes da recente reclassificação dos vírus gigantes, estudos por análises filogenéticas iniciais levaram à formação de três clados distintos, conhecidos como linhagens A, B e C (COLSON *et al.*, 2012). O *Acanthamoeba polyphaga mimivirus* (APMV) e vírus similares a ele, como o isolado de mimivírus brasileiro sambavírus representam a linhagem A (CAMPOS *et al.*, 2014). A linhagem B é formada pelos moumouvírus e seus relacionados (DOS SANTOS SILVA *et al.*, 2020; YOOSUF *et al.*, 2012) e a linhagem C é composta pelos megavírus e outros vírus similares (ARSLAN *et al.*, 2011). Portanto, o gênero *Mimivirus* abrigaria isolados relacionados à linhagem A, o gênero *Moumouvirus* os isolados relacionados à linhagem B e o gênero *Megavirus*, os isolados ligados à linhagem C.

Estudos anteriores mostraram uma predominância de mimivírus da linhagem A isolados em amostras ambientais do Brasil, quando amebas pertencentes aos gêneros *Acanthamoeba* e *Vermamoeba* foram utilizadas como plataformas de isolamento, resultando em sua maioria, em novos isolados pertencentes a essa linhagem (ANDRADE *et al.*, 2018; DORNAS *et al.*, 2015).

Essa predominância é seguida pelos isolados de linhagem C e por último, os mimumovírus que pertencem à linhagem B (DORNAS *et al.*, 2015). Além das características moleculares, é possível observar diferenças na morfologia das fibrilas de cada um desses vírus de acordo com a linhagem à qual estão relacionados, porém até o presente estudo este aspecto das fibrilas ainda não havia sido explorado e estudado mais a fundo no contexto das linhagens evolutivas. O trabalho que descreve o isolamento e caracterização do megavírus chilensis, um mimivírus relacionado à linhagem C, mostra que as fibrilas desses vírus são diferentes quando comparadas às do APMV, porém não se aprofunda no assunto e sugere a necessidade de estudos futuros para compreender a composição química das fibrilas desse isolado (ARSLAN *et al.*, 2011).

O genoma do primeiro mimivírus isolado, o APMV, é composto por uma molécula linear de DNA fita dupla, com um comprimento de 1.181.549 pb. É rico em Adenina-Timina (A-T), que representam 72% dessas bases, e Guanina-Citosina (G-C) correspondem aos 28% restantes do conteúdo de bases (ARSLAN *et al.*, 2011; RAOULT *et al.*, 2004). A densidade de codificação do genoma é de 89%, 1.018 possíveis fases abertas de leitura (ORFs - *open reading frames*) foram preditas, além de sequências para codificar 6 RNAs transportadores (RNAt) e de vários RNAs não codificantes. (RAOULT *et al.*, 2004). Além disso, é importante ressaltar que estes vírus apresentam genes considerados raros ou inéditos entre a maior parte dos vírus, como aqueles capazes de codificar fatores de tradução, RNA transportadores e aminoacil-tRNA sintetases (aaRS), que codificam proteínas funcionais (ABERGEL *et al.*, 2007; ARSLAN *et al.*, 2011; LEGENDRE *et al.*, 2010; SILVA *et al.*, 2015). Íntrons e inteínas foram detectados em genes que codificam a proteína principal do capsídeo e entre outros genes conservados, além de um mobiloma exclusivo do APMV (DESNUES *et al.*, 2012).

Dentro do repertório genômico do APMV encontramos homologias com genes tanto de outros vírus, quanto de bactérias, arqueias e eucariotos (ABERGEL *et al.*, 2015). Os genes que apresentam homologia com outros vírus destacam-se por serem conservados entre os vírus pertencentes ao filo *Nucleocyotviricota* e estão associados às funções de replicação, transcrição de DNA e morfogênese de partículas virais. Entre estes, podemos citar a DNA polimerase B, a helicase D5, a ATPase A32L, a proteína principal do capsídeo e um fator de transcrição (IYER *et al.*, 2001; RAOULT *et al.*, 2004; YUTIN *et al.*, 2009). Já sobre os genes pertencentes a organismos não-virais com os quais o APMV apresenta homologia, foi observada uma variedade de sequências com funcionalidades diversas (KOONIN, 2005). Esses genes foram organizados em 4 conjuntos diferentes de acordo com a sua função: tradução de proteínas, enzimas de reparo do DNA, chaperonas e novas vias enzimáticas (RAOULT *et al.*, 2004). Entre esses, o conjunto que mais chamou a atenção dos pesquisadores foi o de tradução de proteínas,

por se tratarem de genes inéditos para os vírus até então. Dentro desse conjunto encontramos 5 fatores de tradução e 4 tipos de tRNA (ABRAHÃO *et al.*, 2017). A quantidade destes genes pode variar dentro da família *Mimiviridae*, e até entre os isolados pertencentes a uma mesma linhagem, pois mutações acabam levando a deleções ou duplicações de algum gene e alterando assim o número encontrado em cada um. Além disso, foram descritas enzimas de reparo de DNA, que apresentam homologia com genes presentes em bactérias e arqueias, assim como topoisomerasas, DNA glicosilases, uma endo nuclease, e outras (BANDARU *et al.*, 2007; RAOULT *et al.*, 2004; SUZAN-MONTI *et al.*, 2006). Já na categoria das chaperonas, que são enzimas envolvidas no processo de enovelamento de proteínas, o APMV foi o primeiro vírus descrito a apresentar homologia com sequências relacionadas a proteínas de bactérias *Escherichia coli*: proteína de choque térmico (*heat-shock*) e uma ciclofilina (peptidilprolil isomerase) (BARIK, 2018; RAOULT *et al.*, 2004; THAI *et al.*, 2008). Por fim, na categoria de enzimas envolvidas em processos metabólicos diversos, são descritas por exemplo a asparagina sintase e a glutamina sintase, que estão envolvidas na via metabólica de aminoácidos (RAOULT *et al.*, 2004). No genoma do APMV foram descritos diversos tipos de proteínas formadas por múltiplos domínios e repetições. Por exemplo, oito genes para proteínas contendo repetições que formam a estrutura de colágeno composta por tripla hélice são conhecidos, o que só era observado anteriormente em bacteriófagos (LUTHER *et al.*, 2011; RAOULT *et al.*, 2004). Além das proteínas de colágeno, as repetições Kelch; domínio MORN (*membrane occupation, and recognition nexus*); repetição rica em leucina (LRR- *leucine-rich repeat*), repetição do tetratricopeptídeo (TPR); repetição de fenilalanina-asparagina-isoleucina-prolina (FNIP/IP22); repetição triptofano-ácido aspártico (WD40); repetição de anquirina (ANK) e repetição Sel 1 também são encontradas nas proteínas preditas a partir dos genomas dos mimivírus. A presença destas proteínas já foi correlacionada com o tamanho do genoma dos vírus gigantes de forma proporcional, ou seja, quanto maior o genoma, maior a quantidade de proteínas contendo esses domínios e arranjos (SHUKLA *et al.*, 2018).

Por fim, é preciso destacar que apesar do grande e diverso repertório genômico dos mimivírus, uma parte considerável dele é composta por genes ORFans, para os quais não encontramos similaridade nos bancos de dados para a predição de possíveis funções. Muitos esforços têm sido feitos atualmente para elucidar as funções destes genes utilizando metodologias diversas, o que pode nos levar futuramente a não só compreender estas funções, mas também a conhecer novas na virosfera (HAKIM *et al.*, 2012; SAINI; FISCHER, 2007; SOBHAY *et al.*, 2015).

O primeiro mimivírus a ser descoberto, o APMV, chamou muita atenção não apenas pelo tamanho da partícula e genoma, mas também pela aparência complexa de sua partícula viral. O primeiro isolado da família *Mimiviridae*, possui uma partícula viral com um tamanho médio de 750 nm. Essa partícula é composta por um capsídeo proteico com simetria pseudo-icosaédrica, recoberto por uma camada densa de fibrilas externas (revisado por ABRAHÃO *et al.*, 2014; XIAO *et al.*, 2005, 2009). A estrutura do capsídeo é formada por várias camadas, sendo possível identificar uma membrana lipídica envolta externamente por pelo menos três camadas de proteínas. Na parte mais interna da membrana lipídica existe um cerne ou *core* proteico, onde está localizado o genoma viral (ABRAHÃO *et al.*, 2014; XIAO *et al.*, 2009).

A principal proteína que forma a estrutura do capsídeo dos mimivírus é a L425, a proteína principal do capsídeo (MCP- *Major Capsid Protein*) (XIAO *et al.*, 2009). Em um dos vértices do capsídeo é observado o *stargate*, uma estrutura com formato de estrela do mar pela qual o conteúdo interno da partícula desses vírus é liberado, sendo assim uma espécie de portal para a liberação do genoma viral (Figura 4) (ZAUBERMAN *et al.*, 2008). O *stargate* mede cerca de 200 a 250 nm, é recoberto e selado por um complexo proteico denominado *starfish*, sendo a única região do capsídeo que não é recoberta pela camada de fibrilas (KLOSE *et al.*, 2010). A abertura do *stargate* parece ser estimulada por acidificação (ANDRADE *et al.*, 2017).

As fibrilas, são estruturas importantes para essas entidades por agirem como estruturas de adesão viral à superfície de amebas hospedeiras (RODRIGUES *et al.*, 2015). Em relação à morfologia das fibrilas, elas são encontradas frequentemente com uma de suas extremidades livre e associada a uma região terminal globular e a outra anexada a uma única estrutura central (XIAO *et al.*, 2009). Além disso, são resistentes a proteases, quando naturalmente recobertas por uma camada de peptidoglicano e apresentam anéis de densidade sucessivos. A interação entre açúcares encontrados na superfície hospedeira (manose e N-acetilglucosamina) e as fibrilas parece mediar a adesão e, conseqüentemente, estimular a fagocitose do vírus e subsequente penetração na célula hospedeira (RODRIGUES *et al.*, 2015). Fibrilas estão presentes nas partículas não apenas dos mimivírus, mas também em outros vírus gigantes como os Tupanvírus (ABRAHÃO *et al.*, 2018), Orpheovírus (ANDREANI *et al.*, 2018), cedratvírus (MACHADO *et al.*, 2023), cotonvírus (TAKAHASHI *et al.*, 2021), Marseillevírus (BOYER *et al.*, 2009) e mollivírus (LEGENDRE *et al.*, 2015). Logo, são encontradas em abundância na natureza entre os VGs de amebas pertencentes ou não a família *Mimiviridae*, apresentando morfologias diversas.

Estudos sugerem a natureza de possíveis proteínas que compõem as fibrilas de mimivírus. Villalta e colaboradores (2022) demonstraram que o componente principal do nucleocapsídeo proteico do APMV, a 2-glicose-metanol-colina (GMC)-oxirredutase (fibra genômica), é também um dos elementos mais abundantes das fibrilas de superfície que recobrem o capsídeo desses vírus, e essa proteína é codificada pelo gene R135 (VILLALTA *et al.*, 2022). Além disso, as proteínas L829 e L725 também foram associadas à composição das fibrilas de APMV em um estudo anterior. O isolado M4 foi obtido após passagens sucessivas de APMV em amebas em condições alopátricas, resultando na diminuição do genoma e da abundância de fibrilas. Análises de proteômica sugeriram que esse fenótipo quase sem fibrilas das partículas foi associado a falta desses genes (R135, L829 e L275) no genoma do mimivírus M4, quando comparado ao genoma de APMV, que é recoberto por uma densa camada de fibrilas e apresenta esses genes em abundância (BOYER *et al.*, 2011).

Atualmente, a maior parte do conhecimento adquirido sobre as fibrilas e a morfologia das partículas dos mimivírus se baseia em um único isolado, o APMV (RODRIGUES *et al.*, 2015; XIAO *et al.*, 2009). Até então, estudos que avaliem possíveis diferenças entre fenótipos e genótipos dessas estruturas em outros isolados não estão disponíveis na literatura. Apesar disso, é possível observar por meio de microscopias eletrônicas (ME) que as fibrilas do APMV, do *Acanthamoeba polyphaga* mouloumovirus e do megavirus chilensis parecem exibir tamanhos e morfologias diferentes (ARSLAN *et al.*, 2011; XIAO *et al.*, 2009; YOOSUF *et al.*, 2012). Além disso, foi descrito que os capsídeos do *A. polyphaga* mouloumovirus e do *m. chilensis* são maiores do que o descrito para APMV, com diâmetro de aproximadamente 500 e 520 nm, respectivamente (YOOSUF *et al.*, 2012). As fibrilas do *m. chilensis* exibem um ou dois conjuntos mais longos de fibrilas e uma aparência mais eletrodensa nas imagens de ME, medindo cerca de 75 nm em contraste aos 125-150 nm em APMV, enquanto o tamanho das fibrilas do mouloumovirus é de aproximadamente 100 nm (ARSLAN *et al.*, 2011; LA SCOLA *et al.*, 2003; XIAO *et al.*, 2009; YOOSUF *et al.*, 2012).

Para dar início à multiplicação de suas partículas virais, a primeira etapa é a adesão do mimivírus à superfície da ameba hospedeira utilizando as fibrilas que são encontradas na camada mais externa do capsídeo viral (RODRIGUES *et al.*, 2015). Esse processo estimula a fagocitose da partícula pela ameba, culminando na penetração (ANDRADE *et al.*, 2017; SUZAN-MONTI *et al.*, 2007). Uma vez dentro da célula, a partícula viral então presente em um fagossomo, sofre modificações estruturais devido à acidificação deste compartimento. Tal mudança culmina na abertura do *stargate*, impulsionando a fusão da membrana lipídica do fagossomo com a membrana interna da partícula do mimivírus, iniciando assim o processo de

desnudamento e de liberação de todo o conteúdo interno da partícula viral no citoplasma hospedeiro (ANDRADE *et al.*, 2017; SCHRAD *et al.*, 2020).

Durante a fase de desnudamento, partículas virais infecciosas são indetectáveis por se encontrarem desmontadas nesse estágio, sendo este período atribuído à fase de eclipse. Após a liberação da semente viral, que nada mais é do que o conteúdo interno da partícula viral, o citoplasma do hospedeiro passa por uma reorganização induzida por componentes de fase precoce virais, originando uma fábrica viral (FV) precoce (ANDRADE *et al.*, 2017). A fábrica viral dos mimivírus é caracterizada como uma região elétron-densa responsável por abrigar a replicação e transcrição do DNA viral, que resulta na síntese de proteínas virais, aumentando consideravelmente o tamanho da FV, podendo chegar a ocupar até 42% do citoplasma celular quando se encontra no seu ápice de maturação (SUZAN-MONTI *et al.*, 2007). A morfogênese das novas partículas também ocorre dentro das FVs, englobando os processos de síntese dos capsídeos da progênie viral, o preenchimento dos capsídeos com o material genético e a aquisição de fibrilas (ANDRADE *et al.*, 2017; KUZNETSOV *et al.*, 2013). A síntese proteica, que dá origem à matéria prima para a confecção dos capsídeos que posteriormente migram para o interior da FV, ocorre em parte no retículo endoplasmático (MUTSAFI *et al.*, 2013). Os capsídeos, por sua vez, são originados por mudanças de forma e espessura de membranas celulares com estruturas lamelares provenientes do retículo endoplasmático, que migram do interior das FVs para a periferia, formando os capsídeos com simetria pseudo-icosaédrica. Na área de aquisição de fibrilas, localizada na periferia das FVs, a aquisição de fibrilas ocorre concomitantemente ao preenchimento das partículas com o genoma e outras moléculas, por meio do portal localizado do lado oposto ao *stargate* (ANDRADE *et al.*, 2017; ZAUBERMAN *et al.*, 2008). No fim do ciclo, a fábrica viral preenche quase todo o citoplasma celular e a célula é tomada por novas partículas recém-sintetizadas. Estas novas partículas são então liberadas por lise celular (SUZAN-MONTI *et al.*, 2007).

Pouco se sabe sobre o ciclo de moomouvírus e megavírus. Estudos comparativos do ciclo dos três gêneros não foram feitos até então, porém algumas informações na literatura podem ser encontradas nos trabalhos que descrevem isolados. O megavírus chilensis apresenta um ciclo mais lento quando comparado ao APMV, com uma duração de cerca de 17 horas contra 12 horas do APMV (ARSLAN *et al.*, 2011). Essa diferença se deve principalmente ao “estágio de semente viral” que progride mais lentamente até o surgimento das fábricas virais totalmente maduras. Foi observado que o arredondamento das células infectadas também ocorre com um atraso, em comparação às 6 horas pós-infecção (h.p.i) para APMV, e ao contrário do mimivírus, onde as células arredondadas permaneceram aderidas, a maioria delas se solta da monocamada

no caso do *m. chilensis*. Apesar dessas diferenças apontadas no estudo do ciclo desse isolado de megavírus, a maior parte é similar ao que foi descrito anteriormente para APMV (ARSLAN *et al.*, 2011). Quanto ao ciclo de isolados de momeovírus, o que se sabe é que suas fábricas virais e seus ciclos são similares ao que foi descrito para mimivírus e megavírus (BAJRAI *et al.*, 2016; YOOSUF *et al.*, 2012).

Ao longo da evolução, diversas estratégias relacionadas ao processo de infecção/penetração da/célula hospedeira surgiram (ROOSSINCK, 2011). Vários estudos mostram que alguns vírus são capazes de impedir a penetração de novas partículas na célula hospedeira que infectaram, um fenômeno denominado de inibição da superinfecção (CHRISTEN *et al.*, 1990; DOCEUL *et al.*, 2010; HUTCHISON; SINSHEIMER, 1971). Essa estratégia confere a esses vírus um maior sucesso evolutivo por evitar a competição inter e intraespecífica. Além disso, infectar uma célula já parasitada por outro vírus, não geraria uma multiplicação e formação de progênie adequadas, tornando a seleção da inibição desse processo vantajosa. Já foi descrito o processo de inibição da superinfecção por bacteriófagos *Streptococcus thermophilus* TP-J34, que ao expressarem o gene da lipoproteína *ltp* interferem na infecção de fagos exógenos bloqueando a injeção de DNA viral na célula (HUTCHISON; SINSHEIMER, 1971). O vírus HIV também consegue bloquear a superinfecção ao reduzir a expressão do correceptor viral CCR5, inviabilizando a penetração de partículas exógenas (SCHWARTZ *et al.*, 2016). Apesar de não haver descrições na literatura sobre inibição de superinfecção relacionada à vírus gigantes que infectam amebas, dentro dos nucleocitovírus é possível encontrar um ótimo exemplo, os vaccínia vírus. Esses vírus não apenas bloqueiam a infecção por outros vírus, como também são capazes de repelir partículas exógenas para células vizinhas não infectadas por meio da formação de cauda de actina, acelerando a infecção da população de células hospedeiras. Foi demonstrado que expressar as proteínas A33 e A36 precocemente é necessário para que esse processo ocorra (CHRISTEN *et al.*, 1990).

2- JUSTIFICATIVA

Os mimivírus são entidades biológicas diversas geneticamente e amplamente distribuídas pelo planeta. Os anos que sucederam a descrição do APMV, o primeiro mimivírus a ser descoberto, foram marcados por numerosos estudos que revelaram a complexidade estrutural e genômica desse, até então, desconhecido grupo de vírus. Dentre as características estruturais mais marcantes no APMV, as fibrilas de superfície receberam atenção de alguns grupos de pesquisa nos últimos anos. Avanços em relação a sua composição e funcionalidades revelaram uma estrutura única na virosfera, que apesar de não essencial, parece favorecer o processo de penetração do APMV em amebas. Todavia, apesar dos referidos avanços no entendimento das fibrilas de superfície de APMV, há uma importante lacuna em relação a estrutura e função desse componente em outros grupos vírus gigantes, como os moomovírus e megavírus. Muitas perguntas ainda não foram respondidas: como é a estrutura das fibrilas nesses vírus? Como aconteceu a evolução das proteínas que compõem sua estrutura? Como possíveis variações na estrutura das fibrilas de mimi-, moomou- e megavírus podem influenciar no processo de adesão e penetração desses vírus em amebas?

Ainda no contexto da penetração viral em amebas, uma importante lacuna do conhecimento ainda não foi preenchida: existe superinfecção ou sua inibição? Tais fenômenos, anteriormente descritos para vírus de bactérias e animais, ainda não foram estudados em vírus gigantes de amebas. Embora o ciclo do APMV tenha sido analisado por meio de diferentes abordagens, metodologias e diversos grupos de pesquisa, uma pergunta ainda não foi respondida: amebas infectadas por mimivírus são induzidas a bloquear a penetração de novas partículas virais exógenas? Tal pergunta pode ser estendida a outros vírus gigantes de amebas, como os moomovírus e megavírus. No caso de bloqueio de superinfecção, quais os mecanismos envolvidos? É possível reverter tal fenômeno?

Portanto, o presente trabalho buscou investigar aspectos básicos da biologia de mimi-, moomou- e megavírus, no campo estrutural e do ciclo de multiplicação. Acreditamos que as contribuições aqui apresentadas podem preencher lacunas do conhecimento, e auxiliar no entendimento da diversidade e evolução deste grupo de vírus, e sua relação com seus hospedeiros.

3- OBJETIVOS

3.1 Objetivos gerais

Parte 1: Analisar a diversidade estrutural das fibrilas de mimi-, moumou- e megavírus, e investigar como tal diversidade pode impactar na adesão dos vírus em amebas hospedeiras.

Parte 2: Analisar a ocorrência do fenômeno de superinfecção e sua inibição, em amebas infectadas por mimi-, moumou- e megavírus.

3.2 Objetivos específicos

Parte 1:

- Descrever e caracterizar um novo isolado de megavírus;
- Analisar possíveis diferenças estruturais das fibrilas de superfície presentes em mimivírus, moumouvírus e megavírus, anteriormente referidos na literatura como linhagens A, B e C de mimivírus, respectivamente;
- Analisar filogeneticamente sequências de proteínas hipoteticamente envolvidas na estrutura das fibrilas de superfície;
- Analisar a divisão das linhagens A, B e C de mimivírus em relação à morfologia das fibrilas;
- Analisar a relação entre as diferentes organizações de fibrilas de mimi-, moumou- e megavírus e a adesão e penetração desses vírus na célula hospedeira;

Parte 2:

- Investigar a relação de partículas de megavirus caiporensis dentro de vesículas no citoplasma da célula hospedeira com a possibilidade de liberação por exocitose;
- Analisar a possibilidade de indução ou bloqueio da superinfecção em amebas infectadas por mimi-, moumou- ou megavírus;
- Investigar os mecanismos de bloqueio da superinfecção em *Acanthamoeba castellanii* de forma comparativa entre mimi-, moumou- e megavírus.

4. RESULTADOS

Metodologia, resultados e discussões parciais serão apresentados a seguir em forma de artigos publicados precedidos de um breve resumo.


4.1 Artigo 1- Diversity of Surface Fibril Patterns in Mimivirus Isolates.

Este artigo foi publicado no periódico Journal of Virology.

Durante a caracterização do megavirus caiporensis, um novo isolado de vírus gigante de amebas, identificamos diferenças estruturais em suas fibrilas, filamentos proteicos que recobrem a superfície do capsídeo. As fibrilas são importantes para promover a adesão de partículas às células hospedeiras, desencadeando fagocitose e infecção celular. Esse novo isolado, relacionado à linhagem C de mimivírus e ao gênero *Megavirus*, apresenta fibrilas que se organizam formando grumos na superfície do capsídeo. Embora os mimivírus sejam uma das entidades virais mais abundantes em uma infinidade de biomas em todo o mundo, não houve análise comparativa sobre a organização e abundância de fibrilas entre distintos isolados de mimivírus até então. Após essa observação, decidimos expandir nossas análises para outros isolados de mimivírus. Por meio de técnicas incluindo microscopia eletrônica, processamento de imagens, sequenciamento genômico e prospecção viral, obtivemos evidências de pelo menos três padrões principais de fibrilas que podem ser encontrados: (i) isolados contendo partículas com fibrilas abundantes, distribuídas homoganeamente na superfície do capsídeo; (ii) isolados com partículas quase sem fibrilas; e (iii) isolados com partículas contendo fibrilas em abundância, mas organizadas em grumos, como observado em megavirus caiporensis. Um total de 15 isolados virais foram analisados por microscopia eletrônica, e seus genes da subunidade B da DNA polimerase foram sequenciados para análise filogenética. Observamos uma correspondência única entre vírus evolutivamente relacionados e seus perfis de fibrilas. Ensaios biológicos sugeriram que existe relação entre os padrões de fibrilas e a penetração viral nas células hospedeiras. Nossos dados contribuem para o conhecimento da organização e abundância das fibrilas do mimivírus, além de levantar questões sobre a evolução dessas estruturas intrigantes.



Diversity of Surface Fibril Patterns in Mimivirus Isolates

Isabella Luiza Martins de Aquino,^a Mateus Sá Magalhães Serafim,^a Talita Bastos Machado,^a Bruna Luiza Azevedo,^a Denilson Eduardo Silva Cunha,^b Leila Sabrina Ullmann,^c João Pessoa Araújo, Jr.,^c  Jônatas Santos Abrahão^a

^aLaboratório de Vírus, Instituto de Ciências Biológicas, Departamento de Microbiologia, Universidade Federal de Minas Gerais, Belo Horizonte, Minas Gerais, Brazil

^bCentro de Microscopia da UFMG, Universidade Federal de Minas Gerais, Belo Horizonte, Minas Gerais, Brazil

^cLaboratório de Virologia, Departamento de Microbiologia e Imunologia, Instituto de Biotecnologia, Universidade Estadual Paulista, Botucatu, São Paulo, Brazil

ABSTRACT Among the most intriguing structural features in the known virosphere are mimivirus surface fibrils, proteinaceous filaments approximately 150 nm long, covering the mimivirus capsid surface. Fibrils are important to promote particle adhesion to host cells, triggering phagocytosis and cell infection. However, although mimiviruses are one of the most abundant viral entities in a plethora of biomes worldwide, there has been no comparative analysis on fibril organization and abundance among distinct mimivirus isolates. Here, we describe the isolation and characterization of Megavirus caiporensis, a novel lineage C mimivirus with surface fibrils organized as “clumps.” This intriguing feature led us to expand our analyses to other mimivirus isolates. By employing a combined approach including electron microscopy, image processing, genomic sequencing, and viral prospecting, we obtained evidence of at least three main patterns of surface fibrils that can be found in mimiviruses: (i) isolates containing particles with abundant fibrils, distributed homogeneously on the capsid surface; (ii) isolates with particles almost fibrilless; and (iii) isolates with particles containing fibrils in abundance, but organized as clumps, as observed in Megavirus caiporensis. A total of 15 mimivirus isolates were analyzed by microscopy, and their DNA polymerase subunit B genes were sequenced for phylogenetic analysis. We observed a unique match between evolutionarily-related viruses and their fibril profiles. Biological assays suggested that patterns of fibrils can influence viral entry in host cells. Our data contribute to the knowledge of mimivirus fibril organization and abundance, as well as raising questions on the evolution of those intriguing structures.

IMPORTANCE Mimivirus fibrils are intriguing structures that have drawn attention since their discovery. Although still under investigation, the function of fibrils may be related to host cell adhesion. In this work, we isolated and characterized a new mimivirus, called Megavirus caiporensis, and we showed that mimivirus isolates can exhibit at least three different patterns related to fibril organization and abundance. In our study, evolutionarily-related viruses presented similar fibril profiles, and such fibrils may affect how those viruses trigger phagocytosis in amoebas. These data shed light on aspects of mimivirus particle morphology, virus-host interactions, and their evolution.

KEYWORDS amoeba, cell adhesion, diversity, fibrils, mimivirus, structural biology, virus entry

In 2003, *Acanthamoeba polyphaga* mimivirus (APMV) was the first amoeba-associated giant virus to be described and studied (1). The APMV exhibits particles composed of a capsid with pseudo-icosahedral symmetry covered by a dense layer of external fibrils, approximately 750 nm in size. The capsid is formed by several protein layers and an inner lipid membrane, which encompasses the viral core, where the viral genome is located (2). Recently, a study suggested that the APMV genome is organized within a 30-nm helical protein shell composed primarily of 2-glucose-methanol-choline (GMC)

Editor Derek Walsh, Northwestern University
Feinberg School of Medicine

Copyright © 2023 American Society for Microbiology. All Rights Reserved.

Address correspondence to Jônatas Santos Abrahão, jonatas.abrahao@gmail.com.

The authors declare no conflict of interest.

Received 23 November 2022

Accepted 7 December 2022

oxidoreductases (genomic fiber) encoded by the R135 gene, which was also shown to be one of the most abundant elements of the surface fibrils that cover the capsid (3, 4). Fibrils are important structures for adhesion to the surface of amoebas (5). For instance, APMV fibrils are often found with one of their ends free and associated with a globular terminal, while the other is attached to a single central structure (6). In addition, they appear to be associated with a peptidoglycan-like structure, exhibiting successive rings of density (6). Moreover, in addition to R135, the L829 and L725 proteins have also been associated with APMV fibril composition, as the lack of those genes in the genome of mimivirus M4 was linked to an almost-fibrilless phenotype of M4 isolate particles (7). To date, the M4 isolate was obtained after successive passages of APMV in amoebas under allopatric conditions, resulting in genome shrinking and a decrease in fibril abundance (7). Furthermore, the adhesion of mimivirus fibrils to the host membrane seemed to be mediated by sugars found on both the host surface and in the fibrils (e.g., mannose and *N*-acetylglucosamine), allowing the phagocytosis of the virus and subsequent entry to start the cycle (5). Additionally, mimiviruses have a star-shaped structure called a stargate at one of the vertices of their particle, and this structure is responsible for releasing the genome at the beginning of the cycle within the host and is the only region at the capsid uncovered by fibrils (2, 6).

Currently, mimiviruses belong to the genus *Mimivirus*, family *Mimiviridae*, order *Imitervirales*, class *Megaviricetes*, and phylum *Nucleocytoviricota* (8). Metagenomics studies indicate that mimiviruses are among the most abundant viral entities in different biomes worldwide (9, 10). Phylogenetic analyses considering hallmark genes have shown that mimiviruses seem to be divided into three main lineages, A, B, and C (11). Lineage A is represented by APMV and other viruses similar to it, such as the Brazilian isolate sambavirus (12). Lineage B consists of the moutoviruses and related viruses, and lineage C is composed of megaviruses such as *Megavirus chilensis* and other similar viruses (13, 14). Genetic analyses show that mimivirus lineages, despite being evolutionarily related, present important differences between some of their genes. In this context, the possible differences in the morphological organization of mimivirus fibrils have not been explored in a comparative way, considering the three lineages and/or their isolates, and is an open field for study and new discoveries.

In this work, we describe the isolation of a novel mimivirus belonging to lineage C, named *Megavirus caiporensis*. The microscopic and genomic analyses of this virus raised questions on how surface fibrils are organized in different mimivirus isolates and encouraged us to expand this study to 14 other mimivirus isolates. Taken together, our data demonstrate at least three main patterns of fibril organization among isolates from different lineages. Considering the viruses analyzed here, evolutionarily-related isolates present similar fibril profiles. Our data also indicate that, in contrast to previous speculations (7), even the almost-fibrilless isolates (e.g., Borely moutovirus) can have the R135, L829, and L725 genes in their genomes.

RESULTS

Megavirus caiporensis: isolation of a new mimivirus in Brazil. As part of our continuous efforts to discover new giant viruses of amoebas, a new virus was isolated from a water sample collected from an urban lagoon in Belo Horizonte, Brazil. After observing cytopathic effect in the microplate well where this sample was inoculated, we proceeded with characterization of this isolate. By light microscopy, we observed the development and progression of the infection cycle as cytopathic effects emerged and intensified. At 6 h postinfection (hpi), the cells began to round and detach from the monolayer. At 12 hpi, fully rounded cells began to undergo lysis, and at 24 hpi almost all cells were lysed and cellular debris was observed in the supernatant and at the bottom of the flasks (Fig. 1A).

Images obtained by transmission and scanning electron microscopy (TEM and SEM, respectively) allowed us to identify the isolate as a mimivirus (Fig. 1B and C), due to the morphologic characteristics of its particles, composed of capsids with an average

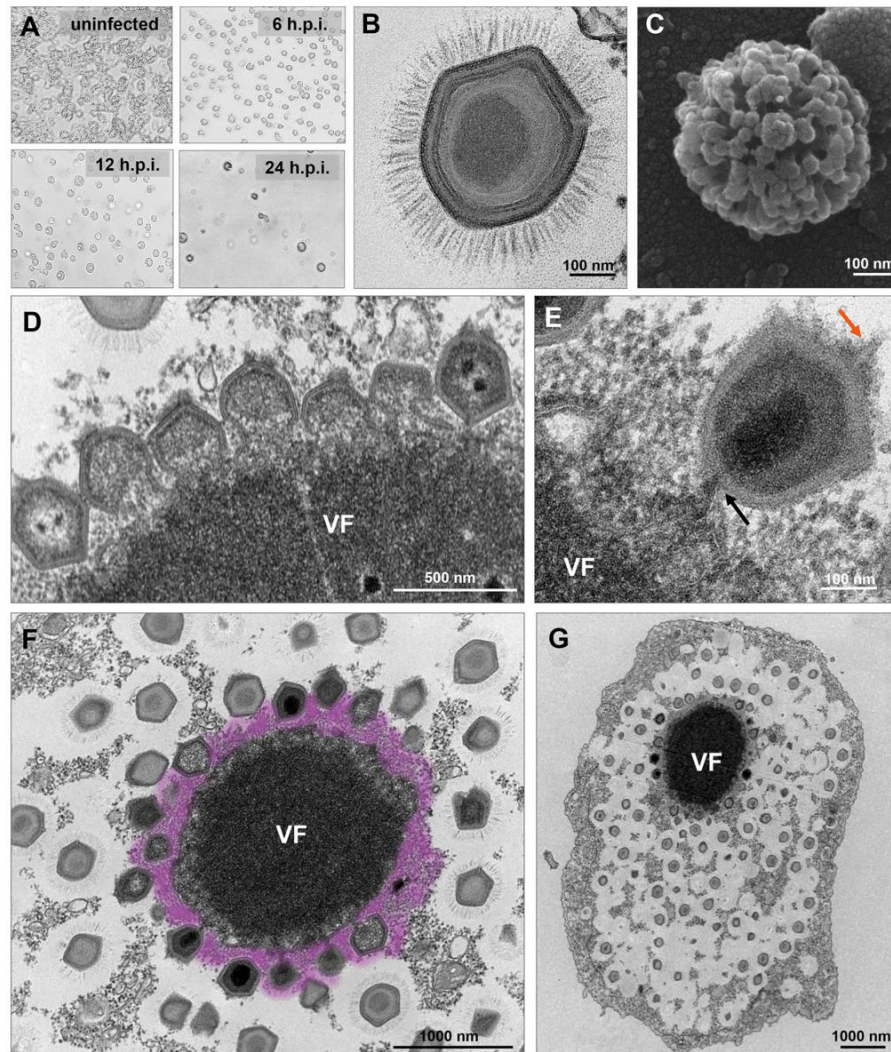


FIG 1 Megavirus caiporensis viral particle and cycle. (A) Cytopathic effects on *A. castellanii* amoeba cells infected with Megavirus caiporensis. For the uninfected cell control, it is possible to observe the cells presenting irregular shapes, vacuoles, and good adhesion forming a monolayer, characteristics that allowed us to verify a healthy culture. From 6 h postinfection (hpi) with the megavirus that we isolated, the cells had already begun to undergo rounding and loosening of the monolayer, as seen in abundance in the supernatant. After 12 hpi, complete rounding and the beginning of cell lysis were observed, which significantly increased after 24 hpi, at which time few cells were still intact. Images were obtained using 100 \times magnification. (B and C) Characteristics of the Megavirus caiporensis viral particle. The Megavirus caiporensis capsid is composed of multiple layers involving the genome, a central and darker region, and a layer of fibrils covering the structure (B). The SEM image of a Megavirus caiporensis particle is shown (C). (D to G) Megavirus caiporensis multiplication cycle stages. (D) Assembly of new Megavirus caiporensis particles, beginning with the filling of the crescent-shaped form with the material present in the viral factory (VF). (E) Megavirus caiporensis viral particle receiving the internal contents through the opposite end (black arrow) to the stargate (orange arrow). (F) Viral factory producing new particles and the fibril acquisition area highlighted in purple. (G) The mature viral factory (VF) occupies a large part of the host cytoplasm of infected amoebas in full production of new Megavirus caiporensis particles.

size of 435 nm, covered by a layer of fibrils of 108 nm, and a total size of 651 nm (average). Interestingly, compared to what has been described for APMV (6), this isolate exhibited fibrils in a different organization, forming small clumps (Fig. 1B and C). Fibrils seemed to be grouped from the point of insertion into the capsid to their outermost portions (Fig. 1B). Here, as the fibrils of this virus are similar to those observed for

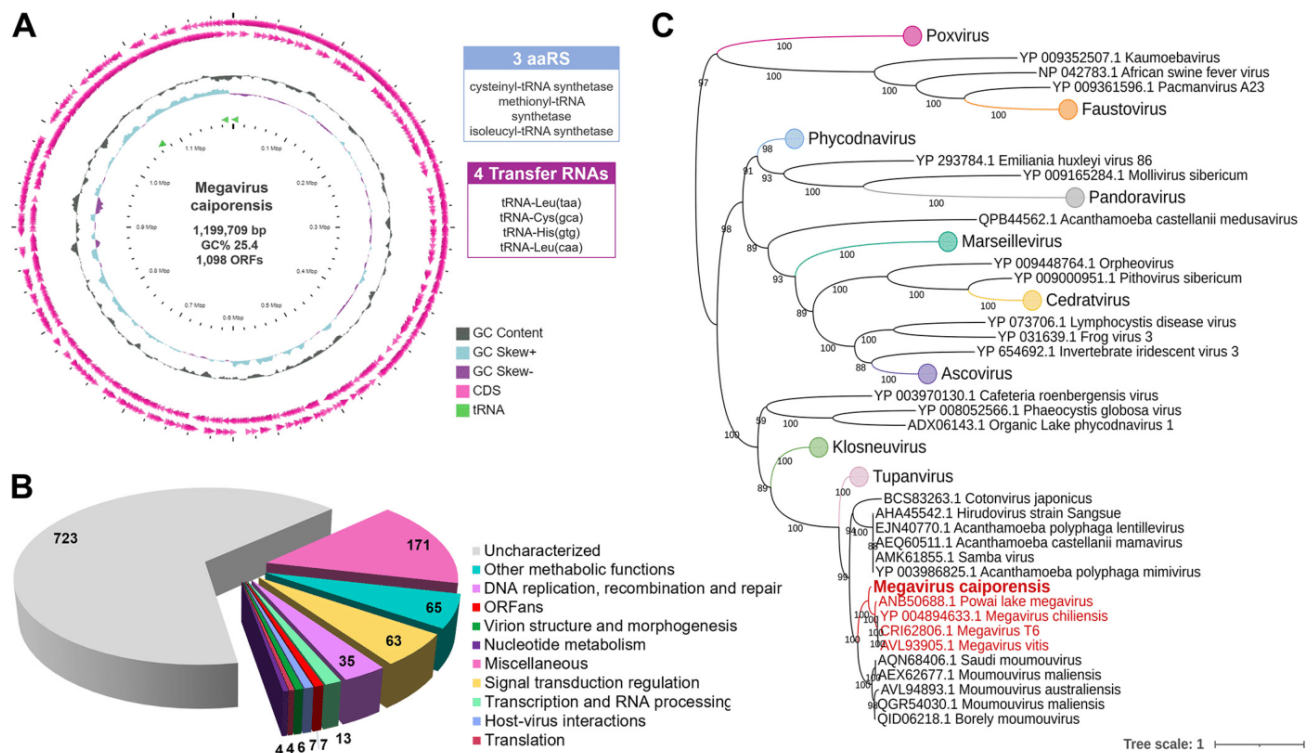


FIG 2 Genomic features of *Megavirus caiporensis*. (A) Circular representation of the *Megavirus caiporensis* genome. Rings, from innermost to outermost, correspond to genome coordinates in kilobases (kb), GC skew, GC content, and predicted protein-coding sequences (CDS) on both the forward and reverse strands. The green arrowheads correspond to transfer RNAs. A colored subtitle is provided on the right side of the figure. The blue and purple boxes at right indicate the three aminoacyl-tRNA synthetases (aaRS) and four tRNAs identified for this virus, respectively. (B) A set of genes from *Megavirus caiporensis*, classified according predicted gene categories. A colored subtitle is provided on the right side of the figure. (C) Phylogenetic analysis of subfamily B DNA polymerase sequences of *Megavirus caiporensis* and *Nucleocytoviricota*-related viruses. A maximum-likelihood phylogenetic tree was constructed with sequences of subfamily B DNA polymerase of mimiviruses and other *Nucleocytoviricota*-associated viruses. In this phylogeny, the new isolate described here, *Megavirus caiporensis*, clustered with lineage C mimiviruses (highlighted in red). The scale bar indicates the rate of evolution.

Megavirus chilensis (13) and considering the sequencing results on this isolate (discussed below), we named it *Megavirus caiporensis*.

TEM images revealed that the entire cycle of *Megavirus caiporensis* is similar to what has been previously described for other mimiviruses (15). For instance, the immature viral factory is formed in the amoeba cytoplasm after virus entry, likely by phagocytosis, initiating the replication cycle. After the formation and maturation of the viral factory, mitochondria can be observed in its periphery, as well as formation of new particles assembling by crescent-shape structures, which gradually increase in size and are filled by the content present in the factory (Fig. 1D and E). During the acquisition of fibrils at the so-called fibril acquisition area, the particles receive their internal content from the opposite side of the stargate (Fig. 1D to F). At the end of the cycle, mature factories occupy a large area in the cell cytoplasm, as described for other mimiviruses (15). The newly formed particles agglomerate into the host cytoplasm, and the factories decrease in size throughout the replication cycle (Fig. 1G). Finally, particle release occurs by cell lysis.

Megavirus caiporensis sequencing and phylogenetic analysis confirmed it belongs to mimivirus lineage C. The genome of *Megavirus caiporensis* is a linear, double-stranded DNA molecule of 1,199,709 bp in length (Fig. 2A). Its genomic content is predicted to encode 1,098 genes (568 located on the negative strand and 530 located on the positive strand) with a coding density of 91.3% and a GC content of 25.4%. Among the predicted proteins, 723 had no known function and were considered uncharacterized. Most functional genes fit into the categories miscellaneous (i.e., domain and repeat proteins; diverse enzymes) (171), other metabolic functions (65), signal transduction regulation (63), and DNA recombination, replication, and repair (35) (Fig. 2B). B-family DNA polymerase, chaperone, helicases, and replication factors

are some of the genes that are incorporated inside the category of DNA recombination, replication, and repair. Seven open reading frames (ORFs) with no detectable homology to other ORFs in a database were detected and were considered ORFans. In addition, genes related to translation, a trademark of mimiviruses, were identified, including three aminoacyl-tRNA-synthetases, four RNA transporters (Fig. 2A), and one GTP binding translation elongation/initiation factor. The Megavirus caiporensis genome presents 13 genes related to transcription and RNA processing, including RNA ligase and different subunits of DNA-directed RNA polymerase. The majority of genes predicted matched those also predicted for Powai Lake megavirus and Megavirus chilensis, including ankyrin repeat proteins (miscellaneous category), putative lipoprotein (other metabolic functions), and putative protein kinases (signal transduction regulation category). Genes associated with host-virus interactions, nucleotide metabolism, and virion structure and morphogenesis were also predicted for Megavirus caiporensis. Additionally, in order to investigate the evolutionary and phylogenetic relationship of Megavirus caiporensis with other *Nucleocytoviricota*, including mimiviruses, we also performed a phylogenetic analysis using the conserved gene that encodes family B DNA polymerase as a target (Fig. 2C). Phylogenetic construction confirmed that Megavirus caiporensis clustered with lineage C mimiviruses.

Mimivirus isolates have at least three patterns of surface fibrils. The isolation and characterization of Megavirus caiporensis intrigued us regarding its structural aspects, as we noticed a different organization of its fibrils, further expanding these analyses to lineage A and B mimiviruses. Thus, we selected APMV (lineage A) and Borely moutoumavirus (lineage B), as they are two viruses for which the whole genomes have been sequenced, as well as their being available in our laboratory. In order to analyze those isolates' fibrils, particles of APMV, Borely moutoumavirus, and Megavirus caiporensis were observed by TEM and SEM (Fig. 3A). As for APMV, it was possible to observe, as previously described in the literature, that its fibrils are long and abundantly surround the capsid (Fig. 3A), herein termed pattern A. In comparison, Borely moutoumavirus (lineage B) appeared to have fewer fibrils around its capsid and these were less homogeneously distributed (Fig. 3A); here, we termed this pattern B. Interestingly, some particles belonging to pattern B were almost fibrilless. Finally, the isolate described here, Megavirus caiporensis, which belongs to lineage C, had an abundant number of fibrils, as seen for lineage A, but they were organized in small groups, as clumps (Fig. 3A); this pattern is herein termed pattern C. In SEM images, the patterns described here for fibrils were maintained, and we also observed very clearly the aforementioned differences among these mimiviruses (Fig. 3B). For instance, APMV exhibited its surface with fibrils homogeneously distributed, while for Megavirus caiporensis fibrils appeared to be organized in groups or clusters. As for Borely moutoumavirus, it is possible to see that the capsid surface exhibits a geometric appearance, which probably is linked with the lower number of fibrils that is usually observed in EM images. We also developed a protocol to estimate the relative abundance of surface fibrils in the particles of mimiviruses, and then we applied it to compare APMV, Borely moutoumavirus, and Megavirus caiporensis (Fig. 3C). After calibration of average values, the analysis revealed that Megavirus caiporensis exhibited the highest relative average contrast, 552-fold higher than Borely moutoumavirus, followed by APMV, for which the contrast was 394-fold higher than Borely moutoumavirus (Fig. 3D). Megavirus caiporensis had the highest relative average contrast and this was possibly related not only to the number of fibrils but also to the clump's organization, while Borely moutoumavirus having the lowest contrast was expected, since it has fewer fibrils surrounding the capsid (Fig. 3D).

It is important to mention that preparation for TEM can influence fibril appearance. To understand whether the different fibril organizations and abundances could be the result of possible artifacts of preparation, we concomitantly analyzed different combinations of mixed purified particles of APMV, Borely moutoumavirus, and Megavirus caiporensis by TEM. Therefore, those different viruses were mixed in the same sample in

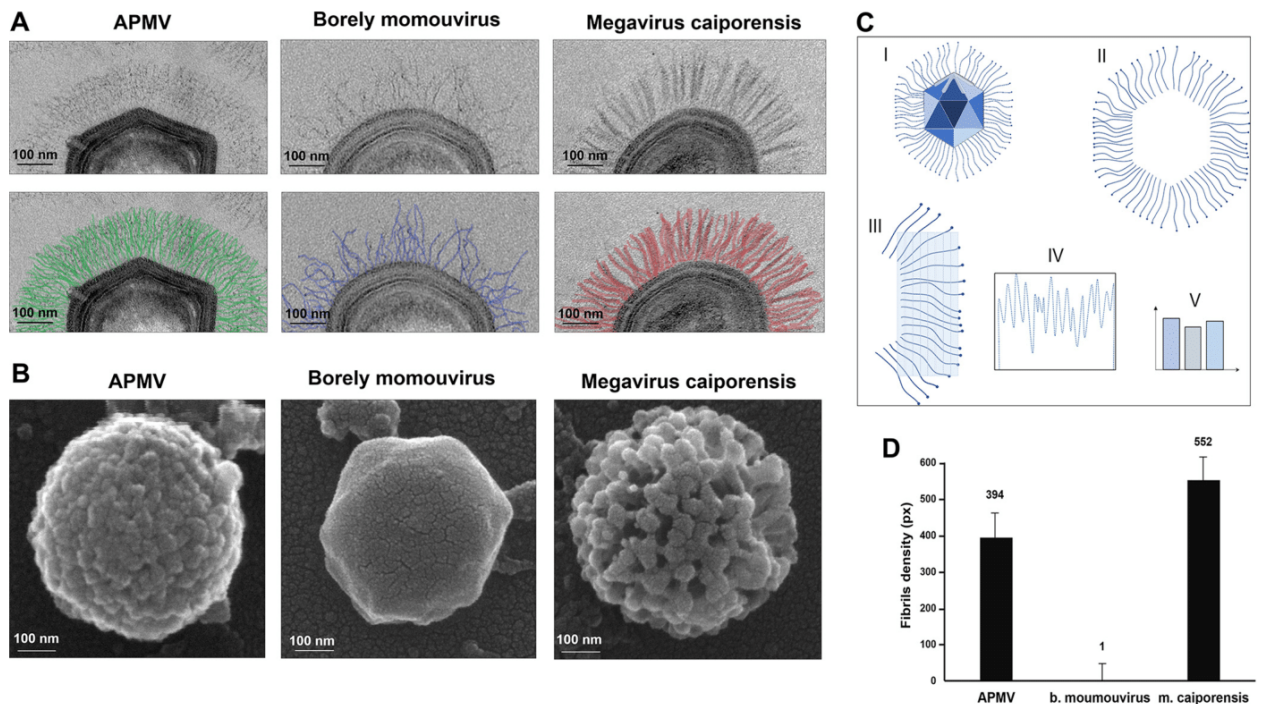


FIG 3 Morphological differences of mimivirus fibrils according to lineages A, B, and C. (A) Different patterns of fibril organization observed by TEM. Mimivirus extern fibrils in TEM images are highlighted with different colors to show the discrepancies of the fibril abundances and organizations (APMV in green, Borely momouvirus in blue, and Megavirus caiporensis in red). (B) Different patterns of fibril organization observed by SEM. SEM images show the fibrils on the surfaces of the particles of APMV, Borely momouvirus, and Megavirus caiporensis, respectively. Scale bars are indicated for each image. (C) Analysis of mimivirus fibril densities. For this illustrative representation of the protocol used to analyze the densities of fibrils of different mimiviruses, we have provided images obtained by TEM for each mimivirus analyzed (I). The fibrils were highlighted in the images manually by using the drawing tool available in Microsoft PowerPoint version 2021, and the background image was erased, leaving only the fibrils that were highlighted. (II) For each of the six sides of the particles, the fibril area was covered with rectangles of the same size and thickness in ImageJ software (version v1.53k). (III) From each rectangle we generated a graph showing curves referring to pixel values read within the demarcated region. (IV) The values obtained were plotted in the form of a table in Excel version 2021 and analyzed. (V) Graph representing the densities of fibrils found for each of the mimiviruses analyzed in this work. The x axis represents the analyzed lineages and the y axis shows the densities of fibrils in pixels. Values were calibrated based on the lowest observed value. Megavirus caiporensis presented the highest value identified among the three (552 pixels), followed by APMV (394 pixels). Finally, Borely momouvirus presented the lowest number among the three (1 pixel), probably due to its lower number of these structures.

trio or pairs (Fig. 4) and then analyzed. All three fibril patterns were observed in the trio preparation (lineages A + B + C) (Fig. 4A). Patterns A and B were observed in preparations containing a mix of particles belonging to lineages A and B (Fig. 4B), and no particles with clumped fibrils were observed. Patterns B and C were the only ones observed in preparations containing lineage B and C viruses (Fig. 4C). Finally, patterns A and C were the only ones observed in preparations containing lineage A and C viruses (Fig. 4D). Taken together, these results confirmed that the distinct patterns of fibril organization and abundances were not likely to be an artifact of analysis related to TEM sample preparation.

Considering these previous results regarding different mimivirus organization and abundance of fibril patterns, we expanded our analyses to other mimivirus isolates obtained by our group in the past 10 years. To date, all viruses isolated in our lab have been inspected by TEM, and their images are stored in a database. We searched for isolates with the three aforementioned fibril patterns (Fig. 2). We selected 15 isolates, 5 of each pattern (Fig. 5), and sequenced their family B DNA polymerase gene, which is considered a hallmark gene for differentiating the three mimivirus lineages. Sequences were used to construct a data set and a phylogenetic tree considering APMV, Borely momouvirus, and Megavirus chilensis (13) as references for lineages A, B, and C, respectively. The results revealed a corresponding match among the three lineages and the predicted fibril morphotypes (Fig. 5 and 6): (i) lineage A, fully covered by fibrils (pattern A), including APMV, Mimivirus PU, Mimivirus capivarensis, Kroon mimivirus,

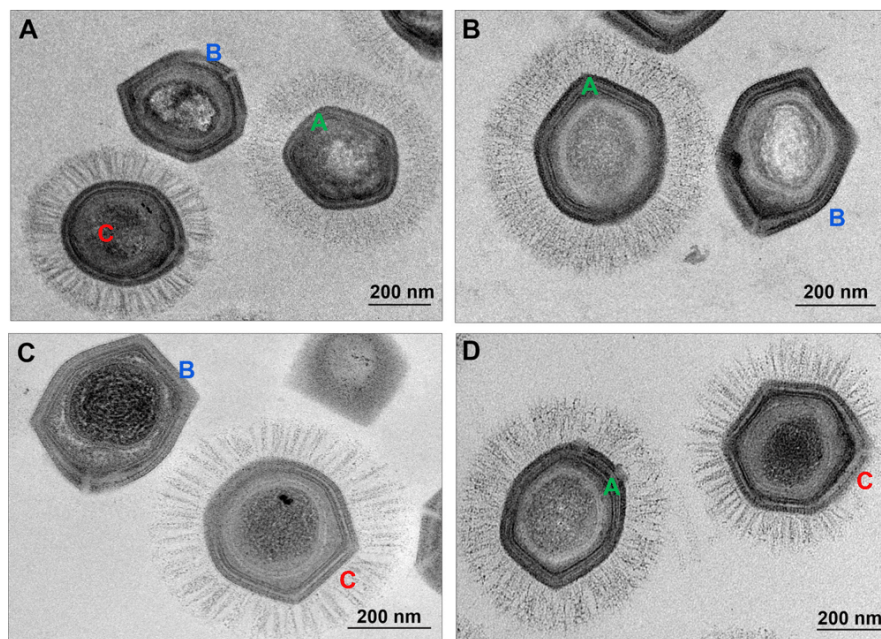


FIG 4 TEM images of trios and pairs of purified mimivirus particles related to lineages A, B, and C obtained in one same sample. (A) Mimivirus trio in the same sample; TEM sample images contain mimivirus A + B + C. (B to D) Mimivirus pairs in the same sample, with TEM sample images for pairs A + B (B), B + C (C), and A + C (D). For the preparations, only purified viral particles were used in combinations in trios or pairs, with APMV representing pattern A; Borely moumouvirus for pattern B; and Megavirus caiporensis representing pattern C. Scale bars are indicated in the images.

and Amazonia mimivirus; (ii) lineage B, almost fibril-less (pattern B), including Borely moumouvirus, Moumouvirus crenensis, Moumouvirus dionensis, Moumouvirus limneidensis, and Moumouvirus naiadiensis; and (iii) lineage C, with fibrils in clumps (pattern C), including Megavirus caiporensis, Megavirus curupirensis, Megavirus botiensis, Megavirus boitataensis, and Megavirus muiraquitaensis. Taken together, our results suggested that, considering our collection of isolates, each lineage is related to a pattern of fibril morphology. A comprehensive search for TEM images of mimivirus isolates in the literature also revealed that at least two of the three patterns of fibrils presented here have already been observed in natural isolates: those with particles fully covered by fibrils (pattern A) (16–18) and those with clumped fibrils (pattern C) (13, 19–21). Although TEM images of lineage B mimivirus particles are scarce in the literature, there is evidence that some moumouvirus have long abundant fibrils, similar to that described for APMV and other lineage A mimiviruses (22), such as those presented here. Therefore, although our isolates indicated a possible correspondence between patterns of fibrils and mimivirus lineages, this feature may not be expandable to all isolates and requires further investigation.

As aforementioned, the M4 isolate was obtained after successive passages of APMV in amoebas under allopatric conditions, resulting in a different set of phenotypes, including almost fibril-less particles. Proteomic analysis of M4 particles indicated the absence of a GMC-oxidoreductase encoded by the APMV R135 gene, while this gene has been reported as a main component of mimivirus fibrils (4, 6). To evaluate this correlation between fibrils and R135, we investigated the presence of R135 orthologues in the Borely moumouvirus genome. Interestingly, although Borely moumouvirus particles have a pattern similar to the M4 isolate, we found an R135 orthologue in its genome with 68.2% similarity to APMV R135, considering predicted amino acid sequences. Other APMV genes previously reported to be related to fibrils but absent in the M4 genome, such as L829 and L725, were also found in the Borely moumouvirus genome, with 62.9%

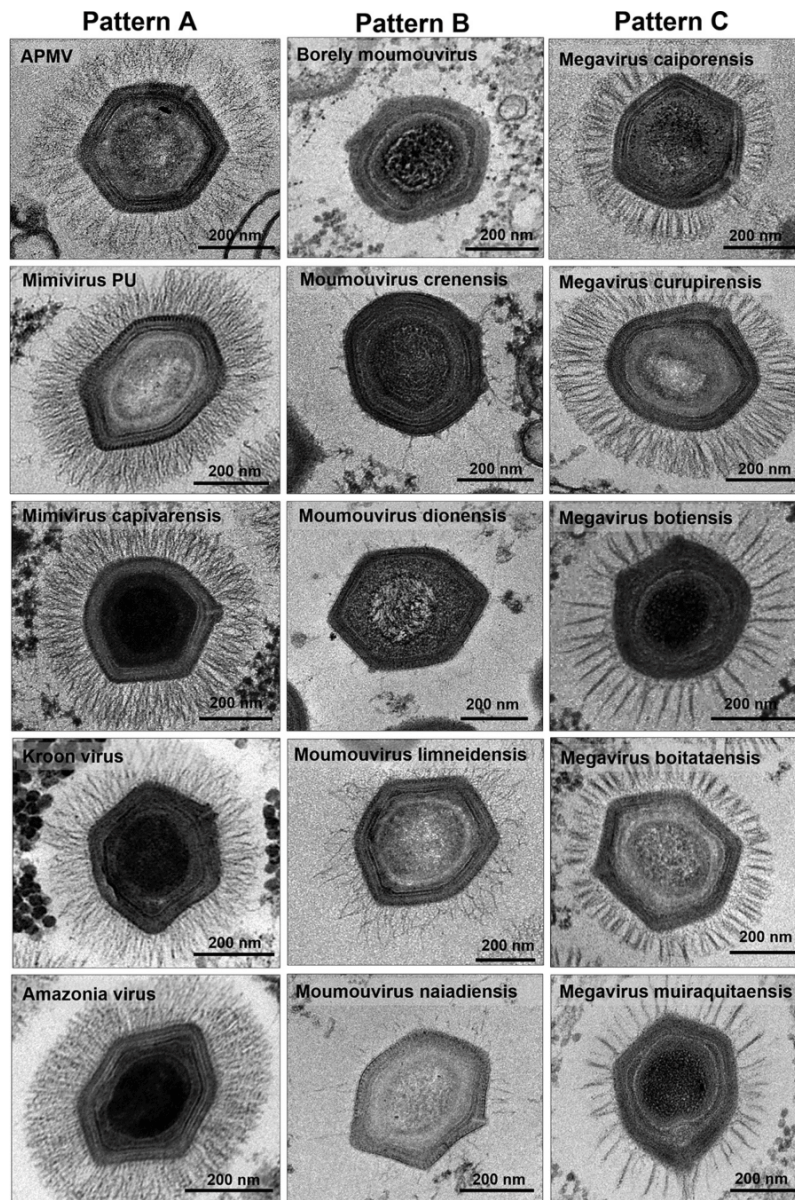


FIG 5 Comparative panel of several mimivirus fibril morphologies related to patterns A, B, and C. Each column represents a pattern of fibril organization for each mimivirus lineage (A, B, or C), exhibited in five different isolates each. Pattern A mimiviruses (first column) fibrils are long and abundantly and homogeneously distributed around the capsid. Pattern B mimiviruses (second column) exhibit many fewer fibrils that are not uniformly distributed, and for some isolates the number of fibrils was too low to be captured by TEM images. Finally, for pattern C mimivirus (third column), the fibrils are organized surrounding the capsid, forming clumps. Some of those fibril clusters are so closely knit that the particle seems to have fewer fibrils (Megavirus muiraquitensis and Megavirus botiensis) compared to others, implicating an interspecific variance between pattern C viruses.

and 54.7% similarity to the APMV predicted proteins, respectively (Table 1). We also observed that those three genes were widespread in most mimiviruses, which were clustered according to their respective lineages (A, B, or C) regardless of their fibrils pattern (Fig. 7A to C).

Fibrils may affect particle incorporation by amoebas. Our group previously demonstrated that mimivirus fibrils may play an important role in viral adhesion to host

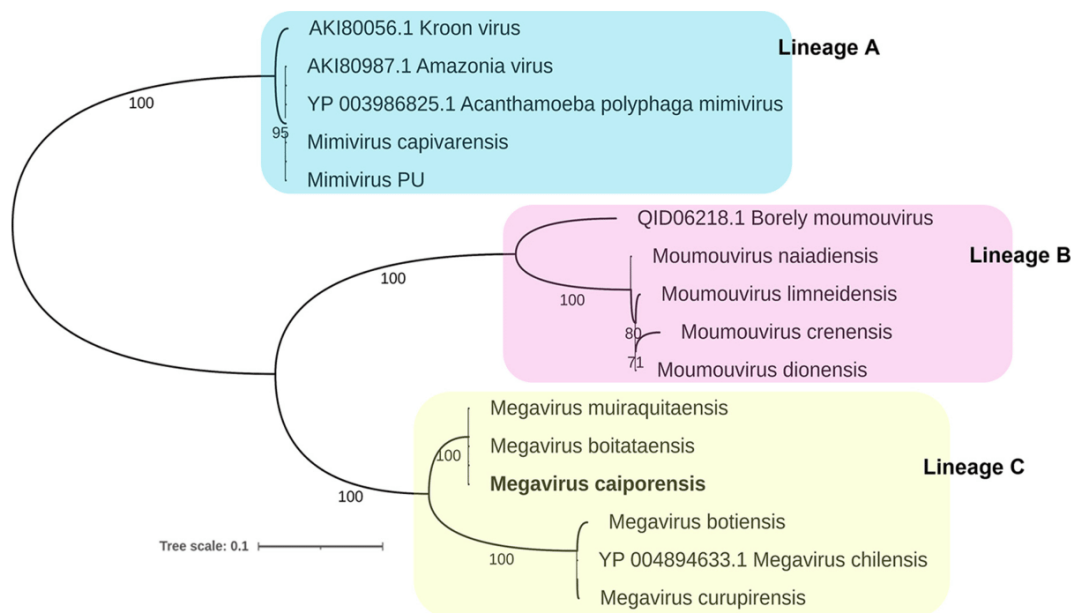


FIG 6 Phylogenetic construction of mimiviruses of patterns A, B, and C. Phylogenetic trees were constructed based on the DNA polymerase gene of subfamily B of 15 mimiviruses, presented previously in a comparative panel of fibril organization patterns. To investigate the history of the relationship of each mimivirus with one lineages, A, B, or C, a representative previously related to each lineage was chosen: APMV for lineage A, Borely moulmouvirus for lineage B, and Megavirus chilensis for lineage C. Our results suggested that different fibril patterns are lineage-associated, considering our analyzed isolates.

amoebas (5). To understand whether the pattern of fibrils could affect the adhesion and entry of the particles in *A. castellanii*, we performed a set of biological assays with viruses presenting patterns A, B, and C. Analysis of TEM images showed pattern A and C particles binding to host plasma membrane, mediated by surface fibrils (Fig. 8A), but no pattern B particles were visualized attached to host cells. To quantitatively evaluate particles adhesion to amoebas, cells were infected at a multiplicity of infection (MOI) of 10, and after 60 min the supernatants were collected and titers were determined. The titration of the samples collected 1 hpi revealed approximately 10 times more Borely moulmouvirus infectious particles than APMV and Megavirus caiporensis, suggesting that Borely moulmouvirus particles (pattern B) were less able to be associated to the amoeba surface than pattern A and C viruses (Fig. 8B). To evaluate the incorporation of lineage A, B, or C isolate particles by amoebas, 50 cells were analyzed by TEM at 30 min pi for each isolate. It is important to mention that these results should be analyzed with care, considering that TEM was performed on a given section of biological samples. Nevertheless, these results are worthwhile to be presented since cells infected by APMV, Borely moulmouvirus, or Megavirus caiporensis were analyzed under the same conditions. Here, 43 of 50 analyzed amoebas had at least two APMV particles internalized, and some cells incorporated a substantial number of APMV particles, up to 34 (Fig. 8C). As for Borely moulmouvirus-inoculated sample, only 4 infected cells were observed, whereas 16 analyzed cells showed Megavirus caiporensis particles internalized (Fig. 8C). Despite those differences in adhesion and entry described for pattern A, B, and C viruses, we were able to observe particle uncoating (stargate opening) for APMV, Borely moulmouvirus, and Megavirus caiporensis (Fig. 8D). Taken together, our results suggest that the pattern of fibrils may affect not only particles adhesion but also their incorporation by amoebas. Finally, the viral factories of viruses belonging to patterns A, B, and C were analyzed by TEM, and this revealed that, in spite of differences in fibril abundances and organization, factories from all viruses presented a fibrils acquisition area, suggesting that further studies on these structures are necessary (Fig. 8E).

TABLE 1 Similarity values of the best hits found by the BLASTp tool from amino acid sequences of proteins R135, L829, and L725^a

Virus	% similarity with protein:		
	R135	L829	L725
APMV	100	100	100
Mimivirus reunion	99.6	99.8	100
<i>Acanthamoeba castellanii</i> mamavirus	99.6	99.8	100
Cotonvirus japonicus	68.4	61.3	66
Borely moudouvirus	68.2	62.9	54.7
Moudouvirus australiensis	68	61.1	55.1
Moudouvirus maliensis	68	62.5	54.7
Moudouvirus monve	68.5	62.2	55.2
Moudouvirus goulette	68.5	61.2	54.3
<i>Acanthamoeba polyphaga</i> moudouvirus	68.5	62.2	55.6
Saudi moudouvirus	68.5	62.3	55.6
Megavirus caiporensis	67.4	59	56.5
Bandra megavirus	68.3	58.5	56.5
Megavirus courdo7	68	58.8	56.5
Megavirus chilensis	68.1	58.3	56.5
Megavirus vitis	68	58.8	56.5
Megavirus lba	68	59	56.5
Powai Lake megavirus	67.8	60.1	56.5

^aAPMV was used as the reference.

DISCUSSION

The isolation of a new lineage C mimivirus in Brazil highlights the diversity and ubiquity of mimiviruses. The role of fibrils for the adhesion of mimiviruses and their consequent success in invading their hosts to start the infection cycle has been reported previously (4–6). Findings from this current work corroborate these data, as we provided evidence that fibril abundance may be related to the entry of mimivirus into amoebas. It is important to highlight that lineage A includes the majority of isolates described worldwide, and most of the mimiviruses isolated by our team in Brazil are related to this lineage (23, 24). A possible explanation for this is the morphology of the fibrils presented by these viruses, which are found abundantly and homogeneously distributed throughout the viral capsid (Fig. 3 and 5). Additionally, the smaller number of isolates related to lineage B can also be related to the same hypothesis, since these viruses have fewer fibrils, which can decrease their abilities to adhere to their hosts and trigger phagocytosis and the consequent entry.

Additionally, regarding fibril morphology, it is also possible to notice an interspecific pattern of clustering of these structures within lineage C (Fig. 5, third column). The organization of the fibrils in clumps starts at the insertion from the capsid and continues until the tips facing the external environment. However, in some particles, these clumps were in smaller quantities and presented with more contrast in TEM images (Fig. 5, Megavirus botiense and Megavirus muraquitaense), while they were more abundant and seemed to cluster fewer fibrils in others (Fig. 5, Megavirus caiporensis, Megavirus curupirensis, and Megavirus boitataense). Understanding the reason for these differences within the same clade, searching for molecular differences that may explain them, and understanding the implications of these data are important perspectives to complement the novelties brought by this work.

Regarding their structure, we also showed that the fibril morphotypes were not the result of preparations for EM analysis but were an intrinsic characteristic of each viral particle pattern's specificity (Fig. 4). Moreover, we found some evidence of molecular differences at important proteins for mimivirus fibrils, namely, R135, L829, and L725 (Fig. 7A to C), which may be closely related to the different phenotypes found among the three lineages. It is important to mention that the scarce number of images from lineage B mimivirus viral particles in the literature was a limiting factor in our study, making our findings concerning fibril patterns dependent on the isolates of each

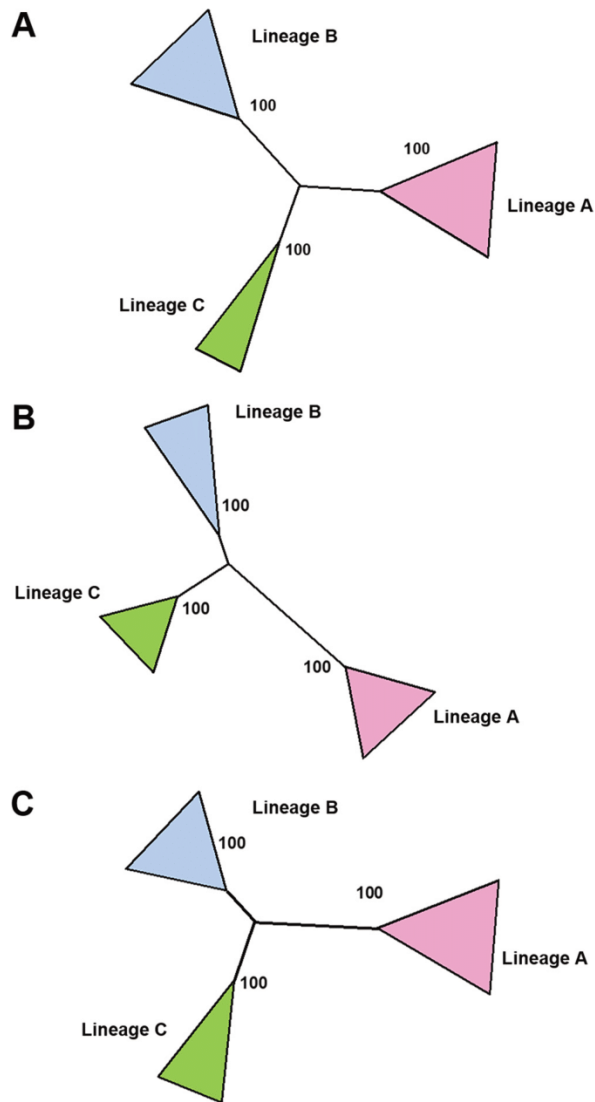


FIG 7 Phylogenetic constructions based on amino acid sequences of proteins associated with mimivirus fibril structures, based on proteins R135 (A), L829 (B), and (C) L275. Our results suggest that those genes are widespread in mimivirus isolates, regardless the lineage.

lineage to which we had access in our database. In addition, although it was clear that the pattern B remained among the isolates of our group, it is essential to attempt to cover future studies with more isolates of lineage B in order to affirm that this pattern can be maintained. Thereby, we propose that fibril morphological characteristics can be considered as indicators of mimivirus relationships to one of the A, B, or C lineages and that they can be complements to molecular traits for the characterization of these viral entities. Understanding the implications of different fibril morphotypes among mimivirus lineages can provide important information about the biology of these viruses and the way they relate to the environment and to their hosts, allowing further unraveling of these features within the family *Mimiviridae*.

MATERIALS AND METHODS

Virus isolation, multiplication, and purification. In August 2017, 10 water samples were collected from Pampulha Lagoon, Belo Horizonte, Brazil. The collection was performed with sterile tubes, and the

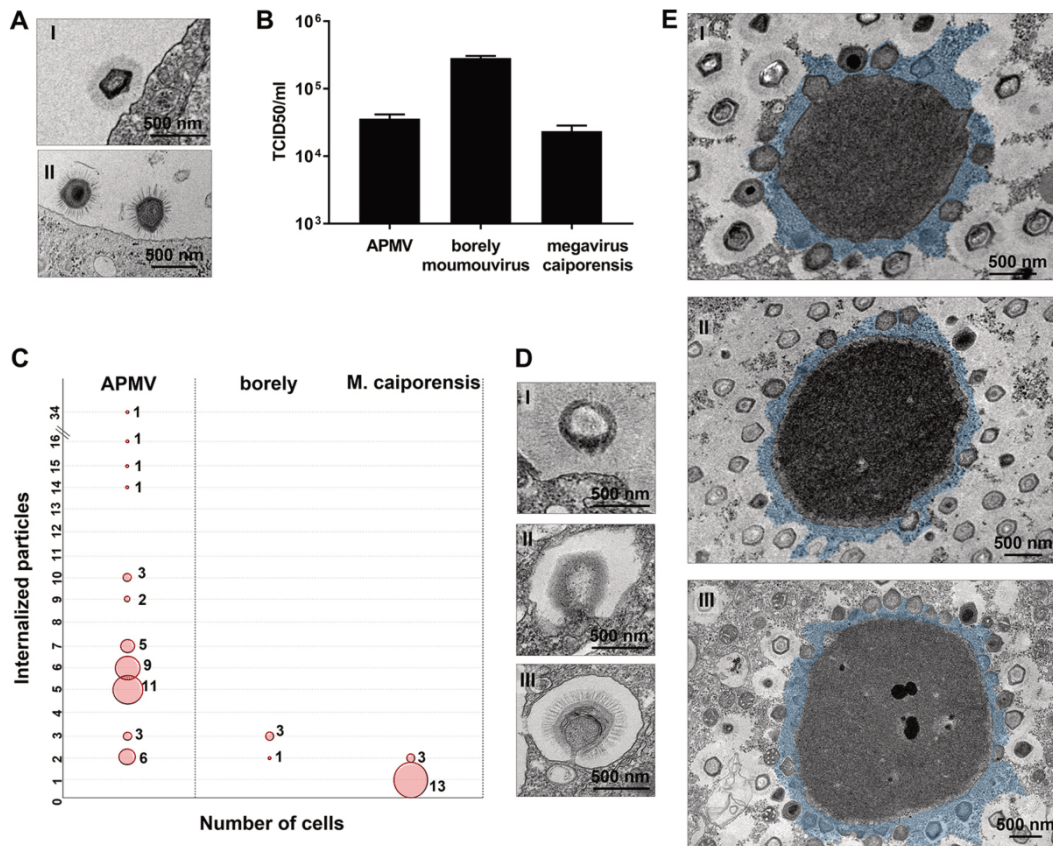


FIG 8 Fibril abundance seems to influence host-amoeba adherence and entry of pattern A, B, and C mimiviruses. (A) TEM images of pattern A (I) and C (II) mimiviruses attached to *Acanthamoeba castellanii* plasma membrane. No images were obtained for pattern B mimivirus. (B) Pattern B mimivirus particles are less incorporated by amoebas than mimivirus pattern A and C particles. Amoebas were infected by pattern A, B, or C at an MOI of 10. Sixty minutes postinfection, the supernatants were collected to verify the number of infectious particles not incorporated by amoebas, and then titers were determined. (C) Graphical representations of the relationship of the number of internalized particles within each amoeba (y axis) versus the number of cells (x axis) for APMV, Borely moutouvirus, and Megavirus caiporensis, respectively. The red circles indicate the number of cells with a specific number of particles internalized. Fifty TEM images of amoebas for each virus were selected randomly for analysis. (D) Mimivirus particles in denudation after entry into the host cell: APMV (I), Borely moutouvirus (II), and Megavirus caiporensis (III), indicating the continuation of the mimivirus cycle. (E) Fibril acquisition areas of mimiviruses related to lineages A, B, and C. Despite the differences in the patterns of fibrils among the three lineages, all three representatives presented a fibril acquisition area (I, APMV; II, Borely moutouvirus; III, Megavirus caiporensis).

samples were stored at 5°C until the inoculation process. The samples were submitted to the process of prospecting and isolation of new giant viruses in *Acanthamoeba castellanii* amoebas, as previously described (25). From this collection of samples, we isolated nine amoeba viruses, including Megavirus caiporensis (mimivirus). These new isolates were registered at the Sistema Nacional de Gestão do Patrimônio Genético e do Conhecimento Tradicional Associado (SisGen), number ABF23CC. After the isolation, the virus was inoculated at a MOI of 0.01 in cell culture roller flasks containing 1.4×10^7 *Acanthamoeba castellanii* cells and 35 mL of peptone-yeast extract-glucose (PYG) medium supplemented with penicillin (100 U/mL; Cellofarm, Brazil), streptomycin (100 µg/mL; Sigma-Aldrich, Burlington, MA, USA), and amphotericin B (0.25 µg/mL; Cultilab, Brazil). The cells were incubated at 30°C under slow rotation (0.2 rpm) on a roller. After the observation of cytopathic effect caused by viral infection (i.e., rounding cells and cellular lysis), the flask contents were collected. This content was subjected to freezing and thawing three times, to lyse the cells that remained intact and release viral particles. Then, it was ultracentrifuged ($36,000 \times g$) in a 22% sucrose cushion for 50 min. The pellet containing purified viral particles was suspended in phosphate-buffered saline (PBS), and the viral titers were obtained by the endpoint method (26).

Electron microscopy. *Acanthamoeba castellanii* cultures infected with different mimivirus strains (belonging to the lineages A, B, and C) and the respective isolated and purified mimiviruses were analyzed by SEM and TEM. Experiments and analyses were performed in the Center of Microscopy at the Universidade Federal de Minas Gerais, Belo Horizonte, Minas Gerais, Brazil (<http://www.microscopia.ufmg.br>).

For SEM assays, samples were fixed by immersion in a solution containing glutaraldehyde (2.5%) in 0.1 M sodium cacodylate buffer (pH 7.2) for 2 h. Following this, postfixation was performed for each sample with 2% osmium tetroxide (OsO_4) for 2 h at room temperature. Fixed samples were dehydrated using a growing series of ethanol dilutions (30%, 50%, 70%, 95%, and 100%) for 10 min in each step. Then, samples were dried with CO_2 at critical point using CPD 030 equipment (Bal-Tec, Liechtenstein). Next, samples were supported in aluminum stubs and metalized with a thin layer (5 nm) of gold particles using MED 020 equipment (Bal-Tec, Liechtenstein). Samples were observed in a FEG-Quanta 200 FEI microscope (FEI Co., Eindhoven, Netherlands) at 15 to 20 kV.

For TEM assays, samples were fixed by immersion in a solution containing glutaraldehyde (2.5%) in 0.1 M sodium phosphate buffer (pH 7.2) for 2 h. After fixation, postfixation was performed with a solution of 1% osmium tetroxide in sodium cacodylate buffer (0.1 M, pH 7.2) for 1 h followed by en bloc counterstaining with uranyl acetate (2% uranyl acetate in deionized water). Samples were gradually dehydrated by immersion in 70%, 80%, and 90% ethanol once for 15 min each and twice in 100% ethanol for 15 min. Next, samples were embedded in Epon resin. Ultrathin sections were obtained using an ultramicrotome with diamond knives (Leica Microsystems), and these sections had a thickness of 70 nm and were placed on a 200 mesh copper screen. The screens were counterstained with Reynold's lead citrate solution for 10 min. Images were obtained using a Tecnai G2-12-SpiritBiotwin FEI electron microscope (FEI Co., Eindhoven, Netherlands) at an acceleration voltage of 120 kV using a charge-coupled-device camera. In order to obtain the Megavirus caiporensis particle medium dimensions, the ImageJ software (version v1.53k, National Institutes of Health) was used to measure seven different particles during the acquisition of images. The measures were used to calculate the medium sizes of the particle and the fibrils.

Sequencing, assembly, and annotation. The samples containing purified virus were sequenced using the Illumina MiSeq system, with a paired-end library and an Illumina DNA Prep kit (Illumina Inc., San Diego, CA, USA). The FastQC program was used to quality control of the obtained reads, which were trimmed using the Trimmomatic tool (27). For genome *de novo* assembly, we used Spades 3.12 with default parameters (28), and the obtained scaffolds were ordered based on a reference genome using MeDuSa online (29). The reference genome used was that of Powai Lake megavirus, obtained from the NCBI database (GenBank accession number KU877344.1). The GeneMarkS tool (30) was used to predict ORFs, considering only proteins that were larger than 50 amino acids. Additionally, the predictions of tRNA coding sequences were performed using Aragorn (31). The predicted ORFs were annotated using BLASTp (expect threshold, 10^{-3}) against the NCBI non-redundant protein sequences (nr) database.

Phylogeny analysis. Phylogenetic trees were constructed employing IQtree software (version 1.6.12) using the maximum-likelihood statistic method, with 1,000 bootstrap replicates as branch support (32). The mimivirus subfamily B DNA polymerase and the gene sequences for proteins R135, L829, and L725 were used. The data sets containing the sequences used for alignments were prepared using BLASTp (expected threshold, 10^{-3}) against the NCBI non-redundant protein sequences (nr) database. The sequences selected were aligned by the Muscle algorithm executed by MEGAX (33, 34). The best-fit substitution models were selected by the ModelFinder algorithm implemented in IQtree (35), and the visualization and editing of the phylogenetic trees were carried out with MEGAX software and iTOL (34, 36).

Fibril morphology and density analysis. In order to analyze differences between the fibrils' morphology and density, we developed some specific protocols. To highlight the fibrils and their morphological differences, TEM images of three mimiviruses were used: APMV (representing lineage A), Borely moutouvirus (representing lineage B), and Megavirus caiporensis (the isolate described here, representing lineage C). First, fibrils were digitally highlighted with colors, emphasizing their peculiarities. For this, fibrils were marked with the aid of the "Marker" or "Watercolor" drawing tools of the Paint 3D (version 2021) program (Microsoft Corporation), with thickness settings between 2 and 4 pixels. Single colors were used for each mimivirus, with a maximum opacity of 35%, to highlight the fibrils with colors without losing their original shape.

For the density analysis, a protocol commonly used to measure the electrophoretic gel band densities was adapted (37). First, 70 TEM images for each one of the three mimiviruses representing lineages A, B, and C were individually highlighted with the tool "Scribble" of Microsoft PowerPoint version 2021 (Microsoft Corporation) very carefully (Fig. 3C, image I). Then, the background image was deleted, leaving only the outlines of the fibrils that were marked (Fig. 3C, image II). Those images were then used in the program ImageJ (version v1.53k, National Institutes of Health) to read the contrast and estimate the fibril densities for the 6 sides of each particle (previously selected, with many rectangles of same size), until the entire area presenting fibrils was fully covered by them (Fig. 3C, image III). After the selection of areas to be measured, the tool plot lanes were used to estimate the contrast from generated graphics (Fig. 3C, image IV). Each rectangle generated a graph with values related to the pixels detected in the analyzed images. These values were then used to interpret the mean contrast values for each of the six sides of the particles, and a total mean value was calculated, considering the standard deviation. The mean values were then normalized to be plotted in graph form (Fig. 3C, image V).

Evaluation of the relationship between fibrils and entry at the host cell. To assess whether the number of fibrils was associated with the success of mimiviruses to adhere and consequently penetrate the host amoebas, we performed *A. castellanii* amoeba infection assays. The same representatives of lineages A, B, and C used previously were used in this experiment. Cell culture flasks (25 cm²; Thermo Fisher Scientific, USA) containing 1×10^6 *A. castellanii* amoebas were infected with APMV, Borely moutouvirus, or Megavirus caiporensis at an MOI of 10. After infection, 30 min of adsorption was carried out at 30°C, with the flasks being gently shaken every 10 min to ensure that the inoculum covered the entire adhered cell monolayer. After adsorption, the inoculum was removed and the monolayer was

washed 2 times with PBS, followed by the addition of 5 mL PYG medium to loosen the monolayer and collect the contents of the flasks. We proceeded with sample preparation for TEM analysis as described above. During imaging, we randomly selected 50 amoebas for each of the samples and counted the number of particles found inside each of the cells, to later analyze and compare the results.

We also tested the inoculums of infections performed in 96-well plates containing 4×10^4 amoebas per well, with inoculums at an MOI of 10 using APMV, Borely moutouvirus, and Megavirus caiporensis. After 1 h of adsorption, the inoculums were collected and the viral titers were obtained by the endpoint method (26).

Data availability. The genome of Megavirus caiporensis is available at GenBank under accession number OP925046.

ACKNOWLEDGMENTS

We are grateful to our colleagues from Laboratório de Vírus and Microscopy Center, Universidade Federal de Minas Gerais, and Laboratório de Virologia, Universidade Estadual Paulista for their excellent technical support. In addition, we acknowledge the financial support from Conselho Nacional de Desenvolvimento Científico e Tecnológico (CNPq), Coordenação de Aperfeiçoamento de Pessoal de Nível Superior (CAPES), Fundação de Amparo à Pesquisa do estado de Minas Gerais (FAPEMIG), Ministério da Ciência, Tecnologia e Inovações (MCTI), and Pro-Reitorias de Pesquisa e Pós-Graduação of UFMG. J.S.A. and J.P.A. are CNPq researchers.

REFERENCES

- La Scola B, Audic S, Robert C, Jungang L, de Lamballerie X, Drancourt M, Birtles R, Claverie J-M, Raoult D. 2003. A giant virus in amoebae. *Science* 299:2033. <https://doi.org/10.1126/science.1081867>.
- Abrahão JS, Dornas FP, Silva LCF, Almeida GM, Boratto PVM, Colson P, La Scola B, Kroon EG. 2014. Acanthamoeba polyphaga mimivirus and other giant viruses: an open field to outstanding discoveries. *Virol J* 11:120. <https://doi.org/10.1186/1743-422X-11-120>.
- Villalta A, Schmitt A, Estrozi LF, Quemim ERJ, Alempic J-M, Lartigue A, Prazák V, Belmudes L, Vasishtan D, Colmant AMG, Honoré FA, Coute Y, Grünwald K, Abergel C. 2022. The giant mimivirus 1.2 Mb genome is elegantly organized into a 30 nm helical protein shield. *bioRxiv*. <https://doi.org/10.1101/2022.02.17.480895>.
- Klose T, Herbst D, Zhu H, Max J, Kenttämaa H, Rossmann M. 2015. A mimivirus enzyme that participates in viral entry. *Structure* 23:1058–1065. <https://doi.org/10.1016/j.str.2015.03.023>.
- Rodrigues RAL, dos Santos Silva LK, Dornas FP, de Oliveira DB, Magalhães TFF, Santos DA, Costa AO, de Macêdo Farias L, Magalhães PP, Bonjardim CA, Kroon EG, La Scola B, Cortines JR, Abrahão JS. 2015. Mimivirus fibrils are important for viral attachment to the microbial world by a diverse glycoside interaction repertoire. *J Virol* 89:11812–11819. <https://doi.org/10.1128/JVI.01976-15>.
- Xiao C, Kuznetsov YG, Sun S, Hafenstein SL, Kostyuchenko VA, Chipman PR, Suzan-Monti M, Raoult D, McPherson A, Rossmann MG. 2009. Structural studies of the giant mimivirus. *PLoS Biol* 7:e92. <https://doi.org/10.1371/journal.pbio.1000092>.
- Boyer M, Azza S, Barrassi L, Klose T, Campocasso A, Pagnier I, Fournous G, Borg A, Robert C, Zhang X, Desnues C, Henrissat B, Rossmann MG, La Scola B, Raoult D. 2011. Mimivirus shows dramatic genome reduction after intraamoebal culture. *Proc Natl Acad Sci U S A* 108:10296–10301. <https://doi.org/10.1073/pnas.1101118108>.
- Koonin EV, Dolja VV, Krupovic M, Varsani A, Wolf YI, Yutin N, Zerbini FM, Kuhn JH. 2020. Global organization and proposed megataxonomy of the virus world. *Microbiol Mol Biol Rev* 84:e00061-19. <https://doi.org/10.1128/MMBR.00061-19>.
- Palermo CN, Fulthorpe RR, Saati R, Short SM. 2019. Metagenomic analysis of virus diversity and relative abundance in a eutrophic freshwater harbour. *Viruses* 11:792. <https://doi.org/10.3390/v11090792>.
- Boratto PVM, Serafim MSM, Witt ASA, Crispim APC, de Azevedo BL, de Souza GAP, de Aquino ILM, Machado TB, Queiroz VF, Rodrigues RAL, Bergier I, Cortines JR, de Farias ST, dos Santos RN, Campos FS, Franco AC, Abrahão JS. 2022. A brief history of giant viruses' studies in Brazilian biomes. *Viruses* 14:191. <https://doi.org/10.3390/v14020191>.
- Colson P, de Lamballerie X, Fournous G, Raoult D. 2012. Reclassification of giant viruses composing a fourth domain of life in the new order Megavirales. *Intervirology* 55:321–332. <https://doi.org/10.1159/000336562>.
- Campos RK, Boratto PV, Assis FL, Aguiar ERGR, Silva LCF, Albarnaz JD, Dornas FP, Trindade GS, Ferreira PP, Marques JT, Robert C, Raoult D, Kroon EG, La Scola B, Abrahão JS. 2014. Samba virus: a novel mimivirus from a giant rain forest, the Brazilian Amazon. *Virol J* 11:95. <https://doi.org/10.1186/1743-422X-11-95>.
- Arslian D, Legendre M, Seltzer V, Abergel C, Claverie J-M. 2011. Distant Mimivirus relative with a larger genome highlights the fundamental features of Megaviridae. *Proc Natl Acad Sci U S A* 108:17486–17491. <https://doi.org/10.1073/pnas.1110889108>.
- Yoosuf N, Yutin N, Colson P, Shabalina SA, Pagnier I, Robert C, Azza S, Klose T, Wong J, Rossmann MG, La Scola B, Raoult D, Koonin EV. 2012. Related giant viruses in distant locations and different habitats: Acanthamoeba polyphaga moutouvirus represents a third lineage of the Mimiviridae that is close to the megavirus lineage. *Genome Biol Evol* 4:1324–1330. <https://doi.org/10.1093/gbe/evs109>.
- Andrade A, Rodrigues RAL, Oliveira GP, Andrade KR, Bonjardim CA, La Scola B, Kroon EG, Abrahão JS. 2017. Filling knowledge gaps for mimivirus entry, uncoating, and morphogenesis. *J Virol* 91:e01335-17. <https://doi.org/10.1128/JVI.01335-17>.
- Andrade KR, Boratto PVM, Rodrigues FP, Silva LCF, Dornas FP, Pilotto MR, La Scola B, Almeida GMF, Kroon EG, Abrahão JS. 2015. Oysters as hot spots for mimivirus isolation. *Arch Virol* 160:477–482. <https://doi.org/10.1007/s00705-014-2257-2>.
- Xiao C, Chipman PR, Battisti AJ, Bowman VD, Renesto P, Raoult D, Rossmann MG. 2005. Cryo-electron microscopy of the giant mimivirus. *J Mol Biol* 353:493–496. <https://doi.org/10.1016/j.jmb.2005.08.060>.
- Akashi M, Takemura M. 2019. Co-isolation and characterization of two pandoraviruses and a mimivirus from a riverbank in Japan. *Viruses* 11:1123. <https://doi.org/10.3390/v11121123>.
- Yoosuf N, Pagnier I, Fournous G, Robert C, La Scola B, Raoult D, Colson P. 2014. Complete genome sequence of Courdo11 virus, a member of the family Mimiviridae. *Virus Genes* 48:218–223. <https://doi.org/10.1007/s11262-013-1016-x>.
- Saadi H, Pagnier I, Colson P, Cherif JK, Beji M, Boughalmi M, Azza S, Armstrong N, Robert C, Fournous G, La Scola B, Raoult D. 2013. First isolation of Mimivirus in a patient with pneumonia. *Clin Infect Dis* 57:e127–e134. <https://doi.org/10.1093/cid/cit354>.
- Saadi H, Reteno D-GI, Colson P, Aherfi S, Minodier P, Pagnier I, Raoult D, La Scola B. 2013. Shan virus: a new mimivirus isolated from the stool of a Tunisian patient with pneumonia. *Intervirology* 56:424–429. <https://doi.org/10.1159/000354564>.
- Gaia M, Benamar S, Boughalmi M, Pagnier I, Croce O, Colson P, Raoult D, La Scola B. 2014. Zamilon, a novel virophage with Mimiviridae host specificity. *PLoS One* 9:e94923. <https://doi.org/10.1371/journal.pone.0094923>.
- Dornas FP, Khalil JYB, Pagnier I, Raoult D, Abrahão J, La Scola B. 2015. Isolation of new Brazilian giant viruses from environmental samples using a panel of protozoa. *Front Microbiol* 6:1086. <https://doi.org/10.3389/fmicb.2015.01086>.
- Andrade A, Arantes TS, Rodrigues RAL, Machado TB, Dornas FP, Landell MF, Furst C, Borges LGA, Dutra LAL, Almeida G, Trindade GdS, Bergier I,

- Abrahão W, Borges IA, Cortines JR, de Oliveira DB, Kroon EG, Abrahão JS. 2018. Ubiquitous giants: a plethora of giant viruses found in Brazil and Antarctica. *Virology* 15:22. <https://doi.org/10.1186/s12985-018-0930-x>.
25. Machado TB, de Aquino ILM, Abrahão JS. 2022. Isolation of giant viruses of *Acanthamoeba castellanii*. *Curr Protoc* 2:e455. <https://doi.org/10.1002/cpz1.455>.
 26. Reed LJ, Muench H. 1938. A simple method of estimating fifty per cent endpoints. *Am J Epidemiol* 27:493–497. <https://doi.org/10.1093/oxfordjournals.aje.a118408>.
 27. Bolger AM, Lohse M, Usadel B. 2014. Trimmomatic: a flexible trimmer for Illumina sequence data. *Bioinformatics* 30:2114–2120. <https://doi.org/10.1093/bioinformatics/btu170>.
 28. Prjibelski A, Antipov D, Meleshko D, Lapidus A, Korobeynikov A. 2020. Using SPAdes de novo assembler. *Curr Protoc Bioinformatics* 70:e102. <https://doi.org/10.1002/cpbi.102>.
 29. Bosi E, Donati B, Galardini M, Brunetti S, Sagot M-F, Lió P, Crescenzi P, Fani R, Fondi M. 2015. MeDuSa: a multi-draft based scaffold. *Bioinformatics* 31:2443–2451. <https://doi.org/10.1093/bioinformatics/btv171>.
 30. Besemer J, Borodovsky M. 2005. GeneMark: web software for gene finding in prokaryotes, eukaryotes and viruses. *Nucleic Acids Res* 33:W451–454. <https://doi.org/10.1093/nar/gki487>.
 31. Laslett D, Canback B. 2004. ARAGORN, a program to detect tRNA genes and tmRNA genes in nucleotide sequences. *Nucleic Acids Res* 32:11–16. <https://doi.org/10.1093/nar/gkh152>.
 32. Nguyen L-T, Schmidt HA, von Haeseler A, Minh BQ. 2015. IQ-TREE: a fast and effective stochastic algorithm for estimating maximum-likelihood phylogenies. *Mol Biol Evol* 32:268–274. <https://doi.org/10.1093/molbev/msu300>.
 33. Edgar RC. 2004. MUSCLE: multiple sequence alignment with high accuracy and high throughput. *Nucleic Acids Res* 32:1792–1797. <https://doi.org/10.1093/nar/gkh340>.
 34. Kumar S, Stecher G, Li M, Knyaz C, Tamura K. 2018. MEGA X: molecular evolutionary genetics analysis across computing platforms. *Mol Biol Evol* 35:1547–1549. <https://doi.org/10.1093/molbev/msy096>.
 35. Kalyaanamoorthy S, Minh BQ, Wong TKF, von Haeseler A, Jermiin LS. 2017. ModelFinder: fast model selection for accurate phylogenetic estimates. *Nat Methods* 14:587–589. <https://doi.org/10.1038/nmeth.4285>.
 36. Letunic I, Bork P. 2021. Interactive Tree Of Life (iTOL) v5: an online tool for phylogenetic tree display and annotation. *Nucleic Acids Res* 49:W293–W296. <https://doi.org/10.1093/nar/gkab301>.
 37. Gallagher SR. 2014. Digital image processing and analysis with ImageJ. *Curr Protoc Essential Lab Tech* 9:A.3C.1–A.3C.29. <https://doi.org/10.1002/9780470089941.eta03cs9>.

4.2 Artigo 2- Surface fibrils on the particles of nucleocyoviruses: A review

*Este artigo foi publicado no periódico **Experimental Biology and Medicine**.*

Após o estudo comparativo de fibrilas em mimivírus, decidimos expandir nossas análises para outros nucleocitovírus. O capsídeo tem um papel central no ciclo de vida dos vírus, desempenhando funções como proteger o genoma viral, bem como promover a interação com as células hospedeiras e desencadear a infecção. Considerando o cenário de múltiplas origens dos vírus ao longo da evolução viral, um número substancial de formas, tamanhos e simetrias de capsídeos foi descrito. Nesse contexto, as fibrilas de superfície encontradas no capsídeo de mimivírus, são uma das características mais intrigantes conhecidas da virosfera. São estruturas de 150 nm de comprimento ligadas a um capsídeo de 450 nm, resultando em uma grande partícula com aparência peluda. Fibrilas de superfície também foram descritas nos capsídeos de outros nucleocitovírus, embora possam diferir substancialmente entre eles. Nesta mini revisão para não especialistas, compilamos as informações mais importantes disponíveis sobre fibrilas de superfície de nucleocitovírus, discutindo suas supostas funções, composição, comprimento, organização e origens.

Minireview

Surface fibrils on the particles of nucleocytoviruses: A review

Isabella Luiza Martins de Aquino, Matheus Gomes Barcelos, Talita Bastos Machado, Mateus Sá Magalhães Serafim and Jônatas Santos Abrahão 

Laboratório de Vírus, Departamento de Microbiologia, Instituto de Ciências Biológicas, Universidade Federal de Minas Gerais, Belo Horizonte 31270-901, Brazil

Corresponding author: Jônatas Santos Abrahão. Email: jonatas.abrahao@gmail.com

Impact Statement

Considering the scenario of multiple origins of viruses along the viral evolution, many peculiar structural features have been reported and described for nucleocytoviruses. In this context, capsids of some of these so-called giant viruses (GV) are highlighted by surface fibrils, which are responsible for adhesion and interaction with their host membranes, such as those in amoeba. Knowing the singularities of these structures promotes the deepening of fundamental knowledge on the biology of these members within the virosphere, ultimately shedding light on their adaptive convergence in evolution, virus–host interactions, and their biological cycle, as well as possibilities for their proteins and viral assembly.

Abstract

The capsid has a central role in viruses' life cycle. Although one of its major functions is to protect the viral genome, the capsid may be composed of elements that, at some point, promote interaction with host cells and trigger infection. Considering the scenario of multiple origins of viruses along the viral evolution, a substantial number of capsid shapes, sizes, and symmetries have been described. In this context, capsids of giant viruses (GV) that infect protists have drawn the attention of the scientific community, especially in the last 20 years, specifically for having bacterial-like dimensions with hundreds of different proteins and exclusive features. For instance, the surface fibrils present on the mimivirus capsid are one of the most intriguing features of the known virosphere. They are 150-nm-long structures attached to a 450-nm capsid, resulting in a particle with a hairy appearance. Surface fibrils have also been described in the capsids of other nucleocytoviruses, although they may differ substantially among them. In this mini review for non-experts, we compile the most important available information on surface fibrils of nucleocytoviruses, discussing their putative functions, composition, length, organization, and origins.

Keywords: Adhesion, fibrils, giant viruses, virus structure

Experimental Biology and Medicine 2023; 248: 2045–2052. DOI: 10.1177/15353702231208410

Introduction

A glimmer of microbial evolution: giants among viruses

The term “giant viruses” has been used to designate a putative monophyletic group of viruses belonging to the phylum Nucleocytoviricota, infecting uni- and pluricellular, hetero- and autotrophic organisms, from protists to animals.¹ Some authors consider bona-fide giant viruses those with capsids larger than 500 nm, which are easily visible by optical microscopy. However, the term “giant viruses” has also been used to refer to smaller nucleocytoviruses, with particles ranging from 150 to 500 nm. Giant viruses are ubiquitous and have already been isolated from different countries,^{2–5} from different environmental^{6,7} and clinical samples.⁸ The first virus to be called a giant virus was *Paramecium bursaria chlorella virus 1* (PBCV-1), which infects algae and which has particles up to approximately 190 nm in diameter,⁹ and a dsDNA genome of approximately 330 kb.¹⁰

Although nucleocytoviruses include historically important representatives, such as poxviruses,¹¹ the discovery of mimivirus in 2003¹² highlighted the remarkable structural complexity of the virions of this group.

Among mimiviruses, the *Acanthamoeba polyphaga* mimivirus (APMV)¹² isolate was the first amoebae-associated GV to be described. APMV was isolated from water samples collected from a hospital cooling tower during a pneumonia outbreak in Bradford, England. After analyzing these samples by Gram stain, researchers noticed small purple-stained dots inside amoebae, similar to gram-positive bacteria. However, after the failure of several techniques used in the identification and characterization of bacteria, questions about the nature of these organisms remained for years. After almost a decade, new techniques were used to study the mysterious microorganism, such as genome sequencing and electron microscopy, which led to the surprising discovery of an actual virus, and not bacteria.¹² This virus attracted the attention of the scientific community due to

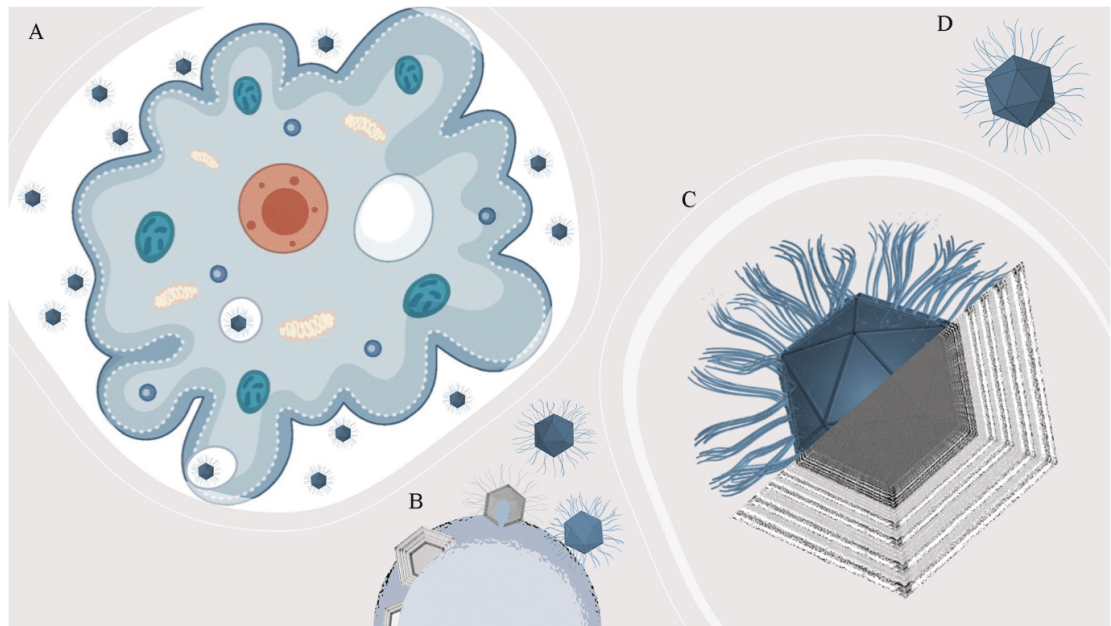


Figure 1. Fibrils' role for giant viruses. (A) Fibrils (~150 nm) are important to the adhesion of mimiviruses onto amoebas, such as APMV. (B) During the morphogenesis, fibrils seem to be acquired in the fibril acquisition area, located at the periphery of the viral factory, concomitantly with the genome acquisition. (C) Fibrils' peptidoglycan-like structures exhibit successive rings of density under electronic microscopy. (D) Schematic representation of a mature APMV particle. Amoeba image was generated from free vectors available at Vecteezy (<https://www.vecteezy.com>).

the large size of its particle and its genome. The APMV particle is approximately 750 nm in diameter, and its genome reaches the million mark, about 1.2 megabases (Mb). Since then, several other amoeba GV groups have been discovered, such as marseillevirus,¹³ pandoravirus,¹⁴ pithovirus,¹⁵ and cedratvirus,¹⁶ among others.

There is great diversity within giant viruses, considering their morphological characteristics. In general, the capsids of giant viruses do not present an external envelope. Instead, the capsids surround an inner lipid sac, which contains the viral genome and proteins related to the early phases of the replication cycle. Particles can have icosahedral symmetry (e.g. marseillevirus¹³ and faustovirus¹⁷), or pseudoicosahedral symmetry, as in mimiviruses, due to the presence of a stargate, that is, a vertex at the capsid that allows for DNA release.¹⁸ They may also be oval (e.g. pithovirus¹⁵ and pandoravirus¹⁴) or even round-shaped (e.g. mollivirus⁴). For instance, one of the largest viruses ever described, Tupanvirus, has a capsid attached to a tail variable in size, allowing the particle to reach up to 2.3 μm .¹⁹ In some GV, we can find some structures decorating their capsids, such as the spherical-headed spikes that cover medusaviruses' surfaces and mimiviruses' fibrils.²⁰

Viral fibrils: an intriguing structural feature among giants

As aforementioned, mimiviruses exhibit particles with a capsid of approximately 750 nm, being 450 nm in diameter and covered by a dense layer of fibrils (~150 nm),²¹ which were

suggested to resemble gram-positive bacteria.¹² This intriguing misunderstanding would be feasible due to its structural fibrils' composition, which is morphologically unique among these viruses,²² and not being fully elucidated yet,²³ with all that is currently known being related to mimiviruses. The fibrils are embedded in a dense layer of peptidoglycan-like structures²⁴ that stain crystal violet in a Gram stain, as those peptidoglycans that are present in the walls of gram-positive bacteria.²⁵ Important to the adhesion onto the amoeba surface (Figure 1(A)), as for APMV, fibrils are often found with one of their ends free while the other end is attached to the viral capsid.²⁶ Moreover, scanning electron microscopy (SEM) and transmission electron microscopy (TEM) analyses have shown different densities of fibrils on GV capsid surfaces, which are simultaneously acquired with the genome acquisition during morphogenesis in the fibril acquisition area, located at the periphery of the viral factories²⁷ (Figure 1(B)). In addition, fibrils' peptidoglycan-like structures exhibit successive so-called rings of density (Figure 1(C)), which supports their key role in viral entry,²⁶ as exemplified for APMV (Figure 1(D)).

Many GV also present fibrils (Figure 2) as APMV, such as: (1) tupanviruses, with a capsid of approximately 450 nm in diameter and a tail attached to it, both covered in fibrils, resulting in particles varying from 1.2 up to 2.3 μm in length;¹⁹ (2) *Cotonvirus japonicus*,²⁸ a mimivirus isolate, with approximately 400 nm in diameter and also surrounded by surface fibrils of approximately 100 nm; (3) Marseillevirus,¹³ with approximately 250 nm of diameter, and 12 nm fibrils surrounding its particles' surface; (4) PBCV-1, an algae

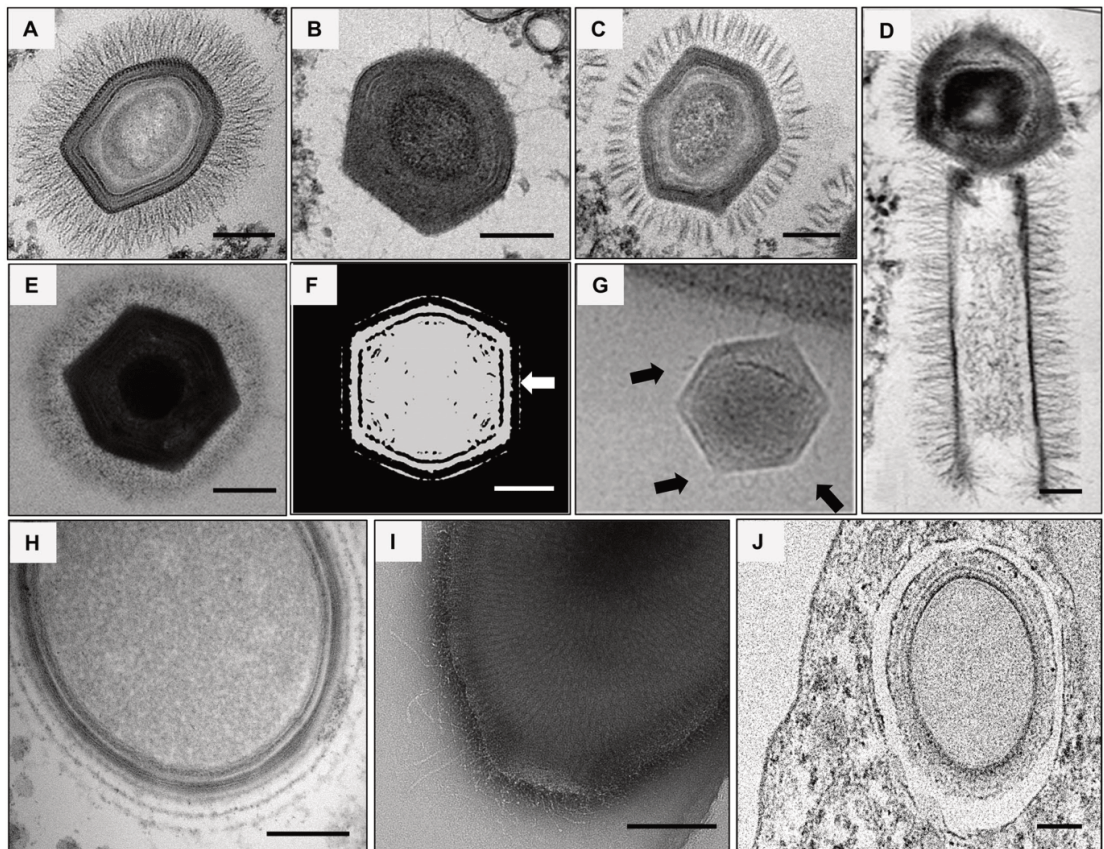


Figure 2. Giant viruses that possess surface fibrils. Electron microscopy images and shaded-surface representation of different GV isolates and their fibrils. (A–C) Lineage A, B, and C mimiviruses: mimivirus puntaullmanensis, momouvirus crenensis, and megavirus caiporensis, respectively. (D) Tupanvirus particle, with its tail, a trademark of this group (adapted from DOI: 10.1038/s41467-018-03168-1). (E) *Cotonivirus japonicus* (adapted from DOI: 10.1128/JVI.00919-21). (F) Marseillevirus shaded representation illustrating the globular portions of its fibrils indicated by the white arrow (adapted from DOI: 10.1038/s41467-018-03168-1). (G) PBCV-1 (adapted from DOI: 10.1073/pnas.1107847108) fibrils are pointed by the black arrows. (H) *Mollivirus sibericum* (credits: provided by Dr Chantal Abergel, IGS UMR7256 CNRS-AMU). (I) *Cedratvirus pambiensis*. (J) Orpheovirus IHUMI-LCC2. Scale bars: 150 nm.

infecting virus with approximately 190 nm in length and small fibrils around the capsid, of nearly 19 nm;⁹ (5) orpheovirus, with particles larger in length than APMV (up to 1.1 μm), but presenting smaller fibrils when compared to these mimiviruses, as well as two tegument layers between the fibrils and the inner membrane;²⁹ (6) *Mollivirus sibericum*,⁴ an almost spherical GV with 500–600 nm in diameter and surrounded by a fibrillar tegument as a mesh of fibrils; (7) cedratviruses, around 500 nm up to 1 μm in length,^{16,30} whose viral factory can be divided in two, one being associated with its fibrils acquisition; and finally (8) *Yasminevirus*,³¹ the first *Klosneuvirus* to be isolated and that presents a particle with approximately 330 nm covered by a thin layer of fibrils.

For instance, Notaro *et al.* demonstrated that fibrils are glycosylated with two different polysaccharides in their composition, whose structures have been elucidated by nuclear magnetic resonance (NMR) analysis, one being L-rhamnose and N-acetylglucosamine (GlcNAc) arranged in a linear repeating pattern, and the other as a branched

repeating unit. Chemical analysis of the monosaccharide composition as acetylated O-methyl glycosides confirmed L-rhamnose (L-Rha), GlcNAc, and 2-O-methyl-4N-acetyl-viosamine (2OMeVio4Nac), including minor amounts of non-methylated Vio4Nac, mannose, and glucose. In addition, glycan-like, or containing, molecules were also a fraction (13.7%) of the structure, showing the influence of the protease digestion protocols in removing protein fractions of the fibrils.³² The glycan composition in fibrils would be related to their binding to host cells, mediating their interactions with hosts' surface glycans (e.g. mannose and GlcNAc), triggering phagocytosis,²⁴ whereas fibrils' peptide fractions are suggested to be putatively more associated with the 2-glucose-methanol-choline (GMC) oxidoreductase's structural composition and assembly.²³

Notaro *et al.* also showed rare amino-acid sugars to be synthesized from different GV of the subfamily Megamimivirinae, which are absent from their hosts and usually found only in bacteria: (1) D-viosamine and rhamnose in

the A-clade; (2) D-Qui2NAc and D-Fuc2NAc in the B-clade; (3) L-RhaNAc and L-Qui2NAc in the C-clade; and (4) bacillosamine (D-diNAcBac) observed only in a few GV so far (*Moumouvirus australiensis*, *Cotonvirus japonicus*, and tupanviruses). Thus, this varied set of glycans decorating capsids could also support the discussion that these structures could mimic bacteria that amoeba feed on, facilitating competition among different organisms and different GV competing for the same host. In addition, differences in sugar compositions and biosynthetic pathways for nucleotide sugars and glycosyltransferases were shown to be related to complex gene clusters (e.g. 6 and up to 33 genes), which are involved in the glycosylation of fibril layers among the subfamily Megamimivirinae and were also shown to be clade-specific.³³

Harboring giants' structural repertoire: genes associated with fibrils

Initially, it was speculated that the mimiviruses' hairy-like appearance could be related to the large number of open reading frame exhibiting the characteristic collagen triple-helix repeat. Thus, fibrils could be linked to collagen and glycosylated proteins, consisting of cross-linked glycosylated collagen.³⁴ However, the fibrils are resistant to collagenases, even after pre-treatment with lysozyme, suggesting that the fibril surfaces are not collagen-linked.³⁵ For instance, the L829 and L725 genes, which codify proteins with unknown functions, and the R135 gene, which codifies a putative GMC-oxidoreductase, were also associated with mimivirus fibrils in previous works.^{36,37} Boyer *et al.* obtained an artificial mimivirus strain called M4 after several blind passages of APMV in axenic amoebae culture. M4 has a reduction of ~200,000 bp in its genome, and its particles have a bald appearance with fewer fibrils. After analysis of purified viral fibers by 2D gel electrophoresis coupled with matrix-assisted laser desorption/ionization mass spectrometry, it was reported that there was an absence of R135, L829, and L725 proteins in M4 particles when compared to the original mimivirus M1. They also compared the protein glycosylation patterns in the M1 and M4 viruses and observed that L829 and R135 proteins were glycosylated only in M1.³⁶ Furthermore, L725, which is encoded by an ORFan gene, that is, genes with no detectable sequence similarities in databases,³⁸ was suggested to be associated with fibrils by RNA silencing experiments.³⁹

In this sense, the R135 protein, APMV's putative GMC-oxidoreductase, was pointed to be part of the fibrils composition and of the helical protein shell that encases mimivirus genomic material by cryo-electron microscopy, cryo-electron tomography, and proteomics,^{32,37} with the only difference between the fibrils and the genomic fiber composition being the presence of a Cys-Pro rich N-terminal domain only in the fibrils. In addition, Aquino *et al.* also discussed those genes in contrast to their previous functionalities or relationships with fibrils, as isolates with fewer fibrils (e.g. Borely moumouvirus) are morphologically similar to mimivirus M4 and present R135 and L829 genes in their genomes.⁴⁰ Interestingly, these three predicted proteins can also be found only in some GV that have fibrils when analyzing search results using the BLASTp tool⁴¹ (Table 1) from the National Center for Biotechnology Information (NCBI). Herein, the

best hits were found for all the proteins among mimiviruses from lineages A, B, and C, and for *Cotonvirus japonicus*, even though lineage B mimiviruses are almost fiberless. As for tupanviruses, a best hit for R135 was not found, and only a best hit for L829 was found for molliviruses, marseillevirus, and cedratvirus. No best hits were found for any of the proteins in PBCV-1 or yasminevirus, which also raises questions about the relationship of these proteins with GV's fibrils. Furthermore, it is also important to highlight that the best hits were also found for R135 and L829 in viruses that do not have surface fibrils described as part of their particles, like pandoravirus and Pithovirus.⁴⁰

Viral attachment: depicting the role of fibrils

Considered intriguing structural features of viruses' morphology until then, fibrils stood out in early studies, and their function remained unknown for more than 10 years after the discovery of APMV. As mentioned, it was described that they play an important role in triggering the host amoeba's phagocytosis by promoting the adhesion of viral particles to the cell surface, mediated by glycans.²⁴ Interestingly, in the presence of high concentrations of certain glycans (e.g. GlcNAc), interaction of the viral particles with other molecules would be prevented, due to the fibrils being saturated by a given carbohydrate. In addition, a smaller number of fibrils does not alter APMV replication but decreases its attachment to *Acanthamoeba castellanii* cells.²⁴

Rodrigues *et al.* treated APMV particles with different enzymatic conditions, such as lysozyme and lysozyme followed by bromelain and proteinase K, both in comparison to APMV and the M4 mimivirus. Interestingly, the presence of more fibrils leads to an increase in viral attachment to the amoebal surface when mediated by mannose and GlcNAc, no changes in viral titers were observed in the presence of glucose or *N*-acetylgalactosamine (GalNAc) at any of the concentrations assessed. The presence of mannose and GlcNAc at different concentrations (>50 and >25 µg/mL, respectively) reduced the viral titer up to 1000-fold. In addition, APMV fibrils also attach differentially to distinct organisms or structures by their glycoside interactions, such as *Aedes sp. legs* (i.e. chitin), *Aspergillus fumigatus* (i.e. mannose and chitin), *Staphylococcus aureus* and *Escherichia coli* (i.e. peptidoglycan), resulting in 18-fold, 7.32-fold, and no differences of the viral particles compared with the control, respectively. Finally, particles were saturated with chitin and peptidoglycan, and the presence of both polymers interfered with APMV adhesion to *A. castellanii* cells, with up to a 100-fold reduction in viral titer at concentrations >25 and >75 µg/mL, respectively.²⁴

These results could suggest that the peptidoglycan-like fraction of fibrils would also be restricted to interactions with *Acanthamoeba* cellular plasma membranes,⁴² which are rich in lipophosphoglycan,⁴³ as well as potentially guaranteeing their host specificity. Furthermore, other functions have been suggested for fibrils, such as: (1) optimizing phagocytosis by expanding particle size;⁴⁴ (2) stimulating phagocytosis in amoeba by partially mimicking bacteria with peptidoglycan-like compounds, which are "food" of amoebae;⁴⁵ (3) acting as a natural decoy for hosts; and (4) increasing resistance under

Table 1. BLASTp best hits for the three genes associated with fibrils: L725, L829, and R135.

Virus	Gene			L829			R135		
	Accession number	Size (aa)	Function	Accession number	Size (aa)	Function	Accession number	Size (aa)	Function
APMV	YP_003987254.1	224	Hypothetical protein	YP_003987362.1	433	Hypothetical protein	YP_003986627.1	720	GMC oxidoreductase
Borely moutouvirus	QID05925.1	223	Hypothetical protein	QID05994.1	395	Hypothetical protein	QID06495.1	661	Choline dehydrogenase-like protein
Megavirus caiporensis	WBF70980.1	225	Hypothetical protein	WBF70952.1	663	Hypothetical protein	WBF70396.1	663	Hypothetical protein
Cotonvirus japonicus	BCS82919.1	225	Hypothetical protein	BCS83575.1	387	Hypothetical protein	BCS83533.1	672	GMC oxidoreductase
Tupanvirus deep ocean	QKU34617.1	238	Hypothetical protein	QKU34326.1	432	Hypothetical protein	-	-	-
Tupanvirus soda lake	QKU35955.1	238	Hypothetical protein	QKU35587.1	432	Hypothetical protein	-	-	-
<i>Mollivirus sibiricum</i>	-	-	-	YP_009165460.1	348	Hypothetical protein	-	-	-
<i>Mollivirus kamchatka</i>	-	-	-	QHN71453.1	418	Hypothetical protein	-	-	-
Orpheovirus	-	-	-	YP_009449253.1	507	Hypothetical protein	YP_009448335.1	546	GMC oxidoreductase
<i>Cedratvirus kamchatka</i>	-	-	-	QIN54245.1	378	Hypothetical protein	-	-	-
<i>Marsellevirus marsellevirus</i>	-	-	-	YP_003406851.1	400	Hypothetical protein	-	-	-
<i>Yasminevirus</i>	-	-	-	-	-	-	-	-	-
PBCV-1	-	-	-	-	-	-	-	-	-

aa: amino acid; APMV: Acanthamoeba polyphaga mimivirus; BLAST: basic local alignment search tool; BLASTp: Protein BLAST; GMC: glucose-methanol-choline; PBCV-1: Paramoecium bursaria chlorella virus 1.

adverse conditions, but more studies remain necessary²⁶ to better understand those propositions.

Uniqueness of an intriguing structure: diversity in surface fibrils pattern

A first glimpse of fibril-like structures was observed with SEM and TEM methods for chloroviruses termed “fibers” at the time.⁴⁶ Subsequent structural²⁶ studies of amoeba GV, such as mimiviruses, helped in the discovery of other GV²² and their fibrils. As fibrils of mimiviruses are polysaccharide-containing structures likely built from their glycosylation machinery, which decorates the capsid as surrounding structures,¹¹ one could argue what the disposition, organization, and composition of different GV’s fibrils would impact their biological cycle and even host specificities. Cultivation-independent approaches (e.g. metagenomics) have enhanced the discovery of new genome sequences of potentially new GV, with the potential for structural and functional diversity of fibrils. Although there are some similarities in how these viruses enter host cells (e.g. fibrils triggering phagocytosis), much is yet to be found about GV and their fibrils, as they can be found nearly anywhere on Earth, and only a small fraction of GV’s genomes have been discovered so far.^{11,47} In this sense, experimental characterization and validation, as demonstrated by Aquino *et al.*, help unravel these differences among different GV’s fibrils. Authors showed that mimiviruses from lineages A (e.g. APMV), B (e.g. Borely moutouvirus), and C (e.g. Megavirus caiporensis) present differences regarding their surface fibrils organization and disposition. SEM and TEM allowed authors to observe that fibrils are (1) long and abundantly surrounding the capsid; (2) fewer in number and less homogeneously distributed; or (3) similarly abundant to the first, but organized in small groups (i.e. clusters or clumps).⁴⁰

For instance, APMV fibrils are homogeneously distributed, whereas Megavirus caiporensis appears in clumps or clusters. Both were estimated for their relative abundance of surface fibrils, whereas Megavirus caiporensis exhibited a 552-fold relative average contrast increase when compared to Borely moutouvirus, in comparison to a 394-fold increase for APMV. In addition, different combinations of the three mimiviruses mixed with purified particles were also compared by TEM, disregarding a potential SEM preparation influencing fibrils appearance and conformation. In addition, adhesion and entry into *A. castellanii* were also quantitatively assessed at a multiplicity of infection (MOI) of 10, showing that APMV and Megavirus caiporensis particles bind to the host plasma membrane approximately 10 times more than Borely moutouvirus after 1h post infection. Finally, more APMV-infected cells were observed (43/50), followed by Megavirus caiporensis (16/50), and Borely moutouvirus (4/50), both under the same experimental conditions.⁴⁰ These results could suggest that the pattern of fibrils may also affect adhesion and their incorporation by amoebas.

Notwithstanding, other GV surface fibrils present some characteristics that distinguish them structurally from those of mimiviruses, such as *Cotonvirus japonicus*,²⁸ which has denser and shorter fibrils in its surface when observed by TEM analysis, which revealed a smoother arrangement

when compared, for example, to lineage A mimiviruses’ particles. As aforementioned, artifacts caused by preparation procedures cannot be excluded, but these structural disposition and size variations are also observed for orpheoviruses, which have larger particles than other mimiviruses (e.g. APMV) but present shorter fibrils.²⁹ In PBCV-1, its external fibrils extend from some of its capsomers and potentially facilitate particle attachment to algae hosts,⁴⁸ similar to the mimiviruses’ mechanism initiating viral infection by attaching to these hosts’ cell walls.

Current knowledge about fibrils: issues and needed studies

The absence of a three-dimensional (3D) solved fibril structure is still a limiting factor for further structural studies, including its binding mechanism onto host membranes during viral entry. Expression, purification, and obtaining crystallized or cryo-EM structures would help in predicting and performing subsequent binding or enzymatic assays. For instance, near-atomic resolution structures of different nucleocytoviruses,^{49,50} yet one of the largest groups of viruses that infect eukaryotic hosts, could also help unravel possibilities for their proteins and assembly,⁵⁰ such as fibrils structural organization.

Moreover, in-depth studies about genes that have already been related to mimivirus fibrils³⁶ are also needed, as is the expansion in search of new genes, both in mimivirus and in other GV with fibrils, which remains a field to be explored. In addition, much of the existing information about these structures was obtained using mimiviruses as a study model, and it would be interesting if new studies with other giant viruses were carried out with the purpose of raising more data and knowledge about the possible diversity of fibrils. In this sense, it was shown that Megavirus chilensis has a gene cluster responsible for producing glycosylated proteins that can be associated with fibrils, and that this profile is shared with several other megaviruses,⁵¹ still in need of more studies. Furthermore, if we consider L725, L829, and R135 as fibril-associated proteins,^{32,36,37,39} the absence of them in some GV that presents fibrils (Table 1) could mean that other genes are responsible for the formation of fibrils in other species of nucleocytoviruses, and it is important to consider that perhaps this characteristic is an adaptive convergence in the evolution of GV.

AUTHORS’ CONTRIBUTIONS

ILMda, MGB, TBM, MSMS, and JSA wrote the review.

DECLARATION OF CONFLICTING INTERESTS

The author(s) declared no potential conflicts of interest with respect to the research, authorship, and/or publication of this article.

FUNDING

The author(s) disclosed receipt of the following financial support for the research, authorship, and/or publication of this article: This work was supported by Conselho Nacional de Desenvolvimento Científico e Tecnológico (grant number 303680/2022-9); Coordenação de Aperfeiçoamento

de Pessoal de Nível Superior/Ministério da Saúde (grant numbers 88882.348380/2010-1, 88887.595578/2020-00, and 88887.684031/2022-00); Fundação de Amparo à Pesquisa do Estado de Minas Gerais (PPM-00732-18); Pró-Reitoria de Pesquisa e de Pós-Graduação from Universidade Federal de Minas Gerais (04/2022); and Centro de Microscopia from Universidade Federal de Minas Gerais (1099). JSA is a Conselho Nacional de Desenvolvimento Científico e Tecnológico researcher (303680/2022-9).

ORCID ID

Jônatas Santos Abrahão  <https://orcid.org/0000-0001-9420-1791>

REFERENCES

- Koonin EV, Yutin N. Origin and evolution of eukaryotic large nucleocytoplasmic DNA viruses. *Intervirology* 2010;**53**:284–92
- Arslan D, Legendre M, Seltzer V, Abergel C, Claverie J-M. Distant mimivirus relative with a larger genome highlights the fundamental features of Megaviridae. *Proc Natl Acad Sci* 2011;**108**:17486–91
- Campos RK, Boratto PV, Assis FL, Aguiar ER, Silva LC, Albarnaz JD, Dornas FP, Trindade GS, Ferreira PP, Marques JT, Robert C, Raoult D, Kroon EG, La Scola B, Abrahão JS. Samba virus: a novel mimivirus from a giant rain forest, the Brazilian Amazon. *Virology* 2014;**461**:95
- Legendre M, Lartigue A, Bertaux L, Jeudy S, Bartoli J, Lescot M, Alempic J-M, Ramus C, Bruley C, Labadie K, Shmakova L, Rivkina E, Couté Y, Abergel C, Claverie J-M. In-depth study of *Mollivirus sibiricum*, a new 30,000-y-old giant virus infecting *Acanthamoeba*. *PNAS* 2015;**112**:E5327–35
- Bajrai LH, Benamar S, Azhar EI, Robert C, Levasseur A, Raoult D, La Scola B. Kaumobavirus, a new virus that clusters with faustoviruses and Asfarviridae. *Viruses* 2016;**8**:278
- Andrade ACDSP, Arantes TS, Rodrigues RAL, Machado TB, Dornas FP, Landell MF, Furst C, Borges LGA, Dutra LAL, Almeida G, Trindade GDS, Bergier I, Abrahão W, Borges IA, Cortines JR, de Oliveira DB, Kroon EG, Abrahão JS. Ubiquitous giants: a plethora of giant viruses found in Brazil and Antarctica. *Virology* 2018;**515**:22
- Boratto PVM, Serafim MSM, Witt ASA, Crispim APC, Azevedo BL, Souza GAP, Aquino ILM, Machado TB, Queiroz VF, Rodrigues RAL, Bergier I, Cortines JR, Farias ST, Santos RND, Campos FS, Franco AC, Abrahão JS. A brief history of giant viruses' studies in Brazilian biomes. *Viruses* 2022;**14**:191
- Scheid P, Balczun C, Schaub GA. Some secrets are revealed: parasitic keratitis amoebae as vectors of the scarcely described pandoraviruses to humans. *Parasitol Res* 2014;**113**:3759–64
- Zhang X, Xiang Y, Dunigan DD, Klose T, Chipman PR, Van Etten JL, Rossmann MG. Three-dimensional structure and function of the Paramecium bursaria chlorella virus capsid. *Proc Natl Acad Sci* 2011;**108**:14837–42
- Yamada T, Onimatsu H, Van Etten JL. Chlorella viruses. *Adv Virus Res* 2006;**66**:293–336
- Schulz F, Abergel C, Woyke T. Giant virus biology and diversity in the era of genome-resolved metagenomics. *Nat Rev Microbiol* 2022;**20**:721–36
- Scola BL, Audic S, Robert C, Jungang L, de Lamballerie X, Drancourt M, Birtles R, Claverie J-M, Raoult D. A giant virus in amoebae. *Science* 2003;**299**:2033
- Boyer M, Yutin N, Pagnier I, Barrassi L, Fournous G, Espinosa L, Robert C, Azza S, Sun S, Rossmann MG, Suzan-Monti M, La Scola B, Koonin EV, Raoult D. Giant Marseillevirus highlights the role of amoebae as a melting pot in emergence of chimeric microorganisms. *Proc Natl Acad Sci* 2009;**106**:21848–53
- Philippe N, Legendre M, Doutre G, Couté Y, Poirot O, Lescot M, Arslan D, Seltzer V, Bertaux L, Bruley C, Garin J, Claverie J-M, Abergel C. Pandoraviruses: amoeba viruses with genomes up to 2.5 Mb reaching that of parasitic eukaryotes. *Science* 2013;**341**:281–6
- Legendre M, Bartoli J, Shmakova L, Jeudy S, Labadie K, Adrait A, Lescot M, Poirot O, Bertaux L, Bruley C, Couté Y, Rivkina E, Abergel C, Claverie J-M. Thirty-thousand-year-old distant relative of giant icosahedral DNA viruses with a pandoravirus morphology. *Proc Natl Acad Sci* 2014;**111**:4274–9
- Andreani J, Aherfi S, Bou Khalil JY, Di Pinto F, Bitam I, Raoult D, Colson P, La Scola B. Cedratvirus, a double-cork structured giant virus, is a distant relative of pithoviruses. *Viruses* 2016;**8**:300
- Reteno DG, Benamar S, Khalil JB, Andreani J, Armstrong N, Klose T, Rossmann M, Colson P, Raoult D, La Scola B. Faustovirus, an asfarvirus-related new lineage of giant viruses infecting amoebae. *J Virol* 2015;**89**:6585–94
- Zauberman N, Mutsafi Y, Halevy DB, Shimoni E, Klein E, Xiao C, Sun S, Minsky A. Distinct DNA exit and packaging portals in the virus *Acanthamoeba polyphaga mimivirus*. *PLoS Biol* 2008;**6**:e114
- Abrahão J, Silva L, Silva LS, Khalil JYB, Rodrigues R, Arantes T, Assis F, Boratto P, Andrade M, Kroon EG, Ribeiro B, Bergier I, Seligmann H, Ghigo E, Colson P, Levasseur A, Kroemer G, Raoult D, La Scola B. Tailed giant Tupanvirus possesses the most complete translational apparatus of the known virosphere. *Nat Commun* 2018;**9**:749
- Colson P, Ominami Y, Hisada A, La Scola B, Raoult D. Giant mimiviruses escape many canonical criteria of the virus definition. *Clin Microbiol Infect* 2019;**25**:147–54
- Abrahão JS, Dornas FP, Silva LC, Almeida GM, Boratto PV, Colson P, La Scola B, Kroon EG. *Acanthamoeba polyphaga mimivirus* and other giant viruses: an open field to outstanding discoveries. *Virology* 2014;**461**:120
- Colson P, La Scola B, Levasseur A, Caetano-Anollés G, Raoult D. Mimivirus: leading the way in the discovery of giant viruses of amoebae. *Nat Rev Microbiol* 2017;**15**:243–54
- Klose T, Herbst DA, Zhu H, Max JP, Kenttämäa HI, Rossmann MG. A mimivirus enzyme that participates in viral entry. *Structure* 2015;**23**:1058–65
- Rodrigues RA, dos Santos Silva LK, Dornas FP, de Oliveira DB, Magalhães TF, Santos DA, Costa AO, de Macêdo Farias L, Magalhães PP, Bonjardim CA, Kroon EG, La Scola B, Cortines JR, Abrahão JS. Mimivirus fibrils are important for viral attachment to the microbial world by a diverse glycoside interaction repertoire. *J Virol* 2015;**89**:11812–9
- Budin G, Chung HJ, Lee H, Weissleder R. A magnetic gram stain for bacterial detection. *Angew Chem Int Ed* 2012;**51**:7752–5
- Xiao C, Kuznetsov YG, Sun S, Hafenstein SL, Kostyuchenko VA, Chipman PR, Suzan-Monti M, Raoult D, McPherson A, Rossmann MG. Structural studies of the giant mimivirus. *PLoS Biol* 2009;**7**:e1000092
- Andrade ACDSP, Rodrigues RAL, Oliveira GP, Andrade KR, Bonjardim CA, La Scola B, Kroon EG, Abrahão JS. Filling knowledge gaps for mimivirus entry, uncoating, and morphogenesis. *J Virol* 2017;**91**:e01335–10117
- Takahashi H, Fukaya S, Song C, Murata K, Takemura M. Morphological and taxonomic properties of the newly isolated Cotonvirus japonicus, a new lineage of the subfamily Megavirinae. *J Virol* 2021;**95**:e0091921
- Andreani J, Khalil JYB, Baptiste E, Hasni I, Michelle C, Raoult D, Levasseur A, La Scola B. Orpheovirus IHUMI-LCC2: a new virus among the giant viruses. *Front Microbiol* 2018;**8**:2643
- Silva LK, dos S, Andrade AC, dos SP, Dornas FP, Rodrigues RAL, Arantes T, Kroon EG, Bonjardim CA, Abrahão JS. Cedratvirus getuliensis replication cycle: an in-depth morphological analysis. *Sci Rep* 2018;**8**:4000
- Bajrai LH, Mougari S, Andreani J, Baptiste E, Delerce J, Raoult D, Azhar EI, La Scola B, Levasseur A. Isolation of Yasminevirus, the first member of Klosneuvirinae isolated in coculture with *Vermamoeba vermiformis*, demonstrates an extended arsenal of translational apparatus components. *J Virol* 2019;**94**:e01534–10119
- Notaro A, Couté Y, Belmudes L, Laugier ME, Salis A, Damonte G, Molinaro A, Tonetti MG, Abergel C, De Castro C. Expanding the occurrence of polysaccharides to the viral world: the case of mimivirus. *Angew Chem Int Ed* 2021;**60**:19897–904
- Notaro A, Poirot O, Garcin ED, Nin S, Molinaro A, Tonetti M, De Castro C, Abergel C. Giant viruses of the Megavirinae subfamily possess

- biosynthetic pathways to produce rare bacterial-like sugars in a clade-specific manner. *MicroLife* 2022;**3**:uqac002
34. Raoult D, Audic S, Robert C, Abergel C, Renesto P, Ogata H, La Scola B, Suzan M, Claverie J-M. The 1.2-megabase genome sequence of mimivirus. *Science* 2004;**306**:1344–50
 35. Klose T, Kuznetsov YG, Xiao C, Sun S, McPherson A, Rossmann MG. The three-dimensional structure of mimivirus. *Intervirology* 2010;**53**:268–73
 36. Boyer M, Azza S, Barrassi L, Klose T, Campocasso A, Pagnier I, Fournous G, Borg A, Robert C, Zhang X, Desnues C, Henrissat B, Rossmann MG, La Scola B, Raoult D. Mimivirus shows dramatic genome reduction after intraamoebal culture. *Proc Natl Acad Sci* 2011;**108**:10296–301
 37. Villalta A, Schmitt A, Estrozi LF, Quemim ERJ, Alempic J-M, Lartigue A, Pražák V, Belmudes L, Vasishtan D, Colmant AMG, Honoré FA, Couté Y, Grünewald K, Abergel C. The giant mimivirus 1.2 Mb genome is elegantly organized into a 30-nm diameter helical protein shield. *Elife* 2022;**11**:e77607
 38. Fischer D, Eisenberg D. Finding families for genomic ORFans. *Bioinformatics* 1999;**15**:759–62
 39. Sobhy H, Gotthard G, Chabrière E, Raoult D, Colson P. Recombinant expression of mimivirus L725 ORFan gene product. *Acta Virol* 2017;**61**:123–6
 40. de Aquino ILM, Serafim MSM, Machado TB, Azevedo BL, Cunha DES, Ullmann LS, Araújo JP, Abrahão JS. Diversity of surface fibril patterns in mimivirus isolates. *J Virol* 2023;**97**:e0182422
 41. McGinnis S, Madden TL. BLAST: at the core of a powerful and diverse set of sequence analysis tools. *Nucleic Acids Res* 2004;**32**:W20–5
 42. Siddiqui R, Khan NA. Biology and pathogenesis of Acanthamoeba. *Parasit Vectors* 2012;**5**:6
 43. Dearborn DG, Korn ED. Lipophosphoglycan of the plasma membrane of *Acanthamoeba castellanii*: FATTY ACID COMPOSITION. *J Biol Chem* 1974;**249**:3342–6
 44. Rodrigues RAL, Abrahão JS, Drumond BP, Kroon EG. Giants among larges: how gigantism impacts giant virus entry into amoebae. *Curr Opin Microbiol* 2016;**31**:88–93
 45. Claverie JM, Ogata H, Audic S, Abergel C, Suhre K, Fournier PE. Mimivirus and the emerging concept of “giant” virus. *Virus Res* 2006;**117**:133–44
 46. Van Etten JL, Lane LC, Meints RH. Viruses and viruslike particles of eukaryotic algae. *Microbiol Rev* 1991;**55**:586–620
 47. Schulz F, Roux S, Paez-Espino D, Jungbluth S, Walsh DA, Deneff VJ, McMahon KD, Konstantinidis KT, Eloe-Fadrosh EA, Kyrpides NC, Woyke T. Giant virus diversity and host interactions through global metagenomics. *Nature* 2020;**578**:432–6
 48. Agarkova IV, Lane LC, Dunigan DD, Quispe CF, Duncan GA, Milrot E, Minsky A, Esmael A, Ghosh JS, Van Etten JL. Identification of a chlorovirus PBCV-1 protein involved in degrading the host cell wall during virus infection. *Viruses* 2021;**13**:782
 49. Fang Q, Zhu D, Agarkova I, Adhikari J, Klose T, Liu Y, Chen Z, Sun Y, Gross ML, Van Etten JL, Zhang X, Rossmann MG. Near-atomic structure of a giant virus. *Nat Commun* 2019;**10**:388
 50. Shao Q, Agarkova IV, Noel EA, Dunigan DD, Liu Y, Wang A, Guo M, Xie L, Zhao X, Rossmann MG, Van Etten JL, Klose T, Fang Q. Near-atomic, non-icosahedrally averaged structure of giant virus *Paramecium bursaria chlorella virus 1*. *Nat Commun* 2022;**13**:6476
 51. Piacente F, De Castro C, Jeudy S, Molinaro A, Salis A, Damonte G, Bernardi C, Abergel C, Tonetti MG. Giant virus *Megavirus chilensis* encodes the biosynthetic pathway for uncommon acetamido sugars. *J Biol Chem* 2014;**289**:24428–39

4.3 Artigo 3- Giant viruses inhibit superinfection by downregulating phagocytosis in *Acanthamoeba*

Este artigo foi publicado no periódico Journal of Virology.

No contexto da virosfera, as partículas virais podem competir pelas células hospedeiras. Nesse cenário, alguns vírus bloqueiam a penetração de partículas exógenas ao infectar uma célula, fenômeno conhecido como inibição de superinfecção. Os mecanismos moleculares associados à inibição da superinfecção variam dependendo da espécie viral e do hospedeiro, mas geralmente, o bloqueio da superinfecção garante a supremacia genética da progênie do vírus que primeiro infecta a célula. Os vírus gigantes que infectam amebas têm atraído a atenção da comunidade científica devido à complexidade de suas partículas e genomas. Porém, não existem estudos sobre a ocorrência de superinfecção e sua inibição induzida por vírus gigantes. Nesse contexto, durante o estudo do ciclo do megavírus caiporensis, notamos a presença de partículas dentro de vesículas em estágios tardios do ciclo, em que a fábrica viral se encontrava funcional para a produção de novas partículas. Após analisarmos que as vesículas não estavam relacionadas a uma liberação por exocitose, como é observado para outros vírus gigantes, partimos para uma investigação de possível fenômeno de superinfecção. Este estudo mostra que mesmo vírus evolutivamente relacionados, como mimivírus, moomovírus e megavírus, exibem diferentes estratégias para a infecção de *Acanthamoeba*. Pela primeira vez, relatamos que o mimivírus e o moomovírus induzem a inibição da superinfecção em amebas, e que os megavírus não exibem esta capacidade, permitindo a entrada contínua de vírions exógenos nas amebas infectadas. Nossa investigação sobre os mecanismos por trás do bloqueio da superinfecção revela que o mimivírus e o moomovírus causam mudanças significativas na morfologia e atividade das células hospedeiras ao inibir a fagocitose amebiana. Em contraste, as amebas infectadas por megavírus continuam incorporando vírions recém-formados, afetando negativamente a progênie viral disponível. Este efeito, entretanto, é reversível com a inibição química da fagocitose. Este trabalho contribui para a compreensão da superinfecção e sua inibição em mimivírus, moomovírus e megavírus, demonstrando que apesar de seu parentesco evolutivo, esses vírus apresentam diferenças profundas em suas interações com seus hospedeiros.



Editor's Pick | Virology | Full-Length Text

Giant viruses inhibit superinfection by downregulating phagocytosis in *Acanthamoeba*

Isabella L. M. Aquino,¹ Erik Sousa Reis,² Rafaella Oliveira Almeida Mattos Moreira,¹ Nidia Esther Colquehuanca Arias,¹ Matheus Gomes Barcelos,¹ Victória Fulgêncio Queiroz,¹ Raquel Duque do Nascimento Arifa,³ Larissa Mendes Barbosa Lucas,³ Juliana Miranda Tatara,⁴ Daniele G. Souza,³ Adriana Costa,⁵ Luiz Rosa,⁶ Gabriel M. F. Almeida,⁴ Erna Geessien Kroon,¹ Jônatas S. Abrahão¹

AUTHOR AFFILIATIONS See affiliation list on p. 15.

ABSTRACT In the context of the virosphere, viral particles can compete for host cells. In this scenario, some viruses block the entry of exogenous virions upon infecting a cell, a phenomenon known as superinfection inhibition. The molecular mechanisms associated with superinfection inhibition vary depending on the viral species and the host, but generally, blocking superinfection ensures the genetic supremacy of the virus's progeny that first infects the cell. Giant amoeba-infecting viruses have attracted the scientific community's attention due to the complexity of their particles and genomes. However, there are no studies on the occurrence of superinfection and its inhibition induced by giant viruses. This study shows that mimivirus, moomovirus, and megavirus, exhibit different strategies related to the infection of *Acanthamoeba*. For the first time, we have reported that mimivirus and moomovirus induce superinfection inhibition in amoebas. Interestingly, megaviruses do not exhibit this ability, allowing continuous entry of exogenous virions into infected amoebas. Our investigation into the mechanisms behind superinfection blockage reveals that mimivirus and moomovirus inhibit amoebic phagocytosis, leading to significant changes in the morphology and activity of the host cells. In contrast, megavirus-infected amoebas continue incorporating newly formed virions, negatively affecting the available viral progeny. This effect, however, is reversible with chemical inhibition of phagocytosis. This work contributes to the understanding of superinfection and its inhibition in mimivirus, moomovirus, and megavirus, demonstrating that despite their evolutionary relatedness, these viruses exhibit profound differences in their interactions with their hosts.

IMPORTANCE Some viruses block the entry of new virions upon infecting a cell, a phenomenon known as superinfection inhibition. Superinfection inhibition in giant viruses has yet to be studied. This study reveals that even closely related viruses, such as mimivirus, moomovirus, and megavirus, have different infection strategies for *Acanthamoeba*. For the first time, we have reported that mimivirus and moomovirus induce superinfection inhibition in amoebas. In contrast, megaviruses do not exhibit this ability, allowing continuous entry of exogenous virions into infected amoebas. Our investigation shows that mimivirus and moomovirus inhibit amoebic phagocytosis, causing significant changes in host cell morphology and activity. Megavirus-infected amoebas, however, continue incorporating newly formed viruses, affecting viral progeny. This research enhances our understanding of superinfection inhibition in these viruses, highlighting their differences in host interactions.

KEYWORDS superinfection, giant virus, phagocytosis, *Acanthamoeba*, virus-host relationship

Editor Kristin N. Parent, Michigan State University, East Lansing, Michigan, USA

Address correspondence to Jônatas S. Abrahão, jonatas.abrahao@gmail.com.

The authors declare no conflict of interest.

See the funding table on p. 16.

Received 13 June 2024

Accepted 6 August 2024

Published 3 September 2024

Copyright © 2024 American Society for Microbiology. All Rights Reserved.

The virosphere is diverse, and different strategies for infecting host cells have evolved throughout evolution (1). Various studies have demonstrated that, during the early stages of infection, some viruses block the entry of other viral particles into cells through a mechanism known as superinfection inhibition (2–5). This phenomenon can genetically favor the particles that first infect the cells in an inter- and intraspecific competition. Another hypothesis explaining the selection of superinfection inhibition mechanisms is based on the fact that an already infected cell would not naturally be a fully productive host for progeny formation (6). Thus, inhibition of penetration would allow such particles to remain in the extracellular environment and eventually find uninfected cells. A notable example of superinfection inhibition has been described for the vaccinia virus, a nucleocyctovirus that, while infecting the host cell, not only blocks the infection by other particles but can also repel exogenous particles to neighboring uninfected cells via actin tail formation, accelerating the infection of the host cell population (3, 4).

Other nucleocyctoviruses, such as mimiviruses, have drawn the attention of the scientific community due to their gigantic particles (750 nm) and complex genome (1.2 Mb) (7). Mimiviruses are giant viruses that, under laboratory conditions, infect *Acanthamoeba*. Recent studies have demonstrated significant genetic diversity within this viral group, supporting its division into different genera, including *Mimivirus*, *Moumouvirus*, and *Megavirus* (8). Although most basic studies have been conducted using mimivirus, it is believed that moumouvirus and megavirus have virus-host interaction mechanisms similar to those described for mimiviruses. For instance, their viral particles enter the host cells after being phagocytosed (9, 10). The acidification of the phagosome induces the release of the genome and early-phase proteins into the host cell cytoplasm (9, 11). Within a few hours, viral factories, micrometric structures involved in the morphogenesis and maturation of viral progeny, are formed (9–12). A few hours later, the host cell lysis releases viral progeny (10). During the amoeba infection by mimivirus, more than one particle can be phagocytosed simultaneously and initiate the replication cycle (9, 10). However, it has not been experimentally shown whether infected amoebas block the penetration of exogenous virions, under what circumstances and when this happens. No such data exist for moumouvirus and megavirus either.

In the present work, we describe for the first time, that mimivirus and moumouvirus induce the process of superinfection inhibition in amoebas. Interestingly, despite being genetically related, megaviruses do not block superinfection, allowing long-lasting entry of exogenous virions into infected amoebas. Investigation of the superinfection blocking mechanisms suggests that mimi- and moumouvirus inhibit the amoebic phagocytosis process, causing significant changes in the morphology and activity of host cells. The constant incorporation of newly formed megavirus virions by infected amoebas impacts the viral progeny released into the supernatant, but the phenomenon is reversible when phagocytosis is chemically inhibited. This work provides information on superinfection and its inhibition in mimi-, moumou-, and megaviruses, highlighting that despite being evolutionarily related, these viruses exhibit profound differences in their relationship with their hosts.

RESULTS

Megavirus particles can be found within vesicles at 6 h post-infection

During our ongoing efforts to discover new amoeba viruses, we recently isolated megavirus caiporensis from an urban lagoon in Belo Horizonte, Brazil. This isolate prompted a comparative study of the surface fibrils of mimi-, moumou-, and megavirus particles (13). Despite the differences in the organization of these fibrils, the viral factories of these three viral groups are similar, being about 3–4 μm in size, electron-dense, and with particles sprouting on their surfaces during morphogenesis (Fig. 1). However, transmission electron microscopy (TEM) analysis of cells infected by megavirus caiporensis revealed the presence of some viral particles enclosed by membranes after the formation of viral factories, 6 h post-infection (hpi), suggesting these particles might be released by exocytosis (Fig. 1 and 2). Although such a release mechanism has

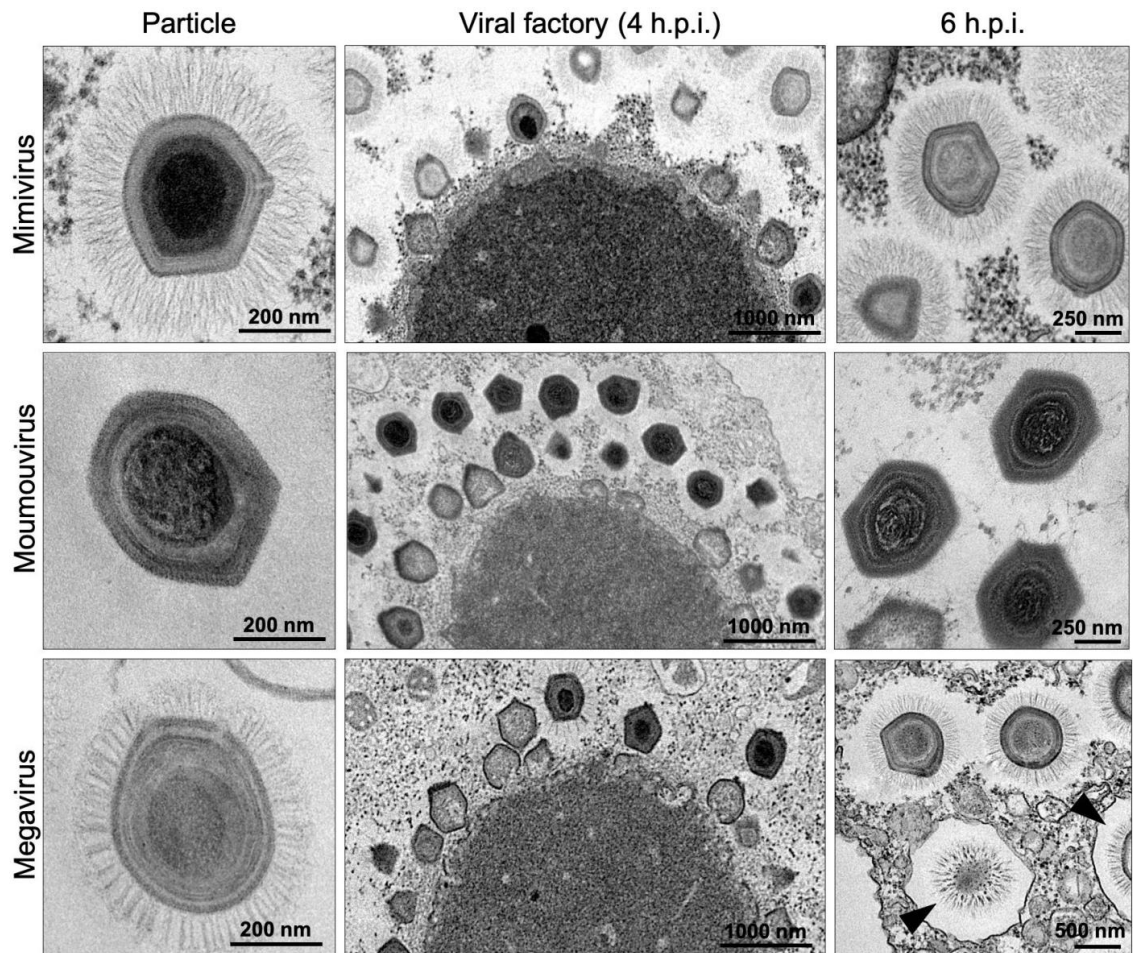


FIG 1 Particle, viral factory, and progeny features of mimi-, moumou-, and megaviruses observed by transmission electron microscopy. This panel shows that mimi-, moumou-, and megaviruses particles exhibit differences in the organization and abundance of surface fibrils, while their viral factories appear very similar. Notably, at 6 h post-infection, some megavirus particles are observed inside vesicles (black arrowheads).

been described for other giant viruses like Pandoravirus, Cedratvirus, Marseillevirus, and Orpheovirus, there is no evidences that the progeny of mimi-, moumou-, and megaviruses are exclusively released by cell lysis (14–17).

To verify if this phenomenon is exclusive to the megavirus caiporensis isolate, we analyzed five other megavirus isolates obtained by our group and one isolate from the University of Tromsø, Norway, by TEM. The analyses revealed that of the seven isolates analyzed, all showed viral particles enclosed by membranes in the stages of infection when the viral factory was fully formed and producing new particles. This result suggested that considering the analyzed megavirus isolates, all appear to release part of their progeny by exocytosis. Analysis of our image library of five mimivirus isolates and five moumouvirus isolates did not reveal the presence of viral particles enclosed by vesicles in the late stages of infection (after the formation of the viral factory). This result suggests the presence of viral particles enclosed by membranes from 6 hpi seems to be an exclusive characteristic of megaviruses compared to the other two viral groups.

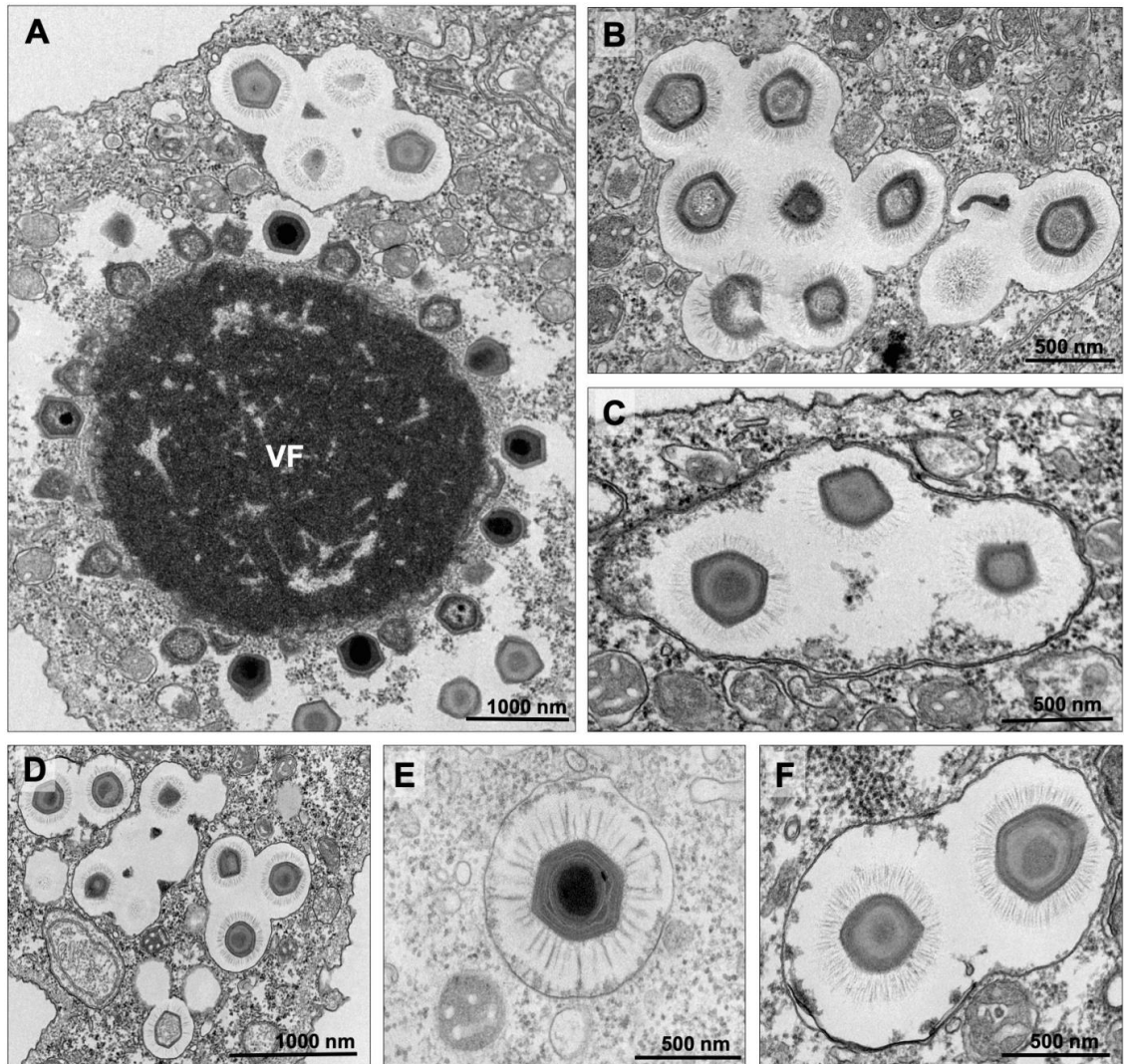


FIG 2 The occurrence of megavirus particles within cytoplasmic vesicles. The replication cycles of megavirus caiporensis and other isolates were analyzed using transmission electron microscopy. All images were captured after the mature viral factory appearance, approximately 4–6 h post-infection. Vesicles contain from one to several megavirus particles.

Megavirus progeny is not released by exocytosis

A viral release experiment was conducted to evaluate whether megavirus caiporensis particles can be released by exocytosis (14, 15). *Acanthamoeba castellanii* trophozoites were infected with mimi-, moumou-, or megavirus at a multiplicity of infection (MOI) of 10. At 0, 2, 4, 8, 12, and 24 hpi, viable amoebas were quantified, and viral particles in the supernatant were titrated. The rationale of this experiment was to verify if there is an increase in viral particles in the supernatant without a reduction in the total number of viable cells, indicating the exocytosis of particles into the supernatant before cell lysis. Although TEM images suggested the possible release of megavirus particles by

exocytosis, the release experiment demonstrated that the increase in mimi-, moumou-, and megaviruses titers in the supernatant of infected cultures was accompanied by a reduction in the number of viable amoeba cells (Fig. 3A through C). As an experimental control, amoebas were infected with cedratvirus, known to be released by exocytosis. As shown in the graph, an increase in cedratvirus particles in the supernatant between 4 and 12 h was observed, not associated with a decrease in the number of viable amoebas, indicating release by exocytosis (Fig. 3D). TEM analysis showed cedratvirus particles inside exosomes at 8 hpi (Fig. 3E through G). These results, therefore, do not support our initial hypothesis of megavirus release by exocytosis.

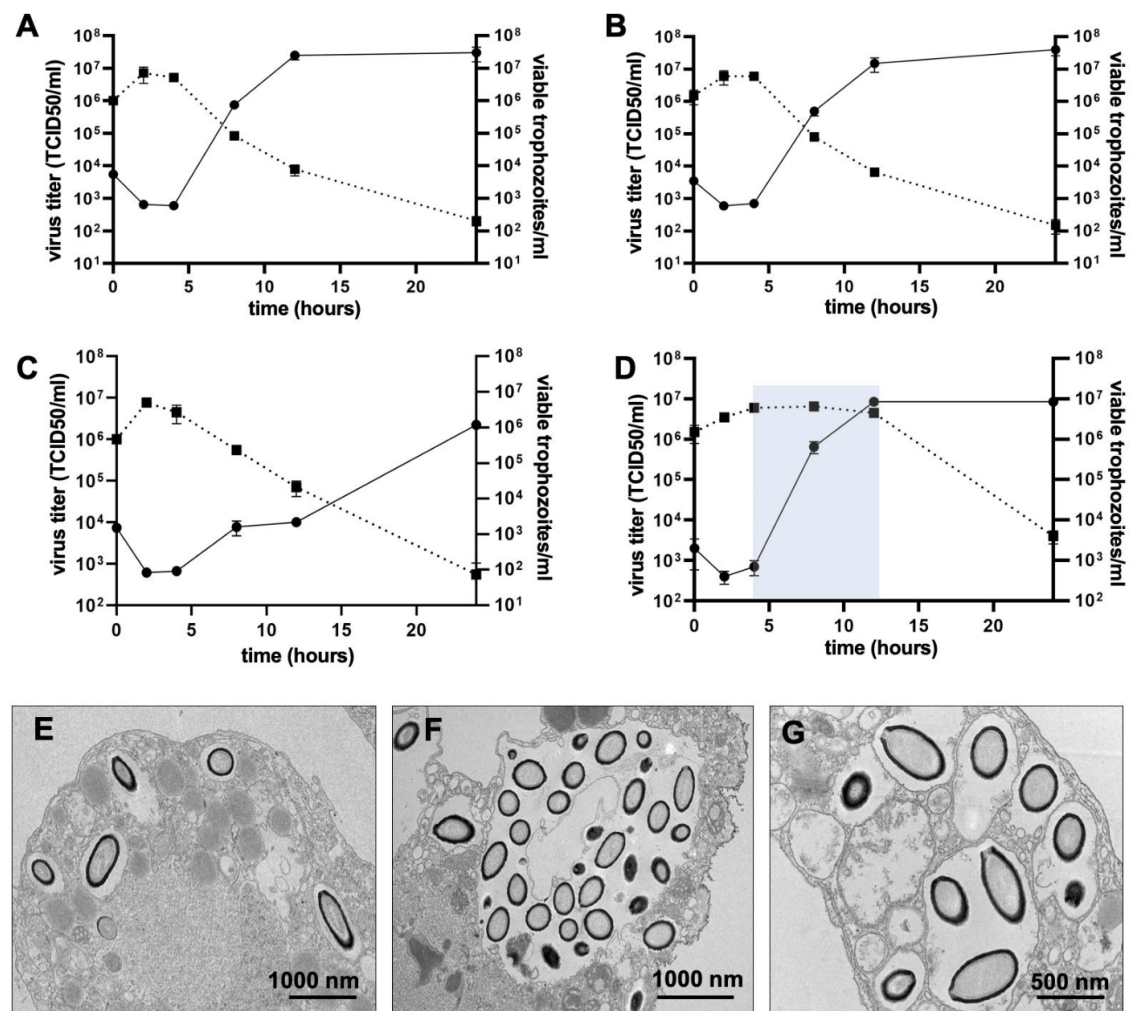


FIG 3 Mimi-, moumou-, and megaviruses are not released via exocytosis in *Acanthamoeba*-infected cells. One-step growth curves of the supernatant from *Acanthamoeba* infected with (A) mimivirus, (B) moumouvirus, (C) megavirus, and (D) cedratvirus. The left Y-axis plots viral titers at different times post-infection. The right Y-axis plots data on viable cells at different times post-infection. The blue box in (D) highlights the period when cedratvirus is primarily released in the supernatant via exocytosis (the number of viable, non-lysed cells remains stable). Solid lines with circles represent virus titers, while dashed lines with squares represent viable cell counts. Panels (E–G) depict cedratvirus particles being released inside exosomes, 8 hpi.

Mimivirus and moulmouvirus, but not megavirus, inhibit superinfection

Considering that the hypothesis of megavirus particle exocytosis was not confirmed, the investigation of megavirus particles enclosed in membranes in the late stages of the cycle continued. Since the particles in vesicles were not being released, we hypothesized that they might be entering cells already infected by megavirus. To verify this hypothesis, we designed an experiment where amoebas infected with mimi-, moulmou-, or megavirus were exposed, 2 hpi, to a “bait” to check for phagocytic activity. After 4 h of exposure to the bait, 6 hpi, the samples were analyzed by confocal immunofluorescence (IF) microscopy. The bait used in this experiment was Orpheovirus particles, at a ratio of 10 particles per amoeba. Orpheovirus was chosen as bait because it cannot replicate in *Acanthamoeba* and thus would not cause major interference with the analyzed cells, despite being internalized. The host of Orpheovirus under laboratory conditions is *Vermamoeba vermiformis* (17).

IF analyses revealed the presence of green-marked Orpheovirus particles primarily attached outside the cells or at intercellular space among cells infected by mimi- or moulmouvirus (Fig. 4A). However, in about 27% of megavirus-infected cells, Orpheovirus particles were visible inside cellular vacuoles (darker regions in the amoeba cytoplasm) (Fig. 4A, B and 5A). Most megavirus-infected cells contained one to two Orpheovirus particles, but some cells had up to six incorporated Orpheovirus particles (Fig. 4B and 5B). Besides the observation and quantification of phagocytosed baits, the supernatant of cells infected by mimi-, moulmou-, or megavirus and subsequently exposed to Orpheovirus was titered in *V. vermiformis* 6 hpi. The results show that almost all the Orpheovirus input used as bait for mimi- or moulmouvirus-infected cells was recovered from the supernatant. In contrast, there was a significant reduction in the input of Orpheovirus particles exposed to megavirus-infected cells, indicating that the cells partially incorporated the baits (Fig. 5C). This result was confirmed by TEM images, where the cells containing formed megavirus viral factories alongside vesicles containing Orpheovirus particles were observed (Fig. 5D).

The above results indicate that mimi- and moulmouvirus, but not megavirus, block the incorporation of new viral particles into infected cells. To evaluate from what time superinfection is inhibited by mimi- and moulmouvirus, amoebas were infected by these viruses or megavirus and exposed to Orpheovirus as bait at different times: 0, 2, 4, 8, and 12 h. After 4 h, the supernatant was collected and titered in *V. vermiformis*. The results indicate that from 2 hpi, mimi- or moulmouvirus-infected cells reduce bait incorporation. In contrast, bait incorporation by megavirus-infected cells was observed even at 12 h, suggesting that superinfection is not entirely blocked by this virus, even in the late stages of infection (Fig. 5E).

Mimivirus and moulmouvirus cause cell size reduction and inhibit the formation of vacuoles and pseudopodia in amoebas

During the previously described experiments, we observed that amoebas infected with mimivirus and moulmouvirus exhibited distinct morphological characteristics compared to amoebas infected with megavirus and the control group (uninfected cells). To better understand this process, amoebas infected with mimi-, moulmou-, or megavirus were observed by immunofluorescence 6 hpi, using Evans blue again as a cytoplasmic marker. The cell size and the number of cytoplasmic vacuoles present in the cells were measured. These vacuoles may be related to the natural phagocytic activity of amoebas, as this pathway represents their main form of feeding/nutrition. Even under axenic conditions, such as laboratory culture, amoebas maintain constant phagocytic activity, forming vacuoles or phagosomes.

Measurement of the cells, considering the largest observed axis, revealed that cells infected with mimi- or moulmouvirus showed a significant size reduction, with an average size of 13 and 14.5 μm , respectively. In contrast, cells infected with megavirus had dimensions similar to uninfected cells, with an average size above 20 μm (Fig. 6A

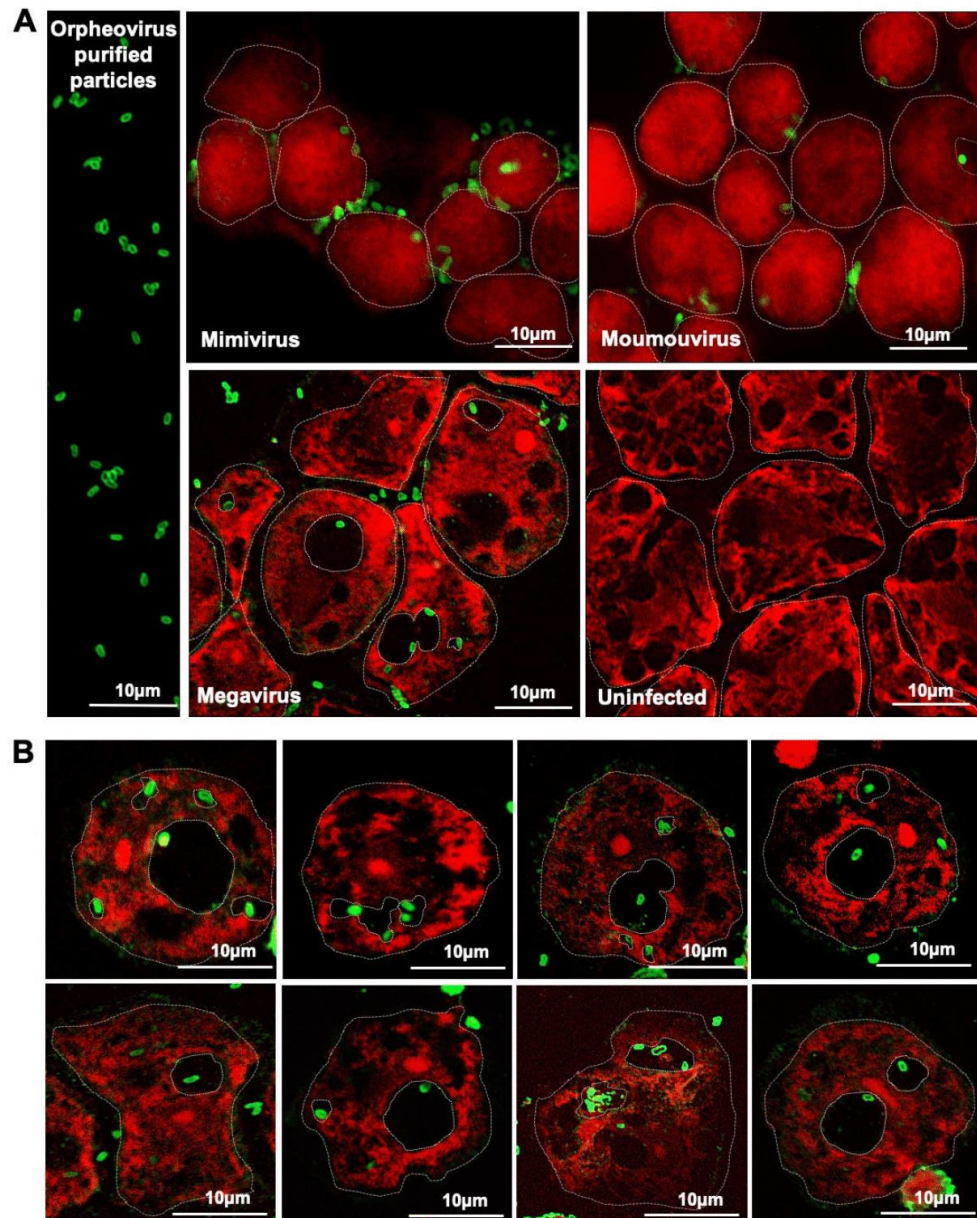


FIG 4 Megavirus-infected cells phagocytose exogenous particles. Amoebas were infected by mimi-, moutmou-, and megaviruses, and 2 h later were exposed to a “bait,” the Orpheovirus particles. At 6 hpi, cells and particles were analyzed by immunofluorescence microscopy. Orpheovirus particles, probed with a mouse primary antibody, appear green, while the amoeba cytoskeleton stained by blue Evans appears red. (A) Cells infected by mimi-, moutmou-, or megavirus and exposed to Orpheovirus (bait). Only Orpheovirus particles colocalizing with amoeba vacuoles (black cytoplasm regions) were considered phagocytized (highlighted with dotted lines inside cells). (B) This panel shows several individual *Acanthamoeba* cells with phagocytized Orpheovirus particles.

and B). This result suggests that mimi- and moutmouvirus cause compaction of the host cells. The count of cytoplasmic vacuoles revealed that cells infected with mimi- or

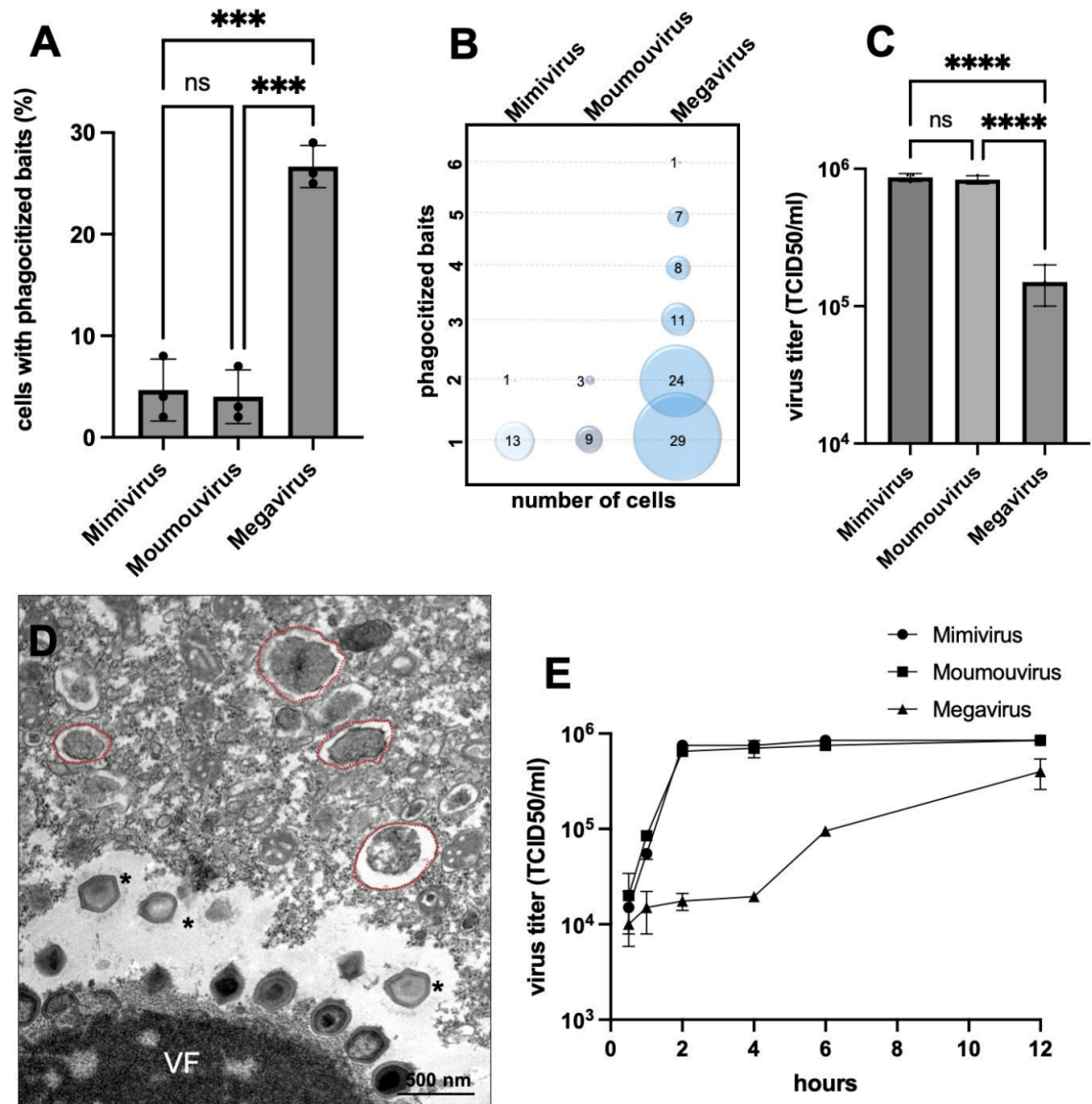


FIG 5 The consequences of superinfection and its inhibition in mimi-, moulou-, and megavirus-infected cells. (A) Megavirus-infected cells phagocytized significantly more exogenous particles than mimi- and moulouvirus-infected cells. This graph was obtained after observing 50 cells infected by mimi-, moulou-, or megavirus and analyzed by immunofluorescence microscopy. The average of three independent replicates is presented. (B) Number of cells versus Orpheovirus-incorporated baits. The graph depicts all analyzed cells belonging to three independent replicates. (C) Titration of the residual Orpheovirus input in *Vermoaeba vermiformis* cells. Mimi-, moulou-, and megavirus-infected cells were inoculated with Orpheovirus baits to verify phagocytosis activity. After 4 h (6 hpi), the supernatants were collected and titered in *Vermoaeba vermiformis*, the laboratory host of Orpheovirus. This graph shows that almost the complete input of Orpheovirus baits was recovered from the supernatant of mimi- and moulouvirus-infected cells, suggesting a significant reduction in phagocytosis activity compared to megavirus-infected cells. (D) Transmission electron microscopy of megavirus-infected cells exposed to Orpheovirus baits. Asterisks denote megavirus particles; VF represents megavirus virus factory; red dashed circles indicate phagosomes containing Orpheovirus particles. (E) Evaluation of superinfection inhibition by mimi-, moulou-, and megaviruses. *Acanthamoeba* cells were infected by mimi-, moulou-, or megavirus at an MOI of 10. At times 30 min, 1 h, 2 h, 4 h, 6 h, and 12 h, cells were exposed to Orpheovirus baits. Four hours after this exposure, culture supernatants were collected and (Continued on next page)

FIG 5 (Continued)

titered in *Veramoeba vermiformis*. The graph shows the almost complete recovery of Orpheovirus inputs from mimi- and moutoumouvirus-infected cultures from 2 hpi. This result indicates that mimi- and moutoumouvirus start to block phagocytosis of exogenous particles at early times post-infection. ***: $P < 0.001$, ****: $P < 0.0001$ (ANOVA, one-way).

moutoumouvirus showed a significant reduction compared to cells infected with megavirus or uninfected cells. On average, about four vacuoles were observed in megavirus-infected cells, while one or no vacuoles were observed in cells infected with mimi- or moutoumouvirus (Fig. 6C). Considering possible cellular alterations caused by preparation for IF, we also evaluated amoebas infected by mimi-, moutou-, or megavirus using scanning electron microscopy. Besides the cellular compaction observed by IF, we also observed that cells infected with mimi- or moutoumouvirus reduced the number and size of pseudopodia at 6 hpi (Fig. 6D). It is important to note that pseudopodia are essential structures for initiating the phagocytosis process in amoebas. Megavirus-infected and control cells exhibited typical trophozoite size and appearance, around 20 μm . Therefore, taken together, our results indicate that mimi- and moutoumouvirus cause host

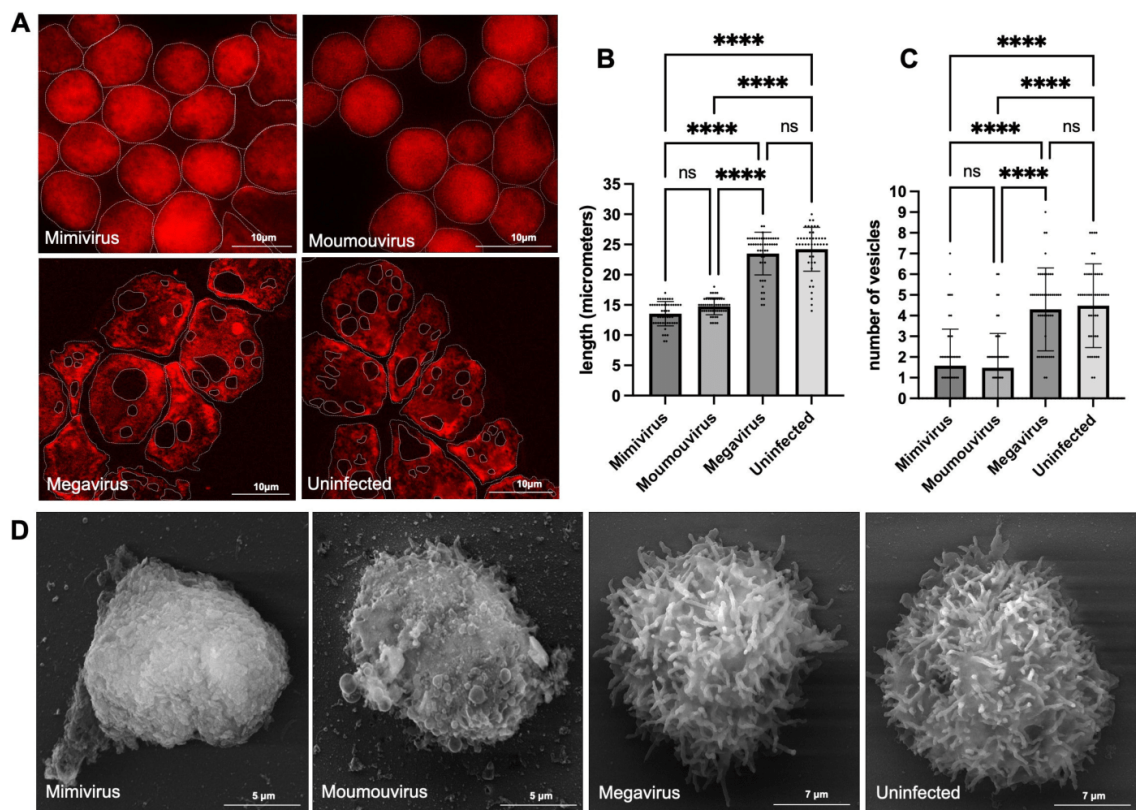


FIG 6 Mimi- and moutoumouvirus cause compaction of the cellular cytoplasm and reduction in the formation of pseudopods and intracellular vacuoles. *Acanthamoeba* cells were infected with mimi-, moutou-, or megavirus at an MOI of 10. At 6 hpi, cells were analyzed by immunofluorescence microscopy. The amoeba cytoskeleton stained with blue Evans is represented in red. (A) Cells infected with mimi- and moutoumouvirus appear rounded and compacted compared to megavirus-infected and uninfected cells. Cell dimensions were measured (B), and vacuole counting (C) was performed by analyzing 50 cells randomly in three independent replicates. (D) Scanning electron microscopy of amoebas infected with mimi-, moutou-, or megavirus, 6 hpi. This panel shows that cells infected with mimi- and moutoumouvirus are smaller and exhibit fewer pseudopods compared to cells infected with megavirus or uninfected cells. ****: $P < 0.0001$ (ANOVA, one-way). Some of the images presented here (panel (A)) were also shown in Fig. 4A and B, as they were obtained from the same experiment.

cell compaction, in addition to reducing the number of pseudopodia and intracellular vacuoles.

The consequences of megavirus superinfection in amoebas

As previously described, the measurement of viral particles in the supernatant of infected cells, revealed a distinct profile for megavirus compared to other viruses (Fig. 3A through C). Although it was clear that the release of megavirus particles is dependent on cell lysis, we observed that the titers of megavirus particles released into the supernatant are lower than that observed for mimi- and moumouvirus, from the beginning to the end of the productive phase of the cycle. It is important to emphasize that the entry process of giant virus particles into host cells is promoted by phagocytosis. As far as we know, it is independent of cellular receptors. Thus, for a mimi-, moumou-, or megavirus to initiate infection, the host must actively phagocytize the viral particle. This naturally causes methodological difficulties in synchronizing the cycle in a population of amoebas, even at high MOIs. Therefore, if they are active, newly formed and released viral particles can be phagocytized by neighboring cells. Considering that, we hypothesized that part of the viral progeny released by lysis from megavirus-infected cells could be incorporated by neighboring cells that are also infected but not yet lysed.

To better understand this process, cells infected by megavirus, 12 hpi, were analyzed by TEM. Similar to what we observed in microscopy of cells infected by megavirus 6 hpi (Fig. 1), we also visualized megavirus particles being massively incorporated by already infected amoebas. However, interestingly, at 12 hpi, most of the phagocytized particles were in the process of uncoating, releasing their genome and viral proteins into a cytoplasm already in an advanced state of degradation due to the primary infection (Fig. 7A through E). Thus, numerous empty megavirus capsids or their inner membrane fused with the phagosome membrane were observed (Fig. 7A through E). In some images, up to three megavirus capsids were seen in a single phagosome, all in the process of uncoating (Fig. 7A). This result suggests that part of the megavirus progeny formed during the cycle can be lost when incorporated by already infected cells, resulting in the superinfection of a cell in an advanced state of degradation. The consequence is a smaller number of megavirus particles in the supernatant of infected cultures compared to cultures infected by mimi- or moumouvirus.

The inhibition of phagocytosis reverses the superinfection by megavirus and increases the number of viral particles in the system

As presented, previous results showed that mimivirus and moumouvirus cause a reduction in the formation of pseudopods, compaction of the cellular cytoplasm, reduction in the formation of intracellular vesicles, and lower incorporation of baits. In contrast, cells infected by megavirus exhibit a phenotype similar to non-infected cells in terms of their morphology and phagocytic activity. Considering the hypothesis that the inability to inhibit superinfection causes a reduction in the total megavirus titers in the supernatant, we decided to investigate the impact of phagocytosis on this process.

For this purpose, amoebas were infected with mimivirus, moumouvirus, or megavirus, and the cells were washed 30 min after infection to remove the remaining particles. Two hours post-infection, amoebas were treated with different endocytic and phagocytic pathways inhibitors. Chloroquine was used as an inhibitor of endocytosis, EIPA as an inhibitor of macropinocytosis and cytochalasin as an inhibitor of phagocytosis. After 24 h of infection (22 h of treatment), the viral particles in the supernatant were quantified. As a control group, amoebas were infected by the viruses and treated 2 h later with the vehicle of the inhibitors. Therefore, in this experiment, we verified the impact of inhibitors on viral progeny incorporation and its effect on the final titer in the culture supernatant.

No changes in the titers of mimivirus and moumouvirus were observed. In both cases, amoebas treated with the inhibitors showed titers similar to those observed in

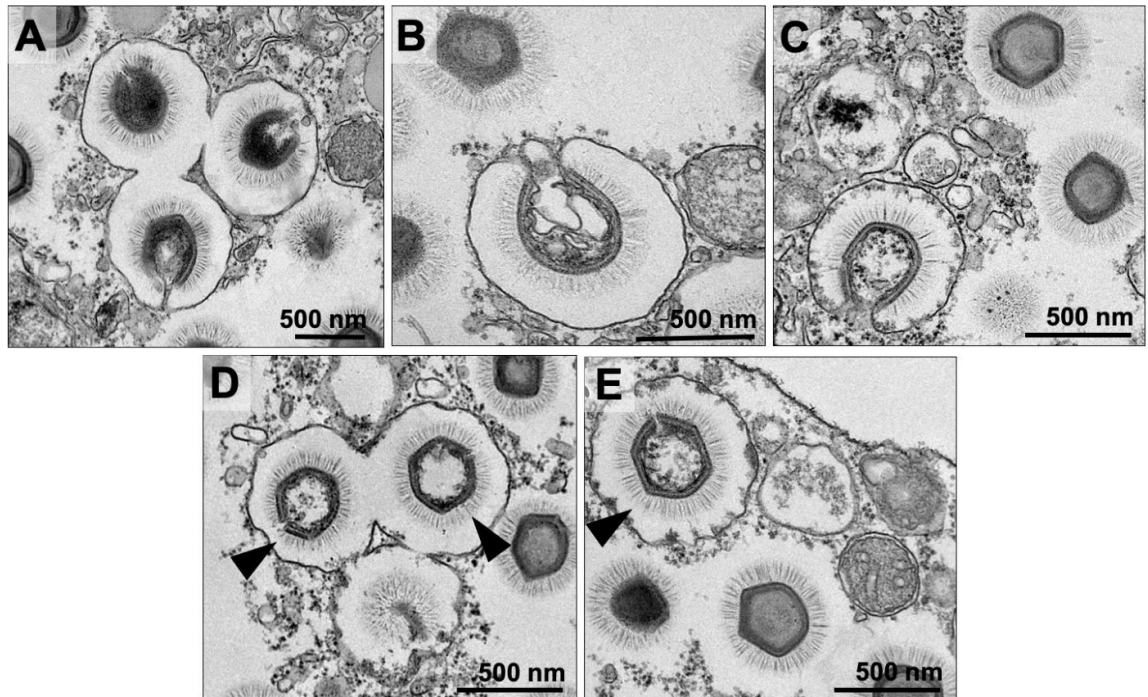


FIG 7 Exogenous particles incorporated by 12-h megavirus-infected cells appear to be undergoing the uncoating process or are already empty. Amoebae were infected with megavirus at an MOI of 10. Twelve hours post-infection, infected cells were analyzed by transmission electron microscopy. (A–C) Megavirus exogenous particles (inside vesicles) undergo the uncoating process. In the images, it is possible to visualize the particle's inner membrane fused with the phagosome membrane. (D and E) Empty exogenous particles inside vesicles (indicated by black arrowheads).

the control (Fig. 8). However, a significant increase in megavirus titers in the supernatant was observed in the group treated with cytochalasin (Fig. 8C). Taken together, this result indicates that inhibiting phagocytosis reduces the phagocytic action on exogenous particles by amoebae previously infected by megavirus, mitigating the process and consequences of superinfection.

DISCUSSION

The mechanisms involved in superinfection inhibition are varied and widespread throughout the virosphere. As mentioned, the phenomenon has been extensively studied in the nucleocyctovirus vaccinia virus. It has been demonstrated that the early expression of the A33 and A36 proteins by the vaccinia virus is necessary to repel exogenous particles by forming actin tails on the surface of infected cells (3). Interestingly, 4 h after infection, the vaccinia virus induces a 90% block of superinfection (4). Superinfection inhibition is also known for bacteriophages. The expression of the lipoprotein gene *ltp* (TP-J34) of the temperate phage *Streptococcus thermophilus* phage TP-J34 interferes with the infection of exogenous phages by blocking the injection of viral DNA into the cell (5). Although the mechanism has not been fully elucidated, it has been shown that the p33 protein of the citrus tristeza virus is essential for inhibiting intraspecific superinfection (18). The HIV virus blocks superinfection by reducing the expression of the viral coreceptor CCR5, making the penetration of exogenous particles unfeasible (2). As far as we know, the entry of giant viruses into amoebae occurs by phagocytosis and does not require a cellular receptor, another point that differentiates these viruses from most of the canonical virosphere. Thus, since amoeba trophozoites

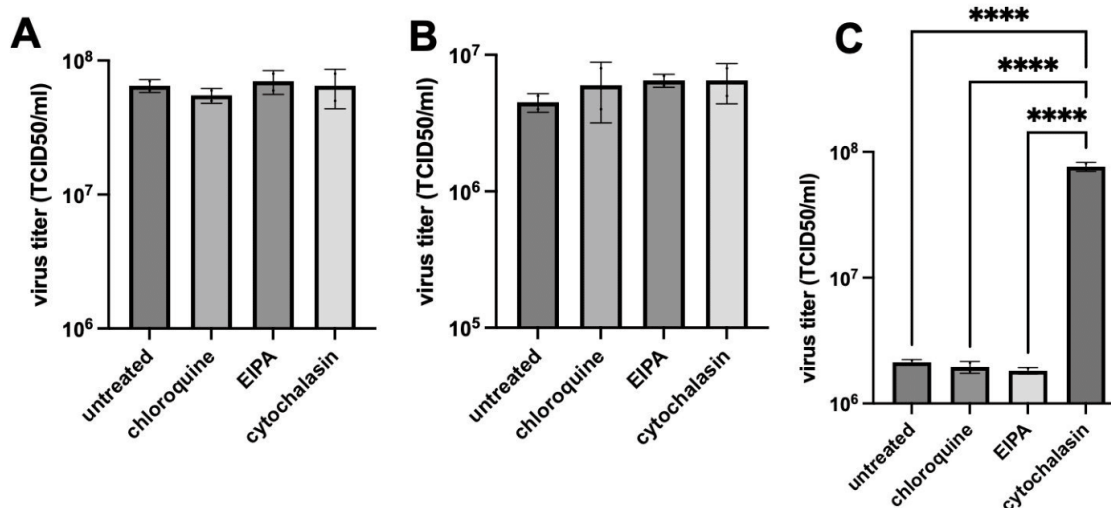


FIG 8 Cytochalasin D reverses the superinfection promoted by megavirus and increases the number of viral particles in the system. *Acanthamoeba* cells were infected with mimi-, moutou-, or megavirus at an MOI of 10. Two hours post-infection, amoebas were treated with different inhibitors of endocytic and phagocytic pathways: 2 μ M of cytochalasin, 100 μ M of chloroquine, or 1 μ M of EIPA. Twenty-four hours post-infection, the culture supernatants were titrated. No significant changes in viral titers were observed in cells infected by mimi- (A) or moutouvirus (B) and treated with any of the mentioned inhibitors. However, cells infected with megavirus (C) and treated with cytochalasin produced significantly increased titers. ****: $P < 0.0001$ (ANOVA, one way).

constantly perform phagocytosis, it would not be intuitive to predict that giant viruses would cause superinfection inhibition.

Free-living amoebas, such as *Acanthamoeba*, must constantly activate the phagocytosis process to obtain nutrients. Weisman and Korn experimentally demonstrated that the phagocytosis process in amoebas is stimulated by particles larger than 500 nm (19). Therefore, most environmental bacteria stimulate phagocytosis in *Acanthamoeba*, their primary source of nutrients. However, the discovery of giant viruses, such as mimi-, moutou-, and megaviruses, revealed that this feeding strategy of amoebas can trigger infection and death of this organism, as these viral entities have particles larger than 500 nm. Some theories hypothesize that the gigantism of giant viruses may have been selected to exploit the niche of entry by phagocytosis (20). Besides gigantism, a series of structural and enzymatic adaptations in viral particles were required to exploit the phagocytic pathway, such as enzymes to control oxidative stress in the phagosomal environment, new uncoating portals like the stargate axis, and the configuration of an inner membrane within the capsid, essential for the genome delivery process in the cytoplasm (21). Therefore, phagocytosis seems to be a crucial phenomenon in the relationship between giant viruses and amoebas.

In the present study, our results indicate that mimi- and moutouviruses induce superinfection inhibition in amoebas starting approximately 2 hpi. These viruses also induce profound changes in amoeba morphology and physiology, such as cytoplasm condensation, reduction in the size and number of pseudopods, diminution in the phagocytosis rate, and a decrease in the number of cytoplasmic vacuoles. In contrast, the cells infected by megavirus retain the fundamental property of amoeba trophozoites: phagocytosis. One consequence of this is the constant incorporation of exogenous viral particles until the late stages of the cycle. However, this property is reversed when a pharmacological phagocytosis inhibitor is employed. To our knowledge, the present study is the first to demonstrate the existence of the superinfection process and its inhibition by giant viruses. It is also the first time that inhibition of the phagocytosis process is associated with the inhibition of viral superinfection in amoebas.

Taken together, our data indicate that the absence of the ability to inhibit superinfection causes a reduction in megavirus titers, as part of the newly formed progeny is promptly phagocytosed and uncoated in already infected cells. During our microscopy analyses, none of the cells infected by megavirus presented more than one viral factory. This indicates that the content uncoated by exogenous megavirus particles does not result in progeny formation. This conclusion is corroborated by the lower titer observed for megavirus compared to mimi- and moomoviruses, regardless of the productive phase of the cycle. From the amoeba population perspective, the phagocytosis of newly formed megavirus particles could be considered an antiviral process, as it reduces the number of viral particles in the extracellular medium, decreasing the chance of neighboring healthy cells' infection. Possibly, mimi- and moomoviruses have overcome this disadvantage by developing mechanisms to control the phagocytic activity of their hosts. The viral proteins involved in this process remain to be investigated, with molecular tools available to delete viral genes involved in cytoskeleton control. In addition, an interesting perspective to investigate is the consequence of superinfection inhibition during viroplasm co-infections. Although the viroplasm entry mechanisms are unknown, it has been hypothesized that these satellite viruses might enter amoebas associated with mimivirus fibrils. In this case, the blocking of superinfection could affect viroplasm infection.

Although the discovery of the first giant amoeba virus occurred just over 20 years ago, numerous unprecedented processes in the relationship between these viruses and their hosts have been described (7, 16, 22–25). The constant investigation of this relationship is crucial, as amoebas and their ancestors are some of the oldest known eukaryotic organisms. The hypothesized scenario for the origin of giant viruses also dates back to ancient times in the context of proto-eukaryotic cells (26). Therefore, although studies involving giant viruses and their hosts represent great novelties in modern virology, such relationships are possibly among the oldest in the history of life on Earth. Understanding these relationships can contribute to a better understanding of the virosphere as a whole.

MATERIALS AND METHODS

Virus multiplication, purification, and titration

The megavirus caiporensis was isolated in 2017 from the Pampulha Lagoon, Belo Horizonte, Brazil (13). The moomovirus B60 was isolated in 2018 from a river in a savanna biome in Brazil (27). The Brazilian cedratvirus was isolated in 2017 from a fishbowl, in Belo Horizonte, Brazil (28). The mimivirus (APMV) and Orpheovirus were kindly provided by Dr. Bernard La Scola (Aix Marseille University). *A. castellanii* ATCC 30,010 cells were kindly provided by Dr. Adriana Oliveira Costa (UFMG). *Vermamoeba vermiformis* cells were also kindly provided by Dr. Bernard La Scola (Aix Marseille University). The study was registered at the Sistema Nacional de Gestão do Patrimônio Genético e do Conhecimento Tradicional Associado (SisGen). For production and purification, each virus was inoculated at an MOI of 0.01 in cell culture T175 flasks containing 1.4×10^7 *A. castellanii* trophozoites and 25 mL of peptone-yeast extract-glucose (PYG) medium supplemented with penicillin (100 U/mL; Cellofarm, Brazil), streptomycin (100 µg/mL; Sigma-Aldrich, Burlington, MA, USA), and amphotericin B (0.25 µg/mL; Cultiab, Brazil). The cells were incubated at 30°C. After observation of the cytopathic effect caused by viral infection (i.e., rounding cells and cellular lysis), the flask contents were collected and ultracentrifuged ($36,000 \times g$) in a 22% sucrose cushion for 50 min. The pellet containing purified viral particles was suspended in phosphate-buffered saline (PBS). All titration assays were performed using the endpoint method (27).

Electron microscopy

A. castellanii cultures infected with different viruses were analyzed by SEM and TEM. Experiments and analyses were performed in the Center of Microscopy at the Universidade Federal de Minas Gerais, Belo Horizonte, Minas Gerais, Brazil (<http://www.microscopia.ufmg.br>). For SEM assays, samples were fixed by immersion in a solution containing glutaraldehyde (2.5%) in 0.1 M sodium cacodylate buffer (pH 7.2) for 2 h. Postfixation was followed for each sample with 2% osmium tetroxide (OsO₄) for 2 h at room temperature. Fixed samples were dehydrated using a growing series of ethanol dilutions (30%, 50%, 70%, 95%, and 100%) for 10 min in each step. Then, samples were dried with CO₂ at a critical point using CPD 030 equipment (Bal-Tec, Liechtenstein). Next, the samples were supported in aluminum stubs and metalized with a thin layer (5 nm) of gold particles using MED 020 equipment (Bal-Tec, Liechtenstein). Samples were observed in a FEG-Quanta 200 FEI microscope (FEI Co., Eindhoven, Netherlands) at 15–20 kV.

For TEM assays, samples were fixed by immersion in a solution containing glutaraldehyde (2.5%) in 0.1 M sodium phosphate buffer (pH 7.2) for 2 h. After fixation, postfixation was performed with a solution of 1% osmium tetroxide in sodium cacodylate buffer (0.1 M, pH 7.2) for 1 h, followed by en bloc counterstaining with uranyl acetate (2% uranyl acetate in deionized water). Samples were gradually dehydrated by immersion in 70%, 80%, and 90% ethanol once for 15 min each and two times in 100% ethanol for 15 min. Next, the samples were embedded in Epon resin. Ultrathin sections were obtained using an ultramicrotome with diamond knives (Leica Microsystems), and these sections had a thickness of 70 nm and were placed on a 200-mesh copper screen. The screens were counterstained with Reynold's lead citrate solution for 10 min. Images were obtained using a Tecnai G2-12-SpiritBiotwin FEI electron microscope (FEI Co., Eindhoven, Netherlands) at an acceleration voltage of 120 kV using a charge-coupled-device camera.

Immunofluorescence microscopy

For immunofluorescence, *A. castellanii* trophozoites were infected with viruses at an MOI of 10, and approximately 2×10^5 cells were collected and centrifuged at $800 \times g$ for 10 min. The pellet was resuspended in 50 μ L of Page's amoebae saline (PAS), and the cells were attached to a slide via cytospin and fixed in methanol for 15 min. After fixation, the cells were incubated with 3% bovine serum albumin (BSA)-PAS for 30 min, followed by three washes with 0.1% PAS-Tween. The cells were stained with polyclonal anti-Orpheovirus whole particle antibody produced in mice—CEUA 235/2023—(1:400 diluted in 3% BSA-PAS) for 1 h at 37°C, followed by three washes with PAS-Tween 0.1%. After a 1-h incubation with an anti-mouse secondary antibody (1:400 diluted in 3% BSA-PAS), one drop of 0.01% Evans Blue (Sigma), which was sufficient to cover the cells, was added and incubated for 15 min at 37°C, followed by three washes with PAS-Tween 0.1%. Uninfected cells (control) were also fixed and prepared as described. Fluorescently labeled cells were observed using a confocal Axio Imager Z2-Apoptome 2 microscope (Zeiss). The Zen Lite software from Zeiss Microscopy was used for image processing. The ImageJ software (version v1.53k, National Institutes of Health) was used to measure 50 different cells during the acquisition of images. The measures were used to calculate the medium sizes and deviate.

One-step growth curves and cell counting

A. castellanii trophozoites were infected by mimivirus, moutouvirus, megavirus, or cedratvirus, at MOI of 10, in T25 culture flasks. Thirty minutes after infection, the supernatants were removed, and fresh medium was added. Then, the supernatants of infected cells were collected at different time points and titrated in 96-well plates containing 40,000 *A. castellanii* cells, by the endpoint method (27). In parallel, the remaining cells of each time and experimental group were quantified using a Neubauer chamber. Viable cells were identified by using trypan blue (Sigma).

Phagocytic activity and superinfection assays

One million of *A. castellanii* trophozoites were infected by mimivirus, moutovirus, or megavirus at MOI of 10, in T25 culture flasks. Thirty minutes after infection, the supernatants were removed, and fresh medium was added. Two hours post-infection, purified Orpheovirus particles were inoculated into the amoeba's monolayers at the MOI of 10. At 6 hpi (4 h post-Orpheovirus inoculation), the cells were collected and analyzed by IF, as previously described. Only particles colocalizing with vacuoles were considered phagocytized. The same experimental groups were analyzed by TEM. The supernatants of each flask were collected and titrated in *V. vermiformis*, using the endpoint method. To verify the superinfection and its inhibition, 1×10^6 of *A. castellanii* cells were infected by mimivirus, moutovirus, or megavirus at MOI of 10, in T25 culture flasks. At different time points, Orpheovirus was inoculated in an MOI of 10. Four hours after this inoculation, the supernatants were collected and titrated in *V. vermiformis*, using the endpoint method (27). IF images obtained from this experiment are presented in both Fig. 4 and 6.

Chemical inhibitors and the reversion of superinfection

Different chemical inhibitors were used to investigate the reversion of superinfection in megavirus-infected cells, including cytochalasin D (a phagocytosis inhibitor), chloroquine (clathrin- and caveolin-dependent of acidification pathways inhibitors), and 5-(N-ethyl-N-isopropyl) amiloride (EIPA), a specific macropinocytosis inhibitor. Cytochalasin D and chloroquine had already been confirmed as inhibitors of endocytic pathways in *Acanthamoeba* (29, 30). A total of 5×10^5 *A. castellanii* trophozoites were infected with mimivirus, moutovirus, or megavirus, and 30 min after infection, the cells were washed with PBS to remove remained particles. Two hours post-infection, the cells were treated with different inhibitors of endocytic and phagocytic pathways: with 2 μ M of cytochalasin (Sigma-Aldrich, USA), 100 μ M of chloroquine (Sigma-Aldrich, USA), or 1 μ M of EIPA (Sigma-Aldrich, USA). The cytotoxicity of the inhibitors was tested in *Acanthamoeba*, and the choice of inhibitor concentrations was based on previous studies (9, 14). After 24 h of infection (22 h of treatment), the viral particles in the supernatant were quantified by the endpoint method. In this experiment, we verified the impact of inhibitors on viral progeny incorporation and its effect on the final titer in the culture supernatant.

ACKNOWLEDGMENTS

The authors would like to thank all colleagues from the Giant Viruses Study Group (www.giantviruses.com) and from Laboratório de Vírus of Universidade Federal de Minas Gerais (UFMG). Also, the authors thank Centro de Microscopia of UFMG for the contribution of microscopy images. The authors thank CNPq (Conselho Nacional de Desenvolvimento Científico e Tecnológico), CAPES (Coordenação de Aperfeiçoamento de Pessoal de Nível Superior), FAPEMIG (Fundação de Amparo à Pesquisa do estado de Minas Gerais), Pro-reitorias de Pós-graduação e Pesquisa da UFMG and the Centre for New Antibacterial Strategies (CANS) of the Arctic University of Norway (project ID #2520855). The manuscript text was corrected by artificial intelligence (ChatGPT). This research is registered at SISGEN. J.S.A., E.G.K., L.H.R., and D.G.S. are CNPq researchers.

AUTHOR AFFILIATIONS

¹Laboratório de Vírus, Instituto de Ciências Biológicas, Departamento de Microbiologia, Universidade Federal de Minas Gerais, Belo Horizonte, Minas Gerais, Brazil

²Laboratório de Virologia Básica e Aplicada (LVBA), Instituto de Ciências Biológicas, Universidade Federal de Minas Gerais, Belo Horizonte, Minas Gerais, Brazil

³Laboratory of Microorganism-Host Interaction, Department of Microbiology, Universidade Federal de Minas Gerais, Belo Horizonte, Minas Gerais, Brazil

⁴The Norwegian College of Fishery Science, Faculty of Biosciences, Fisheries and Economics, UiT - The Arctic University of Norway, Tromsø, Norway

⁵Departamento de Análises Clínicas e Toxicológicas, Faculdade de Farmácia, Universidade Federal de Minas Gerais (UFMG), Belo Horizonte, Minas Gerais, Brazil

⁶Laboratório de Microbiologia Polar e Conexões Tropicais, Departamento de Microbiologia, Instituto de Ciências Biológicas, Universidade Federal de Minas Gerais (UFMG), Belo Horizonte, Minas Gerais, Brazil

AUTHOR ORCID*s*

Daniele G. Souza  <http://orcid.org/0000-0002-7478-5934>

Gabriel M. F. Almeida  <http://orcid.org/0000-0003-2317-5092>

Erna Geessien Kroon  <http://orcid.org/0000-0003-2721-3826>

Jônatas S. Abrahão  <http://orcid.org/0000-0001-9420-1791>

FUNDING

Funder	Grant(s)	Author(s)
Conselho Nacional de Desenvolvimento Científico e Tecnológico (CNPq)	303680/2022-9	Jônatas S. Abrahão
Conselho Nacional de Desenvolvimento Científico e Tecnológico (CNPq)	443344/2023-0	Jônatas S. Abrahão
Coordenação de Aperfeiçoamento de Pessoal de Nível Superior (CAPES)	88882.348380/2010-1	Jônatas S. Abrahão

AUTHOR CONTRIBUTIONS

Isabella L. M. Aquino, Formal analysis, Investigation, Methodology, Writing – review and editing | Erik Sousa Reis, Investigation, Methodology, Writing – review and editing | Rafaella Oliveira Almeida Mattos Moreira, Methodology, Writing – review and editing | Nídia Esther Colquehuanca Arias, Investigation, Methodology, Writing – review and editing | Matheus Gomes Barcelos, Investigation, Methodology, Writing – review and editing | Victória Fulgêncio Queiroz, Methodology, Writing – review and editing | Raquel Duque do Nascimento Arifa, Methodology, Writing – review and editing | Larissa Mendes Barbosa Lucas, Methodology, Writing – review and editing | Juliana Miranda Tatará, Methodology, Writing – review and editing | Daniele G. Souza, Resources, Writing – review and editing | Adriana Costa, Resources, Writing – review and editing | Luiz Rosa, Project administration, Writing – review and editing | Gabriel M. F. Almeida, Resources, Writing – review and editing | Erna Geessien Kroon, Formal analysis, Resources, Writing – review and editing | Jônatas S. Abrahão, Conceptualization, Data curation, Formal analysis, Funding acquisition, Investigation, Methodology, Project administration, Resources, Supervision, Validation, Writing – original draft, Writing – review and editing

DATA AVAILABILITY

The data that support the findings of this study are available from the corresponding author, upon reasonable request.

REFERENCES

- Roossinck MJ. 2011. The good viruses: viral mutualistic symbioses. *Nat Rev Microbiol* 9:99–108. <https://doi.org/10.1038/nrmicro2491>
- Schwartz EJ, Biggs KRH, Bailes C, Ferolito KA, Vaidya NK. 2016. HIV dynamics with immune responses: perspectives from mathematical modeling. *Curr Clin Microbiol Rep* 3:216–224. <https://doi.org/10.1007/s40588-016-0049-z>
- Doceul V, Hollinshead M, van der Linden L, Smith GL. 2010. Repulsion of superinfecting virions: a mechanism for rapid virus spread. *Science* 327:873–876. <https://doi.org/10.1126/science.1183173>
- Christen L, Seto J, Niles EG. 1990. Superinfection exclusion of vaccinia virus in virus-infected cell cultures. *Virology* 174:35–42. [https://doi.org/10.1016/0042-6822\(90\)90051-r](https://doi.org/10.1016/0042-6822(90)90051-r)
- Hutchison CA, Sinsheimer RL. 1971. Requirement of protein synthesis for bacteriophage phi X174 superinfection exclusion. *J Virol* 8:121–124. <https://doi.org/10.1128/JVI.8.1.121-124.1971>
- Biggs KRH, Bailes CL, Scott L, Wichman HA, Schwartz EJ. 2021. Ecological approach to understanding superinfection inhibition in bacteriophage. *Viruses* 13:1389. <https://doi.org/10.3390/v13071389>
- La Scola B, Audic S, Robert C, Jungang L, de Lamballerie X, Drancourt M, Birtles R, Claverie J-M, Raoult D. 2003. A giant virus in amoebae. *Science* 299:2033. <https://doi.org/10.1126/science.1081867>
- Aylward FO, Abrahão JS, Brussaard CPD, Fischer MG, Moniruzzaman M, Ogata H, Suttle CA. 2023. Taxonomic update for giant viruses in the

- order Imitervirales (phylum Nucleocytoviricota). Arch Virol 168:283. <https://doi.org/10.1007/s00705-023-05906-3>
9. Andrade A, Rodrigues RAL, Oliveira GP, Andrade KR, Bonjardim CA, La Scola B, Kroon EG, Abrahão JS. 2017. Filling knowledge gaps for mimivirus entry, uncoating, and morphogenesis. J Virol 91:e01335-17. <https://doi.org/10.1128/JVI.01335-17>
 10. Suzan-Monti M, La Scola B, Barrassi L, Espinosa L, Raoult D. 2007. Ultrastructural characterization of the giant volcano-like virus factory of *Acanthamoeba polyphaga* mimivirus. PLoS One 2:e328. <https://doi.org/10.1371/journal.pone.0000328>
 11. Schrad JR, Abrahão JS, Cortines JR, Parent KN. 2020. Structural and proteomic characterization of the initiation of giant virus infection. Cell 181:1046–1061. <https://doi.org/10.1016/j.cell.2020.04.032>
 12. Mutsafi Y, Zauberman N, Sabanay I, Minsky A. 2010. Vaccinia-like cytoplasmic replication of the giant mimivirus. Proc Natl Acad Sci U S A 107:5978–5982. <https://doi.org/10.1073/pnas.0912737107>
 13. de Aquino ILM, Serafim MSM, Machado TB, Azevedo BL, Cunha DES, Ullmann LS, Araújo JP, Abrahão JS. 2023. Diversity of surface fibril patterns in mimivirus isolates. J Virol 97:e0182422. <https://doi.org/10.1128/jvi.01824-22>
 14. Silva LKDS, Andrade ACDSP, Dornas FP, Rodrigues RAL, Arantes T, Kroon EG, Bonjardim CA, Abrahão JS. 2018. Cedratvirus getuliensis replication cycle: an in-depth morphological analysis. Sci Rep 8:4000. <https://doi.org/10.1038/s41598-018-22398-3>
 15. Pereira Andrade A, Victor de Miranda Boratto P, Rodrigues RAL, Bastos TM, Azevedo BL, Dornas FP, Oliveira DB, Drumond BP, Kroon EG, Abrahão JS. 2019. New isolates of pandoraviruses: contribution to the study of replication cycle steps. J Virol 93:e01942-18. <https://doi.org/10.1128/JVI.01942-18>
 16. Arantes TS, Rodrigues RAL, Dos Santos Silva LK, Oliveira GP, de Souza HL, Khalil JYB, de Oliveira DB, Torres AA, da Silva LL, Colson P, Kroon EG, da Fonseca FG, Bonjardim CA, La Scola B, Abrahão JS. 2016. The large marseillevirus explores different entry pathways by forming giant infectious vesicles. J Virol 90:5246–5255. <https://doi.org/10.1128/JVI.00177-16>
 17. Souza F, Rodrigues R, Reis E, Lima M, La Scola B, Abrahão J. 2019. In-depth analysis of the replication cycle of Orpheovirus. Virol J 16:158. <https://doi.org/10.1186/s12985-019-1268-8>
 18. Folimonova SY. 2012. Superinfection exclusion is an active virus-controlled function that requires a specific viral protein. J Virol 86:5554–5561. <https://doi.org/10.1128/JVI.00310-12>
 19. Weisman RA, Korn ED. 1967. Phagocytosis of latex beads by *Acanthamoeba*. I. Biochemical properties. Biochemistry 6:485–497. <https://doi.org/10.1021/bi00854a017>
 20. Rodrigues RAL, Abrahão JS, Drumond BP, Kroon EG. 2016. Giants among larges: how gigantism impacts giant virus entry into amoebae. Curr Opin Microbiol 31:88–93. <https://doi.org/10.1016/j.mib.2016.03.009>
 21. Colson P, La Scola B, Levasseur A, Caetano-Anollés G, Raoult D. 2017. Mimivirus: leading the way in the discovery of giant viruses of amoebae. Nat Rev Microbiol 15:243–254. <https://doi.org/10.1038/nrmicro.2016.197>
 22. Oliveira G, Silva L, Leão T, Mougari S, da Fonseca FG, Kroon EG, La Scola B, Abrahão JS. 2019. Tupanvirus-infected amoebae are induced to aggregate with uninfected cells promoting viral dissemination. Sci Rep 9:183. <https://doi.org/10.1038/s41598-018-36552-4>
 23. Yoshikawa G, Blanc-Mathieu R, Song C, Kayama Y, Mochizuki T, Murata K, Ogata H, Takemura M. 2019. Medusavirus, a novel large DNA virus discovered from hot spring water. J Virol 93:e02130-18. <https://doi.org/10.1128/JVI.02130-18>
 24. Boratto P, Albarnaz JD, Almeida G de F, Botelho L, Fontes ACL, Costa AO, Santos D de A, Bonjardim CA, La Scola B, Kroon EG, Abrahão JS. 2015. *Acanthamoeba polyphaga* mimivirus prevents amoebal encystment-mediating serine proteinase expression and circumvents cell encystment. J Virol 89:2962–2965. <https://doi.org/10.1128/JVI.03177-14>
 25. Queiroz VF, Tatará JM, Botelho BB, Rodrigues RAL, Almeida G de F, Abrahão JS. 2024. The consequences of viral infection on protists. Commun Biol 7:306. <https://doi.org/10.1038/s42003-024-06001-2>
 26. Krupovic M, Dolja VV, Koonin EV. 2023. The virome of the last eukaryotic common ancestor and eukaryogenesis. Nat Microbiol 8:1008–1017. <https://doi.org/10.1038/s41564-023-01378-y>
 27. Dos Santos Silva LK, Rodrigues RAL, Dos Santos Pereira Andrade AC, Hikida H, Andreani J, Levasseur A, La Scola B, Abrahão JS. 2020. Isolation and genomic characterization of a new mimivirus of lineage B from a Brazilian river. Arch Virol 165:853–863. <https://doi.org/10.1007/s00705-020-04542-5>
 28. Rodrigues RAL, Andreani J, Andrade A, Machado TB, Abdi S, Levasseur A, Abrahão JS, La Scola B. 2018. Morphologic and genomic analyses of new isolates reveal a second lineage of cedratviruses. J Virol 92:e00372-18. <https://doi.org/10.1128/JVI.00372-18>
 29. Alsam S, Sissons J, Dudley R, Khan NA. 2005. Mechanisms associated with *Acanthamoeba castellanii* (T4) phagocytosis. Parasitol Res 96:402–409. <https://doi.org/10.1007/s00436-005-1401-z>
 30. Moon EK, Kim SH, Hong Y, Chung DI, Goo YK, Kong HH. 2015. Autophagy inhibitors as a potential anti-amoebic treatment for *Acanthamoeba* keratitis. Antimicrob Agents Chemother 59:4020–4025. <https://doi.org/10.1128/AAC.05165-14>

5- DISCUSSÃO

Desde o isolamento do primeiro mimivírus, APMV, em 2003, vários outros mimivírus e vírus gigantes que infectam amebas foram descritos na literatura (LA SCOLA *et al.*, 2003). Apesar de não ter se tornado um foco de estudo até então, é possível observar que diferenças morfológicas e genéticas entre estes isolados já eram exibidas por meio de imagens de microscopias eletrônicas (ME) das partículas e dos dados de sequenciamento e anotação dos genomas em trabalhos anteriores (ANDRADE *et al.*, 2018; ARSLAN *et al.*, 2011; DOS SANTOS SILVA *et al.*, 2020; LA SCOLA *et al.*, 2003).

Com base nessas observações, nas observações do banco de isolados do nosso grupo de pesquisa e no isolamento e caracterização de um novo isolado similar a mimivírus, decidimos tornar o estudo comparativo de diferentes mimivírus o foco deste trabalho. Durante o processo, nomeamos o novo vírus de megavírus caiporensis, fazendo menção à literatura folclórica brasileira e ao gênero ao qual foram relacionados por meio de análises de genoma e filogenias. Além disso, a caracterização morfológica desse isolado chamou nossa atenção acerca das fibrilas desses vírus, que exibem um padrão de organização em grumos (DE AQUINO *et al.*, 2023).

Durante nosso estudo, mostramos que existem pelo menos três padrões diferentes de fibrilas para mimivírus. Esses padrões estão ligados à forma como esses vírus são capazes de interagir com a ameba hospedeira, estimulando a fagocitose e iniciando a infecção no citoplasma (DE AQUINO *et al.*, 2023). Considerando que as fibrilas são estruturas importantes para a adesão ao hospedeiro (RODRIGUES *et al.*, 2015), vírus que apresentam maior quantidade de fibrilas homogeneamente distribuídas em torno de seus capsídeos, como os mimivírus, apresentarão uma maior superfície de contato para a adesão, levando conseqüentemente ao sucesso na penetração viral. Em contrapartida, os momouvírus, que exibem menos fibrilas e que não estão distribuídas ao longo de todo o capsídeo, sofrerão o efeito contrário, exibindo uma menor capacidade de estímulo da fagocitose pela ameba hospedeira desencadeada pela adesão mediada pelas fibrilas de superfície. Isso pode explicar os maiores títulos virais recuperados de inóculos de infecção em *Acanthamoeba* com momouvírus quando comparado à mimivírus e megavírus. Ou seja, uma quantidade menor de partículas de momouvírus foi capaz de estimular a fagocitose por adesão e penetrar no citoplasma hospedeiro, ficando disponível no sobrenadante titulado. Apesar de os megavírus apresentarem muitas fibrilas, a organização em forma de grumos também pode diminuir a superfície de contato desses vírus com a ameba hospedeira (DE AQUINO *et al.*, 2023). Ao fornecer

evidências de que a abundância das fibrilas está ligada à penetração dos vírus na célula hospedeira, esse trabalho corrobora dados anteriores da literatura sobre o papel das fibrilas de superfície dos mimivírus (RODRIGUES *et al.*, 2015). Além disso, é importante destacar que o número maior de isolados de mimivírus descritos relacionados à linhagem A (ANDRADE *et al.*, 2018; DORNAS *et al.*, 2015), possivelmente está ligado a um maior fitness conferido pelo padrão de organização de fibrilas apresentado por esses vírus.

Quanto à estrutura das fibrilas, mostramos que é possível encontrar diferenças a nível molecular nas proteínas R135, L829 e L725; relacionadas à composição das mesmas em trabalhos anteriores. A manutenção da topologia separando os isolados em linhagens A, B e C ao construirmos filogenias com base nas sequências de aminoácidos dessas proteínas, mostra que essas diferenças moleculares podem estar ligadas aos diferentes fenótipos aqui observados. Durante nossas análises, encontrar imagens de isolados relacionados à linhagem B de mimivírus se mostrou uma tarefa difícil, uma vez que são escassas na literatura. Por isso, apesar de o padrão B ter se mantido entre os nossos isolados, é importante que essa análise seja expandida. Com os resultados apresentados, propomos que o padrão de fibrilas pode ser utilizado como um marcador viral de relação com as linhagens A, B e C de mimivírus (ou mimi-, mimumou- e megavírus) e que podem servir como complementos para dados moleculares na caracterização de novos isolados (DE AQUINO *et al.*, 2023).

Ao expandir nossos estudos sobre fibrilas de superfície para os nucleocitovírus, percebemos o quão diversas essas estruturas podem ser. No entanto, é preciso destacar que a maior parte das informações encontradas na literatura são referentes às fibrilas de vírus gigantes que infectam amebas. Isso mostra a necessidade de se investir na busca por mais conhecimento acerca delas, como estruturas tridimensionais (3D) de fibrilas; expressão, purificação e obtenção de estruturas cristalizadas ou criomicroscopia eletrônica. Análises desse tipo podem ajudar a elucidar a organização estrutural das fibrilas. Atualmente, é possível encontrar imagens em alta resolução geradas por microscopia de força atômica de fibrilas do APMV na literatura, que são a maior fonte de conhecimento acerca da composição bioquímica dessas estruturas (BOYER *et al.*, 2011). Uma vez que aqui apontamos que existem diferenças morfológicas entre as fibrilas de mimivírus, mimumovírus e megavírus, é de interesse que se realize análises futuras como essas para se compreender a composição bioquímica das fibrilas de vírus relacionados aos outros dois gêneros. Aprofundar os estudos sobre a composição genética das fibrilas é de suma importância, bem como a utilização de outros modelos que não o APMV para diversificar nosso conhecimento acerca dessas estruturas e sua evolução (AQUINO *et al.*, 2023).

Assim como o estudo de fibrilas, o ciclo dos mimivírus mais bem estudado teve como modelo o APMV (ANDRADE *et al.*, 2017; SUZAN-MONTI *et al.*, 2007). Apesar de os trabalhos que descrevem isolados de mimi, moomou e megavírus muitas vezes citarem as etapas críticas do ciclo desses vírus e às vezes até ilustrar (ARSLAN *et al.*, 2011; DOS SANTOS SILVA *et al.*, 2020; YOOSUF *et al.*, 2012), poucos se aprofundam em ciclos de representantes de um dos dois outros gêneros, como encontramos para *Mimivirus*. Dessa forma, procurando contribuir com mais informações sobre o ciclo dos megavírus, decidimos que analisaríamos o ciclo desse vírus de forma mais profunda, principalmente após notarmos nas etapas de multiplicação viral do m. caiporensis que esse isolado parecia ser mais lento quando comparado ao APMV na produção de novas partículas virais. O ciclo do m. caiporensis se assemelha muito ao descrito para o megavírus chilensis, trabalho no qual Arslan e colaboradores (2011) já haviam demonstrado que a duração do ciclo é maior em comparação ao APMV (ARSLAN *et al.*, 2011). Com uma duração de 17 horas em comparação a 12h do APMV (ARSLAN *et al.*, 2011), os megavírus são mais lentos, e no caso do nosso isolado, um pouco mais, uma vez que por volta de 20 h.p.i em uma MOI de 10, é que observamos o rompimento massivo de células infectadas com o nosso isolado em imagens geradas por MET (AQUINO *et al.*, 2024).

Após observarmos, durante o estudo do ciclo, a presença de partículas dentro de vesículas a partir de 6 h.p.i e adiante, sendo visualizadas até 24 h.p.i, analisamos a possibilidade de exocitose como forma de liberação, algo que poderia ser inédito para mimivírus em geral. Porém, em nossos resultados essa possibilidade foi descartada, mostrando mais uma vez a similaridade do ciclo do m. caiporensis com o m. chilensis, onde a liberação de partículas foi descrita como lise celular (ARSLAN *et al.*, 2011). Descartada a hipótese de exocitose, partimos para a pesquisa da possibilidade de superinfecção de *Acanthamoeba castellanii* por megavirus caiporensis e de as vesículas se tratarem na verdade de fagossomos. Até então, não havia sido descrito esse fenômeno ou sua inibição relacionado a vírus gigantes que infectam amebas, mas sim para outro nucleocitovírus, o vaccínia vírus, também em bacteriófagos e para o vírus HIV (CHRISTEN *et al.*, 1990; DOCEUL *et al.*, 2010; HUTCHISON; SINSHEIMER, 1971; SCHWARTZ *et al.*, 2016). Nossos resultados mostraram que não só esse fenômeno pode ser encontrado para vírus gigantes de amebas, como existe uma diferença na interação dos vírus com a célula hospedeira que permita ou não a ocorrência da superinfecção. Pela primeira vez, descrevemos que mimivírus e moomouvírus são capazes de induzir a inibição da superinfecção de *A. castellanii* ao impedirem a fagocitose após a penetração, estimulando mudanças celulares significativas como a redução do tamanho e a inibição da formação de vacúolos e pseudópodes pela célula hospedeira. Já os megavírus não inibem o processo, e uma consequência disso é a

incorporação constante de partículas virais exógenas até os estágios finais do ciclo. No entanto, esta propriedade pode ser revertida quando um inibidor farmacológico da fagocitose é empregado (AQUINO *et al.*, 2024).

Ao observarmos partículas dentro de fagossomos sofrendo desnudamento 12 h.p.i, liberando seus genomas e proteínas virais em um citoplasma já em estágios finais da morfogênese de novas partículas, entendemos que parte da progênie recém-formada é prontamente fagocitada e sofre desnudamento em células já infectadas. Porém, não observamos em nossas análises de imagens por microscopia eletrônica de transmissão (MET) mais de uma fábrica viral, sugerindo que partículas exógenas fagocitadas não são capazes de causar uma infecção produtiva e resultar na formação de progênie. Ao pensarmos pela perspectiva da população de amebas, a fagocitose de partículas recém-formadas de megavírus poderia ser considerada um processo antiviral, uma vez que a quantidade reduzida de partículas virais no meio extracelular diminui a chance de infecção das células vizinhas saudáveis. Possivelmente, os mimi e moumouvírus superaram esta desvantagem desenvolvendo mecanismos para controlar a atividade fagocítica de seus hospedeiros (AQUINO *et al.*, 2024).

Esse trabalho contribui com informações pioneiras e adicionais sobre o estudo dos vírus gigantes e de nucleocitovírus. Ao buscar informações sobre a morfologia, biologia, genética, filogenia e relações ecológicas e com o hospedeiro, nos aproximamos mais alguns passos para a compreensão da evolução de vírus gigantes.

6- CONCLUSÕES

- Descrevemos pela primeira vez diferentes padrões de organização para fibrilas de superfície de mimi-, mougou- e megavírus, que se diferem de acordo a linhagem/gênero com o qual estão intimamente relacionados;
- O sequenciamento do genoma e análise filogenética indica o megavírus caiporensis como um mimivírus pertencente à linhagem C/gênero *Megavirus*;
- Mostramos que a abundância e organização das fibrilas parece estar relacionada com a capacidade de adesão e conseqüentemente desencadeamento de fagocitose e penetração na ameba hospedeira;
- Encontramos diferenças importantes nas sequências de aminoácido preditas para proteína mais abundante relacionada às fibrilas, GMC-oxidoreductase (gene R135), ao compararmos diversos isolados pertencentes aos mimi-, mougou- e megavírus;
- O estudo das fibrilas sugere que estas podem representar um possível marcador para identificação de mimi-, mougou- e megavírus;
- O estudo do ciclo do megavirus caiporensis mostrou que apesar de partículas terem sido observadas em vesículas em estágios tardios, esses vírus não são liberados por exocitose;
- Demonstramos pela primeira vez, a existência do processo de superinfecção por vírus gigantes que infectam amebas, e sua inibição;
- Mimivírus e mougovírus induzem o bloqueio da superinfecção em amebas por meio da inibição da fagocitose, causando redução do volume celular e inibindo a formação de vacúolos e pseudópodes;

- Megavírus não são capazes de induzir o bloqueio da fagocitose e conseqüentemente, a superinfecção, permitindo a incorporação contínua de vírions recém-formados, afetando negativamente a progênie viral disponível;
- Apesar do parentesco evolutivo, mimi-/moumou- e megavírus exibem diferenças profundas em suas interações com a ameba hospedeira.

7- PERSPECTIVAS

- Explorar a fibrila de outros vírus gigantes, em relação à morfologia, composição, etc;
- Explorar a composição molecular e a diversidade morfológica das fibrilas de mousmouvírus e megavírus;
- Explorar a superinfecção em outros vírus de amebas, incluindo aqueles que penetram utilizando mecanismos diferentes da fagocitose;
- Analisar quais genes estão envolvidos com a inibição da superinfecção em mimivírus;
- Avaliar a natureza da superinfecção em megavírus, incluindo a possibilidade de se tratar de um mecanismo antiviral de *Acanthamoeba*.

REFERÊNCIAS

- ABERGEL, C.; LEGENDRE, M.; CLAVERIE, J.-M. The rapidly expanding universe of giant viruses: Mimivirus, Pandoravirus, Pithovirus and Mollivirus. **FEMS microbiology reviews**, [s. l.], v. 39, n. 6, p. 779–796, 2015.
- ABERGEL, C.; RUDINGER-THIRION, J.; GIEGÉ, R.; CLAVERIE, J.-M. Virus-encoded aminoacyl-tRNA synthetases: structural and functional characterization of mimivirus TyrRS and MetRS. **Journal of Virology**, [s. l.], v. 81, n. 22, p. 12406–12417, 2007.
- ABRAHÃO, J. S.; ARAÚJO, R.; COLSON, P.; SCOLA, B. L. The analysis of translation-related gene set boosts debates around origin and evolution of mimiviruses. **PLOS Genetics**, [s. l.], v. 13, n. 2, p. e1006532, 2017.
- ABRAHÃO, J. S.; DORNAS, F. P.; SILVA, L. C. F.; ALMEIDA, G. M.; BORATTO, P. V. M.; COLSON, P.; LA SCOLA, B.; KROON, E. G. Acanthamoeba polyphaga mimivirus and other giant viruses: an open field to outstanding discoveries. **Virology Journal**, [s. l.], v. 11, p. 120, 2014.
- ABRAHÃO, J.; SILVA, L.; SILVA, L. S.; KHALIL, J. Y. B.; RODRIGUES, R.; ARANTES, T.; ASSIS, F.; BORATTO, P.; ANDRADE, M.; KROON, E. G.; RIBEIRO, B.; BERGIER, I.; SELIGMANN, H.; GHIGO, E.; COLSON, P.; LEVASSEUR, A.; KROEMER, G.; RAOULT, D.; LA SCOLA, B. Tailed giant Tupanvirus possesses the most complete translational apparatus of the known virosphere. **Nature Communications**, [s. l.], v. 9, n. 1, p. 749, 2018.
- ANDRADE, A. C. D. S. P.; ARANTES, T. S.; RODRIGUES, R. A. L.; MACHADO, T. B.; DORNAS, F. P.; LANDELL, M. F.; FURST, C.; BORGES, L. G. A.; DUTRA, L. A. L.; ALMEIDA, G.; TRINDADE, G. de S.; BERGIER, I.; ABRAHÃO, W.; BORGES, I. A.; CORTINES, J. R.; DE OLIVEIRA, D. B.; KROON, E. G.; ABRAHÃO, J. S. Ubiquitous giants: a plethora of giant viruses found in Brazil and Antarctica. **Virology Journal**, [s. l.], v. 15, n. 1, p. 22, 2018.
- ANDRADE, A. C. D. S. P.; RODRIGUES, R. A. L.; OLIVEIRA, G. P.; ANDRADE, K. R.; BONJARDIM, C. A.; LA SCOLA, B.; KROON, E. G.; ABRAHÃO, J. S. Filling Knowledge Gaps for Mimivirus Entry, Uncoating, and Morphogenesis. **Journal of Virology**, [s. l.], v. 91, n. 22, p. e01335-17, 2017.
- ANDREANI, J.; KHALIL, J. Y. B.; BAPTISTE, E.; HASNI, I.; MICHELLE, C.; RAOULT, D.; LEVASSEUR, A.; LA SCOLA, B. Orpheovirus IHUMI-LCC2: A New Virus among the Giant Viruses. **Frontiers in Microbiology**, [s. l.], v. 8, 2018. Disponível em: <https://www.frontiersin.org/articles/10.3389/fmicb.2017.02643>. Acesso em: 29 nov. 2022.
- AQUINO, I. L. M. de; BARCELOS, M. G.; MACHADO, T. B.; SERAFIM, M. S. M.; ABRAHÃO, J. S. Surface fibrils on the particles of nucleocytoviruses: A review. **Experimental Biology and Medicine (Maywood, N.J.)**, [s. l.], v. 248, n. 22, p. 2045–2052, 2023.
- AQUINO, I. L. M.; REIS, E. S.; MOREIRA, R. O. A. M.; ARIAS, N. E. C.; BARCELOS, M. G.; QUEIROZ, V. F.; ARIFA, R. D. do N.; LUCAS, L. M. B.; TATARA, J. M.; SOUZA, D. G.; COSTA, A.; ROSA, L.; ALMEIDA, G. M. F.; KROON, E. G.; ABRAHÃO, J. S. Giant viruses inhibit superinfection by downregulating phagocytosis in Acanthamoeba. **Journal of Virology**, [s. l.], v. 98, n. 10, p. e0104524, 2024.

- ARSLAN, D.; LEGENDRE, M.; SELTZER, V.; ABERGEL, C.; CLAVERIE, J.-M. Distant Mimivirus relative with a larger genome highlights the fundamental features of Megaviridae. **Proceedings of the National Academy of Sciences of the United States of America**, [s. l.], v. 108, n. 42, p. 17486–17491, 2011.
- BAJRAI, L. H.; DE ASSIS, F. L.; AZHAR, E. I.; JARDOT, P.; ROBERT, C.; ABRAHÃO, J.; RAOULT, D.; LA SCOLA, B. Saudi Mousmouvirus, the First Group B Mimivirus Isolated from Asia. **Frontiers in Microbiology**, [s. l.], v. 7, 2016. Disponível em: <https://www.frontiersin.org/articles/10.3389/fmicb.2016.02029>. Acesso em: 26 set. 2022.
- BANDARU, V.; ZHAO, X.; NEWTON, M. R.; BURROWS, C. J.; WALLACE, S. S. Human endonuclease VIII-like (NEIL) proteins in the giant DNA Mimivirus. **DNA repair**, [s. l.], v. 6, n. 11, p. 1629–1641, 2007.
- BARIK, S. A Family of Novel Cyclophilins, Conserved in the Mimivirus Genus of the Giant DNA Viruses. **Computational and Structural Biotechnology Journal**, [s. l.], v. 16, p. 231–236, 2018.
- BOYER, M.; AZZA, S.; BARRASSI, L.; KLOSE, T.; CAMPOCASSO, A.; PAGNIER, I.; FOURNOUS, G.; BORG, A.; ROBERT, C.; ZHANG, X.; DESNUES, C.; HENRISSAT, B.; ROSSMANN, M. G.; LA SCOLA, B.; RAOULT, D. Mimivirus shows dramatic genome reduction after intraamoebal culture. **Proceedings of the National Academy of Sciences of the United States of America**, [s. l.], v. 108, n. 25, p. 10296–10301, 2011.
- BOYER, M.; YUTIN, N.; PAGNIER, I.; BARRASSI, L.; FOURNOUS, G.; ESPINOSA, L.; ROBERT, C.; AZZA, S.; SUN, S.; ROSSMANN, M. G.; SUZAN-MONTI, M.; LA SCOLA, B.; KOONIN, E. V.; RAOULT, D. Giant Marseillevirus highlights the role of amoebae as a melting pot in emergence of chimeric microorganisms. **Proceedings of the National Academy of Sciences of the United States of America**, [s. l.], v. 106, n. 51, p. 21848–21853, 2009.
- CAMPOS, R. K.; BORATTO, P. V.; ASSIS, F. L.; AGUIAR, E. R. G. R.; SILVA, L. C. F.; ALBARNAZ, J. D.; DORNAS, F. P.; TRINDADE, G. S.; FERREIRA, P. P.; MARQUES, J. T.; ROBERT, C.; RAOULT, D.; KROON, E. G.; LA SCOLA, B.; ABRAHÃO, J. S. Samba virus: a novel mimivirus from a giant rain forest, the Brazilian Amazon. **Virology Journal**, [s. l.], v. 11, p. 95, 2014.
- CHRISTEN, L.; SETO, J.; NILES, E. G. Superinfection exclusion of vaccinia virus in virus-infected cell cultures. **Virology**, [s. l.], v. 174, n. 1, p. 35–42, 1990.
- COLSON, P.; LAMBALLERIE, X. de; FOURNOUS, G.; RAOULT, D. Reclassification of Giant Viruses Composing a Fourth Domain of Life in the New Order Megavirales. **Intervirology**, [s. l.], v. 55, n. 5, p. 321–332, 2012.
- DE AQUINO, I. L. M.; SERAFIM, M. S. M.; MACHADO, T. B.; AZEVEDO, B. L.; CUNHA, D. E. S.; ULLMANN, L. S.; ARAÚJO, J. P.; ABRAHÃO, J. S. Diversity of Surface Fibril Patterns in Mimivirus Isolates. **Journal of Virology**, [s. l.], v. 97, n. 2, p. e0182422, 2023.
- DESNUES, C.; LA SCOLA, B.; YUTIN, N.; FOURNOUS, G.; ROBERT, C.; AZZA, S.; JARDOT, P.; MONTEIL, S.; CAMPOCASSO, A.; KOONIN, E. V.; RAOULT, D. Provirophages and transpovirons as the diverse mobilome of giant viruses. **Proceedings of the National Academy of Sciences of the United States of America**, [s. l.], v. 109, n. 44, p. 18078–18083, 2012.

- DOCEUL, V.; HOLLINSHEAD, M.; VAN DER LINDEN, L.; SMITH, G. L. Repulsion of superinfecting virions: a mechanism for rapid virus spread. **Science (New York, N.Y.)**, [s. l.], v. 327, n. 5967, p. 873–876, 2010.
- DORNAS, F. P.; KHALIL, J. Y. B.; PAGNIER, I.; RAOULT, D.; ABRAHÃO, J.; LA SCOLA, B. Isolation of new Brazilian giant viruses from environmental samples using a panel of protozoa. **Frontiers in Microbiology**, [s. l.], v. 6, p. 1086, 2015.
- DOS SANTOS SILVA, L. K.; RODRIGUES, R. A. L.; DOS SANTOS PEREIRA ANDRADE, A. C.; HIKIDA, H.; ANDREANI, J.; LEVASSEUR, A.; LA SCOLA, B.; ABRAHÃO, J. S. Isolation and genomic characterization of a new mimivirus of lineage B from a Brazilian river. **Archives of Virology**, [s. l.], v. 165, n. 4, p. 853–863, 2020.
- HAKIM, M.; EZERINA, D.; ALON, A.; VONSHAK, O.; FASS, D. Exploring ORFan domains in giant viruses: structure of mimivirus sulfhydryl oxidase R596. **PLoS One**, [s. l.], v. 7, n. 11, p. e50649, 2012.
- HUTCHISON, C. A.; SINSHEIMER, R. L. Requirement of protein synthesis for bacteriophage phi X174 superinfection exclusion. **Journal of Virology**, [s. l.], v. 8, n. 1, p. 121–124, 1971.
- IYER, L. M.; ARAVIND, L.; KOONIN, E. V. Common origin of four diverse families of large eukaryotic DNA viruses. **Journal of Virology**, [s. l.], v. 75, n. 23, p. 11720–11734, 2001.
- KLOSE, T.; KUZNETSOV, Y. G.; XIAO, C.; SUN, S.; MCPHERSON, A.; ROSSMANN, M. G. The three-dimensional structure of Mimivirus. **Intervirology**, [s. l.], v. 53, n. 5, p. 268–273, 2010.
- KOONIN, E. V. Virology: Gulliver among the Lilliputians. **Current biology: CB**, [s. l.], v. 15, n. 5, p. R167-169, 2005.
- KUZNETSOV, Y. G.; KLOSE, T.; ROSSMANN, M.; MCPHERSON, A. Morphogenesis of mimivirus and its viral factories: an atomic force microscopy study of infected cells. **Journal of Virology**, [s. l.], v. 87, n. 20, p. 11200–11213, 2013.
- LA SCOLA, B.; AUDIC, S.; ROBERT, C.; JUNGANG, L.; DE LAMBALLERIE, X.; DRANCOURT, M.; BIRTLES, R.; CLAVERIE, J.-M.; RAOULT, D. A giant virus in amoebae. **Science (New York, N.Y.)**, [s. l.], v. 299, n. 5615, p. 2033, 2003.
- LEGENDRE, M.; AUDIC, S.; POIROT, O.; HINGAMP, P.; SELTZER, V.; BYRNE, D.; LARTIGUE, A.; LESCOT, M.; BERNADAC, A.; POULAIN, J.; ABERGEL, C.; CLAVERIE, J.-M. mRNA deep sequencing reveals 75 new genes and a complex transcriptional landscape in Mimivirus. **Genome Research**, [s. l.], v. 20, n. 5, p. 664–674, 2010.
- LEGENDRE, M.; LARTIGUE, A.; BERTAUX, L.; JEUDY, S.; BARTOLI, J.; LESCOT, M.; ALEMPIC, J.-M.; RAMUS, C.; BRULEY, C.; LABADIE, K.; SHMAKOVA, L.; RIVKINA, E.; COUTÉ, Y.; ABERGEL, C.; CLAVERIE, J.-M. In-depth study of Mollivirus sibericum, a new 30,000-y-old giant virus infecting Acanthamoeba. **Proceedings of the National Academy of Sciences of the United States of America**, [s. l.], v. 112, n. 38, p. E5327-5335, 2015.
- LUTHER, K. B.; HÜLSMEIER, A. J.; SCHEGG, B.; DEUBER, S. A.; RAOULT, D.; HENNET, T. Mimivirus collagen is modified by bifunctional lysyl hydroxylase and glycosyltransferase enzyme. **The Journal of Biological Chemistry**, [s. l.], v. 286, n. 51, p. 43701–43709, 2011.
- MACHADO, T. B.; PICORELLI, A. C. R.; DE AZEVEDO, B. L.; DE AQUINO, I. L. M.; QUEIROZ, V. F.; RODRIGUES, R. A. L.; ARAÚJO, J. P.; ULLMANN, L. S.; DOS SANTOS, T. M.; MARQUES, R. E.; GUIMARÃES, S. L.; ANDRADE, A. C. S. P.; GULARTE, J. S.;

DEMOLINER, M.; FILIPPI, M.; PEREIRA, V. M. A. G.; SPILKI, F. R.; KRUPOVIC, M.; AYLWARD, F. O.; DEL-BEM, L.-E.; ABRAHÃO, J. S. Gene duplication as a major force driving the genome expansion in some giant viruses. **Journal of Virology**, [s. l.], v. 97, n. 12, p. e0130923, 2023.

MUTSAFI, Y.; SHIMONI, E.; SHIMON, A.; MINSKY, A. Membrane assembly during the infection cycle of the giant Mimivirus. **PLoS pathogens**, [s. l.], v. 9, n. 5, p. e1003367, 2013.

RAOULT, D.; AUDIC, S.; ROBERT, C.; ABERGEL, C.; RENESTO, P.; OGATA, H.; LA SCOLA, B.; SUZAN, M.; CLAVERIE, J.-M. The 1.2-megabase genome sequence of Mimivirus. **Science (New York, N.Y.)**, [s. l.], v. 306, n. 5700, p. 1344–1350, 2004.

RODRIGUES, R. A. L.; DOS SANTOS SILVA, L. K.; DORNAS, F. P.; DE OLIVEIRA, D. B.; MAGALHÃES, T. F. F.; SANTOS, D. A.; COSTA, A. O.; DE MACÊDO FARIAS, L.; MAGALHÃES, P. P.; BONJARDIM, C. A.; KROON, E. G.; LA SCOLA, B.; CORTINES, J. R.; ABRAHÃO, J. S. Mimivirus Fibrils Are Important for Viral Attachment to the Microbial World by a Diverse Glycoside Interaction Repertoire. **Journal of Virology**, [s. l.], v. 89, n. 23, p. 11812–11819, 2015.

ROOSSINCK, M. J. The good viruses: viral mutualistic symbioses. **Nature Reviews. Microbiology**, [s. l.], v. 9, n. 2, p. 99–108, 2011.

SAINI, H. K.; FISCHER, D. Structural and functional insights into Mimivirus ORFans. **BMC genomics**, [s. l.], v. 8, p. 115, 2007.

SCHRAD, J. R.; ABRAHÃO, J. S.; CORTINES, J. R.; PARENT, K. N. Structural and Proteomic Characterization of the Initiation of Giant Virus Infection. **Cell**, [s. l.], v. 181, n. 5, p. 1046-1061.e6, 2020.

SCHWARTZ, E. J.; BIGGS, K. R. H.; BAILES, C.; FEROLITO, K. A.; VAIDYA, N. K. HIV Dynamics With Immune Responses: Perspectives From Mathematical Modeling. **Current Clinical Microbiology Reports**, [s. l.], v. 3, n. 4, p. 216–224, 2016.

SHUKLA, A.; CHATTERJEE, A.; KONDABAGIL, K. The number of genes encoding repeat domain-containing proteins positively correlates with genome size in amoebal giant viruses. **Virus Evolution**, [s. l.], v. 4, n. 1, p. vex039, 2018.

SILVA, L. C. F.; ALMEIDA, G. M. F.; ASSIS, F. L.; ALBARNAZ, J. D.; BORATTO, P. V. M.; DORNAS, F. P.; ANDRADE, K. R.; LA SCOLA, B.; KROON, E. G.; DA FONSECA, F. G.; ABRAHÃO, J. S. Modulation of the expression of mimivirus-encoded translation-related genes in response to nutrient availability during *Acanthamoeba castellanii* infection. **Frontiers in Microbiology**, [s. l.], v. 6, p. 539, 2015.

SOBHY, H.; SCOLA, B. L.; PAGNIER, I.; RAOULT, D.; COLSON, P. Identification of giant Mimivirus protein functions using RNA interference. **Frontiers in Microbiology**, [s. l.], v. 6, p. 345, 2015.

SUZAN-MONTI, M.; LA SCOLA, B.; RAOULT, D. Genomic and evolutionary aspects of Mimivirus. **Virus Research**, [s. l.], v. 117, n. 1, Comparative Genomics and Evolution of Complex Viruses, p. 145–155, 2006.

SUZAN-MONTI, M.; SCOLA, B. L.; BARRASSI, L.; ESPINOSA, L.; RAOULT, D. Ultrastructural Characterization of the Giant Volcano-like Virus Factory of *Acanthamoeba polyphaga* Mimivirus. **PLOS ONE**, [s. l.], v. 2, n. 3, p. e328, 2007.

TAKAHASHI, H.; FUKAYA, S.; SONG, C.; MURATA, K.; TAKEMURA, M. Morphological and Taxonomic Properties of the Newly Isolated Cotonvirus japonicus, a New Lineage of the Subfamily Megavirinae. **Journal of Virology**, [s. l.], v. 95, n. 18, p. 10.1128/jvi.00919-21, 2021.

THAI, V.; RENESTO, P.; FOWLER, C. A.; BROWN, D. J.; DAVIS, T.; GU, W.; POLLOCK, D. D.; KERN, D.; RAOULT, D.; EISENMESSER, E. Z. Structural, biochemical, and in vivo characterization of the first virally encoded cyclophilin from the Mimivirus. **Journal of Molecular Biology**, [s. l.], v. 378, n. 1, p. 71–86, 2008.

VILLALTA, A.; SCHMITT, A.; ESTROZI, L. F.; QUEMIN, E. R. J.; ALEMPIC, J.-M.; LARTIGUE, A.; PRAŽÁK, V.; BELMUDES, L.; VASISHTAN, D.; COLMANT, A. M. G.; HONORÉ, F. A.; COUTÉ, Y.; GRÜNEWALD, K.; ABERGEL, C. **The giant Mimivirus 1.2 Mb genome is elegantly organized into a 30 nm helical protein shield**. [S. l.]: bioRxiv, 2022. Disponível em: <https://www.biorxiv.org/content/10.1101/2022.02.17.480895v1>. Acesso em: 12 jul. 2022.

XIAO, C.; CHIPMAN, P. R.; BATTISTI, A. J.; BOWMAN, V. D.; RENESTO, P.; RAOULT, D.; ROSSMANN, M. G. Cryo-electron Microscopy of the Giant Mimivirus. **Journal of Molecular Biology**, [s. l.], v. 353, n. 3, p. 493–496, 2005.

XIAO, C.; KUZNETSOV, Y. G.; SUN, S.; HAFENSTEIN, S. L.; KOSTYUCHENKO, V. A.; CHIPMAN, P. R.; SUZAN-MONTI, M.; RAOULT, D.; MCPHERSON, A.; ROSSMANN, M. G. Structural studies of the giant mimivirus. **PLoS biology**, [s. l.], v. 7, n. 4, p. e92, 2009.

YOOSUF, N.; YUTIN, N.; COLSON, P.; SHABALINA, S. A.; PAGNIER, I.; ROBERT, C.; AZZA, S.; KLOSE, T.; WONG, J.; ROSSMANN, M. G.; LA SCOLA, B.; RAOULT, D.; KOONIN, E. V. Related giant viruses in distant locations and different habitats: Acanthamoeba polyphaga moutoumavirus represents a third lineage of the Mimiviridae that is close to the megavirus lineage. **Genome Biology and Evolution**, [s. l.], v. 4, n. 12, p. 1324–1330, 2012.

YUTIN, N.; WOLF, Y. I.; RAOULT, D.; KOONIN, E. V. Eukaryotic large nucleo-cytoplasmic DNA viruses: clusters of orthologous genes and reconstruction of viral genome evolution. **Virology Journal**, [s. l.], v. 6, p. 223, 2009.

ZAUBERMAN, N.; MUTSAFI, Y.; HALEVY, D. B.; SHIMONI, E.; KLEIN, E.; XIAO, C.; SUN, S.; MINSKY, A. Distinct DNA Exit and Packaging Portals in the Virus Acanthamoeba polyphaga mimivirus. **PLOS Biology**, [s. l.], v. 6, n. 5, p. e114, 2008.

EVENTOS CIENTÍFICOS E PRODUÇÕES

Participações em eventos científicos

- Participação e submissão de resumo expandido no VIII Simpósio de Microbiologia da UFMG- ConectaSIM, 2021, Online.
- Participação no XXXII Congresso Brasileiro de Virologia e XVI Encontro de Virologia do Mercosul, 2021, Online.
- Participação e apresentação oral concorrendo ao melhor trabalho na categoria de Virologia Básica no XXXIII Congresso Brasileiro de Virologia e XVII Encontro de Virologia do Mercosul, 2022, Bahia.
- Participação e apresentação de pôster no IX Simpósio de Microbiologia da UFMG- A Microbiologia no Brasil: a ciência de hoje para soluções dos problemas de amanhã, 2022, Belo Horizonte.
- Participação no Curso de Inverno em Bioinformática 2023 da UFMG, 2023, Belo Horizonte.
- Participação e apresentação de pôster no V FAMERP- UTMB: Emerging infections in the Americas- Common interests and collaboration between North-South, 2023, São José do Rio Preto/SP.
- Participação da comissão avaliadora da XXXII Semana da Iniciação Científica da UFMG, 2023, Belo Horizonte;
- Participação e apresentação oral concorrendo ao prêmio Helio Gelli Pereira no XXXIV Congresso Brasileiro de Virologia e XVIII Encontro de Virologia do Mercosul, 2023, Ouro Preto.
- Participação e apresentação oral concorrendo ao prêmio Cláudio Bonjardim no XI Simpósio de Microbiologia da UFMG-, 2023, Belo Horizonte.

Formação complementar

- Minicurso Filogenia Viral (4h) no Curso de Inverno em Bioinformática 2023 da UFMG, 2023, Belo Horizonte.

- Treinamento teórico/prático sobre biossegurança e trabalho em laboratório de biossegurança nível 3 (20h). Laboratório NB3- ICB, UFMG, 2024, Belo Horizonte.
- Treinamento de Gestão de Calibração (6h), 2024, Novus Gestão Empresarial, online.

Atividades de extensão

- Participação como analista de laboratório voluntária no enfrentamento a pandemia de coronavírus pela iniciativa Rede de Laboratórios – UFMG, 2021, Laboratório de Vírus, Belo Horizonte.
- Construção de um modelo 3D de Tupanvírus para apresentação na Mostra de Profissões da UFMG 2023, Belo Horizonte.
- Produção de banner contendo imagens de microscopias eletrônicas de Tupanvírus para apresentação na Mostra de Profissões da UFMG 2023, Belo Horizonte.

Atividades didáticas

- Produção, gravação e edição de três aulas de virologia com 1h de duração para o Curso de Especialização em Diagnóstico Microbiológico do Programa de Pós-Graduação em Microbiologia da UFMG, 2023, sobre os seguintes conteúdos:
 - Arboviroses: Dengue, Zika e Chikungunya
 - Influenza e Paramixovírus
 - Sarampo, Caxumba e Rubéola

Coorientação

- Coorientação da aluna de iniciação científica e graduanda em Ciências Biológicas pela UFMG, Rafaella Oliveira Almeida Mattos Moreira. Projeto intitulado: Prospecção de Vírus Gigantes em Biomas Brasileiros. 2022, Laboratório de Vírus, Belo Horizonte.

Participação em bancas

- Participação em banca de defesa de Trabalho de Conclusão de Curso (Graduação em Ciências Biológicas) de Douglas Fernandes Lourenço. Caracterização genômica de vírus gigantes da família *Phycodnaviridae*: Prospecção *in silico* de enzimas virais para aplicação biotecnológica. 2023, Universidade Federal de Minas Gerais, Belo Horizonte.

Artigos científicos publicados

1. **AQUINO, ISABELLA L.M.**; REIS, ERIK V.S.; MOREIRA, RAFAELLA O.A.M.; ARIAS, NIDIA E.C.; BARCELOS, MATHEUS G.; QUEIROZ, VICTÓRIA F.; ARIFA, RAQUEL D.; LUCAS, LARISSA M.B.; TATARA, JULIANA M.; SOUZA, DANIELLE G.; COSTA, ADRIANA O.; ROSA, LUIZ H.; ALMEIDA, GABRIEL M.F.; KROON, ERNA G.; ABRAHÃO, JÔNATAS S. Giant viruses inhibit superinfection by downregulating phagocytosis in *Acanthamoeba*. *Journal of Virology*, v. 98, p. e0104524, 2024.
2. DE AZEVEDO, BRUNA L.; QUEIROZ, VICTÓRIA F.; **DE AQUINO, ISABELLA L.M.**; MACHADO, TALITA B.; DE ASSIS, FELIPE L.; REIS, ERIK; ARAÚJO JR, JOÃO P.; ULLMANN, LEILA S.; COLSON, PHILIPPE; GREUB, GILBERT; AYLWARD, FRANK; RODRIGUES, RODRIGO A.L.; ABRAHÃO, JÔNATAS S. The genomic and phylogenetic analysis of *Marseillevirus cajuinensis* raises questions about the evolution of *Marseilleviridae* lineages and their taxonomical organization. *Journal of Virology*, v. 98, p. e0051324, 2024.
3. MACHADO, TALITA B.; **DE AQUINO, ISABELLA L.M.**; AZEVEDO, BRUNA L.; SERAFIM, MATEUS S.; BARCELOS, MATHEUS G.; ANDRADE, ANA CLÁUDIA S.P.; REIS, ERIK V.; ULLMANN, LEILA S.; ARAÚJO JR., JOÃO P.; COSTA, ADRIANA O.; ROSA, LUIZ H.; ABRAHÃO, JÔNATAS S. A long-term prospecting study on giant viruses in terrestrial and marine Brazilian biomes. *Virology Journal*, v. 21, p. 135, 2024.

4. MACHADO, TALITA B.; PICORELLI, AGNELLO C.L.; AZEVEDO, BRUNA L.; **DE AQUINO, ISABELLA L.M.**; QUEIROZ, VICTORIA F.; RODRIGUEZ, RODRIGO A.L.; ARAÚJO JR., JOÃO P.; ULLMANN, LEILA S.; DOS SANTOS, THIAGO M.; MARQUES, RAFAEL E.; GUIMARÃES, SAMUEL L.; ANDRADE, ANA CLÁUDIA S.P.; GULARTE, JULIANA S.; DEMOLINER, MERIANE; FILIPPI, MICHELI; PEREIRA, VYCTORIA M.A.G.; SPILKI, FERNANDO R.; KRUPOVIC, MART; AYLWARD, FRANK O.; DEL-BEM, LUIZ-EDUARDO; ABRAHÃO, JÔNATAS S. A. Gene duplication as a major force driving the genome expansion in some giant viruses. *Journal of Virology*, v. 97, p. e01309-23, 2023.
5. **DE AQUINO, ISABELLA L.M.**; SERAFIM, MATEUS S.M.; MACHADO, TALITA B.; AZEVEDO, BRUNA L.; CUNHA, DENILSON E.S.; ULLMANN, LEILA S.; ARAÚJO JR, JOÃO P.; ABRAHÃO, JÔNATAS S. Diversity of Surface Fibril Patterns in Mimivirus Isolates. *JOURNAL OF VIROLOGY*, v. 97, p. e0182422, 2023.
6. **AQUINO, ISABELLA L.M.**; BARCELOS, MATHEUS G.; MACHADO, TALITA BASTOS; SERAFIM, MATEUS S.M.; ABRAHÃO, JÔNATAS S. Surface fibrils on the particles of nucleocytoviruses: A review. *Experimental Biology and Medicine*, p. 2045-2052, 2023.
7. MACHADO, TALITA B.; **AQUINO, ISABELLA L.M.**; ABRAHÃO, JÔNATAS S. Isolation of Giant Viruses of *Acanthamoeba castellanii*. *Current Protocols*, v. 2, p. 1, 2022.
8. BORATTO, PAULO V.M.; SERAFIM, MATEUS S.M.; WITT, AMANDA S.A.; CRISPIM, ANA PAULA C.; AZEVEDO, BRUNA L.; SOUZA, GABRIEL A.P.; **AQUINO, ISABELLA L.M.**; MACHADO, TALITA B.; QUEIROZ, VICTÓRIA F.; RODRIGUES, RODRIGO A.L.; BERGIER, IVAN; CORTINES, JULIANA R.; FARIAS, SÁVIO T.; SANTOS, RAÍSSA N.; CAMPOS, FABRÍCIO S.; FRANCO, ANA CLÁUDIA; ABRAHÃO,

JÔNATAS S. A Brief History of Giant Viruses' Studies in Brazilian Biomes.
Viruses-Basel, v. 14, p. 191, 2022.

ANEXOS- OUTROS ARTIGOS PUBLICADOS DURANTE O DOUTORADO



Journal of
Virology



Virology | Full-Length Text

The genomic and phylogenetic analysis of *Marseillevirus cajuinensis* raises questions about the evolution of Marseilleviridae lineages and their taxonomical organization

Bruna Luiza de Azevedo,¹ Victória Fulgêncio Queiroz,¹ Isabella Luiza Martins de Aquino,¹ Talita Bastos Machado,¹ Felipe Lopes de Assis,¹ Erik Reis,¹ João Pessoa Araújo Júnior,² Leila Sabrina Ullmann,² Philippe Colson,^{3,4,5} Gilbert Greub,⁶ Frank Aylward,^{7,8} Rodrigo Araújo Lima Rodrigues,¹ Jônatas Santos Abrahão¹

AUTHOR AFFILIATIONS See affiliation list on p. 17.

ABSTRACT Marseilleviruses (MsV) are a group of viruses that compose the Marseilleviridae family within the Nucleocyotiviricota phylum. They have been found in different samples, mainly in freshwater. MsV are classically organized into five phylogenetic lineages (A/B/C/D/E), but the current taxonomy does not fully represent all the diversity of the MsV lineages. Here, we describe a novel strain isolated from a Brazilian saltwater sample named *Marseillevirus cajuinensis*. Based on genomics and phylogenetic analyses, *M. cajuinensis* exhibits a 380,653-bp genome that encodes 515 open reading frames. Additionally, *M. cajuinensis* encodes a transfer RNA, a feature that is rarely described for Marseilleviridae. Phylogeny suggests that *M. cajuinensis* forms a divergent branch within the MsV lineage A. Furthermore, our analysis suggests that the common ancestor for the five classical lineages of MsV diversified into three major groups. The organization of MsV into three main groups is reinforced by a comprehensive analysis of clusters of orthologous groups, sequence identities, and evolutionary distances considering several MsV isolates. Taken together, our results highlight the importance of discovering new viruses to expand the knowledge about known viruses that belong to the same lineages or families. This work proposes a new perspective on the *Marseilleviridae* lineages organization that could be helpful to a future update in the taxonomy of the Marseilleviridae family.

IMPORTANCE Marseilleviridae is a family of viruses whose members were mostly isolated from freshwater samples. In this work, we describe the first *Marseillevirus* isolated from saltwater samples, which we called *Marseillevirus cajuinensis*. Most of *M. cajuinensis* genomic features are comparable to other Marseilleviridae members, such as its high number of unknown proteins. On the other hand, *M. cajuinensis* encodes a transfer RNA, which is a gene category involved in protein translation that is rarely described in this viral family. Additionally, our phylogenetic analyses suggested the existence of, at least, three major Marseilleviridae groups. These observations provide a new perspective on Marseilleviridae lineages organization, which will be valuable in future updates to the taxonomy of the family since the current official classification does not capture all the Marseilleviridae known diversity.

KEYWORDS Marseillevirus, Marseilleviridae, lineages, phylogeny, taxonomy, evolution

Some years after the mimivirus discovery (1), the Marseilleviridae family became the second described group of large/giant viruses that are able to infect amoebas. The first Marseilleviridae isolate was obtained from water samples collected in a cooling tower in Paris, France (2). Typically, the members of the Marseilleviridae family exhibit

Editor Kristin N. Parent, Michigan State University, East Lansing, Michigan, USA

Address correspondence to Jônatas Santos Abrahão, jonatas.abrahao@gmail.com.

The authors declare no conflict of interest.

Received 19 March 2024

Accepted 19 April 2024

Published 16 May 2024

Copyright © 2024 American Society for Microbiology. All Rights Reserved.

icosahedral particles with an average diameter of approximately 250 nm. The discovery of the first *Marseillevirus* (MsV) paved the way to describe several new isolates. Amoebae are likely marseillevirus hosts in the environment, and *Acanthamoeba* was the species used at the laboratory to isolate these viruses. Most of them were obtained from freshwater samples, including Lausannevirus, Tunisvirus, Melbournevirus, Cannes 8 virus, Noumeavirus, Brazilian marseillevirus, and Tokyovirus (3–9). Samples from other environments have been tested leading to the discovery of new *Marseilleviridae* isolates. Golden marseillevirus and Insectomime virus, for example, were isolated from golden mussels and internal organs of insect larvae, respectively (10, 11). In addition to several isolates already described, metagenomic studies have reported five divergent *Marseilleviridae* sequences detected in sediments from a hydrothermal vent (Loki's Castle), in the Atlantic Ocean (12). These discoveries in different types of environments, such as deep ocean regions, have expanded our understanding about the ecology of these viruses and locations where they can be isolated.

Marseilleviridae genomes are composed by circular double-stranded DNA molecules that range in size from 348 to 404 kbp (13). The G-C content ranges from 42.9% to 44.8%, and the number of predicted genes varies from 386 to 491 (13). Most part of *Marseillevirus* genomes encodes uncharacterized proteins. This is a general characteristic for giant viruses. Besides, *Marseilleviruses* do not have a diversity of genes involved in protein translation as observed in other giant viruses, such as those of *Mimiviridae* family (14). Although genes encoding translation factors have been described, it is not common to find in *Marseilleviruses* genome genes that encode transfer RNAs (tRNA) and aminoacyl-tRNA synthetases (13, 15). Considering tRNAs, they are currently described only in Tokyovirus and in the Loki's Castle metagenomic sequences (8, 12). As other Nucleocytoviricota phylum viruses, *Marseillevirus* genomes present a high mosaicism, which means that they have sets of genes of multiple origins (2).

The International Committee on Taxonomy of Viruses (ICTV) classifies all members of the *Marseilleviridae* family within the Nucleocytoviricota phylum, Pimascorivales order (16, 17). Currently, *Marseilleviridae* is composed by one genus (*Marseillevirus*), in which two species are included: *Marseillevirus marseillevirus* and *Senegalvirus marseillevirus*. There are two other species in the family, which are not included in any genus, the species *Lausannevirus* and *Tunisvirus* (16). However, a new organization and nomenclature for *Marseillevirus*-related taxa was recently proposed and is under approval for official publishing by ICTV. Phylogenetic analyses based on DNA polymerase proteins revealed the existence of five different *Marseillevirus* phylogenetic lineages, named A, B, C, D, and E. Lineage A is represented by the first isolate, *Marseillevirus marseillevirus* (2). Lineage B is represented by Lausannevirus, the second *Marseilleviridae* isolated (3). Lineages A and B have the largest number of isolates. The lineage C is represented by Tunisvirus and Insectomime virus (5, 17), while lineages D and E are composed of the Brazilian isolates, Brazilian marseillevirus and Golden marseillevirus, respectively (9, 11). Taking that into account, the known diversity of *Marseilleviridae* members is not being completely represented by the official taxonomy of the group. For example, the representatives of lineages D and E are not considered yet.

Almost 15 years after the discovery of the first *Marseillevirus*, it becomes apparent that the isolation of new viruses is important to elucidate the evolutionary history of this family. In this study, we report the discovery of *Marseillevirus cajuinensis*, a new isolate obtained from a saltwater sample from the Northeast coast of Brazil. This discovery paved the way for a genomic and phylogenetic characterization that suggested the existence of at least three major consistent *Marseilleviridae* groups. Analysis involving Clusters of Orthologous Groups (COGs), relative evolutionary distance (RED), and average amino acid/nucleotide identity (AAI and ANI) reinforces this three-group organization and helps to establish parameters for a future taxonomic organization of *Marseilleviridae* into three genera and different species. These findings provide a new perspective on *Marseilleviridae* lineages, which will be valuable in evolutive studies and future updates to the taxonomy of the family.

RESULTS

Marseillevirus cajuinensis: a new amoebae-infecting virus isolated from saltwater

From a saltwater sample collected in the Northeast coast of Brazil, we identified a new viral isolate able to infect *Acanthamoeba castellanii*. The transmission electronic microscopy (TEM) images containing infected amoebae showed icosahedral particles presenting shape similar to members of Marseilleviridae (Fig. 1A). With TEM analysis, it was also possible to observe some general morphological aspects from the isolate replication cycle. For example, we observed viral factories (VF) with an electron lucent aspect that occupied a large part of the cell cytoplasm (Fig. 1B, highlighted in pink). The images showed several viral particles in different maturation stages inside the VF (Fig. 1C, black arrow). Amorphous structures were also observed inside VFs (Fig. 1B through D), some of them horseshoe shaped (Fig. 1C and D, yellow arrows), resembling the crescent precursors of viral particles found in poxvirus and mimivirus viral factories (18, 19). Also, we observed giant vesicles harboring several viral particles at the end of the replication cycle. One of these giant vesicles reached a size of 5 μm (Fig. 1E, red arrow).

Besides TEM, the viral sample was analyzed by genome sequencing for a more accurate identification of the virus. Next-generation sequencing generated 225,574 reads that were assembled into a 166 \times depth single scaffold containing 380,653 bp. When compared with the National Center for Biotechnology Information (NCBI) database, the genome sequence best matched with a member of the Marseilleviridae family, presenting 79% of average nucleotide identity with Tokyovirus. Since we could confirm that the isolate is a Marseilleviridae, we named it *Marseillevirus cajuinensis*.

Marseillevirus cajuinensis genome

The circular double-stranded DNA molecule that composes *M. cajuinensis* genome has a G-C content of 45.24%. A total of 515 open reading frames (ORFs) were predicted that encode proteins with sizes ranging from 50 to 1,520 amino acids. GenBank sequence database searches suggested that 40 of the 515 proteins encoded by *M. cajuinensis* genome have functions related to DNA replication, recombination, and repair (Fig. 2A). This category includes a chaperone, a DNA topoisomerase, different nucleases, helicases, histones, and the DNA polymerase protein, which is commonly used as a marker for phylogeny. Other remarkable categories include signal transduction regulation and miscellaneous (Fig. 2A). The former primarily comprises serine/threonine protein kinases, while the latter consists of proteins whose function cannot be reliably predicted due to the presence of non-specific domains and/or repeats, such as ankyrin repeat-containing proteins and zinc finger proteins. *M. cajuinensis* genome also encodes for proteins involved in different metabolic processes, such as lipases and proteases. Furthermore, the major capsid protein (MCP) and the A32-like packaging ATPase are important proteins found in the virion structure and morphogenesis category.

More than half (59%) of the 515 *M. cajuinensis* proteins were classified as uncharacterized (Fig. 2A). Another 38 proteins were considered as ORFans since they had no hits with any other sequence in the used databases (Fig. 2A). Since several Marseilleviridae isolates have been described, it could be considered a high number of ORFans for a new isolate. However, by analyzing the ORFans' sizes, we observed that most of them (27/38) correspond to short polypeptides ranging from 50 to 100 amino acids (Fig. 2B). The possible high number of ORFans and their short sizes was intriguing. To confirm these results, a new gene prediction was performed using a different program. Thus, Prodigal was used instead of GeneMarkS. After this new analysis, 493 proteins (bigger than 50 amino acids) were predicted by Prodigal, 22 less than the 515 that were predicted by GeneMarkS. Interestingly, the number of predicted ORFans decreased considerably. Instead of 38, the new prediction returned only 9 ORFans. When analyzing the size of these newly predicted ORFans, it was possible to note that the number of ORFans bigger than 150 amino acids was increased, while the number of ORFans that were composed

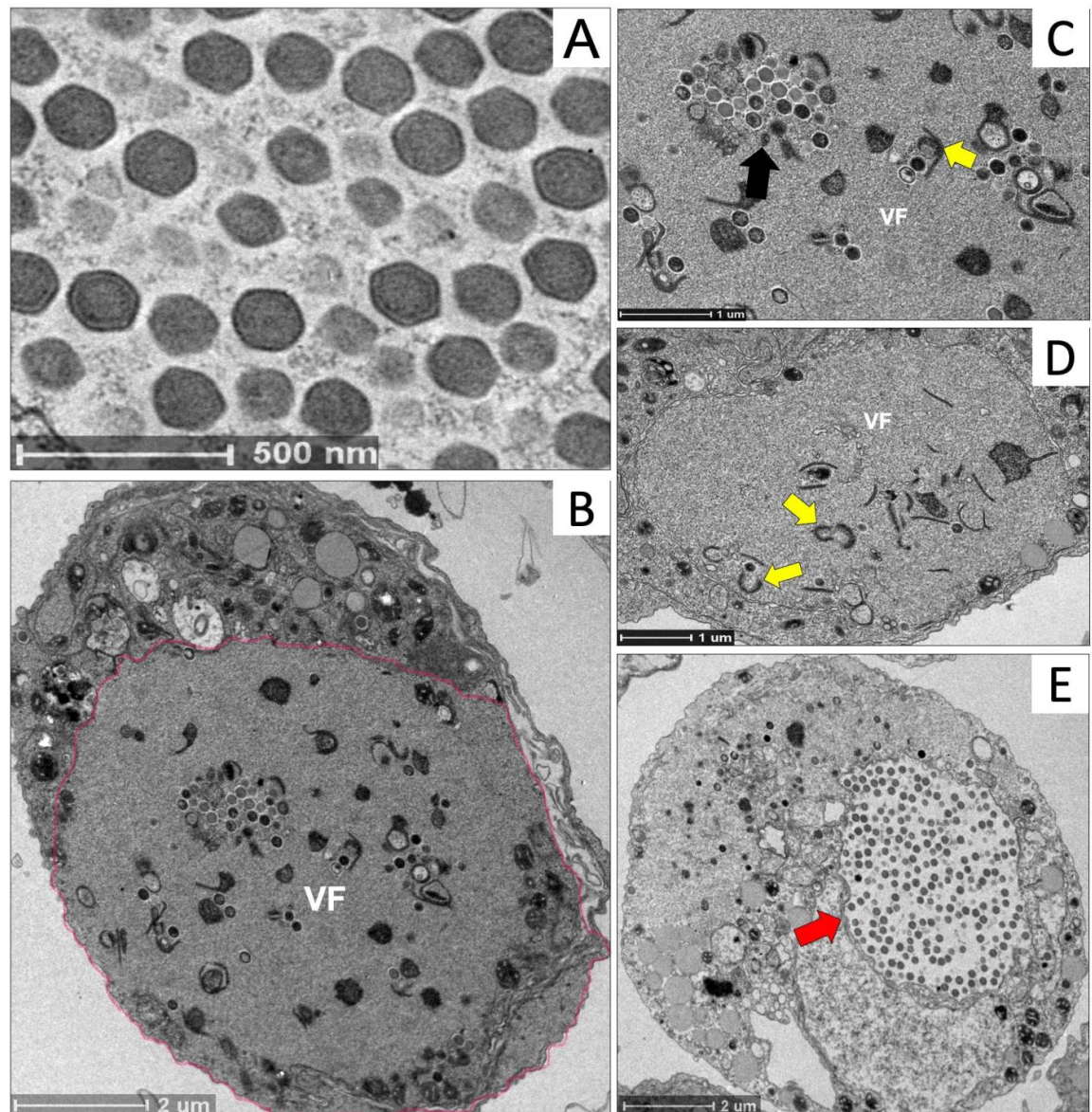


FIG 1 Transmission electron microscopy images showing morphological characteristics from the new isolate inside *Acanthamoeba castellanii* cells. (A) Several icosahedral Marseillevirus-like particles. (B) *Acanthamoeba castellanii* cell containing a viral factory occupying a large portion of the cell. Viral factory boundaries are highlighted in pink. (C) A portion of Fig. 1B seen closer, showing a VF containing particles in different maturation stages (black arrow) and horseshoe-shaped structures (yellow arrow). (D) Another amoeba cell containing a VF filled with amorphous and horseshoe-shaped structures (yellow arrows). (E) Giant vesicle (red arrow) harboring several viral particles in a final stage of the cycle.

by less than 100 amino acids was considerably low (Fig. 2B). Here, predictions generated by GeneMarkS were selected to perform all the analysis in this work because this tool was the one the most consistently used for Marseilleviruses in previous works (2, 4–6, 9, 10, 17, 20).

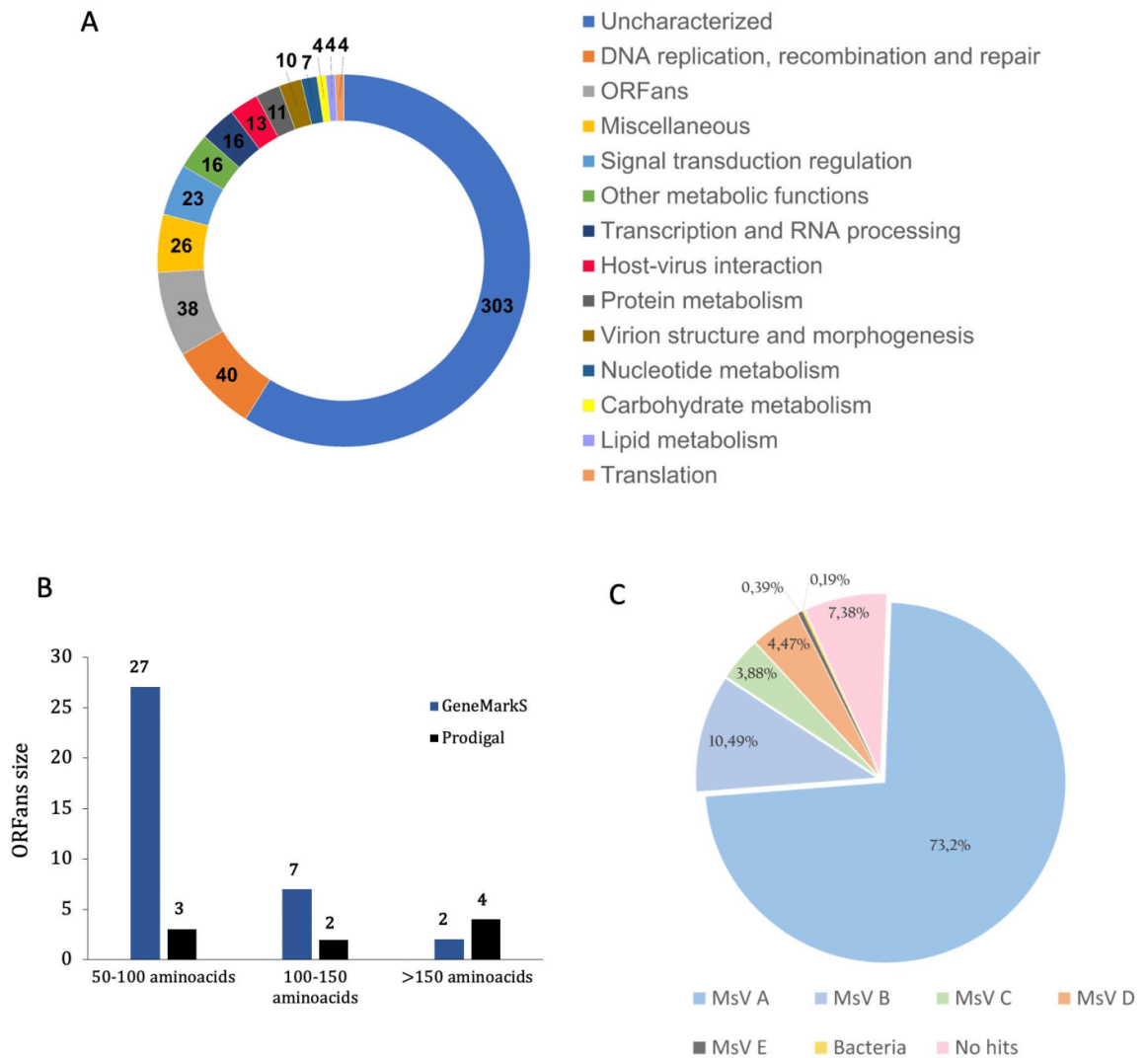


FIG 2 Genomic analysis of the *Marseillevirus cajuinensis* genome. (A) Number of *M. cajuinensis* proteins according to the function predicted during genome annotation. $n = 515$. (B) Comparison between the number of *M. cajuinensis* ORFans and their sizes when using different gene prediction tools. (C) Percentage of *Marseillevirus cajuinensis* proteins that presented best hit (BLASTp) with the five different Marseilleviridae lineages currently described (A–E). $n = 515$.

To know which organisms had their sequences considered as best hits with *M. cajuinensis* proteins, we analyzed hit by hit the results obtained in the BLASTp searches. Thus, for more than half (73.2%) of *M. cajuinensis* proteins, best hits from GenBank database, were Marseillevirus lineage A sequences (MsV A) (Fig. 2C). This suggests that *M. cajuinensis* could present a closer evolutionary relationship with lineage A, which can be confirmed by phylogeny. Also, this best hit analysis showed one *M. cajuinensis* protein (P86) whose best hit was a sequence encoded by a bacterium (Fig. 2C). P86 was the only protein for which no best hits were sequences from other members of the family Marseilleviridae.

Genome synteny analysis of different members of Marseilleviridae lineages highlighted the relatedness between *M. cajuinensis* and previously described lineage A members.

It is possible to observe that the organization of the *M. cajuinensis* genome blocks, separated and colored according to similarity, is more like that of the representative member of lineage A than of viruses from other lineages (Fig. 3). In this analysis, it is also possible to observe that in all the genomes analyzed, there is a region that appears to be more conserved, being approximately the last third of genome lengths (Fig. 3). Such conserved region in *Marseilleviridae* genomes was already described before and called a “core region” (21). More detailed synteny analysis containing different *Marseillevirus* isolates from the five lineages can be found in Supplementary Figure 1 at <https://www.giantviruses.com/sup-material-of-papers/sup-material-the-genomic-and-phylogenetic-analysis-of-marseillevirus-cajuinensis-raises-questions-about-the-evolution-of-marseilleviridae-lineages-and-their-taxonomical-organization>.

Marseillevirus cajuinensis’ translation-related genes and detection of tRNAs in different *Marseillevirus*s

The genomic analysis showed that *M. cajuinensis* encodes four different translation factors. No aminoacyl-tRNA-synthetase genes were found. Additionally, a search for transfer RNA sequences in *M. cajuinensis* genome was performed. To perform this search, two different programs (Aragorn and tRNAscanSE) were used. No tRNA sequence was found in *M. cajuinensis* genome by using tRNAscanSE. However, Aragorn was able to detect 1 tRNA sequence (tRNA-Gln-CTG) that has a 1,379-nucleotide intron.

Considering all the known giant/large amoeba-infecting viruses, tRNA encoding is not commonly described for *Marseilleviridae* isolates neither for other families from Pimascovirales. Otherwise, in groups phylogenetically related to the Pimascovirales order, such as cedratviruses and orpheoviruses, tRNAs were already described (22). Because of the difference in results between the two programs used to predict the tRNA, we carried out a search for tRNA in genomes from the five classical *Marseilleviridae* lineages that had complete sequences available in GenBank (March 2023). For this, we used both Aragorn and tRNAscanSE. The Aragorn program allows changing its parame-

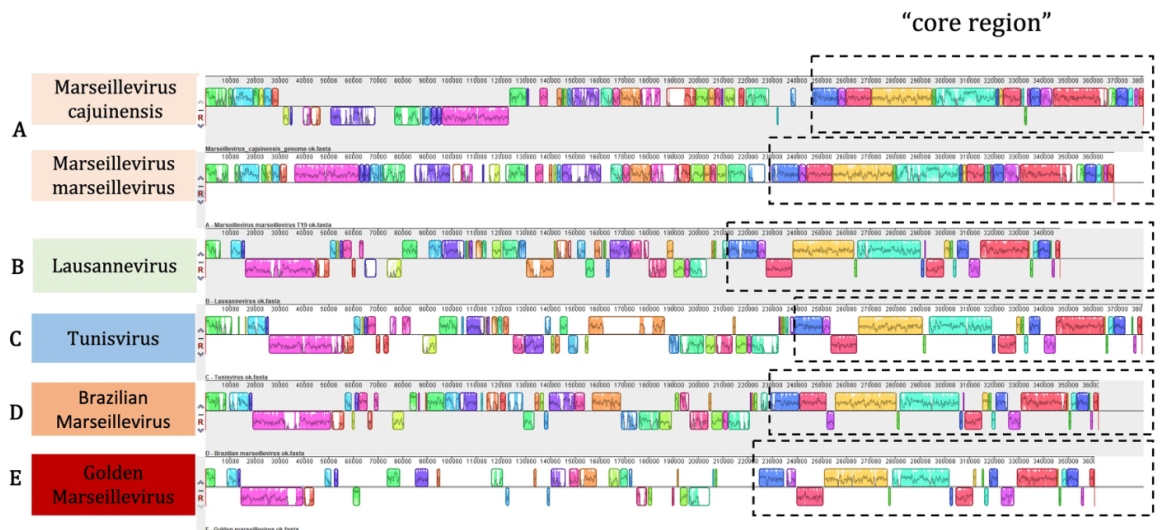


FIG 3 Genome synteny analysis of *Marseilleviridae* isolates representing the five currently described lineages and *Marseillevirus cajuinensis*. Each line represents the sequence of a different virus, which is identified in the legend on the left. The letters A, B, C, D, and E indicate the respective phylogenetic lineages of each analyzed virus. Blocks of the same color indicate similar regions between sequences. The areas without any colored blocks represent regions exclusive to that virus, that is, which do not show similarity with other viruses used in the analysis. Note: As they have a circular topology, the sequences were adjusted to start from the MCP aiming to facilitate interpretation of this figure. *Marseillevirus marseillevirus* was used as the reference genome.

ters to consider or not the presence of introns, and we performed the analysis in both conditions.

Thus, we detected tRNA sequences in Tokyovirus, *Marseillevirus marseillevirus*, Melbournevirus, Insectomime virus, Tunisvirus, and Golden marseillevirus using the Aragorn program with parameter allowing introns detection. When introns detection was not considered, it was only possible to detect tRNA in Tokyovirus, as the two sequences encoded by this virus do not have introns. Using tRNAscanSE, it was possible to detect tRNA only in the Tokyovirus sequence. Interestingly, tRNAscanSE detected three tRNA sequences in Tokyovirus, while Aragorn detected only two (see Supplementary Figure 2 at <https://www.giantviruses.com/sup-material-of-papers/sup-material-the-genomic-and-phylogenetic-analysis-of-marseillevirus-cajuinensis-raises-questions-about-the-evolution-of-marseilleviridae-lineages-and-their-taxonomical-organization>). Considering all tRNA sequences detected in different Marseillevirus, only two of the Tokyovirus tRNA were already described (8). Albeit little described in the Marseilleviruses of the five previously reported lineages, tRNAs have already been described in the sequences detected by metagenomics from samples from Loki's Castle. Although genomes assembled from metagenomes should be considered with caution, one of these sequences, called LCMAC202, was reported to encode 26 types of tRNA (12).

Phylogeny of different Nucleocytoviricota conserved proteins raises questions about Marseilleviridae lineages organization

To better elucidate the evolutionary relationship of *M. cajuinensis* with other Marseilleviridae members, phylogenetic analyses were performed using protein sequences that are considered conserved in Nucleocytoviricota. This set of conserved proteins includes the DNA polymerase, the A32-like packaging ATPase, and the late transcription factor VLT3 like, which were used as markers to construct phylogenetic trees (Fig. 4). It is noteworthy that the topology within lineages or genera varies not only among Marseilleviruses but also among other amoebal viruses, depending on the gene analyzed. Virus evolution is modular, with each gene subject to various nuances of a multitude of selective pressures.

Analyzing all phylogenies, it was possible to observe that *M. cajuinensis* groups together with sequences from Marseilleviruses of lineage A but represents a more divergent branch within this group (Fig. 4). Similar results were described for Tokyovirus within lineage A in previous works (8). It is noteworthy that *M. cajuinensis* and Tokyovirus cluster together in separate branch in the VLT3-like tree but not in all constructed trees, including the concatenated one. It is important to note that the divergence of *M. cajuinensis* within lineage A is comparable with the divergence that separates two different lineages (C and D). It raises questions about which criteria should be used to define what can be considered a new lineage or a new genus within the Marseilleviridae family. For example, by comparing lineage C and D branches, Brazilian marseillevirus is currently considered as a different lineage. Based on this, *M. cajuinensis*, and even Tokyovirus, could also be considered new lineages.

In addition to this questioning, it is also possible to observe the clear divergence of the common ancestor of the five classical Marseilleviridae lineages into three major groups: one that groups the current members of lineage A, corresponding to the current genus *Marseillevirus*, another that groups members of the current lineages B-C-D, and finally Golden marseillevirus (lineage E) in a third group. Noteworthy, the lineage E is closer from B-C-D branch than from the *Marseillevirus* genus (lineage A) but still presents a high divergence within its clade. Indeed, this same topology can be observed in a concatenated phylogenetic tree based on the three conserved sequences former analyzed individually (Fig. 4D).

Marseillevirus cajuinensis expands the pangenome of Marseilleviridae isolates

To understand the impact of the *M. cajuinensis* isolation on the pangenome and core genome of Marseilleviridae isolates, we searched for Clusters of Orthologous Groups of

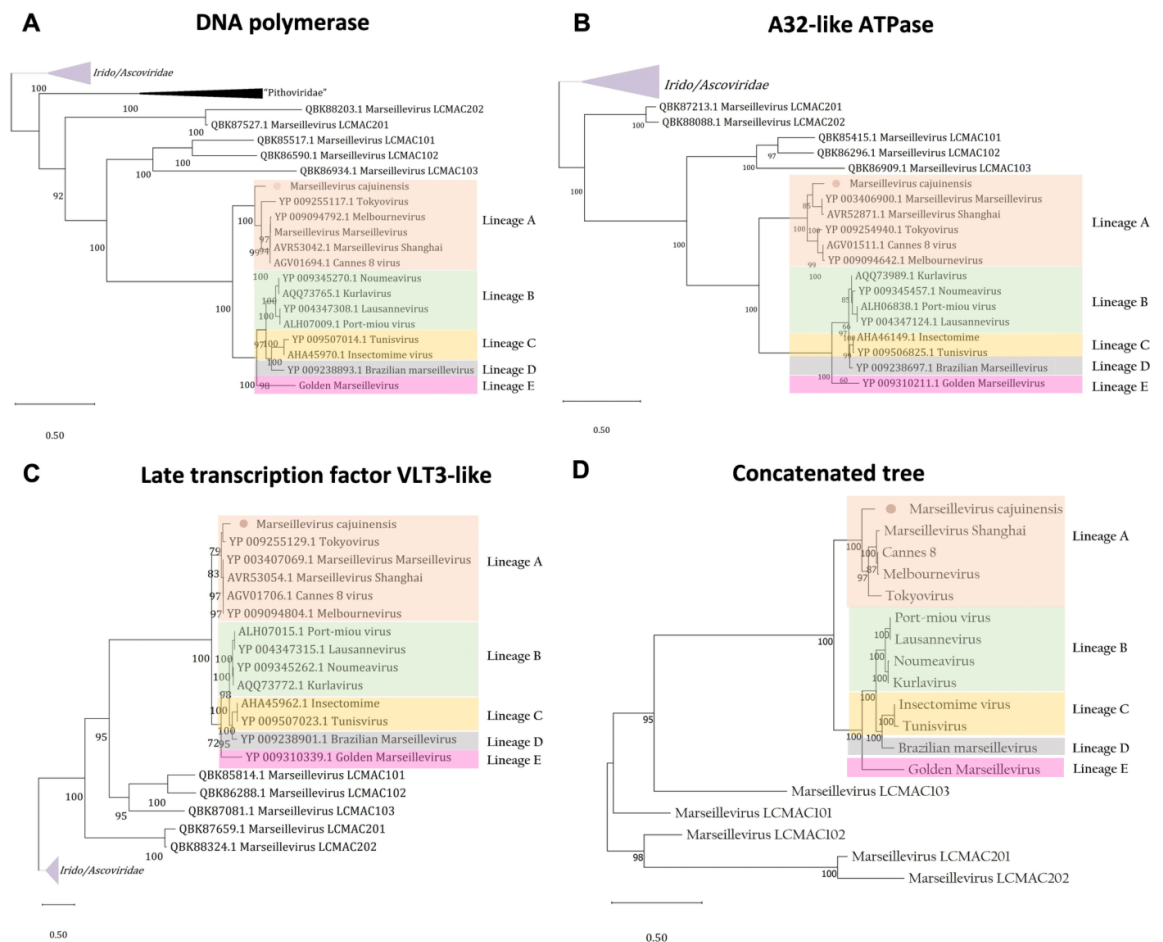


FIG 4 Marseilleviridae phylogeny using different conserved protein sequences. (A) Phylogeny based on DNA polymerase sequences. (B) Phylogenetic tree based on the A32-like packaging ATPase sequences. (C) Phylogeny based on the amino acid sequence of the VLT3-like late transcription factor sequences. (D) Concatenated sequence tree based on DNA polymerase, A32-like packaging ATPase, and VLT3-like late transcription factor sequences. *Marseillevirus cajuinensis* sequence is labeled in the tree with a pink disk. The trees were built using the maximum likelihood method, with statistical support based on 1,000 replicates (bootstrap). The best model, selected by IQtree (ModelFinder), for the trees was VT + F + I + G4 for (A), LG + G4 for (B), LG + I + G4 for (C), and VT + F + I + G4 for (D). The trees shown in A, B, and C were rooted on Iridoviridae branch as an outgroup. Concatenated tree was rooted at the midpoint. The tree scale bars represent the number of amino acid substitutions per site.

proteins shared between complete genome sequences of the isolates available in GenBank. Thus, it was possible to analyze the pangenome and core genome of isolated members of the Marseilleviridae family after including *M. cajuinensis* (Fig. 5) as well as the sharing of COGs between each lineage. It was observed that the pangenome of Marseilleviridae isolates increases from 598 to 1,626 when 13 new isolates are added in the analysis (Fig. 5). The first inserted sequence was Golden marseillevirus because it is the most divergent member of the five lineages. It was expected that with each new discovery of a different virus, the number of total COGs (pangenome) increases. This shows that the Marseilleviridae pangenome is still expanding and that the discovery of new additional viruses is warranted and important, as it will consequently lead to the discovery of new genes.

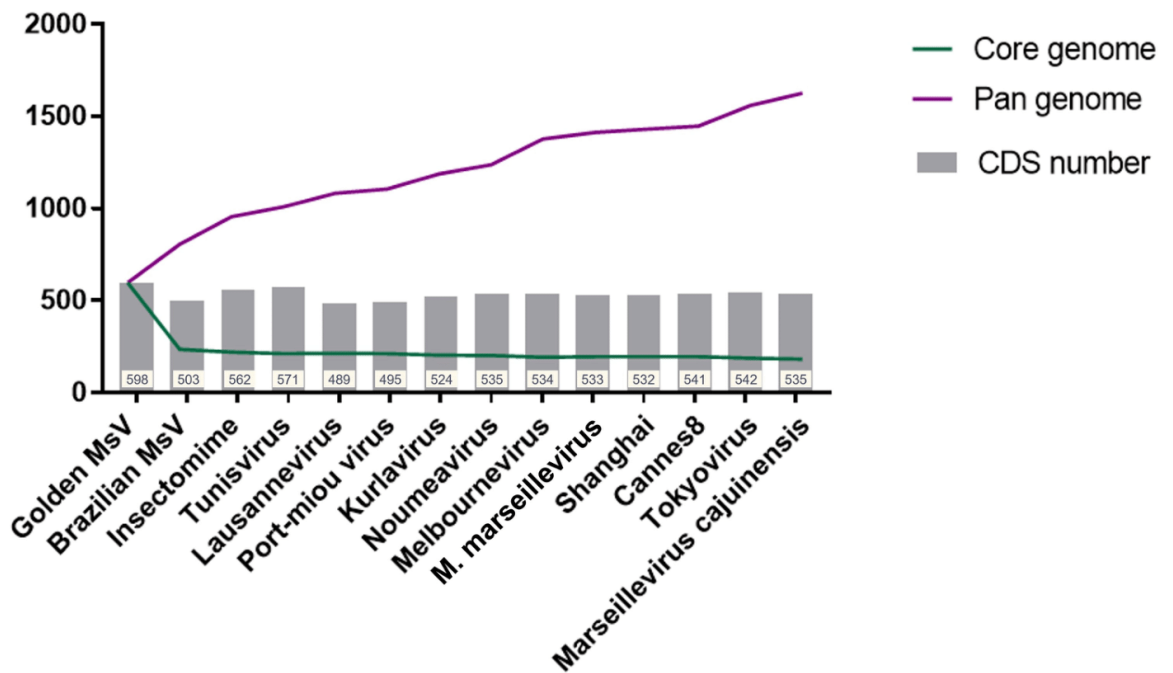


FIG 5 Analysis of the pangenome and core genome of Marseilleviridae isolates, including *Marseillevirus cajuinensis*. The curves indicate the variation in the number of Clusters of Orthologous Groups as new sequences are inserted in analysis. White boxes in the bottom of gray bars indicate the number of coding sequences (CDS) for each virus. Note: The number of CDS is based on the new gene prediction performed exclusively to this analysis.

On the other hand, the number of COGs shared by all the analyzed viruses (core genome) is 182 (Fig. 5). The graph analysis suggests that the core genome of Marseilleviridae isolates appears to have reached a plateau, suggesting that the gene content essential for the existence of these viruses is already relatively well defined, although the functions of most of these genes still need to be deciphered.

A detailed analysis of COGs shared between different Marseilleviruses reinforces the organization of Marseilleviridae in three major groups

In addition to pangenome and coregenome analyses, our data indicate the number of COGs that are shared between the members of the five Marseilleviridae classical lineages (Fig. 6). This analysis shows that *M. cajuinensis* (Fig. 6A, VI, red arrow) has 65 singletons, that is, clusters of proteins that are found only in its sequence. Among the members of lineage A (Fig. 6A, red disks), *M. cajuinensis* (VI, red arrow) and Tokyovirus (I) are those that have the greatest numbers of singletons. This reinforces the assumption that both viruses are the most divergent members of the lineage, corroborating the phylogeny results mentioned above. Altogether, the members of lineage A analyzed here share a total of 370 COGs that are unique to their lineage (Fig. 6A, red disks).

Among the other Marseilleviridae lineages analyzed, in lineage B (Fig. 6A, blue disks), it is possible to observe that all the four lineage members share 137 COGs that are absent in other lineages. Similarly, the lineage C members (Fig. 6A, purple disks) share 133 COGs that are exclusive to their lineage. On the other hand, the only known member of lineage D, Brazilian marseillevirus, has 52 singletons (Fig. 6A, gray arrow). This virus is described to compose its own lineage; however, in this analysis, it presents a smaller number of COGs than *M. cajuinensis* and Tokyovirus which are considered members of a same phylogenetic lineage (lineage A). Golden marseillevirus, the only known representative member of lineage E, has 294 singletons (Fig. 6A, orange arrow). The comparison of the

A

- Lineage A**
 - I. Tokyovirus (542 CDS)
 - II. Marseillevirus Shanghai (532 CDS)
 - III. Cannes 8 virus (541 CDS)
 - IV. Melbourne virus (534 CDS)
 - V. Marseillevirus Marseillevirus (533 CDS)
 - VI. Marseillevirus cajuinensis (535 CDS)
- Lineage B**
 - VII. Lausannevirus (489 CDS)
 - VIII. Port-miou virus (495 CDS)
 - IX. Noumeavirus (535 CDS)
 - X. Kurlavirus (524 CDS)
- Lineage C**
 - XI. Tunisvirus (571 CDS)
 - XII. Insetomime virus (562 CDS)
- Lineage D**
 - XIII. Brazilian Marseillevirus (503 CDS)
- Lineage E**
 - XIV. Golden Marseillevirus (598 CDS)

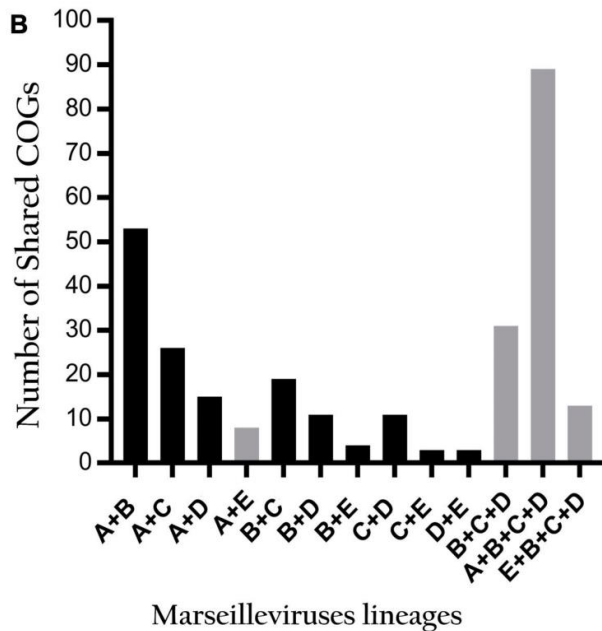
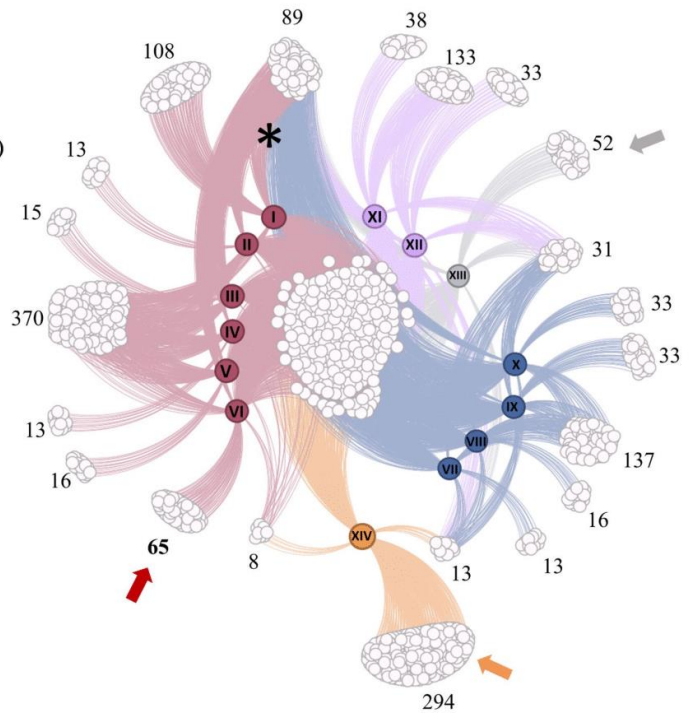


FIG 6 The sharing of Clusters of Orthologous Groups among different viruses belonging to the five classical lineages of Marseilleviruses. (A) Network showing the distribution of COGs among viruses. White circles represent COGs. The colored circles represent the analyzed viruses, separated by color, according to their respective phylogenetic lineages. Roman numerals individually identify each virus analyzed, while Arabic numbers indicate the number of COGs contained (Continued on next page)

FIG 6 (Continued)

in each cluster. Note: The number of proteins obtained through GeneMarkS is indicated in parentheses for each virus. *Marseillevirus cajuinensis* is highlighted by a red arrow, Golden marseillevirus is highlighted by an orange arrow, Brazilian marseillevirus is highlighted by a gray arrow, and the sharing of COGs between lineages A, B, C, and D is highlighted by an asterisk. (B) Graph detailing the number of exclusive COGs shared between combinations of different classical Marseilleviridae lineages. The black bars correspond to combinations of lineages that are not represented in Fig. 6A, while the gray bars correspond to combinations already represented in Fig. 6A. Note: Some of the lineage's combinations were not represented in Fig. 6A because some of them often overlap themselves in the network, making analysis hard.

number of exclusive shared COGs between the different lineages is detailed in Fig. 6B. In this graph, it is possible to analyze the sharing of COGs between different lineages in a simpler way. Lineages A and E (A + E), for example, share only eight COGs. This number decreases when comparing the other lineages with lineage E. Lineages B and E (B + E) share only four COGs, while lineages C and E (C + E), and D and E (D + E) share only COGs. Together, lineages A, B, C, and D (A + B + C + D) share 89 COGs that are not found in lineage E (Fig. 6A, asterisk). Thus, these data reinforce the divergence of lineage E among Marseilleviridae and support its assignment in a distinct group of the family.

Using the data obtained in COGs analysis described above, a hierarchical clustering phenophyletic tree was constructed based on the presence and absence of COGs in the analyzed sequences (Fig. 7). In this figure, it was possible to observe a topology very similar to what was observed in the phylogenetic trees described in this work. Representatives of lineage A are organized into a group (group I) that represents the current genus *Marseillevirus* and apart from representatives of lineages B, C, D (group II), and E (group III) (Fig. 7).

Within lineage A, it was possible to observe the organization of the viruses into two subgroups, one was composed of *M. cajuinensis* and Tokyovirus, and the other was composed of the other lineage A viruses (Fig. 7). The same happens in group II since there are three subgroups composed by each member of lineages B, C, and D

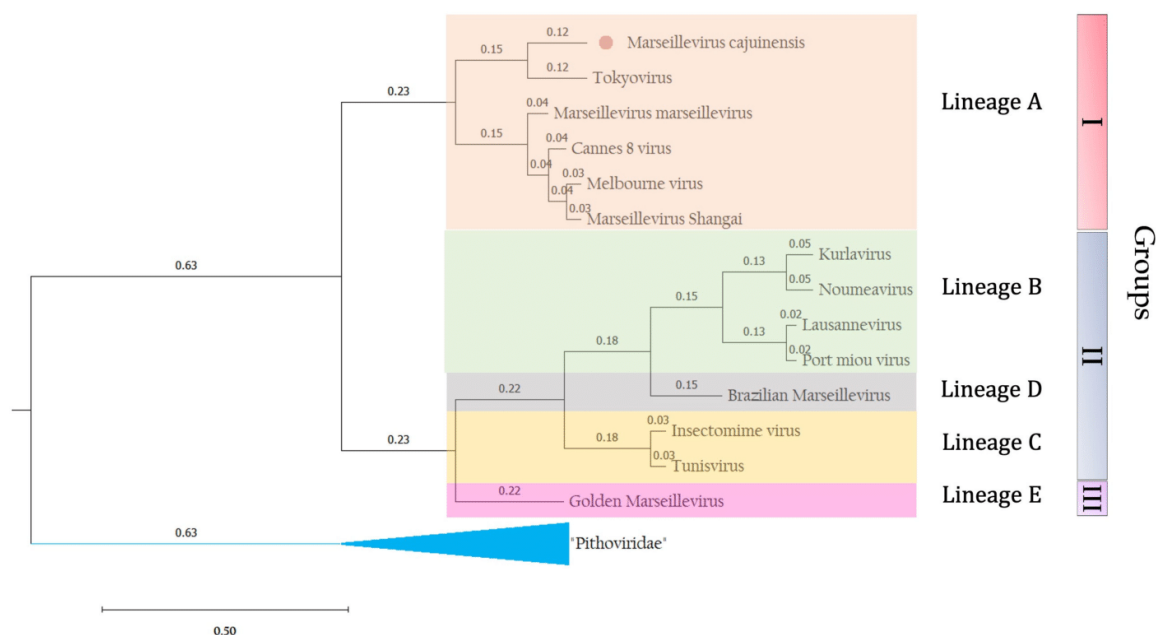


FIG 7 Hierarchical clustering tree considering the presence and absence of Clusters of Orthologous Groups in different viruses of Marseilleviridae family. *Marseillevirus cajuinensis* is labeled in the tree with a pink circle. Scale bar represents arbitrary values that express the evolutionary distance based on presence-absence of COGs.

(Fig. 7). These results reinforce what was observed in phylogeny and genomic analyses. Also, they reinforce the questions raised about the classical organization of *Marseilleviridae* viruses in five lineages. For example, if the tree branches (lineages B, C, and D) that compose group II are represented by viruses originally classified into three different lineages, this could justify that *Marseillevirus cajuinensis* and *Tokyovirus* could be classified in its own lineages. On the other hand, the different branches that compose the classical *Marseilleviridae* lineages could also be considered as members of major groups.

Relative evolutionary distance and average amino acid/nucleotide identity analyses suggest the organization of *Marseilleviridae* isolates in three putative genera

To quantify all these observations and make them more consistent, an RED analysis was performed. Thus, we considered three groups for this analysis based on the three major clades observed in DNA polymerase phylogeny: group I (lineage A), group II (lineages B, C, D), and group III (lineage E) (Fig. 8A). DNA polymerase phylogeny was selected because it is the main phylogenetic marker for Nucleocytoviricota, but the same topology was observed for all phylogenies (Fig. 4) and for the hierarchical clustering tree as well (Fig. 7).

RED values varies from 0 to 1, and threshold values for different taxonomic levels in Nucleocytoviricota were defined previously (23). The previously reported RED values for genus ranged from 0.69 to 0.995 (23). The present analysis showed that group I (lineage A) had a RED value of 0.86, while group II (lineages B, C, and D) had a RED value of 0.83 (Fig. 8A). These numbers are consistent with values expected for the genus level (23). Because group III (lineage E) is composed by a single genome (Golden marseillevirus), RED analysis cannot be performed. However, when Golden marseillevirus sequence is included in group II (lineages B, C, and D), the RED value decreases to 0.78. Although this value could still classify group II as a genus while including Golden marseillevirus, the lower RED value makes group II less consistent when comparing with group I. Thus, excluding lineage E from group II and considering it as a separate group were most consistent here.

Additionally, sequences of the *Marseillevirus* isolates previously analyzed in this work were submitted to an average nucleotide identity analysis. The ANI analysis delineated three main groups of *Marseilleviruses*, considering an ANI cutoff >75% (Fig. 8B). This value corroborates with our phylogenetic analyses and hierarchical clustering of COGs, revealing the existence of three distinct groups in *Marseilleviridae*, possibly corresponding to three distinct genera. Within groups, we can use pairwise ANI >95% to define viral species, as used for members of *Imitervirales* (24). In this case, we can define eight viral species, among which three belong to group I—one of them corresponding to the *Marseillevirus cajuinensis*; four belong to group II; and only one, consisting of the Golden marseillevirus isolate, belongs to group III. Also, an average amino acid identity analysis was performed. The same three groups could be observed in the bidirectional AAI analysis, with AAI >65% (Fig. 8B). Moreover, in the AAI estimation, we clearly saw eight putative viral species, with AAI >95%.

DISCUSSION

In this work, we describe the isolation of *M. cajuinensis* from a saltwater sample from the Northeast coast of Brazil. Although members of the family *Marseilleviridae* have already been isolated from samples of different sources (2, 10, 11, 17, 25), most of them were obtained from freshwater or mud from rivers and lakes (2–4, 6–8). To our knowledge, this is the first time that a *Marseilleviridae* member has been isolated from ocean water, although they have already been detected in this type of environment through metagenomic analyses (12).

TEM images revealed that the replication cycle of *M. cajuinensis* shares similar characteristics with other members of the *Marseilleviridae* family, such as the presence of

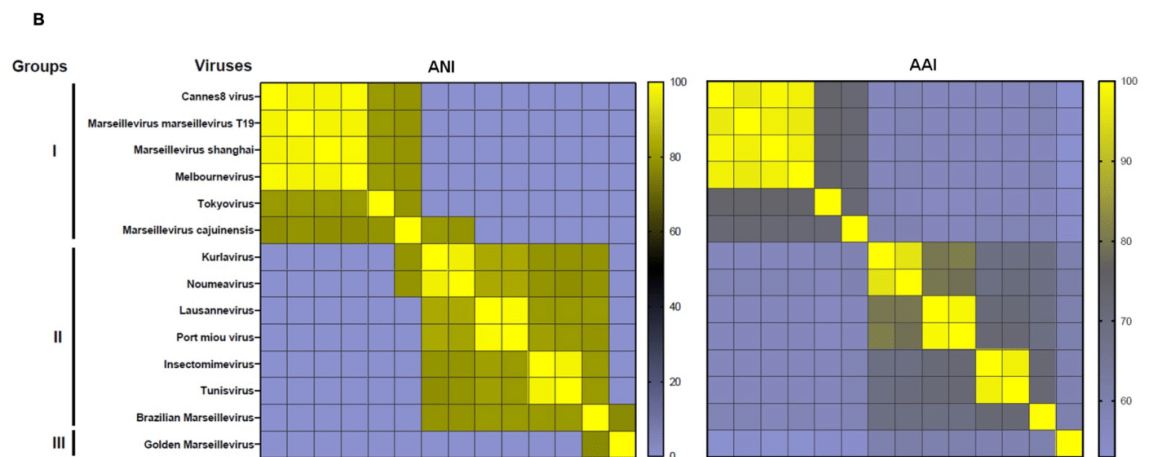
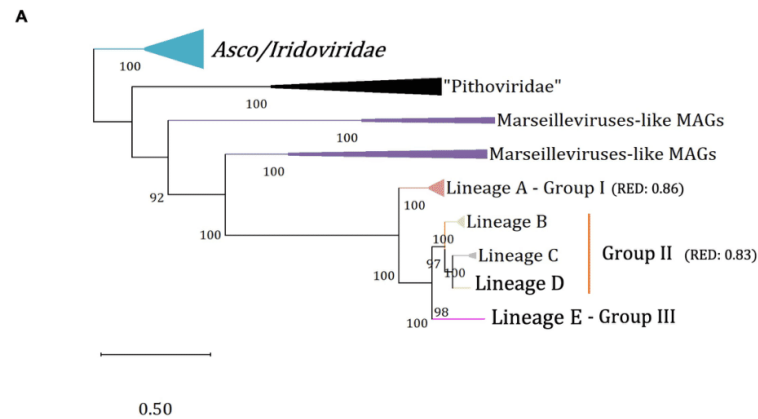


FIG 8 (A) DNA polymerase phylogenetic tree illustrating the three-group proposal for *Marseilleviridae*. RED values are indicated for groups I and II, and the numbers are consistent with the genus level for taxonomy. Group III does not have a RED value because there is only one virus in lineage E. The tree was built using the maximum likelihood method, with statistical support based on 1,000 replicates (bootstrap). The best model, selected by IQtree (ModelFinder), for the tree was VT + F + I + G4. The tree was rooted on *Iridoviridae* branch as an outgroup. The tree scale bars represent the number of amino acid substitutions per site. Note: MAGs, metagenome-assembled genomes. (B) Average nucleotide identity and average amino acid identity analysis of *Marseilleviridae*. Fourteen *Marseilleviruses* are grouped based on a similarity matrix composed by ANI (left heatmap) and AAI (right heatmap). The three viral groups are indicated. ANI <75% was set to zero. ANI values ranged from 77 to 100, and AAI values ranged from 53 to 100.

giant vesicles by the end of the cycle (26). These vesicles are important structures for their replication cycles, as the viruses can be released from the cell inside these vesicles, referred to as “expelled vesicles” (27, 28). This mechanism is important to ensure greater effectiveness in the subsequent entry of particles into another amoeba to start new cycle, corresponding to a sort of Trojan horse strategy. Alternatively, such structure may be related to the exocytosis of the viral progeny (26) and their increased resistance to harsh environments when being outside amoebae, waiting for new hosts. The presence of amorphic and horseshoe-like structures inside the viral factory (Fig. 1C and D) requires further investigations, and more detailed analyses of the replication cycle are needed to infer a biological function to these structures. It is known that in the initial stages of *Marseilleviridae* isolates viral factory formation, endosomal membranes are recruited. These recruited membranes are involved in the formation of the internal membranes that compose viral capsids (26). Therefore, it can be hypothesized that *M. cajunensis* VF

structures have been recruited from some cellular component to perform a function that is not yet known.

After analyzing the genome of *M. cajuinensis*, we observed that its genome size, GC content, and number of genes are compatible with that described for other members of the *Marseilleviridae* family (2, 3, 5, 9, 11, 13). The functional categorization of proteins suggests that more than half of the *M. cajuinensis* genome encode proteins with unknown functions. This is a very common characteristic among giant amoeba viruses and reinforces the need for new studies that aim the elucidation of the unknown functions of these proteins (1, 29, 30). Also, we detected 38 ORFans in a first gene prediction, but most of them have sizes that range from 50 to 100 amino acids. This puts in doubt whether these sequences are real proteins or whether they are artifacts due to the main gene prediction protocol used in this study. When using a new gene prediction tool, the number of ORFans decreased to 9. This considerable difference in results might be due to the lack in updates of prediction tools that currently are mostly indicated for prokaryotes, eukaryotes, and for viruses that have smaller and fewer complex genomes. The number of ORFs was also affected when different parameters and tools for prediction are utilized. In addition, we detected a gene that encodes a tRNA, which is not commonly described in members of the family *Marseilleviridae* (13, 14). By analyzing sequences from other *Marseilleviridae* members using different programs and parameters, we detected tRNAs in five *Marseilleviruses* that, to our knowledge, have not been previously described as encoding such sequences. The absence of tRNA detection might be attributed to the use of a single algorithm in most previous analyses. Our current analysis shows a difference in the sensitivity of tRNA detection, with Aragorn being more sensitive than the tRNAscanSE algorithm tested in parallel. This is likely due to the different tRNA search models and parameters used by each tool (31, 32). For example, the Aragorn does not depend on the taxonomic lineage specification as parameter to achieve maximum search sensitivity, whereas the tRNAscan-SE does (31). Thus, current gene prediction algorithms lack updates that consider the singularities of giant viruses. This highlights the importance to systematically use more than one algorithm for ORFs and tRNA prediction, as they can complement each other and can stimulate deeper investigations.

Comparisons between *M. cajuinensis* and members of the *Marseillevirus* genus, conducted through genomic and phylogenetic analyses, showed that they are all grouped within the lineage A. Despite this, *M. cajuinensis* and Tokyovirus form a divergent branch within this lineage. Phylogenetic analyses also showed that the common ancestor of the five classical *Marseilleviridae* lineages is in fact diversified into three main branches, which we refer to as group I (lineage A), group II (lineages B, C, and D), and group III (lineage E). After analyzing parameters such as RED, AAI, and ANI, it is possible to suggest that these three groups could potentially be considered as three genera. Taxonomically, group I currently corresponds to *Marseillevirus* genus, and group II corresponds to the recently proposed *Losanna* genus (that includes the *L. lausannense* and the *L. tunisiense* species). Group III and some members of the other proposed groups (e.g. Brazilian marseillevirus) remain to be officially assigned taxonomically. Also, AAI and ANI analyses suggested the organization of *Marseilleviridae* isolates in eight species (see Supplementary Figure 3 at <https://www.giantviruses.com/sup-material-of-papers/sup-material-the-genomic-and-phylogenetic-analysis-of-marseillevirus-cajuinensis-raises-questions-about-the-evolution-of-marseilleviridae-lineages-and-their-taxonomical-organization>), according to the percentage of sequence identity between each other. This could be helpful to classify the isolates that are still not considered officially.

The analyses of COGs shared between different lineages highlight conserved and variable COGs in each lineage. An in-depth analysis to understand the function of each protein belonging to the clusters was not performed here, and most part of these proteins might not have a known function. However, it is possible to hypothesize that conserved COGs might represent important genes to the lineage, possibly inherited

from their common ancestor. Conversely, the proteins belonging to clusters that vary among lineages might have different origins. The presence/absence of COGs analysis complemented the phylogeny and reinforced both the greater divergence of *Marseillevirus cajuinensis* within lineage A and the organization of Marseilleviridae classical lineages into three groups. However, is it worth mentioning that defining the number of Marseilleviridae lineages/genera is a big challenge and might be treacherous as it depends on the methods and the viruses considered in the analysis. Taking that into account, it is clear that there is a need to continue efforts to obtain new isolates as the Marseilleviridae pangenome is still open. The raised questions about the number of lineages within the Marseilleviridae family reflect the impact of new virus discovery on taxonomists' perspectives, as these new strains add new information to the analyses, sometimes leading to different tree topologies. Such new topologies call for updating phylogenetic organization and taxonomy to ensure that genus and species taxonomic levels better reflect the reality of diversity in a given taxon, rather than being biased due to sampling mostly specific habitats, such as freshwater. For this taxonomic update to happen, it is necessary to first establish the parameters that are needed to classify these viruses into new species or genus. Thus, this work represents a contribution to shape future updates in Marseilleviridae taxonomy.

MATERIALS AND METHODS

Viral isolation, multiplication, purification, and titration

The isolate was obtained through the collection of saltwater samples at Cajueiro da Praia city, located in Piauí state (Northeast coast of Brazil). The protocol was based on the inoculation of the collected samples on 96-well plates containing *Acanthamoeba castellanii* cells (33). The inoculated wells that presented cytopathic effects (i.e., rounding cells and cellular lysis) had their content collected and analyzed through transmission electron microscopy. After confirming the isolation, the virus was inoculated at a multiplicity of infection (MOI) of 0.01 in cell culture flasks containing 1.4×10^7 *Acanthamoeba castellanii* cells and 35 mL of peptone-yeast extract-glucose (PYG) medium, supplemented with penicillin (100 U/mL; Cellofarm, Brazil), streptomycin (100 µg/mL; Sigma-Aldrich, USA), and amphotericin B (0.25 µg/mL; Cultilab, Brazil). The cells were incubated at 32°C. Non-infected cells maintained in the same conditions were used as control. When viral-induced cytopathic effects were observed, the flask's content was collected. This content was filtered through 0.45 µm pores, and then it was ultracentrifuged (36,000 x g) in a 25% sucrose cushion for 2 hours. The pellet containing purified viral particles was homogenized in 300 µL of phosphate-buffered saline (PBS 1×). All the viral titers were obtained and calculated using the end-point method (34).

Transmission electron microscopy

To analyze the morphology of isolated viral particles, the samples were prepared for TEM. First, 7×10^6 *A. castellanii* cells, cultured in 25 mL of PYG medium, were inoculated with the virus at an MOI of 0.01. Once cytopathic effects were observed, we performed two consecutive washes with 0.1 M sodium phosphate buffer, and we subsequently fixed the cells for 2 hours at room temperature under rotation in an orbital mixer. The fixation solution consisted of 0.1 M sodium phosphate buffer and 2.5% glutaraldehyde. Following this initial fixation step, the cells underwent a secondary fixation with 2% osmium tetroxide before being embedded in Epon resin. This resin allowed an ultramicrotomy, and the 60-nm-thick sections were then examined using a transmission electron microscope (Spirit Biotwin FEI-120 kV) at the Center of Microscopy of the Federal University of Minas Gerais (CM-UFMG).

Sequencing, assembly, and annotation

The purified virus was sequenced using an Illumina MiSeq instrument with a paired-end library using the Illumina DNA Prep Kit (Illumina Inc., San Diego, CA, USA). The FastQC program was used for quality control of the obtained reads, and the per base sequence quality was considered satisfactory (phred >28). The reads were trimmed using the Trimmomatic tool (35). Genome *de novo* assembly was performed using Spades 3.12 program with default parameters (36, 37). The obtained scaffold was compared with sequences from the NCBI database, using BLASTn (database: nr/nt; expect threshold: 10^{-3}). Open reading frames were predicted with the GeneMarkS tool and Prodigal (38, 39), considering only proteins that were bigger than 50 amino acids. Additionally, tRNA-coding sequences (CDSs) were predicted using ARAGORN (parameters – type: tRNA; allow intron: yes and no (alternately); topology: circular; strand- both) and tRNAscanSE (parameters - Sequence source: general tRNA model; Search mode: default; Genetic Code for tRNA Isotype Prediction: universal) (31, 32). ORFs were annotated using BLASTp (expect threshold: 10^{-3}) against the NCBI non-redundant protein sequence (nr) database aiming to search for similar sequences in this database. The functional categorization of predicted proteins was carried out based on the Nucleo-Cytoplasmic Virus Orthologous Groups (40, 41).

Synteny and phylogenetic analysis

To perform synteny analyses, genome sequences of different MsV isolates were obtained from the NCBI GenBank database. Only genomes from isolated *Marseillevirus* (excluding those built from metagenomic data) and that were complete and available in GenBank (March 2023) were selected. As they have a circular topology, the sequences were manually curated to start from the major capsid protein aiming to facilitate image interpretation. After curating the sequences, synteny analysis was performed using the MAUVE program, with default parameters (42). The following genome sequences were retrieved from GenBank and then analyzed: Tokyovirus (NC_030230.1); *Marseillevirus marseillevirus* (GU071086.1); Cannes 8 virus (KF261120.1); *Marseillevirus Shanghai* (MG827395.1); Melbournevirus (KM275475.1); Kurlavirus (KY073338.1); Lausannevirus (HQ113105.1); Noumeavirus (KX066233.1); Port-miou virus (KT428292.1); Insectomime (HG428764.1); Tunisivirus (KF483846.1); Brazilian MsV (KT752522.1); Golden MsV (KT835053.1).

Phylogenetic trees were constructed using the IQtree software (version 1.6.12) with 1,000 bootstrap replicates as branch support (43). To prepare the data sets for alignment, a search for similar sequences was performed using the NCBI non-redundant protein sequences (nr) database and BLASTp with an expected threshold of 10^{-3} . Sequence alignment was performed using the MUSCLE algorithm (44). The best-fit substitution models were determined using the ModelFinder algorithm within IQtree (45). Finally, the resulting phylogenetic trees were visualized and edited using MEGA X software (46).

Relative evolutionary distance analyses were performed using phylogeny constructed according to parameters mentioned above. RED values were calculated using the R package “castor” (47), and the thresholds for taxonomic levels were defined as described in the Results section based in a previous work (23).

Pangenome and COGs analysis

All complete MsV sequences that were previously obtained for synteny analyses from GenBank were also subjected to a new gene prediction using GeneMarkS (38). The amino acid sequences of each predicted CDS were analyzed using the ProteinOrtho software (parameters - selfblast, identity: 30%, coverage: 50%, and e-value of 10^{-5}) (48). The output files generated by ProteinOrtho were used to analyze the pangenome and core genome of isolated MsV. Also, output files of orthologous proteins were used to compare the number of Clusters of Orthologous Groups that are shared between the studied viruses and to construct a hierarchical clustering based on the presence and absence of COGs

in different MsV. To analyze the sharing of COGs between different MsV, a network representation was constructed using the Gephi 0.10 software. For this, data obtained in ProteinOrtho analysis were used to create spreadsheets containing the “nodes” (viruses and COGs) and the “edges” (presence of COGs in each virus). Network representation was built using an algorithm based on attraction and repulsion forces (Force Atlas). To perform COGs presence and absence analysis, a binary file was generated, and a phenetic tree was created in the MultiExperiment Viewer program, version 4.9.0, using the hierarchical clustering algorithm and the Pearson correlation as distance metric (49).

Average nucleotide and amino acid identities

Whole-genome average nucleotide identity analysis was performed using FastANI (50) implemented on Galaxy Server (<https://usegalaxy.eu/>), on the complete genomes of 14 Marseilleviruses obtained from the NCBI GenBank database. ANI <75% was considered 0. Average amino acid identity was calculated using reciprocal best hits (two-way AAI) between two Marseilleviruses’ protein genomic data sets, considering an identity cutoff of 20%. AAI was estimated using the AAI calculator (<http://enve-omics.ce.gatech.edu/aai/>).

ACKNOWLEDGMENTS

We would like to thank all colleagues from Grupo de Estudo e Prospecção de Vírus Gigantes (GEPVIG) and from Laboratório de Vírus of Universidade Federal de Minas Gerais (UFMG). Also, we thank Centro de Microscopia of UFMG for the contribution of microscopy images.

We thank CNPq (Conselho Nacional de Desenvolvimento Científico e Tecnológico), CAPES (Coordenação de Aperfeiçoamento de Pessoal de Nível Superior), and FAPEMIG (Fundação de Amparo à Pesquisa do estado de Minas Gerais) for research funding.

This research is registered at SISGEN and SISBIO.

J.S.A., J.P.A.J., and R.A.L.R. are CNPq researchers.

P.C., G.G., and J.S.A. are contributors of the ICTV Marseillevirus study group (2016-2023).

AUTHOR AFFILIATIONS

¹Laboratório de Vírus, Departamento de Microbiologia, Universidade Federal de Minas Gerais (UFMG), Belo Horizonte, Minas Gerais, Brazil

²Laboratório de Virologia, Departamento de Microbiologia e Imunologia, Instituto de Biotecnologia, Universidade Estadual Paulista (Unesp), Alameda das Tecomarias s/n, Chácara Capão Bonito, Botucatu, Brazil

³IHU Méditerranée Infection, Marseille, France

⁴Microbes Evolution Phylogeny and Infections (MEPHI), Aix-Marseille University, Marseille, France

⁵Assistance Publique-Hôpitaux de Marseille (AP-HM), Marseille, France

⁶Centre for Research on Intracellular Bacteria and Giant Viruses, Institute of Microbiology, University Hospital Centre and University of Lausanne, Lausanne, Switzerland

⁷Department of Biological Sciences, Virginia Tech, Blacksburg, Virginia, USA

⁸Center for Emerging, Zoonotic, and Arthropod-Borne Infectious Disease Virginia Tech, Blacksburg, Virginia, USA

AUTHOR ORCIDs

Gilbert Greub  <http://orcid.org/0000-0001-9529-3317>

Frank Aylward  <http://orcid.org/0000-0002-1279-4050>

Rodrigo Araújo Lima Rodrigues  <http://orcid.org/0000-0001-7148-4012>

Jônatas Santos Abrahão  <http://orcid.org/0000-0001-9420-1791>

DATA AVAILABILITY

The *M. cajuinensis* genome sequence is available in GenBank under accession number OR991738.

REFERENCES

- Scola BL, Audic S, Robert C, Jungang L, de Lamballerie X, Drancourt M, Birtles R, Claverie J-M, Raoult D. 2003. A giant virus in amoebae. *Science* 299:2033–2033. <https://doi.org/10.1126/science.1081867>
- Boyer M, Yutin N, Pagnier I, Barrassi L, Fournous G, Espinosa L, Robert C, Azza S, Sun S, Rossmann MG, Suzan-Monti M, La Scola B, Koonin EV, Raoult D. 2009. Giant *Marseillevirus* highlights the role of amoebae as a melting pot in emergence of chimeric microorganisms. *Proc Natl Acad Sci U S A* 106:21848–21853. <https://doi.org/10.1073/pnas.0911354106>
- Thomas V, Bertelli C, Collyn F, Casson N, Telenti A, Goesmann A, Croxatto A, Greub G. 2011. Lausannevirus, a giant amoebal virus encoding histone doublets. *Environ Microbiol* 13:1454–1466. <https://doi.org/10.1111/j.1462-2920.2011.02446.x>
- Aherfi S, Pagnier I, Fournous G, Raoult D, La Scola B, Colson P. 2013. Complete genome sequence of Cannes 8 virus, a new member of the proposed family “*Marseilleviridae*”. *Virus Genes* 47:550–555. <https://doi.org/10.1007/s11262-013-0965-4>
- Aherfi S, Boughalmi M, Pagnier I, Fournous G, La Scola B, Raoult D, Colson P. 2014. Complete genome sequence of Tunisivirus, a new member of the proposed family *Marseilleviridae*. *Arch Virol* 159:2349–2358. <https://doi.org/10.1007/s00705-014-2023-5>
- Doutre G, Philippe N, Abergel C, Claverie J-M. 2014. Genome analysis of the first *Marseilleviridae* representative from Australia indicates that most of its genes contribute to virus fitness. *J Virol* 88:14340–14349. <https://doi.org/10.1128/JVI.02414-14>
- Fabre E, Jeudy S, Santini S, Legendre M, Trauchessec M, Couté Y, Claverie J-M, Abergel C. 2017. Noumeavirus replication relies on a transient remote control of the host nucleus. *Nat Commun* 8:15087. <https://doi.org/10.1038/ncomms15087>
- Takemura M. 2016. Morphological and taxonomic properties of *Tokyovirus*, the first *Marseilleviridae* member isolated from Japan. *Microbes Environ* 31:442–448. <https://doi.org/10.1264/jsme2.ME16107>
- Dornas FP, Assis FL, Aherfi S, Arantes T, Abrahão JS, Colson P, La Scola B. 2016. A Brazilian marseillevirus is the founding member of a lineage in family *Marseilleviridae*. *Viruses* 8:76. <https://doi.org/10.3390/v8030076>
- Colson P, Fancello L, Gimenez G, Armougom F, Desnues C, Fournous G, Yoosuf N, Million M, La Scola B, Raoult D. 2013. Evidence of the megavirome in humans. *J Clin Virol* 57:191–200. <https://doi.org/10.1016/j.jcv.2013.03.018>
- Dos Santos RN, Campos FS, Medeiros de Albuquerque NR, Finoketti F, Corrêa RA, Cano-Ortiz L, Assis FL, Arantes TS, Roehle PM, Franco AC. 2016. A new marseillevirus isolated in Southern Brazil from *Limnoperna fortunei*. *Sci Rep* 6:35237. <https://doi.org/10.1038/srep35237>
- Bäckström D, Yutin N, Jørgensen SL, Dharamshi J, Homa F, Zaremba-Niedwiedzka K, Spang A, Wolf YI, Koonin EV, Ettema TJG. 2019. Virus genomes from deep sea sediments expand the ocean megavirome and support independent origins of viral gigantism. *mBio* 10:e02497-18. <https://doi.org/10.1128/mBio.02497-18>
- Sahmi-Bounsiar D, Rolland C, Aherfi S, Boudjemaa H, Levasseur A, La Scola B, Colson P. 2021. Marseilleviruses: an update in 2021. *Front Microbiol* 12:648731. <https://doi.org/10.3389/fmicb.2021.648731>
- Rodrigues RAL, da Silva LCF, Abrahão JS. 2020. Translating the language of giants: translation-related genes as a major contribution of giant viruses to the virosphere. *Arch Virol* 165:1267–1278. <https://doi.org/10.1007/s00705-020-04626-2>
- Abrahão JS, Araújo R, Colson P, La Scola B. 2017. The analysis of translation-related gene set boosts debates around origin and evolution of mimiviruses. *PLoS Genet* 13:e1006532. <https://doi.org/10.1371/journal.pgen.1006532>
- Current ICTV taxonomy release. ICTV. Available from: <https://ictv.global/taxonomy>. Retrieved 01 Oct 2022.
- Boughalmi M, Pagnier I, Aherfi S, Colson P, Raoult D, La Scola B. 2013. First isolation of a Marseillevirus in the Diptera Syrphidae *Eristalis tenax*. *Intervirology* 56:386–394. <https://doi.org/10.1159/000354560>
- Andrade A, Rodrigues RAL, Oliveira GP, Andrade KR, Bonjardim CA, La Scola B, Kroon EG, Abrahão JS. 2017. Filling knowledge gaps for mimivirus entry, uncoating, and morphogenesis. *J Virol* 91:e01335-17. <https://doi.org/10.1128/JVI.01335-17>
- Maruri-Avidal L, Weisberg AS, Moss B. 2013. Association of the vaccinia virus A11 protein with the endoplasmic reticulum and crescent precursors of immature virions. *J Virol* 87:10195–10206. <https://doi.org/10.1128/JVI.01601-13>
- Chatterjee A, Kondabagil K. 2017. Complete genome sequence of Kurlavirus, a novel member of the family *Marseilleviridae* isolated in Mumbai, India. *Arch Virol* 162:3243–3245. <https://doi.org/10.1007/s00705-017-3469-z>
- Blanca L, Christo-Foroux E, Rigou S, Legendre M. 2020. Comparative analysis of the circular and highly asymmetrical *Marseilleviridae* genomes. *Viruses* 12:1270. <https://doi.org/10.3390/v12111270>
- Queiroz VF, Carvalho J, de Souza FG, Lima MT, Santos JD, Rocha KLS, de Oliveira DB, Araújo JP, Ullmann LS, Rodrigues RAL, Abrahão JS. 2023. Analysis of the genomic features and evolutionary history of pithovirus-like isolates reveals two major divergent groups of viruses. *J Virol* 97:e0041123. <https://doi.org/10.1128/jvi.00411-23>
- Aylward FO, Moniruzzaman M, Ha AD, Koonin EV. 2021. A phylogenomic framework for charting the diversity and evolution of giant viruses. *PLOS Biol* 19:e3001430. <https://doi.org/10.1371/journal.pbio.3001430>
- Aylward FO, Abrahão JS, Brussaard CPD, Fischer MG, Moniruzzaman M, Ogata H, Suttle CA. 2023. Taxonomic update for giant viruses in the order Imitervirales (phylum *Nucleocytoviricota*). *Arch Virol* 168:283. <https://doi.org/10.1007/s00705-023-05906-3>
- Doutre G, Arfib B, Rochette P, Claverie J-M, Bonin P, Abergel C. 2015. Complete genome sequence of a new member of the *Marseilleviridae* recovered from the brackish submarine spring in the Cassis Port-Miou Calanque, France. *Genome Announc* 3:e01148-15. <https://doi.org/10.1128/genomeA.01148-15>
- Arantes TS, Rodrigues RAL, Dos Santos Silva LK, Oliveira GP, de Souza HL, Khalil JYB, de Oliveira DB, Torres AA, da Silva LL, Colson P, Kroon EG, da Fonseca FG, Bonjardim CA, La Scola B, Abrahão JS. 2016. The large Marseillevirus explores different entry pathways by forming giant infectious vesicles. *J Virol* 90:5246–5255. <https://doi.org/10.1128/JVI.00177-16>
- Greub G, Raoult D. 2004. Microorganisms resistant to free-living amoebae. *Clin Microbiol Rev* 17:413–433. <https://doi.org/10.1128/CMR.17.2.413-433.2004>
- Greub G, Raoult D. 2002. Crescent bodies of *Parachlamydia acanthamoeba* and its life cycle within *Acanthamoeba polyphaga*: an electron micrograph study. *Appl Environ Microbiol* 68:3076–3084. <https://doi.org/10.1128/AEM.68.6.3076-3084.2002>
- Boratto PVM, Oliveira GP, Machado TB, Andrade A, Baudoin J-P, Klose T, Schulz F, Azza S, Decloquement P, Chabrière E, Colson P, Levasseur A, La Scola B, Abrahão JS. 2020. Yaravirus: a novel 80-nm virus infecting *Acanthamoeba castellanii*. *Proc Natl Acad Sci U S A* 117:16579–16586. <https://doi.org/10.1073/pnas.2001637117>
- Legendre M, Bartoli J, Shmakova L, Jeudy S, Labadie K, Adrait A, Lescot M, Poirot O, Bertaux L, Bruley C, Couté Y, Rivkina E, Abergel C, Claverie J-M. 2014. Thirty-thousand-year-old distant relative of giant icosahedral DNA viruses with a pandoravirus morphology. *Proc Natl Acad Sci U S A* 111:4274–4279. <https://doi.org/10.1073/pnas.1320670111>
- Laslett D, Canback B. 2004. ARAGORN, a program to detect tRNA genes and tmRNA genes in nucleotide sequences. *Nucleic Acids Res* 32:11–16. <https://doi.org/10.1093/nar/gkh152>
- Chan PP, Lowe TM. 2019. tRNAscan-SE: searching for tRNA genes in genomic sequences. *Methods Mol Biol* 1962:1–14. https://doi.org/10.1007/978-1-4939-9173-0_1

33. Machado TB, de Aquino ILM, Abrahão JS. 2022. Isolation of giant viruses of *Acanthamoeba castellanii*. *Curr Protoc* 2:e455. <https://doi.org/10.1002/cpz1.455>
34. Reed LJ, Muench H. 1938. A simple method of estimating fifty per cent endpoints. *Am J Epidemiol* 27:493–497. <https://doi.org/10.1093/oxfordjournals.aje.a118408>
35. Bolger AM, Lohse M, Usadel B. 2014. Trimmomatic: a flexible trimmer for Illumina sequence data. *Bioinformatics* 30:2114–2120. <https://doi.org/10.1093/bioinformatics/btu170>
36. Bankevich A, Nurk S, Antipov D, Gurevich AA, Dvorkin M, Kulikov AS, Lesin VM, Nikolenko SI, Pham S, Pribelski AD, Pyshkin AV, Sirotkin AV, Vyahhi N, Tesler G, Alekseyev MA, Pevzner PA. 2012. SPAdes: a new genome assembly algorithm and its applications to single-cell sequencing. *J Comput Biol* 19:455–477. <https://doi.org/10.1089/cmb.2012.0021>
37. Pribelski A, Antipov D, Meleshko D, Lapidus A, Korobeynikov A. 2020. Using spades de novo assembler. *Curr Protoc Bioinformatics* 70:e102. <https://doi.org/10.1002/cpbi.102>
38. Besemer J, Borodovsky M. 2005. GeneMark: web software for gene finding in prokaryotes, eukaryotes and viruses. *Nucleic Acids Res* 33:W451–W454. <https://doi.org/10.1093/nar/gki487>
39. Hyatt D, Chen G-L, Locascio PF, Land ML, Larimer FW, Hauser LJ. 2010. Prodigal: prokaryotic gene recognition and translation initiation site identification. *BMC Bioinformatics* 11:119. <https://doi.org/10.1186/1471-2105-11-119>
40. Yutin N, Wolf YI, Raoult D, Koonin EV. 2009. Eukaryotic large nucleocytoplasmic DNA viruses: clusters of orthologous genes and reconstruction of viral genome evolution. *Virol J* 6:223. <https://doi.org/10.1186/1743-422X-6-223>
41. Rodrigues RAL, Queiroz VF, Ghosh J, Dunigan DD, Van Etten JL. 2022. Functional genomic analyses reveal an open pan-genome for the chloroviruses and a potential for genetic innovation in new isolates. *J Virol* 96:e0136721. <https://doi.org/10.1128/JVI.01367-21>
42. Darling ACE, Mau B, Blattner FR, Perna NT. 2004. Mauve: multiple alignment of conserved genomic sequence with rearrangements. *Genome Res* 14:1394–1403. <https://doi.org/10.1101/gr.2289704>
43. Nguyen L-T, Schmidt HA, von Haeseler A, Minh BQ. 2015. IQ-TREE: a fast and effective stochastic algorithm for estimating maximum-likelihood phylogenies. *Mol Biol Evol* 32:268–274. <https://doi.org/10.1093/molbev/msu300>
44. Edgar RC. 2004. MUSCLE: multiple sequence alignment with high accuracy and high throughput. *Nucleic Acids Res* 32:1792–1797. <https://doi.org/10.1093/nar/gkh340>
45. Kalyaanamoorthy S, Minh BQ, Wong TKF, von Haeseler A, Jermin LS. 2017. ModelFinder: fast model selection for accurate phylogenetic estimates. *Nat Methods* 14:587–589. <https://doi.org/10.1038/nmeth.4285>
46. Kumar S, Stecher G, Li M, Knyaz C, Tamura K. 2018. MEGA X: molecular evolutionary genetics analysis across computing platforms. *Mol Biol Evol* 35:1547–1549. <https://doi.org/10.1093/molbev/msy096>
47. Louca S, Doebeli M. 2018. Efficient comparative phylogenetics on large trees. *Bioinformatics* 34:1053–1055. <https://doi.org/10.1093/bioinformatics/btx701>
48. Lechner M, Findeiss S, Steiner L, Marz M, Stadler PF, Prohaska SJ. 2011. Proteinortho: detection of (Co-)orthologs in large-scale analysis. *BMC Bioinformatics* 12:124. <https://doi.org/10.1186/1471-2105-12-124>
49. Howe E, Holton K, Nair S, Schlauch D, Sinha R, Quackenbush J. 2010. MeV: MultiExperiment viewer, p 267–277. In Ochs MF, Casagrande JT, Davuluri RV (ed), *Biomedical informatics for cancer research*. Springer US, Boston, MA.
50. Jain C, Rodriguez-R LM, Phillippy AM, Konstantinidis KT, Aluru S. 2018. High throughput ANI analysis of 90K prokaryotic genomes reveals clear species boundaries. *Nat Commun* 9:5114. <https://doi.org/10.1038/s41467-018-07641-9>



Gene duplication as a major force driving the genome expansion in some giant viruses

Talita B. Machado,¹ Agnello C. R. Picorelli,² Bruna L. de Azevedo,¹ Isabella L. M. de Aquino,¹ Victória F. Queiroz,¹ Rodrigo A. L. Rodrigues,¹ João Pessoa Araújo Jr.,³ Leila S. Ullmann,³ Thiago M. dos Santos,⁴ Rafael E. Marques,⁵ Samuel L. Guimarães,⁵ Ana Cláudia S. P. Andrade,⁶ Juliana S. Gularte,⁷ Meriane Demoliner,⁷ Micheli Filippi,⁷ Vyctoria M. A. G. Pereira,⁷ Fernando R. Spilki,⁷ Mart Krupovic,⁸ Frank O. Aylward,^{9,10} Luiz-Eduardo Del-Bem,⁴ Jônatas S. Abrahão¹

AUTHOR AFFILIATIONS See affiliation list on p. 14.

ABSTRACT Giant viruses with their gigantic genomes are among the most intriguing components of the virosphere. How these viruses attained such giant genomes remains unclear, despite considerable efforts to understand this phenomenon. Here, we describe the discovery of cedratvirus pambiensis, an amoebal giant virus isolated in Brazil. Although the virion morphology and replication cycle of *c. pambiensis* are very similar to those described for other cedratviruses, whole genome sequencing revealed the largest cedratvirus genome ever described, with 623,564 base pairs and 842 predicted protein-coding genes (among them, 76 ORFans). Genome analysis has revealed an unprecedented number of paralogous genes, with ~73% of the *c. pambiensis* genome being composed of genes with two or more copies. Large families of functionally diverse paralogous genes included up to >70 copies and were distributed across the genome. The in-depth investigation of the mechanisms and origins of gene duplications revealed that both tandem-like duplications and distal transfer of syntenic blocks of genes contributed to the *c. pambiensis* genomic expansion. Finally, a comprehensive genome analysis of viruses from all known giant virus families suggested that gene duplication is one of the key mechanisms underlying genomic gigantism across the phylum *Nucleocytoviricota*. The expansion of viral genomes through successive duplications followed by subfunctionalization and exaptation of the paralogous gene copies may promote the adaptation of giant viruses to a variety of niches.

IMPORTANCE Giant viruses are noteworthy not only due to their enormous particles but also because of their gigantic genomes. In this context, a fundamental question has persisted: how did these genomes evolve? Here we present the discovery of cedratvirus pambiensis, featuring the largest genome ever described for a cedratvirus. Our data suggest that the larger size of the genome can be attributed to an unprecedented number of duplicated genes. Further investigation of this phenomenon in other viruses has illuminated gene duplication as a key evolutionary mechanism driving genome expansion in diverse giant viruses. Although gene duplication has been described as a recurrent event in cellular organisms, our data highlights its potential as a pivotal event in the evolution of gigantic viral genomes.

KEYWORDS giant virus, *Pithoviridae*, cedratvirus pambiensis, genome expansion, paralogous genes, *Nucleocytoviricota*

Gene and genomic segment duplication is a critical mechanism underlying the evolution of cellular organisms by providing raw genetic material for the emergence of new gene functions and pathways (1). Duplicated genes can undergo subfunctionalization by acquiring mutations, resulting in the evolution of new protein

Editor Colin R. Parrish, Cornell University Baker Institute for Animal Health, Ithaca, New York, USA

Address correspondence to Jônatas S. Abrahão, jonatas.abrahao@gmail.com, or Luiz-Eduardo Del-Bem, delbem@ufmg.br.

The authors declare no conflict of interest.

See the funding table on p. 15.

Received 23 August 2023

Accepted 26 October 2023

Published 21 November 2023

Copyright © 2023 American Society for Microbiology. All Rights Reserved.

functions. The significance of this phenomenon in evolution is evidenced by the widespread occurrence of duplicated genes across all domains of life (2–5). It has been estimated that around 30%–65% of the genes in multicellular eukaryotes, such as humans, have emerged through duplication (6, 7).

Giant viruses of amoeba are characterized by their large genome sizes and complex gene repertoires (8–11). Although the driving forces that led to the genome gigantism of those viruses are not fully understood, horizontal gene transfer, *de novo* gene emergence, and gene duplication have all been hypothesized to have contributed to genome expansion (12–18). Large families of functionally diverse paralogous genes have been identified in giant viruses of amoebas, including genes encoding ankyrin repeat-containing proteins, receptors for ubiquitination targets, and proteins with glycosyltransferase domains. In addition, many of these gene families are composed of unknown proteins or ORFan genes (13, 19). Although studies on gene duplication in giant viruses are scarce, there is convincing evidence showing that approximately one-third of the mimivirus genome and 50% of pandoravirus genomes are composed of multi-copy genes (13, 19).

Here, we report the discovery of cedratvirus pambiensis, a giant amoeba virus with the largest genome size ever described for the cedratvirus group, comprising 623,564 base pairs. The investigation of the architecture of the genome revealed an unprecedented abundance of duplicated genes, which constitute up to 72% of the total genome, a proportion on par with or surpassing that observed in cellular organisms. Most of these genes are grouped into six major gene families. Only 27.7% of the genome is composed of single-copy genes (non-duplicated genes). The expansion of the analyses to other varidnaviruses revealed extensive gene duplications in most groups of giant viruses, most markedly in members of the “Pithoviridae”-related viruses (which includes cedratviruses), pandoraviruses, and some mimiviruses. The discovery of *c. pambiensis* expands our understanding of the diversity and complexity of giant viruses, emphasizing the role of gene duplication in driving their genome expansion and shaping the genomic content.

RESULTS

Cedratvirus pambiensis particles and replication cycle

As part of our ongoing efforts to characterize the diversity of giant viruses infecting amoeba, we have isolated a new cedratvirus, *c. pambiensis*, from a water sample collected in a small, forested area at the Federal University of Minas Gerais (UFMG) campus, Belo Horizonte, Brazil. Inoculated amoebas exhibited cytopathic effects such as rounding and lysis, and upon light microscopy examination, it was possible to visualize viral particles. To gain a more comprehensive understanding of the particles' characteristics, we analyzed images obtained by transmission electron microscopy (TEM), negative staining electron microscopy (NSEM) (Fig. 1), and scanning electron microscopy (SEM) (see Supplementary Fig. 1a posted at <https://www.giantviruses.com/sup-material-of-papers/sup-material-gene-duplication-as-a-major-force-driving-the-genome-expansion-in-some-giant-viruses>). The virus particles were oval-shaped, measuring approximately 1 μm in length and 500 nm in width (Fig. 1a). The capsid is composed of parallel striations (Fig. 1a) and may have one or two apical “corks.” Most observed particles had two corks, which is consistent with previous descriptions of cedratviruses. Notably, the capsid of *c. pambiensis* exhibited surface fibrils, a structure that has not been previously documented in cedratviruses (Fig. 1c). Although not visible by TEM and SEM, these fibrils were present in all images obtained by NSEM.

The replication cycle of *c. pambiensis* is a complex process that involves several steps (Fig. 1). It begins with the entry of viral particles into the host cell, which probably occurs via phagocytosis. Once inside the cell, the viral particles undergo uncoating, followed by an eclipse period which typically lasts for around 3 hours (Supplementary Fig. 1b posted at <https://www.giantviruses.com/sup-material-of-papers/sup-material-gene-duplication-as-a-major-force-driving-the-genome-expansion-in-some-giant-viruses>). The uncoating

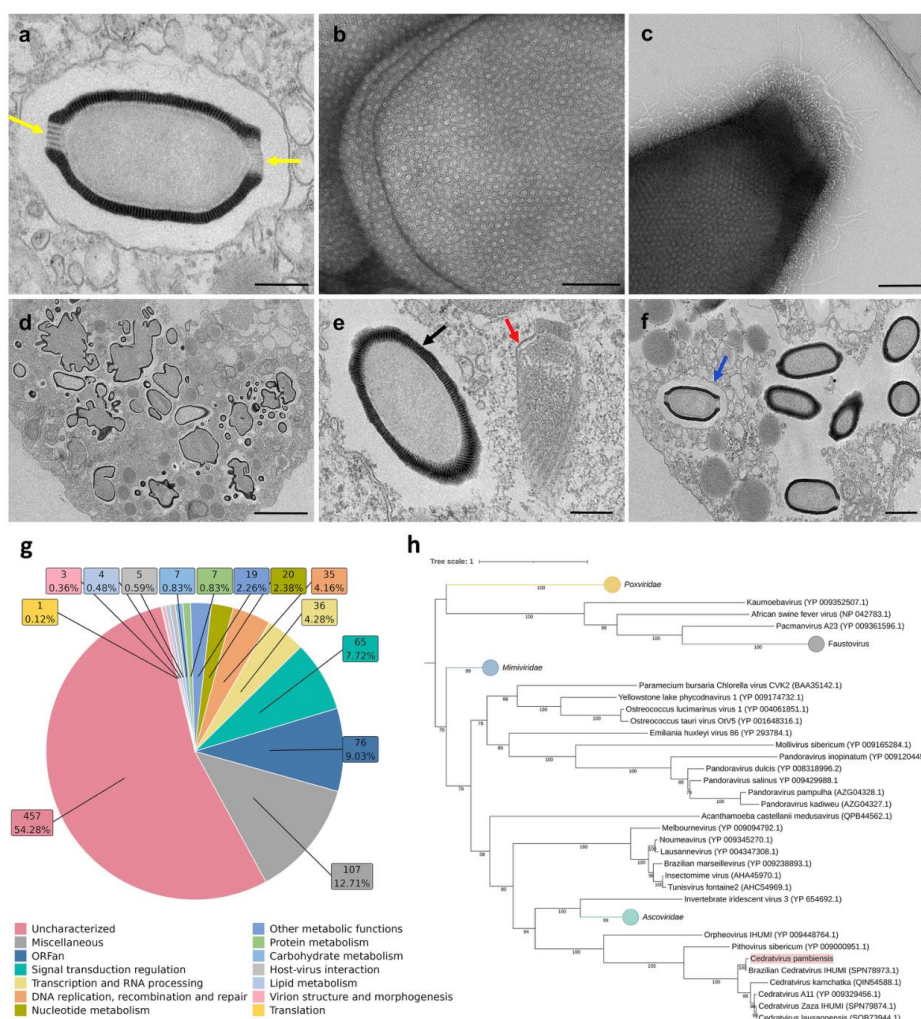


FIG 1 Particle, replication cycle, and genomic features of *C. pambiensis*. (a) Cedratvirus particle showing an oval shape with two apical corks (yellow arrows). Scale bar: 200 nm. (b) Zoom in the particle, showing the parallel striated structures of the capsid. Scale bar: 100 nm. (c) Observation of surface fibrils on the capsid. Scale bar: 100 nm. (d) Amorphous structures with no defined function in the cytoplasm of an infected amoeba. Scale bar: 2 μ m. (e) Assembly of new viral progeny. It is possible to observe structures of early particles being formed (red arrow) and mature particles (black arrow) at the same time inside the cells. Scale bar: 200 nm. (f) A viral particle was observed inside a vesicle after assembly (blue arrow), suggesting release by exocytosis before cell lysis. Scale bar: 500 nm. (g) Functional categories of *C. pambiensis* predicted genes. The color legend is provided below the graph. (h) Maximum likelihood phylogenetic tree constructed with amino acid sequences from the DNA polymerase subunit B of cedratviruses and other nucleocytoviruses. The new isolate described here, *C. pambiensis* (highlighted in pink), clustered with other cedratviruses, closer to the Brazilian cedratvirus. The scale bar indicates the genetic distance.

involves the removal of the viral cork to release the viral genome into the cytoplasm of the host cell. The next step is the formation of the viral factory, which is a region within the host cell that supports viral replication. In electron micrographs, the viral factory appears as a space that is unbounded and electron-lucent. Within the factory, amorphous electron-dense structures can be observed (Fig. 1d). Although the function of

TABLE 1 Comparison between the genomes of all cedratviruses with published genomes

Virus	Genome size	Predicted proteins	% Intergenic regions
Cedratvirus A11	589,068 bp	574	18.99
Cedratvirus lausannensis	575,161 bp	643	17.15
Cedratvirus zaza	560,887 bp	636	15.69
Brazilian cedratvirus	460,038 bp	533	14.43
Cedratvirus kamchatka	466,767 bp	545	18.26
Cedratvirus pambiensis	623,564 bp	842	10.59

these structures is unknown, they appear to be composed of material that is similar to that of the viral capsid, as seen in Fig. 1a. During the assembly of new viral particles, initial structures that will contribute to the formation of new virions can be observed, as shown in Fig. 1e. At 12 hours post-infection (hpi), viral production reaches its maximum level, after which it plateaus, as seen in Supplementary Fig. 1b posted at <https://www.giantviruses.com/sup-material-of-papers/sup-material-gene-duplication-as-a-major-force-driving-the-genome-expansion-in-some-giant-viruses>. The final step in the replication cycle is the release of viral progeny, which occurs via cell lysis. However, exocytosis may also play a role in this process, as depicted in Fig. 1f, where particles can be visualized inside vesicles close to the cell plasma membrane at the end of the infection cycle.

Cedratvirus pambiensis has an unprecedented abundance of paralogous genes

Genomic characterization of *c. pambiensis* yielded a circular dsDNA molecule of 623,564 bp and encoding 842 predicted proteins. Until then, the largest cedratvirus genome was described for cedratvirus A11, with 589,068 bp, and the largest number of predicted proteins was described for cedratvirus lausannensis, with 643. Thus, *c. pambiensis* is the cedratvirus with the largest genome and highest number of predicted proteins among all cedratviruses published to date (Table 1). As gene prediction methods may vary among different studies, we performed the gene prediction of all available cedratviruses using the same parameters that we applied to *c. pambiensis*. Although we observed a general increase in the number of predicted genes for all viruses, *c. pambiensis* still holds the record for the largest number of predicted genes among the isolated viruses. Functional analysis of the predicted proteins (Fig. 1g) revealed that most of them are uncharacterized (54.24%), and ORFans (9.03%). Proteins related to the regulation of signal transduction; transcription and RNA processing; DNA replication, recombination and repair, and different types of metabolism were also identified. The construction of a phylogenetic tree using amino acid sequences from the family B DNA polymerase showed that the new isolate clustered with other cedratviruses (Fig. 1h), and most closely to the Brazilian cedratvirus. The synteny analysis reinforces the proximity of these two cedratviruses, when compared to the other cedratviruses (see Supplementary Fig. 2 posted at <https://www.giantviruses.com/sup-material-of-papers/sup-material-gene-duplication-as-a-major-force-driving-the-genome-expansion-in-some-giant-viruses>).

Initially, we hypothesized that the increase in the genome size could be due to the presence of a new class of genes or a substantial number of ORFans. However, the annotation of the *c. pambiensis* genome revealed a gene content that is similar to that of other cedratviruses. Next, we investigated the intergenic content of *c. pambiensis* genome and compared it to that of other cedratviruses. However, after analyzing the intergenic content in all cedratviruses with available genomes, we observed that *c. pambiensis* has the lowest percentage (10.59%) of predicted intergenic regions among all of them (mean of 16.90%) (see Supplementary Table 1 posted at <https://www.giantviruses.com/sup-material-of-papers/sup-material-gene-duplication-as-a-major-force-driving-the-genome-expansion-in-some-giant-viruses>).

Then, we tested whether the larger genome size of *c. pambiensis* could be explained by the increase in the number of paralogous genes, which occurs due to gene and genomic segment duplications. We performed an all-against-all BLASTp analysis of the predicted proteins of *c. pambiensis*, which revealed an unexpectedly large number of paralogous groups with more than three genes, as well as paralogs grouped in pairs and triplets (Fig. 2). Only 27.7% of the *c. pambiensis* genome consists of single copy genes (Fig. 2). At least six large gene families (>20 genes) were identified in *c. pambiensis* genome, encoding functionally diverse proteins, including ankyrin-domain containing proteins, collagen-like proteins, serine-threonine protein kinases, hypothetical proteins, proteins containing F-box domain, ORFans, and others. Certain families presented genes with more than one predicted function or domain, suggesting progressive differentiation after duplication (Fig. 2). All the information about the paralogous genes is described in Supplementary Material 1 posted at <https://www.giantviruses.com/sup-material-of-papers/sup-material-gene-duplication-as-a-major-force-driving-the-genome-expansion-in-some-giant-viruses>.

Of 842 total genes, 609 (72.3%) are part of multi-gene families while only 233 (27.7%) are single-copy genes (Fig. 3a). We observed that a large fraction of these paralogous groups (34.6%) are composed of tandem genomic segment duplications (Fig. 3a and b). We then evaluated the percentage of tandemly duplicated genes across gene families, showing that these events are much more common in the six largest gene clusters (57%), while in low-copy number families present in triplets (9%) or pairs of genes (10%) tandem duplication events are less frequent (Fig. 3c). This finding suggests that tandem duplications are primarily responsible for the formation and expansion of large gene families.

To better understand the tandem duplication events and their effect on the genome evolution of these viruses, we constructed phylogenetic trees with the protein sequences for the six largest gene families (or clusters). Analysis of the phylogenetic trees showed that two types of duplication events occurred: proximal tandem duplications (involving more recent duplications) and chromosomal segment duplications (when an entire block of tandem genes appears to have been copied from one part of the genome and pasted into another, occasionally disrupting the preexisting genes). As an example, these analyses were detailed for the phylogenetic tree of cluster 3 (Fig. 3d), in which tandem genes were identified (Fig. 3e). Both proximal tandem duplication events (Fig. 3f) and chromosome segment duplication events (Fig. 3g) can be observed, and we note that these events can follow each other. Taking the tandem genes of groups A (207-208-209-210-211) and B (241-242-243-244) as an example, two interpretations can be made: (i) a copy-paste event occurred from group A to group B, and a gene was lost afterward; (ii) there was a copy-paste event from group B to group A, and subsequently, a proximal tandem duplication gave rise to gene 208. The phylogenetic trees for the other large gene families can be seen in Supplementary Fig. 3 posted at <https://www.giantviruses.com/sup-material-of-papers/sup-material-gene-duplication-as-a-major-force-driving-the-genome-expansion-in-some-giant-viruses>. We quantified the two events (proximal tandem duplications and chromosomal segment duplications) for the six largest gene families (see Supplementary Fig. 4 posted at <https://www.giantviruses.com/sup-material-of-papers/sup-material-gene-duplication-as-a-major-force-driving-the-genome-expansion-in-some-giant-viruses>) and noticed that they are frequent and seem to have a great influence on the genome evolution of this virus.

After a gene duplication event, the copies follow different evolutionary paths. When one of the copies suffers an extreme reduction in its coding sequence (CDS) caused by the emergence of a premature stop codon, we can infer that a pseudogenization event has occurred (resulting in a progressive loss of gene function). Our data suggest that there was a significant difference in CDS length and identity among genes within the

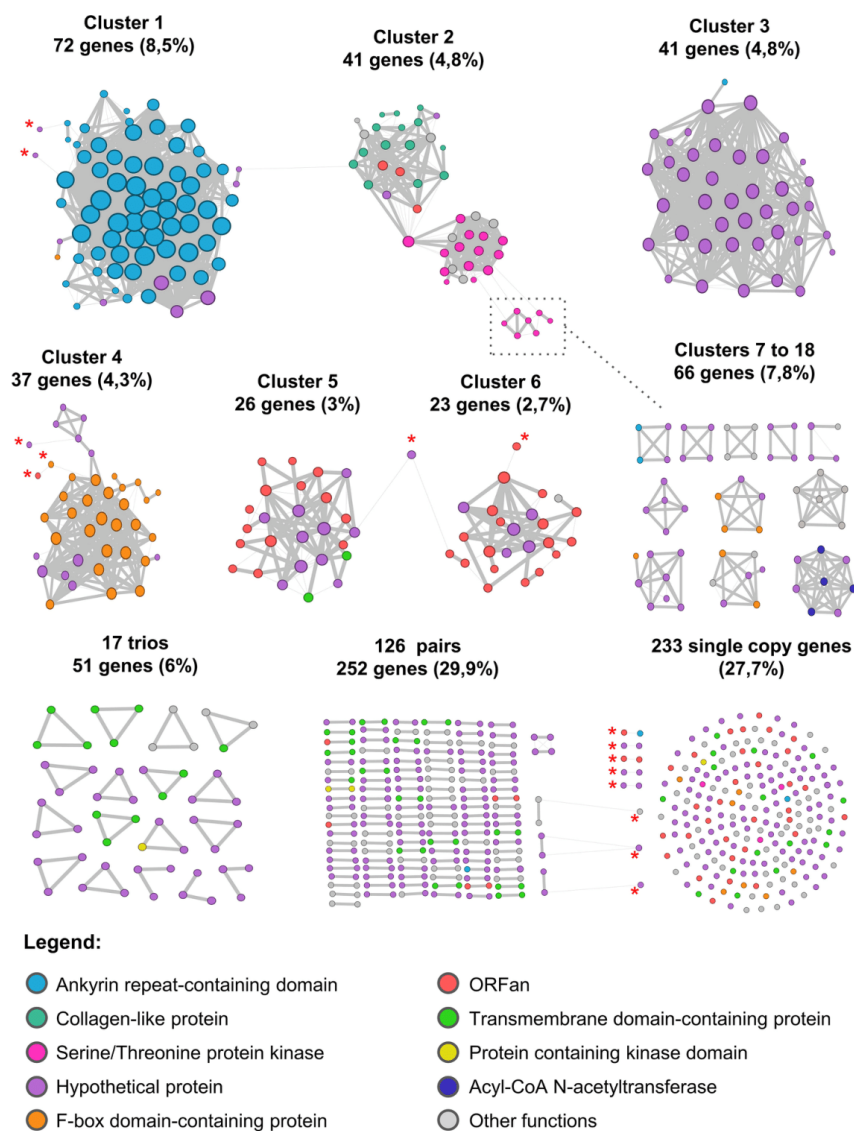


FIG 2 Network of clusters, trios, pairs, and single copy genes in the *C. pambiensis* genome. Reciprocal BLASTp-hits (coverage ≥ 30 and $e\text{-value} < 1e-4$) between two proteins are represented by thicker lines, while non-reciprocal BLASTp-hits are represented by thinner lines. Considering the defined criteria, to be part of the cluster, the gene must: (1) have a reciprocal match with some gene within the cluster (thick line) or (2) have at least two non-reciprocal matches with genes within the cluster (thin line). Genes that only had one non-reciprocal match with a gene within the cluster were not considered part of that cluster. Asterisks indicate single genes, which were not included within the clusters according to the aforementioned criteria. The square highlights cluster 10, in which has non-reciprocal hits with cluster 2. The color legend is provided below the image.

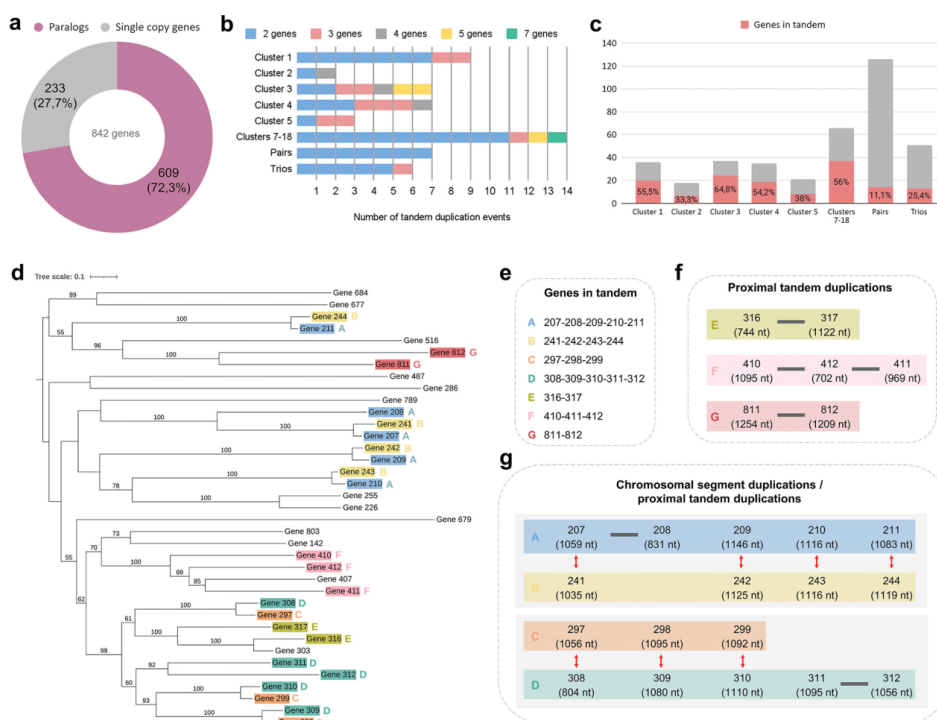


FIG 3 Gene duplication analyses in the *c. pambiensis* genome. (a) Number and percentage of genes in paralog groups or single copy genes in *c. pambiensis* genome. (b) Number of tandem duplication events observed within paralog clusters with more than three genes and low-copy number clusters composed of trios and pairs of genes. (c) Percentage of tandem duplication events observed within paralogs clusters, trios, and pairs. (d) Maximum likelihood phylogenetic tree constructed with protein sequences encoded by cluster 3 genes. Tandem genes are highlighted and colored in the tree according to the organization shown in (e). (e) Tandem genes highlighted in (d). They were organized in ascending order. (f) Proximal tandem duplication events are identified in (d). (g) Chromosomal segment duplications plus proximal duplication events identified in (d). In (f) and (g), the length of the gene in nucleotides is depicted below the gene ID.

same family, indicating non-negligible pseudogenization (Fig. 4a, and see Supplementary Fig. 5 and 6 posted at <https://www.giantviruses.com/sup-material-of-papers/sup-material-gene-duplication-as-a-major-force-driving-the-genome-expansion-in-some-giant-viruses>). In addition to gene size/coverage variation, we also observed considerable sequence divergence of the paralogous proteins, so that some of the cluster members were not reciprocally identifiable as homologous in BLASTp analysis, suggesting independent and progressive evolution after gene duplication (Fig. 3 and 4, and see Supplementary Fig. 5 and 6 posted at <https://www.giantviruses.com/sup-material-of-papers/sup-material-gene-duplication-as-a-major-force-driving-the-genome-expansion-in-some-giant-viruses>).

The chromosome position of the paralogs can provide clues about how genome expansion has evolved. We observed that some clusters (1, 3, and 4) appear to have more gene copies concentrated in a given region within the genome, while others (2, 5, and 6) are more spread throughout the genome (Fig. 4b). But in general, the paralogs belonging to those six major gene families are scattered throughout the *c. pambiensis* genome (see Supplementary Fig. 7 posted at <https://www.giantviruses.com/sup-material-of-papers/>

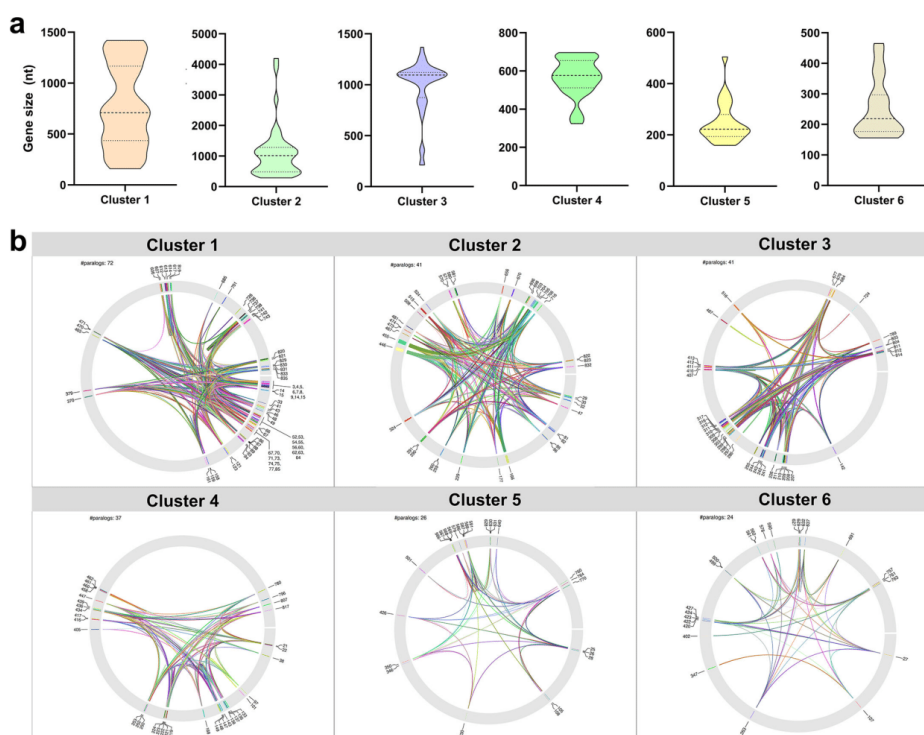


FIG 4 Size and location of paralogous genes comprising each large family of genes (clusters 1 to 6). (a) Violin plots showing gene size variation considering each cluster. Coding sequences far below the mean may suggest possible pseudogenization events. The dashed line represents the mean. Dotted lines delimit the interquartile range. (b). Gene location considering each cluster. Clusters 1, 3, and 4 seem to have some polarity in the genome, while clusters 2, 5, and 6 do not seem to have any pattern and are scattered throughout the genome.

[sup-material-gene-duplication-as-a-major-force-driving-the-genome-expansion-in-some-giant-viruses](#)), indicating multiple and successive events of gene/chromosome segment duplication.

Gene duplication as a driving force of genome gigantism in giant viruses

To explore the prevalence and distribution of paralogs in cedratviruses, we expanded our analysis to include all available cedratvirus genomes in public databases (Fig. 5). By performing BLASTp searches of predicted proteins against the complete set of proteins of each cedratvirus, we identified a range of gene families with varying sizes and predicted functions. Firstly, it is noteworthy that *c. pambiensis* has an atypical and unprecedented relative abundance of duplicated genes compared to other cedratviruses, accounting for 72.3% of its genome. Nevertheless, a significant contribution of paralogs was observed in all cedratvirus genomes, ranging from 43.34% in Brazilian cedratvirus to 52.26% in *c. lausannensis*. In addition, all cedratviruses share some large gene families, such as families mainly related to ankyrin repeat-containing domain and hypothetical proteins, as well as other functions such as collagen-like proteins, serine/threonine kinases and F-box domain-containing proteins. We further expanded our analysis to include the pithovirus-like group, to which cedratviruses belong. Interestingly, pithovirus and orpheovirus present a similar proportion of duplicated genes in their genomes, at 42.61% and 52.29%, respectively, but other protein domains were

overrepresented, such as collagen-like and MORN-repeat proteins, suggesting that extensive duplications have occurred independently following the radiation of the pithovirus-like group.

Expanding the analysis to other members of the phylum *Nucleocytoviricota* and yaravirus revealed that gene duplications are, again, quite abundant (Fig. 6a). In addition to cedratviruses, gene duplication also seems to be an important factor in the evolution of the genome of other giant viruses, particularly for pandoraviruses (mean of 47.28%) and some mimiviruses (e.g., 49.46% for cottonvirus). Despite the different proportions, all analyzed genomes have duplicated genes. However, it is important to highlight that even after expanding our analysis to other nucleocytoviruses, *c. pambiensis* remains the virus with the highest percentage of the genome composed of duplicated genes (72.3%). We note, however, that for some viruses, mechanisms other than gene duplication may be acting synergistically or concurrently.

It is generally expected to observe a positive correlation between viral genome size and the number of genes. The isolation of *c. pambiensis* raised questions about this correlation and the existence of a correlation between genome size and the number of paralogs. To address these questions, we compared genome size with the overall number of genes and the number of duplicated genes across a large sample of giant viruses (Fig. 6b and c). As aforementioned, variations on gene prediction methods must be considered, but the overall available data strongly suggest the presence of a strong positive correlation between genome size and both the total number of genes ($\rho = 0.90$, P -value $< 2.2e-16$) and the number of paralogs ($\rho = 0.87$, P -value = $1.4e-14$) per genome. The linear regression analysis reveals that, although all cedratviruses show a similar correlation between genome size and the number of predicted genes, *c. pambiensis* stands out as an exceptional case due to the significant contribution of paralogs in its genome (Fig. 6c).

DISCUSSION

The genome gigantism observed in giant viruses represents an intriguing unanswered question. A number of giant viruses have been discovered in recent years, revealing an increasing variety of particles, genome sizes, and predicted genes. Although deserving attention has been given to the functional content of the giant virus genomes, few studies have investigated why the genomes of these viruses are so large, reaching up to 2.8 Mb (8–11, 14, 16). The early efforts to answer this question were hampered by the scarcity of genomic information available at the time, precluding generalizing conclusions. However, the constant efforts of several research teams to isolate novel giant viruses worldwide have now set the stage for a more comprehensive analysis of giant virus genome evolution. Here, we presented the evidence that gene duplication is a primary mechanism for genome expansion among several groups of giant viruses.

Gene duplication has been recognized as an important source of genetic diversity in cellular organisms (2–5). Through gene duplication, new functions can emerge, as duplicated genes typically experience lower negative selection pressures, and the encoded proteins can gain new properties and functions. Gene families within a given organism typically emerge as a result of duplication events followed by divergence (20). In addition to potential functional divergence, the multi-copy gene families can contribute to the increased gene expression via so-called gene dosage phenomenon. Some of the well-known examples of multi-gene families include genes encoding cytomotive filament-forming proteins, globins, and ribosomal units (20–22). As a result, gene duplication is consistently considered a major mechanism in the evolution of cellular organisms. However, the understanding of the consequences of gene duplication in viruses remains limited. There are ample examples showing that gene duplication followed by exaptation of one of the gene copies has played a key role in adaptation and diversification throughout virus evolution (23, 24). Nevertheless, in viruses with small capsids, experimental studies have shown that gene duplications are prohibitive and lead to the loss of infectivity, primarily dictated by the limited packaging capacity of

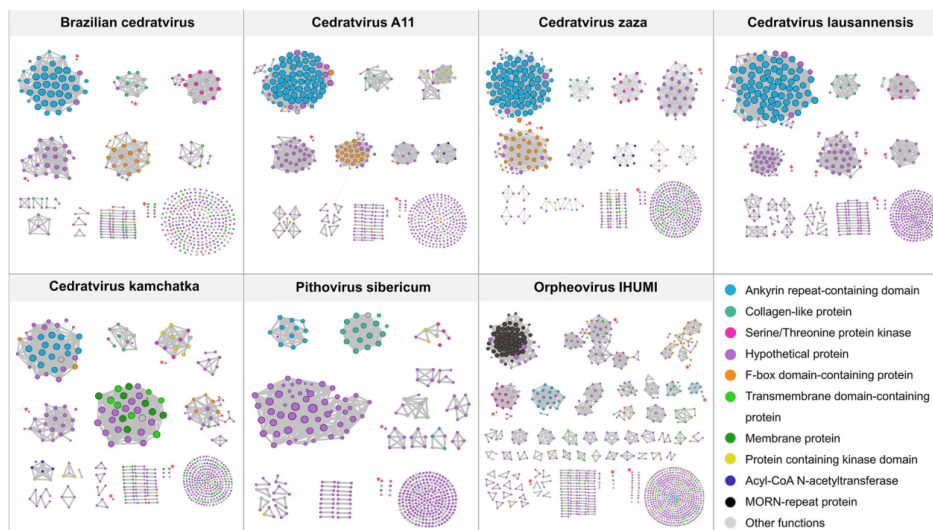


FIG 5 Comparison of gene families in the genome of members of the pithovirus-like group. These networks were made in the same way as for *c. pambiensis* (Fig. 2). Color legend is provided on the image.

small capsids (25). The situation in giant viruses, which show overall low packaging densities (26), is radically different compared to viruses with small capsids. Thus, genome evolution in giant viruses is apparently not constrained by the capsid size, allowing them to reap the benefits of gene duplication, which has shaped the genomes of cellular organisms.

In this study, we have described that genes in *c. pambiensis* appear to duplicate through several mechanisms, involving both tandem gene and distal genomic segment duplications. Tandem duplications in cellular organisms may occur through replication slippage, ectopic recombination, or aberrant DNA break repair. Distal duplications typically involve unequal crossing-over rearrangements of gene clusters with similar gene content. This mechanism may become progressively more frequent as the number of paralogs increases, providing more regions with similar content available for recombination (1). It is notable that the largest paralogous gene families encode proteins that themselves consist of repetitive domains, such as ankyrin repeats, leucine-rich repeats, and MORN repeats. Conceivably, the repetitive nucleotide sequences within these genes promote both tandem and long-distance genomic duplications. Furthermore, considering that a substantial number of viral genome copies are produced and compacted within viral factories, and considering the fact that the cedratvirus genome is circular dsDNA, it is reasonable to believe that ectopic recombination and unequal crossing-over may generate both tandem and distal duplications in cedratviruses. Additionally, the role of transposons should be considered in relation to gene duplication, as they have been described in the genomes of amoeba and certain groups of giant viruses (27, 28). Considering that the *Nucleocytoviricota* may have arisen from smaller and simpler viruses infecting early eukaryotes (29–31), the expansion of their genomes might involve a general mechanism conserved in the entire phylum. While genome expansion by extensive gene gain through horizontal gene transfer and *de novo* gene creation seem to be characteristic of only some groups of nucleocytoviruses (13, 15), our data indicate that gene duplication is an evolutionary mechanism common for several groups of giant viruses, especially those capable of infecting amoebas.

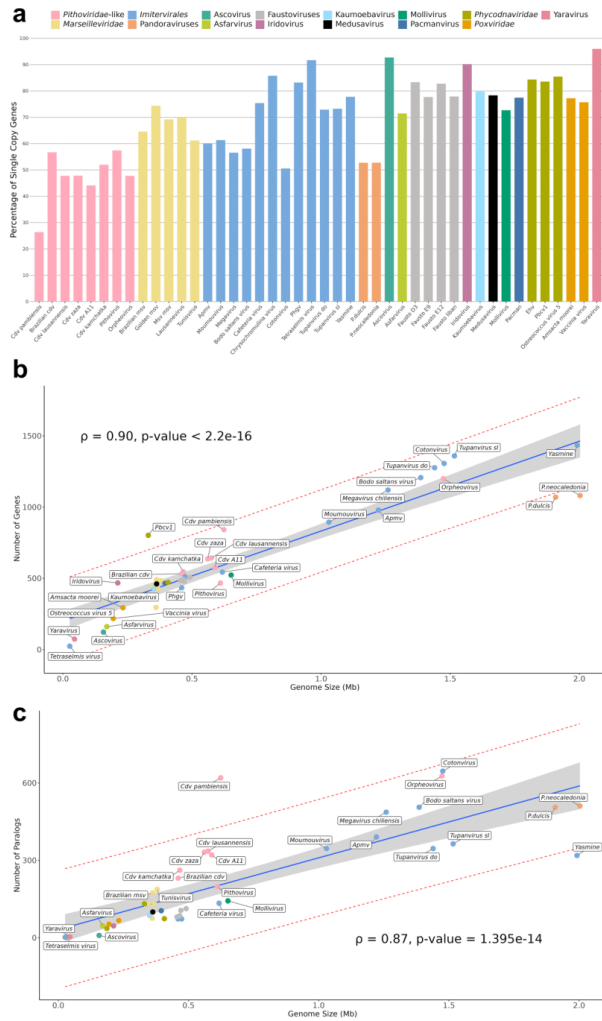


FIG 6 The contribution of paralogs genes in the genomes of giant viruses. (a) Comparison of the percentage of single copy genes in the genome for members of *Nucleocytoviricota* and yaravirus. The representatives of each group were depicted with distinct colors, as described in the legend. The percentage of single-copy genes is shown for each genome. Spearman correlation plots of the relationship between genome size and total number of predicted genes (b) and the relationship between genome size and total number of paralogs (c). Yasminevirus and *c. pambiensis* are outliers. The solid blue line marks the linear regression while the shaded gray area illustrates the 95% confidence interval associated with the linear regression line. The outer red lines delineate the 95% prediction interval, encapsulating the range within which we anticipate 95% of gene/paralog numbers to fall based on a given genome size. ρ : Spearman correlation coefficient; p -value: associated P -value.

One question that arises is why cedratviruses have so many duplicated genes in their genome. Maintaining duplicated copies may be important for creating genetic redundancy, and protecting the virus from deleterious mutations in essential genes since

additional copies could maintain the organism's functionality and fitness (32). Indeed, some of the *c. pambiensis* duplicated genes are potentially essential, such as the major capsid protein, early transcription factors, and transcriptional enzymes. Furthermore, as aforementioned, gene duplication is a phenomenon that provides raw material for evolution. The additional gene copies can be repurposed for functions unrelated to those of the original genes, which appears to be the main trend in virus evolution (23, 33). Furthermore, the duplicated genomic regions provide the raw genetic material for *de novo* gene emergence, a route extensively explored by pandoraviruses (13). Both mechanisms can lead to genetic innovation, increasing the genetic repertoire of these viruses. This is supported by the presence of different identifiable domains/functional categories in certain clusters of paralogous genes in *c. pambiensis* and other pitho-like viruses (Fig. 2 and 5). Further exploration of the giant virus diversity should further refine our understanding of the mechanisms of genome expansion and evolutionary traits associated with this remarkable group of viruses.

MATERIALS AND METHODS

Sample collection and isolation

To obtain the sample, a plastic container was placed in a small, forested area at the UFMG campus for a few days, collecting rainwater and organic matter present in that environment. From this collected water, the method of co-culture with amoebae of the species *Acanthamoeba castellanii* was carried out, as described in a published protocol (34). Collection authorization: SISBIO 89441-1. Brazilian genetic resources access authorization: SISGEN A2291C9.

Production, purification, and titration

To produce the new isolate, *A. castellanii* were infected with an MOI of 0.01 in glass culture flasks (300 cm²) with 35 mL of PYG medium and kept at 30°C in a rotary cell oven. After complete lysis of the cells, the contents of the flask were collected. This content was added to a sucrose cushion (40%) and then ultracentrifuged in a Comborvall Rotor AH-62va centrifuge at 14,000 rotations per minute (AH-629 rotor) for 1 hour, between 4°C and 8°C. The final pellet was resuspended in phosphate-buffered saline. Titration was performed by the limiting dilution method (35) in 96-well plates and the titer was expressed in TCID₅₀ per milliliter. The viral stock was kept at -20°C until use.

Electron microscopy and one-step growth curve

Three electron microscopy methods were used during this work, for a better description of the viral particle: TEM, negative contrast electron microscopy, and SEM. For TEM, *A. castellanii* cells cultivated in a PYG medium were infected with an MOI of 0.01 for 24 hours. Cells were then collected and fixed with 2.5% glutaraldehyde + phosphate for 2 hours at room temperature. Subsequently, fixation was performed with 2% osmium tetroxide, and incorporation in EPON resin, in sequence ultrathin sections was made. Image analyses were performed using a transmission electron microscope (FEI SpiritBiotwin 120 kV). For NSEM, the purified virus was diluted 1:10 in water, and 3 μL of this diluted sample was applied onto glow-discharged 400-mesh copper grids covered with a Lacey carbon support film and an ultrathin carbon layer (15 mA, negative charge for 40 seconds, 01824—Ted Pella, USA). After 1 minute, the excess liquid was drained gently touching the edge of the grid with a filter paper. The grid was stained twice with 3 μL uranyl acetate solution (2%) for 30 seconds. The excess solution was drained with filter paper and the grid was allowed to dry at room temperature. Images were collected using a 4k × 4k Ceta CMOS Camera coupled on a Talos F200C Transmission Electron Microscope (200 kV, Thermo Fisher Scientific) at LNNano/CNPEM. For SEM, *A. castellanii* cultivated in PYG medium were infected with an MOI of 0.01 for 24 hours. The cells were then collected, transferred to a coverslip containing poly-L-lysine, and fixed

with 2.5% glutaraldehyde + cacodylate for 2 hours at room temperature. Subsequently, fixation was performed with 1% osmium tetroxide, washing with 0.1 M cacodylate buffer, and immersion in 0.1% tannic acid. Then, dehydration was performed using serial passages in ethanol solutions with different concentrations. Subsequently, a critical point drying process using CO₂ was carried out. Finally, the samples were accommodated in metal supports (called stubs) and metalized with a layer of gold. Image analyses were performed using a scanning electron microscope (FEI Quanta 200 FEG).

For the one-step-growth curve assay, *A. castellanii* cells were infected in duplicates with an MOI of 10 to obtain a synchronous cycle. After 30 minutes of adsorption, the inoculum was removed, and fresh PYG medium was added. The collections of the supernatant with the cells were performed at 0, 1, 3, 6, 9, 12, 24, 48, and 72 hpi, considering the time 0 hpi right after the adsorption. All times were titrated later, and the curve was constructed from the titration result.

Sequencing, assembly, annotation, and phylogenetic analyses

The samples containing the purified virus were sequenced twice using the equipment Illumina MiSeq, with a paired-end library using the kit Illumina DNA Prep (Illumina Inc., San Diego, CA, USA). First, a *de novo* assembly was performed using the SPAdes 3.13.1 software (36). To increase the *de novo* assembly, the SOAPdenovo2 1.12 (37) program was used. Subsequently, a reference genome (the best hit, Brazilian cedratvirus) was used in the Medusa 1.3 program (38) and the final genome was obtained. For the prediction of the open reading frames (ORFs), the GeneMarkS 4.28 software (39) was used, and the sequences smaller than 50 amino acids were removed from the analyses. Gene prediction using GeneMarkS was performed using both prokaryotic and viral parameters. Since the results were very similar, we opted to use data from prokaryotic parameters because several studies on giant viruses employed this strategy. Therefore, some *c. pambiensis* (and other pitho-like viruses) genes were predicted to start with alternative start codons, different from ATG. The functional annotation of the predicted proteins was performed using BLASTp against the NCBI NR database considering 1e−5 e-value. The annotation was also done for the six largest clusters of genes using HHpred, with similar results.

For the construction of the phylogenetic trees, the amino acid sequences of the viruses of interest were obtained by the BLASTp tool (default parameters) from the NCBI Genbank database (40). These sequences were aligned with that of *c. pambiensis* using the MUSCLE 3.8.1551 software (41). The phylogenetic tree was built by the IQtree 1.6.12 program (42) using the best-fitted VT+F+R5 model for amino acid substitution and the likelihood-based method aLRT SH-like with 1,000 pseudoreplicates to estimate branch support values. As aforementioned, substantial variation in coverage was observed in genes belonging to the six largest clusters. This result posed challenges to our phylogenetic analyses due to the potential lack of negative selection in pseudogenes that leads to sequence degeneration. To improve the reliability of our analyses, we defined a cut-off point, in which the gene with the longest CDS was considered as a reference and all the other genes with a CDS shorter than half the size of this gene were removed from the alignment. For cluster 2, the procedure was a little different, as it has three genes much longer than all the others (mean of 427.5% larger than the family median). Therefore, for this cluster, the three largest genes were removed from the analysis and the fourth largest one was considered as a reference.

Detection and mapping of duplicated genes

To detect duplicated genes, we BLASTp the predicted proteins of *c. pambiensis* against themselves, and hits with coverage ≥30% and e-value <1e−4 were considered paralogs. Higher stringent cutoffs were evaluated (i.e., 50%) revealing very similar results. To cluster the paralogs, the Gephi 0.9.7 software (43) was used, based on the list of hits obtained in the previous step. To better understand the duplication events happening within the

genome, we constructed phylogenetic trees for the six largest gene families (more than 20 genes) using amino acid sequences. The programs and parameters used to build these trees were the same used previously.

With the groups of paralogs established, we decided to investigate how these genes spread within the genome. The gene and protein prediction steps gave us the coordinates of each gene, so we developed an R script to construct a Circos plot-like using the *circize* 0.4.15 package (44) that draws a line between paralog genes.

Statistical analysis

Spearman correlations were used to assess correlations between genome size and total number of paralogs or total number of genes with a significance level of $P < 0.05$. Data distribution was assessed by the Shapiro-Wilk test. Testing and plotting results were all done in Rstudio (45).

ACKNOWLEDGMENTS

We thank the Laboratório de Vírus of Universidade Federal de Minas Gerais for all the support provided and the Microscopy Center of UFMG, in particular the technicians Denilson Cunha, Rodrigo Ferreira, Altair Mendes, Thalita Arantes, Marilene Oliveira, and Breno Moreira, who collaborated from the preparation to the session for observation of the samples.

We would also like to thank the Conselho Nacional de Desenvolvimento Científico e Tecnológico (CNPq), Coordenação de Aperfeiçoamento de Pessoal de Nível Superior (CAPES), Fundação de Amparo à Pesquisa do Estado de Minas Gerais (FAPEMIG), and Pró-Reitorias de Pesquisa e Pós-Graduação da UFMG (PRPG-UFMG) for the financial support, and LNNano/CNPEM for access to the EM facility via project 20230751. J.S.A., J.P.A.J., and F.R.S. are CNPq researchers.

T.B.M., L.E.D.B., and J.S.A. designed the study and experiments. All authors performed experiments and/or analyses. All authors wrote the manuscript. The text has been entirely written by the authors, and English revision was partially performed using artificial intelligence. All authors approved the final manuscript.

AUTHOR AFFILIATIONS

¹Laboratório de Vírus, Departamento de Microbiologia, Instituto de Ciências Biológicas, Universidade Federal de Minas Gerais (UFMG), Belo Horizonte, Brazil

²Laboratório de Genômica Evolutiva, Departamento de Genética, Evolução, Microbiologia e Imunologia, Instituto de Biologia, Universidade Estadual de Campinas (UNICAMP), Campinas, Brazil

³Laboratório de Virologia, Departamento de Microbiologia e Imunologia, Instituto de Biotecnologia, Universidade Estadual Paulista (UNESP), Botucatu, Brazil

⁴Del-Bem Lab, Departamento de Botânica, Instituto de Ciências Biológicas, Universidade Federal de Minas Gerais (UFMG), Belo Horizonte, Brazil

⁵Brazilian Biosciences National Laboratory (LNBio), Brazilian Center for Research in Energy and Materials (CNPEM), Campinas, Brazil

⁶Centre de Recherche du Centre Hospitalier Universitaire de Québec- Université Laval, Laval, Québec, Canada

⁷Laboratório de Microbiologia Molecular, Universidade Feevale, Novo Hamburgo, Brazil

⁸Archaeal Virology Unit, Institut Pasteur, Université Paris Cité, CNRS UMR6047, Paris, France

⁹Department of Biological Sciences, Virginia Tech, Blacksburg, Virginia, USA

¹⁰Center for Emerging, Zoonotic, and Arthropod-Borne Infectious Disease Virginia Tech, Blacksburg, Virginia, USA

AUTHOR ORCID*s*Rodrigo A. L. Rodrigues  <http://orcid.org/0000-0001-7148-4012>Frank O. Aylward  <http://orcid.org/0000-0002-1279-4050>Luiz-Eduardo Del-Bem  <http://orcid.org/0000-0001-8472-4476>Jônatas S. Abrahão  <http://orcid.org/0000-0001-9420-1791>**FUNDING**

Funder	Grant(s)	Author(s)
Conselho Nacional de Desenvolvimento Científico e Tecnológico (CNPq)	303680/2022-9	Jônatas S. Abrahão
Ministério da Ciência, Tecnologia e Inovação (MCTI)	405249/2022-5, 406441/2022-7	Jônatas S. Abrahão
Coordenação de Aperfeiçoamento de Pessoal de Nível Superior (CAPES)	88882.348380/2010-1	Jônatas S. Abrahão

AUTHOR CONTRIBUTIONS

Talita B. Machado, Data curation, Formal analysis, Investigation, Methodology, Writing – original draft | Agnello C. R. Picorelli, Data curation, Formal analysis, Investigation | Bruna L. de Azevedo, Formal analysis, Writing – original draft | Isabella L. M. de Aquino, Formal analysis, Investigation, Writing – original draft | Victória F. Queiroz, Data curation, Formal analysis, Investigation, Methodology, Writing – original draft | Rodrigo A. L. Rodrigues, Formal analysis, Methodology, Writing – original draft | João Pessoa Araújo Jr., Methodology, Writing – original draft | Leila S. Ullmann, Methodology | Thiago M. dos Santos, Methodology, Writing – original draft | Rafael E. Marques, Methodology, Writing – original draft | Samuel L. Guimarães, Methodology, Writing – original draft | Ana Cláudia S. P. Andrade, Investigation, Writing – original draft | Juliana S. Gularte, Methodology, Writing – original draft | Meriane Demoliner, Methodology, Writing – original draft | Micheli Filippi, Methodology, Writing – original draft | Vyctoria M. A. G. Pereira, Investigation, Writing – original draft | Fernando R. Spilki, Methodology, Writing – original draft | Mart Krupovic, Investigation, Methodology, Validation, Writing – original draft | Frank O. Aylward, Investigation, Writing – original draft | Luiz-Eduardo Del-Bem, Conceptualization, Funding acquisition, Investigation, Methodology, Validation, Writing – original draft.

DATA AVAILABILITY

The genome of cedratvirus pambiensis is available at GenBank under accession number [OR343515](https://www.ncbi.nlm.nih.gov/nucl/11861471). The genome sequence (fasta) is also available at our research group website (<https://5c95043044c49.site123.me/sup-material-of-papers/sup-material-gene-duplication-as-a-major-force-driving-the-genome-expansion-in-some-giant-viruses>).

REFERENCES

- Krebs JE, Goldstein ES, Kilpatrick ST. 2017. Lewin's genes twelve. Jones & Bartlett Learning.
- Cannon SB, Mitra A, Baumgarten A, Young ND, May G. 2004. The roles of segmental and tandem gene duplication in the evolution of large gene families in *Arabidopsis thaliana*. *BMC Plant Biol* 4:10. <https://doi.org/10.1186/1471-2229-4-10>
- Reams AB, Neidle EL. 2004. Selection for gene clustering by tandem duplication. *Annu Rev Microbiol* 58:119–142. <https://doi.org/10.1146/annurev.micro.58.030603.123806>
- Wapinski I, Pfeffer A, Friedman N, Regev A. 2007. Natural history and evolutionary principles of gene duplication in fungi. *Nature* 449:54–61. <https://doi.org/10.1038/nature06107>
- Persi E, Wolf YI, Karamycheva S, Makarova KS, Koonin EV. 2023. Compensatory relationship between low-complexity regions and gene
- paralogy in the evolution of prokaryotes. *Proc Natl Acad Sci U S A* 120:e2300154120. <https://doi.org/10.1073/pnas.2300154120>
- Li WH, Gu Z, Wang H, Nekrutenko A. 2001. Evolutionary analyses of the human genome. *Nature* 409:847–849. <https://doi.org/10.1038/35057039>
- Zhang J. 2003. Evolution by gene duplication: an update. *Trends Ecol Evol* 18:292–298. [https://doi.org/10.1016/S0169-5347\(03\)00033-8](https://doi.org/10.1016/S0169-5347(03)00033-8)
- Scola BL, Audic S, Robert C, Jungang L, de Lamballerie X, Drancourt M, Birtles R, Claverie J-M, Raoult D. 2003. A giant virus in amoebae. *Science* 299:2033–2033. <https://doi.org/10.1126/science.1081867>
- Philippe N, Legendre M, Doutre G, Coutè Y, Poirot O, Lescot M, Arslan D, Seltzer V, Bertaux L, Bruley C, Garin J, Claverie J-M, Abergel C. 2013. Pandoraviruses: amoeba viruses with Genomes up to 2.5 MB reaching that of parasitic eukaryotes. *Science* 341:281–286. <https://doi.org/10.1126/science.1239181>

10. Abrahão J, Silva L, Silva LS, Khalil JYB, Rodrigues R, Arantes T, Assis F, Boratto P, Andrade M, Kroon EG, Ribeiro B, Bergier I, Seligmann H, Ghigo E, Colson P, Levasseur A, Kroemer G, Raoult D, La Scola B. 2018. Tailed giant tupanvirus possesses the most complete translational apparatus of the known virosphere. *Nat Commun* 9:749. <https://doi.org/10.1038/s41467-018-03168-1>
11. Moniruzzaman M, Martinez-Gutierrez CA, Weinheimer AR, Aylward FO. 2020. Dynamic genome evolution and complex virocell metabolism of globally-distributed giant viruses. *Nat Commun* 11:1710. <https://doi.org/10.1038/s41467-020-15507-2>
12. Boyer M, Yutin N, Pagnier I, Barrassi L, Fournous G, Espinosa L, Robert C, Azza S, Sun S, Rossmann MG, Suzan-Monti M, La Scola B, Koonin EV, Raoult D. 2009. Giant marseillevirus highlights the role of amoebae as a melting pot in emergence of chimeric microorganisms. *Proc Natl Acad Sci U S A* 106:21848–21853. <https://doi.org/10.1073/pnas.0911354106>
13. Legendre M, Fabre E, Poirat O, Jeudy S, Lartigue A, Alempic J-M, Beucher L, Philippe N, Bertaux L, Christo-Fouroux E, Labadie K, Couté Y, Abergel C, Claverie J-M. 2018. Diversity and evolution of the emerging pandoraviridae family. *Nat Commun* 9:2285. <https://doi.org/10.1038/s41467-018-04698-4>
14. Filée J. 2015. Genomic comparison of closely related giant viruses supports an accordion-like model of evolution. *Front Microbiol* 6:593. <https://doi.org/10.3389/fmicb.2015.00593>
15. Filée J, Pouget N, Chandler M. 2008. Phylogenetic evidence for extensive lateral acquisition of cellular genes by nucleocytoplasmic large DNA viruses. *BMC Evol Biol* 8:320. <https://doi.org/10.1186/1471-2148-8-320>
16. Filée J, Chandler M. 2008. Convergent mechanisms of genome evolution of large and giant DNA viruses. *Res Microbiol* 159:325–331. <https://doi.org/10.1016/j.resmic.2008.04.012>
17. Yutin N, Wolf YI, Koonin EV. 2014. Origin of giant viruses from smaller DNA viruses not from a fourth domain of cellular life. *Virology* 466–467:38–52. <https://doi.org/10.1016/j.virol.2014.06.032>
18. Koonin EV, Yutin N. 2019. Evolution of the large nucleocytoplasmic DNA viruses of eukaryotes and convergent origins of viral gigantism. *Adv Virus Res* 103:167–202. <https://doi.org/10.1016/bs.avir.2018.09.002>
19. Suhre K. 2005. Gene and genome duplication in acanthamoeba polyphaga Mimivirus. *J Virol* 79:14095–14101. <https://doi.org/10.1128/JVI.79.22.14095-14101.2005>
20. Moradkhani K, Prêhu C, Old J, Henderson S, Balamitsa V, Luo H-Y, Poon M-C, Chui DHK, Wajcman H, Patrinos GP. 2009. Mutations in the paralogous human α -globin genes yielding identical hemoglobin variants. *Ann Hematol* 88:535–543. <https://doi.org/10.1007/s00277-008-0624-3>
21. Wickstead B, Gull K. 2011. The evolution of the cytoskeleton. *J Cell Biol* 194:513–525. <https://doi.org/10.1083/jcb.201102065>
22. Malik Ghulam M, Catala M, Reulet G, Scott MS, Abou Elela S. 2022. Duplicated ribosomal protein paralogs promote alternative translation and drug resistance. *Nat Commun* 13:4938. <https://doi.org/10.1038/s41467-022-32717-y>
23. Koonin EV, Dolja VV, Krupovic M. 2022. The logic of virus evolution. *Cell Host Microbe* 30:917–929. <https://doi.org/10.1016/j.chom.2022.06.008>
24. Butkovic A, Dolja VV, Koonin EV, Krupovic M. 2023. Plant virus movement proteins originated from jelly-roll capsid proteins. *PLoS Biol* 21:e3002157. <https://doi.org/10.1371/journal.pbio.3002157>
25. Willemssen A, Zwart MP, Higuera P, Sardanyés J, Elena SF. 2016. Predicting the stability of homologous gene duplications in a plant RNA virus. *Genome Biol Evol* 8:3065–3082. <https://doi.org/10.1093/gbe/evw219>
26. Chaudhari HV, Inamdar MM, Kondabagil K. 2021. Scaling relation between genome length and particle size of viruses provides insights into viral life history. *iScience* 24:102452. <https://doi.org/10.1016/j.isci.2021.102452>
27. Filée J. 2018. Giant viruses and their mobile genetic elements: the molecular symbiosis hypothesis. *Curr Opin Virol* 33:81–88. <https://doi.org/10.1016/j.coviro.2018.07.013>
28. Sun C, Feschotte C, Wu Z, Mueller RL. 2015. DNA transposons have colonized the genome of the giant virus pandoravirus salinus. *BMC Biol* 13:38. <https://doi.org/10.1186/s12915-015-0145-1>
29. Krupovic M, Dolja VV, Koonin EV. 2023. The virome of the last eukaryotic common ancestor and eukaryogenesis. *Nat Microbiol* 8:1008–1017. <https://doi.org/10.1038/s41564-023-01378-y>
30. Bisio H, Legendre M, Giry C, Philippe N, Alempic J-M, Jeudy S, Abergel C. 2023. Evolution of giant pandoravirus revealed by CRISPR/Cas9. *Nat Commun* 14:428. <https://doi.org/10.1038/s41467-023-36145-4>
31. Koonin EV, Krupovic M, Yutin N. 2015. Evolution of double-stranded DNA viruses of eukaryotes: from bacteriophages to transposons to giant viruses. *Ann N Y Acad Sci* 1341:10–24. <https://doi.org/10.1111/nyas.12728>
32. Rodrigues RAL, Andreani J, Andrade ACDS, Machado TB, Abdi S, Levasseur A, Abrahão JS, La Scola B. 2018. Morphologic and genomic analyses of new isolates reveal a second lineage of cedratviruses. *J Virol* 92:e00372-18. <https://doi.org/10.1128/JVI.00372-18>
33. Koonin EV, Krupovic M. 2018. The depths of virus exaptation. *Curr Opin Virol* 31:1–8. <https://doi.org/10.1016/j.coviro.2018.07.011>
34. Machado TB, de Aquino ILM, Abrahão JS. 2022. Isolation of giant viruses of *Acanthamoeba castellanii*. *Curr Protoc* 2:e455. <https://doi.org/10.1002/cpz1.455>
35. Reed LJ, Muench H. 1938. A simple method of estimating fifty per cent endpoints. *Am J Epidemiol* 27:493–497. <https://doi.org/10.1093/oxfordjournals.aje.a118408>
36. Bankevich A, Nurk S, Antipov D, Gurevich AA, Dvorkin M, Kulikov AS, Lesin VM, Nikolenko SI, Pham S, Pribelski AD, Pyshkin AV, Sirotkin AV, Vyahhi N, Tesler G, Alekseyev MA, Pevzner PA. 2012. SPAdes: a new genome assembly algorithm and its applications to single-cell sequencing. *J Comput Biol* 19:455–477. <https://doi.org/10.1089/cmb.2012.0021>
37. Luo R, Liu B, Xie Y, Li Z, Huang W, Yuan J, He G, Chen Y, Pan Q, Liu Y, Tang J, Wu G, Zhang H, Shi Y, Liu Y, Yu C, Wang B, Lu Y, Han C, Cheung DW, Yiu S-M, Peng S, Xiaoqian Z, Liu G, Liao X, Li Y, Yang H, Wang J, Lam T-W, Wang J. 2012. SOAPdenovo2: an empirically improved memory-efficient short-read de novo assembler. *Gigascience* 1:18. <https://doi.org/10.1186/2047-217X-1-18>
38. Bosi E, Donati B, Galardini M, Brunetti S, Sagot M-F, Lió P, Crescenzi P, Fani R, Fondi M. 2015. MeDUSA: a multi-draft based scaffold. *Bioinformatics* 31:2443–2451. <https://doi.org/10.1093/bioinformatics/btv171>
39. Besemer J, Borodovsky M. 2005. Genemark: web software for gene finding in prokaryotes, eukaryotes and viruses. *Nucleic Acids Res* 33:W451–4. <https://doi.org/10.1093/nar/gki487>
40. Benson DA, Clark K, Karsch-Mizrachi I, Lipman DJ, Ostell J, Sayers EW. 2014. Genbank. *Nucleic Acids Res* 42:D32–7. <https://doi.org/10.1093/nar/gkt1030>
41. Edgar RC. 2004. MUSCLE: multiple sequence alignment with high accuracy and high throughput. *Nucleic Acids Res* 32:1792–1797. <https://doi.org/10.1093/nar/gkh340>
42. Minh BQ, Schmidt HA, Chernomor O, Schrempf D, Woodhams MD, von Haeseler A, Lanfear R. 2020. IQ-TREE 2: New models and efficient methods for phylogenetic inference in the genomic era. *Mol Biol Evol* 37:1530–1534. <https://doi.org/10.1093/molbev/msaa131>
43. Bastian M, Heymann S, Jacomy M. 2009. Gephi: an open source software for exploring and manipulating networks. *ICWSM* 3:361–362. <https://doi.org/10.1609/icwsml.v3i1.13937>
44. Gu Z, Gu L, Eils R, Schlesner M, Brors B. 2014. Brors, circlize implements and enhances circular visualization in R. *Bioinformatics* 30:2811–2812. <https://doi.org/10.1093/bioinformatics/btu393>
45. Posit team. 2022. Rstudio: integrated development environment for R, Posit software. Available from: <http://www.posit.co>

RESEARCH

Open Access



A long-term prospecting study on giant viruses in terrestrial and marine Brazilian biomes

Talita B. Machado¹, Isabella L. M. de Aquino¹, Bruna L. Azevedo¹, Mateus S. Serafim¹, Matheus G. Barcelos¹, Ana Cláudia S. P. Andrade², Erik Reis³, Leila Sabrina Ullmann⁴, João Pessoa Jr.⁵, Adriana O. Costa⁶, Luiz H. Rosa⁷ and Jônatas S. Abrahão^{1*}

Abstract

The discovery of mimivirus in 2003 prompted the search for novel giant viruses worldwide. Despite increasing interest, the diversity and distribution of giant viruses is barely known. Here, we present data from a 2012–2022 study aimed at prospecting for amoebal viruses in water, soil, mud, and sewage samples across Brazilian biomes, using *Acanthamoeba castellanii* for isolation. A total of 881 aliquots from 187 samples covering terrestrial and marine Brazilian biomes were processed. Electron microscopy and PCR were used to identify the obtained isolates. Sixty-seven amoebal viruses were isolated, including mimiviruses, marseilleviruses, pandoraviruses, cedratviruses, and yaraviruses. Viruses were isolated from all tested sample types and almost all biomes. In comparison to other similar studies, our work isolated a substantial number of Marseillevirus and cedratvirus representatives. Taken together, our results used a combination of isolation techniques with microscopy, PCR, and sequencing and put highlight on richness of giant virus present in different terrestrial and marine Brazilian biomes.

Keywords Giant virus, Amoebas, Biomes, Diversity, Richness

*Correspondence:

Jônatas S. Abrahão

jonatas.abrahao@gmail.com; jsa@icb.ufmg.br

¹Laboratório de vírus, Departamento de Microbiologia, Instituto de Ciências Biológicas, Universidade Federal de Minas Gerais (UFMG), Belo Horizonte city, Minas Gerais, Brazil

²Centre de Recherche du Centre Hospitalier Universitaire de Québec, Université Laval, Laval city, Québec, Canada

³Laboratório de virologia básica e aplicada, Departamento de Microbiologia, Instituto de Ciências Biológicas, Universidade Federal de Minas Gerais (UFMG), Belo Horizonte city, Minas Gerais, Brazil

⁴Laboratório de Virologia Veterinária, Faculdade de Medicina Veterinária e Zootecnia (FAMEZ), Universidade Federal de Mato Grosso do Sul (UFMS), Campo Grande city, Mato Grosso do Sul, Brazil

⁵Laboratório de Virologia, Departamento de Microbiologia e Imunologia, Instituto de Biotecnologia, Universidade Estadual Paulista (UNESP), Botucatu city, São Paulo, Brazil

⁶Departamento de Análises Clínicas e Toxicológicas, Faculdade de Farmácia, Universidade Federal de Minas Gerais (UFMG), Belo Horizonte city, Minas Gerais, Brazil

⁷Laboratório de Microbiologia Polar e Conexões Tropicais, Departamento de Microbiologia, Instituto de Ciências Biológicas, Universidade Federal de Minas Gerais (UFMG), Belo Horizonte city, Minas Gerais, Brazil



© The Author(s) 2024. **Open Access** This article is licensed under a Creative Commons Attribution 4.0 International License, which permits use, sharing, adaptation, distribution and reproduction in any medium or format, as long as you give appropriate credit to the original author(s) and the source, provide a link to the Creative Commons licence, and indicate if changes were made. The images or other third party material in this article are included in the article's Creative Commons licence, unless indicated otherwise in a credit line to the material. If material is not included in the article's Creative Commons licence and your intended use is not permitted by statutory regulation or exceeds the permitted use, you will need to obtain permission directly from the copyright holder. To view a copy of this licence, visit <http://creativecommons.org/licenses/by/4.0/>. The Creative Commons Public Domain Dedication waiver (<http://creativecommons.org/publicdomain/zero/1.0/>) applies to the data made available in this article, unless otherwise stated in a credit line to the data.

Introduction

Amoeba giant viruses are well-known for their structural and genomic complexity. Since the mimivirus discovery in 2003 [1], several groups of giant viruses have been described. Metagenomics and prospective studies involving virus isolation revealed that giant amoeba viruses are distributed in a diverse range of environments and substrates [2–8]. These entities have been already isolated from water samples, animals' bodies, permafrost, ocean depths, thermal springs, and soda lakes [9–12].

Brazil is one of the countries with the highest biodiversity and species richness in the world [13]. Its tropical forests, such as the Amazon, are globally renowned for their complexity and their role in regulating the world's climate. However, tropical forests represent just a part of the vast Brazilian territory. Brazil is described as having six major biomes: Amazon (i) and Atlantic Forest (ii), both typical of humid tropical forests and biodiversity hotspots; Cerrado (iii), a savanna biome with a rich network of rivers and a high number of endemic species; Caatinga (iv), an arid biome with species well-adapted to water scarcity; Pantanal (v), one of the world's largest wetland plains; and Pampas (vi), a biome typical of the cooler regions of Brazil, composed of grasslands [14]. In this context, our group has been prospecting viruses of amoebas in Brazilian territory, and we have described completely new species, including Tupanvirus and Yaravirus [11, 15].

In this present work, we describe our efforts in the prospective study of giant viruses from 2012 to 2022. A total of 67 viruses were isolated and identified, from almost all Brazilian biomes. Our study provides information into the isolation and richness of giant amoeba viruses across Brazilian territory, shedding light on their presence in both natural and urban environments.

Materials and methods

Cells and medium

The free-living amoeba of the species *Acanthamoeba castellanii* from the American Type Culture Collection (ATCC 30,234; Maryland, USA) was used in all experiments. The amoebas were propagated in cell culture flasks using peptone-yeast extract-glucose medium (PYG) supplemented with 100 IU/mL of penicillin (Cel-lofarm, Brazil), 0.25 µg/mL of amphotericin B (Cultilab, Brazil), and 0.1 mg/mL of streptomycin (Sigma-Aldrich, USA). To perform the subcultures, the amoebas were mechanically detached from the monolayer by tapping the bottle, quantified in a Neubauer chamber, and the necessary amount was inoculated into a new flask with fresh medium.

Samples collection

The samples were collected from 2012 to 2022. It is important to note that this study does not intend to test a similar number of samples per biome, state, or substrate. This is a descriptive work on the richness of giant viruses found in Brazil in a 11-years study. Brazil has a vast territory, and reaching some regions can be challenging due to logistical or funding issues. Therefore, several collections prospected here were donated to our group by local researchers. The collections were carried out with authorization from the Biodiversity Authorization and Information System (SISBIO) under the identification numbers: 33326-2 and 34293-2; and SISGEN: A2291C9. Most of the collections were made using mainly sterile 1.5 mL microtubes or 50 mL conical tubes. After collection, the samples underwent three cycles of freezing and thawing (a process to reduce contamination) and were organized into collections. For this purpose, each sample was aliquoted into 1.5 mL microtubes, with 1 to 10 aliquots of 1 mL, depending on the initial quantity of the sample, and stored at -20 °C. At the end of the organization, 24 collections were obtained, collected from different Brazilian states and biomes (Fig. 1A). Samples were obtained from different Brazilian states: Amazonas, Bahia, Goiás, Maranhão, Mato Grosso do Sul, Minas Gerais, Piauí, Rio Grande do Sul, Santa Catarina, and São Paulo. These samples resulted in 1 collection from the Pantanal biome, 1 collection from the Caatinga biome, 1 collection from the Amazon biome, 1 collection from the Pampa biome, 6 collections from the Atlantic Forest biome, 13 collections from the Cerrado biome (Sup. Table 1). At last, 61 samples were also collected from the Atlantic Ocean inside the Brazilian Exclusive Economic Zone (EEZ) from Rio de Janeiro to Rio Grande do Norte, corresponding to 1 collection. From those 24 collections, a total of 881 aliquots of 187 samples were tested for giant viruses. The majority of the samples originated from freshwater (459 aliquots), followed by sewage (110 aliquots), saltwater (300 aliquots), mud (10 aliquots), and soil (2 aliquots) (Fig. 1B).

Prospection of giant viruses in *Acanthamoeba castellanii*

For prospection of giant viruses, preliminary processing of the samples is carried out. For water and sewage samples, a dilution was performed at a ratio of 1:10 for each aliquot. For mud samples, it was necessary to wait 24 h at 10 °C for the sediment to settle first and then perform a dilution at a ratio of 1:10 for each aliquot with the liquid content of the supernatant. For soil samples, 100 g of sediment was collected and 300 µL of sterile distilled water was added, resulting in an initial dilution of 1:4; this content was then vortexed, and the sample was left in the refrigerator overnight for sediment settling. After this period, a dilution at a ratio of 1:10 for each aliquot was

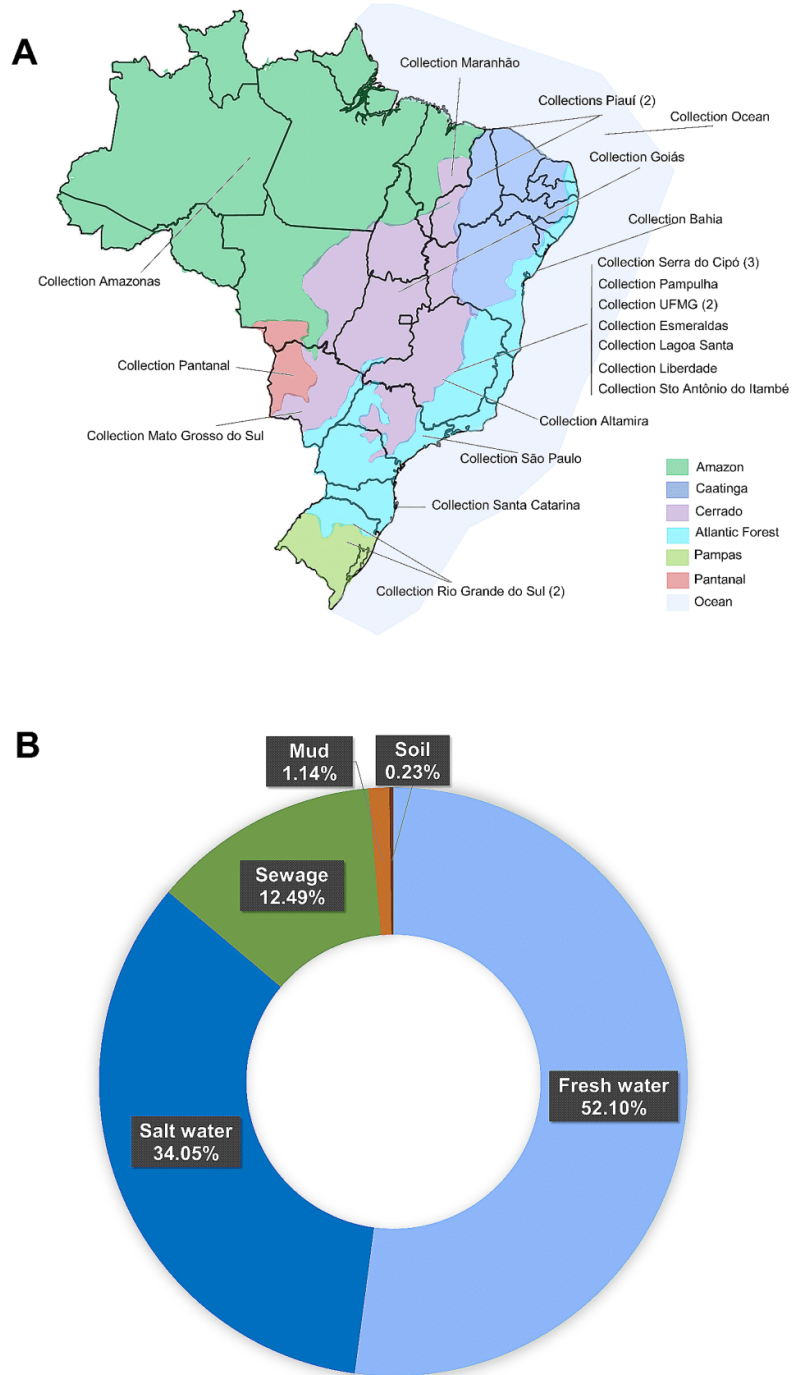


Fig. 1 (A) Map with the distribution of collections. Location of each collection based on its geographical coordinates. Brazilian biomes are represented by different colors, as per the figure legend. (B) Types of samples considering all the collections

performed with the liquid content of the supernatant. The 1:10 dilutions were made using 1x phosphate-buffered saline (PBS). Virus isolation was performed in *Acanthamoeba castellanii* seeded in 96-well plates (Kasvi, Brazil) in PYG medium supplemented with three additional antibiotics: 0.004 mg/mL vancomycin (Inlab, Brazil), 0.004 mg/mL ciprofloxacin (Sigma-Aldrich, USA), and 0.020 mg/mL doxycycline (Sigma-Aldrich, USA). Inoculated amoebas were monitored for seven days, during three rounds of blind passages. In case of cytopathic effects, the extract of amoebas was collected and sent to virus identification [16].

Transmission electron microscopy

For transmission electron microscopy (TEM), 1.5×10^7 cells of *A. castellanii* were added to T-75 cell culture flasks (Kasvi, Brazil). The cells were infected with the newly isolated viruses during this work at a multiplicity of infection (MOI) of 0.01 and maintained in incubators at a temperature of approximately 30 °C until the cytopathic effect appearance. After observing the cytopathic effect, the contents of the bottle were collected into a 50 mL conical tube and centrifuged at 1308 x g (Sorvall RT6000B) for 10 min. Following centrifugation, the supernatant was discarded, and the pellet was washed with 5 mL of 0.1 M monosodium phosphate buffer, and the contents were transferred to a 15 mL conical tube and centrifuged again at 1308 x g (Sorvall RT6000B) for 10 min, washing and centrifugation were performed twice. After washing, the supernatant was discarded, and the pellet was resuspended in 1.5 mL of fixative composed of 2.5% glutaraldehyde and 0.1 M monosodium phosphate buffer and kept in a homogenizer for 2 h at room temperature. After the incubation period with the fixative, the contents of the conical tube were centrifuged at 145 x g (Sorvall RT6000B) for 10 min, the supernatant was discarded, and the pellet was resuspended with 1 mL of 0.1 M monosodium phosphate buffer, the contents were transferred to a 1.5 mL microtube and centrifuged again at 0.8 x g (Eppendorf 5415R) for 10 min. After this final centrifugation, the material was correctly identified and stored in the refrigerator until it was sent to the Microscopy Center of UFMG. There, it underwent subsequent fixation with 2% osmium tetroxide, embedding in EPON resin, and preparation of ultra-thin sections. Image analysis was performed using a transmission electron microscope (FEI SpiritBiotwin 120 kV). The identification of the viruses was performed based on multiple features from the particles (morphology, size, unique structures and capsid characteristics) combined with impact of infection on the host (viral factory appearance and reorganization of host cytoplasm).

PCR identification and sequencing

Following the identification of cultures exhibiting a cytopathic effect, screening was conducted via PCR targeting specific giant virus groups (Sup. Table 2). DNA extraction was performed using the phenol-chloroform method from 200 µL of the collected content from positive aliquots, yielding DNA at a concentration of approximately 50 µg/µL, utilized as a template for PCR assays. PCR assays targeted various genes, including the major capsid protein gene of mimivirus, Marseillevirus and yaravirus; and the DNA polymerase gene of Pandoravirus, pithovirus and cedratvirus. Design and standardization of primers and reactions were ensured to prevent cross-amplification among analyzed viruses available on GenBank.

PCR assays utilized 1 µL of extracted DNA (~50 nanograms) in an amplification reaction mix containing 5 µL of SYBR Green Master Mix (Thermo Fisher Scientific, USA) and 0.4 µL (10 µM) of forward and reverse primers, adjusted with ultrapure water to a final volume of 10 µL. Thermal cycling conditions on the StepOne thermal cycler (Applied Biosystem, USA) comprised initial denaturation at 95 °C for 10 min, followed by 40 cycles of 95 °C for 15 s and 60 °C for 1 min, with a final step of 95 °C for 15 s, 60 °C for 1 min, and 95 °C for 15 s. Positive samples exhibited amplification with specific melting temperatures, while negative samples showed no specific amplification. As negative controls, DNA extracted from non-inoculated amoebas with purified viruses or samples was used, while DNA from amoebae infected with purified virus served as a positive control.

Phylogenetic analyses

Some representative viruses of each group were sequenced. The samples containing purified virus underwent sequencing using the Illumina MiSeq system, employing a paired-end library and an Illumina DNA Prep kit (Illumina Inc., San Diego, CA, USA). Quality control of the obtained reads was conducted using the FastQC program, followed by read trimming with the Trimmomatic tool. Genome de novo assembly was performed using Spades 3.12 with default parameters [17].

Phylogenetic trees were constructed using IQtree software (version 1.6.12) employing the maximum-likelihood method, with 1,000 bootstrap replicates for branch support [18]. For tree construction, sequences of different genes were utilized. Data sets containing sequences for alignments were prepared using BLASTp against the NCBI non-redundant protein sequences (nr) database with an expected threshold of 10^{-3} [19]. Alignments were performed using the Muscle software 3.8.1551 [20]. The best-fit substitution models were selected using the ModelFinder algorithm implemented in IQtree. Visualization

and editing of phylogenetic trees were carried out using iTOL.

Results

In this prospective study, covering all Brazilian biomes, a total of 67 amoeba-associated viruses were isolated (Fig. 2). These viruses induced rounding and lysis as cytopathic effects in *Acanthamoeba*. Additionally, one of the isolates caused cell aggregation (Sup. Table 3). Only four isolates were obtained during the 1st passage, 11 isolates during the 2nd passage and the others (52) were detected during the 3rd passage of the prospecting procedures (Sup. Table 3). In addition, no isolates were obtained from the Amazon and Atlantic Ocean samples.

All isolates were first submitted to transmission electron microscopy (TEM) for identification (Figs. 2, 3 and 4). Here we will describe the types of isolated viruses and the criteria we used to identify them by TEM:

–1 Pandoravirus isolate, with its typical ovoid shape particle and approximately 1 μm in length. It presents an apical ostiole, serving as an entry point for interactions with host cells. Within the host cell's cytoplasm, an electron-lucent viral factory is discernible, indicative of active viral replication and assembly processes taking place (Figs. 2 and 3F).

–13 mimiviruses, in which the viral structure exhibits pseudo-icosahedral symmetry, with a diameter measuring approximately 450 nm. Surrounding the capsid is a layer of fibrils, measuring approximately 125 nm in length. The capsid consists of multiple layers of protein. Enclosed within is an internal lipid membrane. Notably, the presence of the “stargate” feature. Within the host cell's cytoplasm, an electron-dense viral factory is discernible, indicative of active viral replication and assembly processes (Figs. 2, 3A and 4A).

–26 marseilleviruses, with icosahedral symmetry, these viral particles have a diameter of 180–250 nm. They may be observed individually or clustered together, inside vesicles. Within the host cell's cytoplasm, an electron-luminous viral factory is evident, indicating active viral replication and assembly processes (Figs. 2, 3B and 4C and D).

–24 pitho/cedrat-like viruses: The viral structure presents an ovoid shape, ranging from 600 nm to 1.5 μm in length. Its capsid is characterized by parallel vertical striations. Notably, one or two apical corks, also striated, can be observed. By electron microscopy, it is not possible to be sure if the isolate is a cedrat- or pithovirus, because particles with one or two corks have already been described for both groups of viruses. Within the

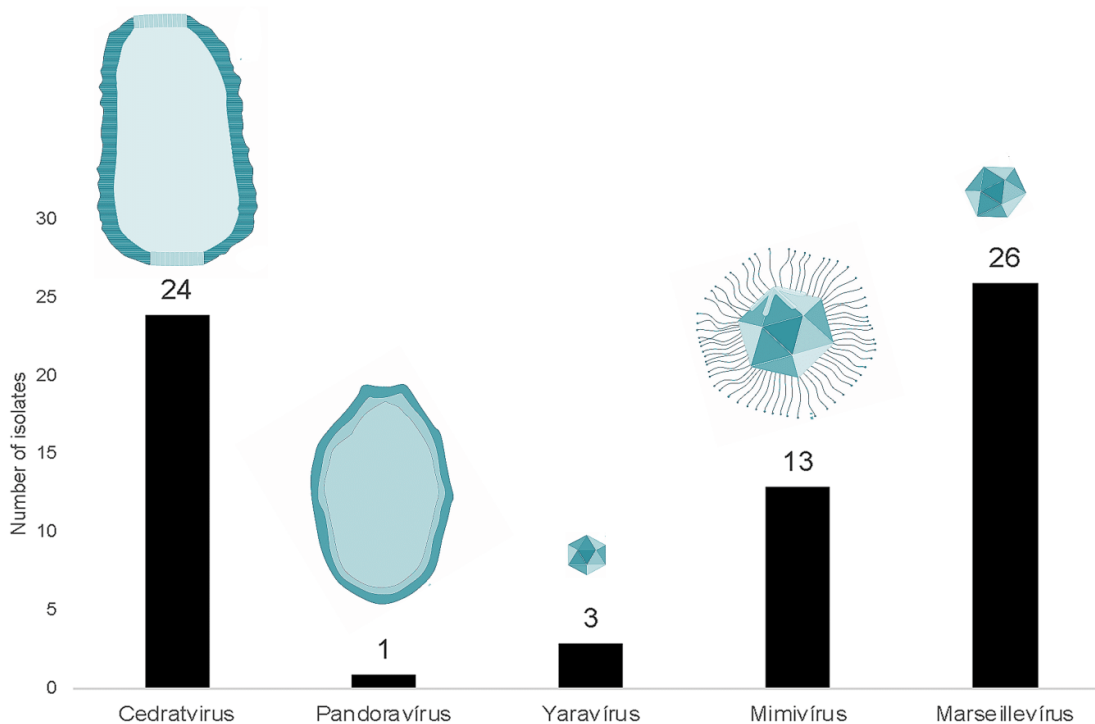


Fig. 2 Number and variety of viruses isolated during this study. A total of 67 isolates were obtained from Brazilian biomes

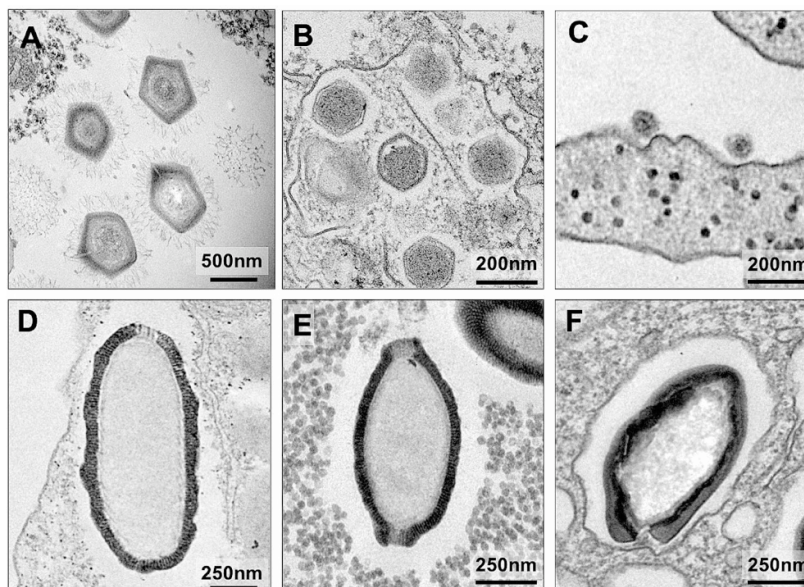


Fig. 3 Transmission electron microscopy of isolated viral particles. (A) Mimivirus particles exhibiting its surface fibrils. (B) Marseillevirus particles with their typical icosahedral symmetry. (C) Yaravirus particles attached to the *Acanthamoeba castellanii* plasma membrane. (D) Cedratvirus particle with a single cork. (E) Cedratvirus particle with two corks. (F) Oval-shaped Pandoravirus particle, with its typical ostiole

host cell's cytoplasm, an electron-luminous viral factory is noticeable, accompanied by the presence of electron-dense amorphous structures, indicative of active viral replication and assembly processes (Figs. 2, 3D and E and 4B).

–3 yaraviruses: With icosahedral symmetry, the viral particles exhibit a diameter of approximately 80 nm. Within the host cell's cytoplasm, the viral factory has two different areas: a granular, containing replicated genomic units; and an electron-lucent, containing empty capsids (Figs. 2, 3C and 4E).

Considering the identification of isolates by PCR, the viruses underwent reactions corresponding to all available targets, including Pandoravirus, mimivirus, Marseillevirus, cedratvirus, pithovirus, and Yaravirus. PCR results corresponded with TEM identification for all isolates, comprising 1 Pandoravirus, 13 mimiviruses, 26 marseilleviruses, 24 cedratviruses, and 3 yaraviruses. Therefore, the PCR indicated that all the isolates identified (Sup. Table 3) by TEM as pitho/cedrat-like viruses were, actually, cedratviruses.

Considering the increasing prevalence of giant virus prospective research in laboratories worldwide, we deem it pertinent and valuable to examine the relationships among variables such as substrates, biomes, and isolates. However, it is important to note that this analysis is descriptive in nature. As previously mentioned, the representativeness of explored substrates and biomes

may not be equivalent due to logistical and financial constraints.

New isolates were obtained from all types of samples tested (Fig. 5A). The largest quantity came from freshwater samples (45 isolates), which also exhibited the highest richness of isolated viral groups (at least 4 groups). From the less representative samples (soil and mud), only 1 Marseillevirus was isolated from soil samples, while 3 yaraviruses were obtained from mud samples. Saltwater and sewage samples yielded an equal number of isolates (9 isolates), but sewage samples showed greater richness of viral groups (3 groups) compared to saltwater samples (1 group).

The largest quantity of isolates was obtained from the Cerrado biome (30 new isolates), followed by the Atlantic Forest (24 isolates). However, the number of viral groups was the same for both (4 groups). From the Cerrado biome, isolates of Marseillevirus, mimivirus, Pandoravirus, and cedratviruses were obtained, while from the Atlantic Forest biome, isolates of mimivirus, Marseillevirus, cedratvirus, and Yaravirus were obtained (Fig. 5B).

In addition, representative viruses from each group were selected for genome sequencing to confirm their prior identification. For mimivirus, Pandoravirus, cedratvirus, and Marseillevirus, a phylogenetic tree was constructed using DNA polymerase, a common marker for giant virus phylogenetic analysis. In the case of Yaravirus, the major capsid protein (MCP) gene was utilized for tree

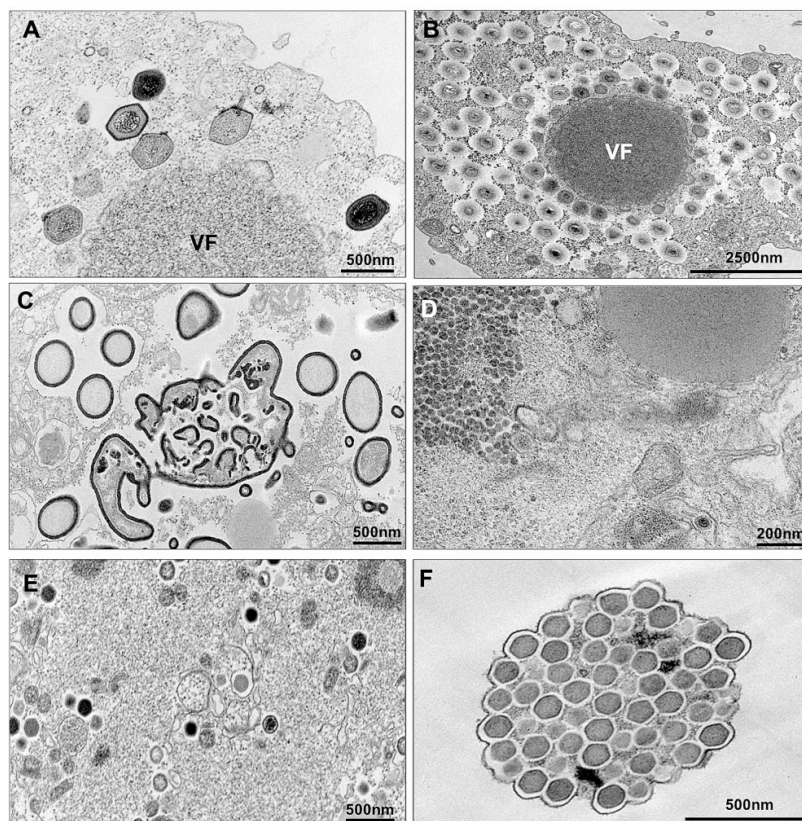


Fig. 4 Transmission electron microscopy of *Acanthamoeba castellanii* cells infected by different viral isolates. (A and B) Mimivirus spherical electron-dense viral factory with particles under morphogenesis. VF – viral factory. (C) Cedratvirus viral factory. In the center, an amorphous structure that likely is related to the tegument morphogenesis. (D) Yaravirus viral factory. At top-left, genomic granular area. It is possible to visualize a particle at bottom-right (E) Marseillevirus electron-lucent viral factory. It is possible to visualize viral particles in different stages of morphogenesis. (F) A Marseillevirus giant vesicle containing dozens of viral particles

construction. The results indicate that the previous identification of the isolates through TEM and PCR aligns with phylogenetic analysis, confirming the identification of the viruses (Fig. 6).

Discussion

The remarkable biodiversity of organisms in Brazilian natural and urban environments pose questions and supports virology studies employing a prospecting approach as employed in this study. Consequently, the ongoing isolation and characterization of giant viruses may contribute to the understanding of their ecological roles, evolutionary dynamics, and potential impact on host populations and ecosystems. In this sense, obtaining several environmental samples from different biomes, collected over a span of 11 years yielded a total of 67 new isolates belonging to at least five distinct viral groups, including Pandoravirus, mimivirus, Marseillevirus,

cedratvirus, and Yaravirus. Over time, other prospecting studies on amoebal viruses were also performed in Brazilian biomes. Dornas et al. (2015) and Andrade et al. (2019) described the isolation of different types of *Acanthamoeba*-infecting giant viruses. However, in contrast to the present study, mimivirus was previously the most frequently isolated virus.

Information on the distribution patterns of isolated viruses across different biomes and sample types may be useful for future prospecting studies. Despite logistical and financial constraints, our study successfully captured the diversity of giant virus diversity present in Brazilian environments in a span of 11 years of research. However, it is important to acknowledge the limitations of our sampling approach, particularly regarding the representativeness of explored substrates and biomes. Future studies should aim to address these limitations and further

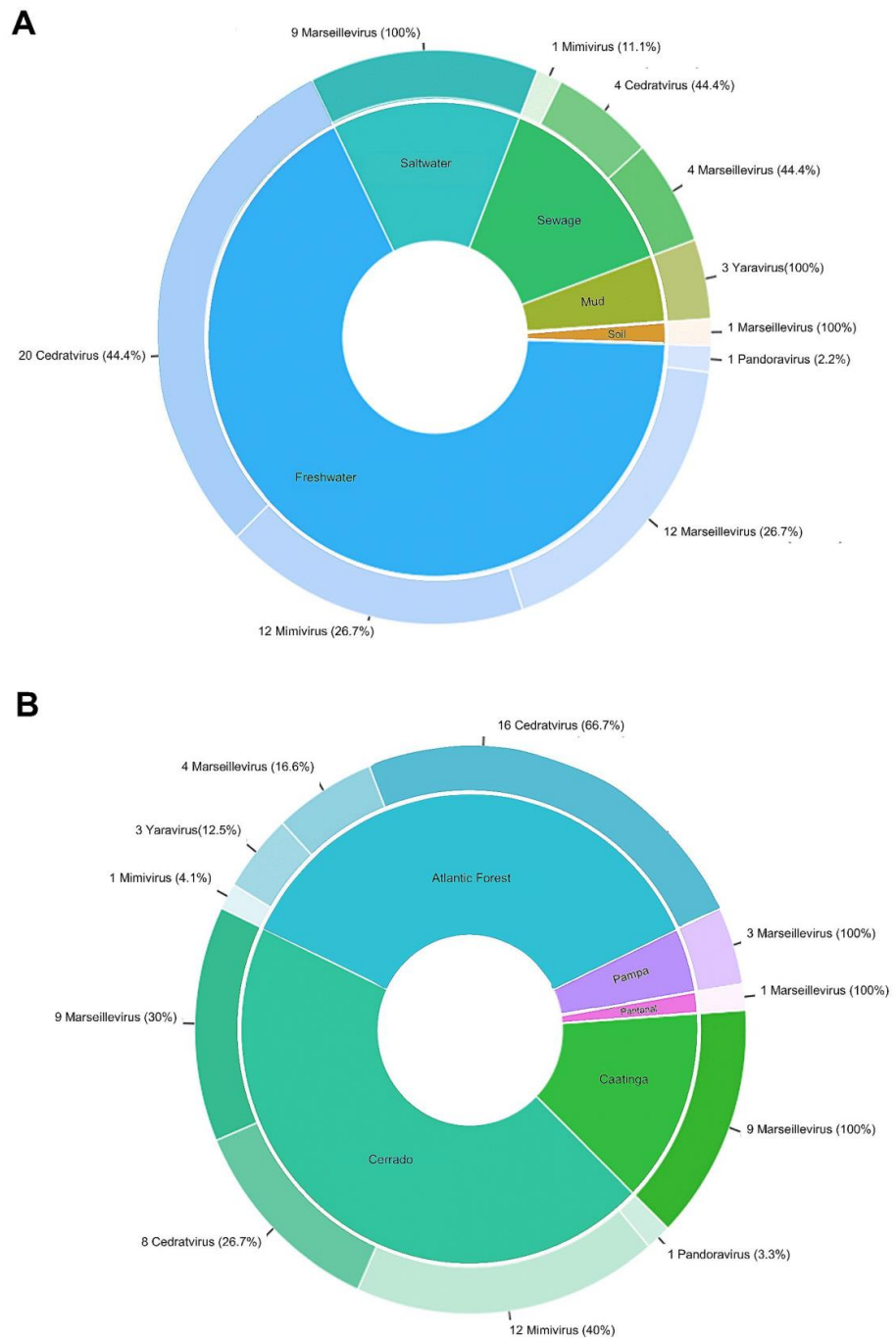


Fig. 5 Isolates, samples and biomes. **(A)** Quantity and representativeness of each viral group isolated within each type of sample (substrate). The greatest variety of viral groups was obtained in freshwater. **(B)** Quantity and representativeness of each viral group isolated within each biome. The greatest variety of viral groups was obtained in Cerrado samples

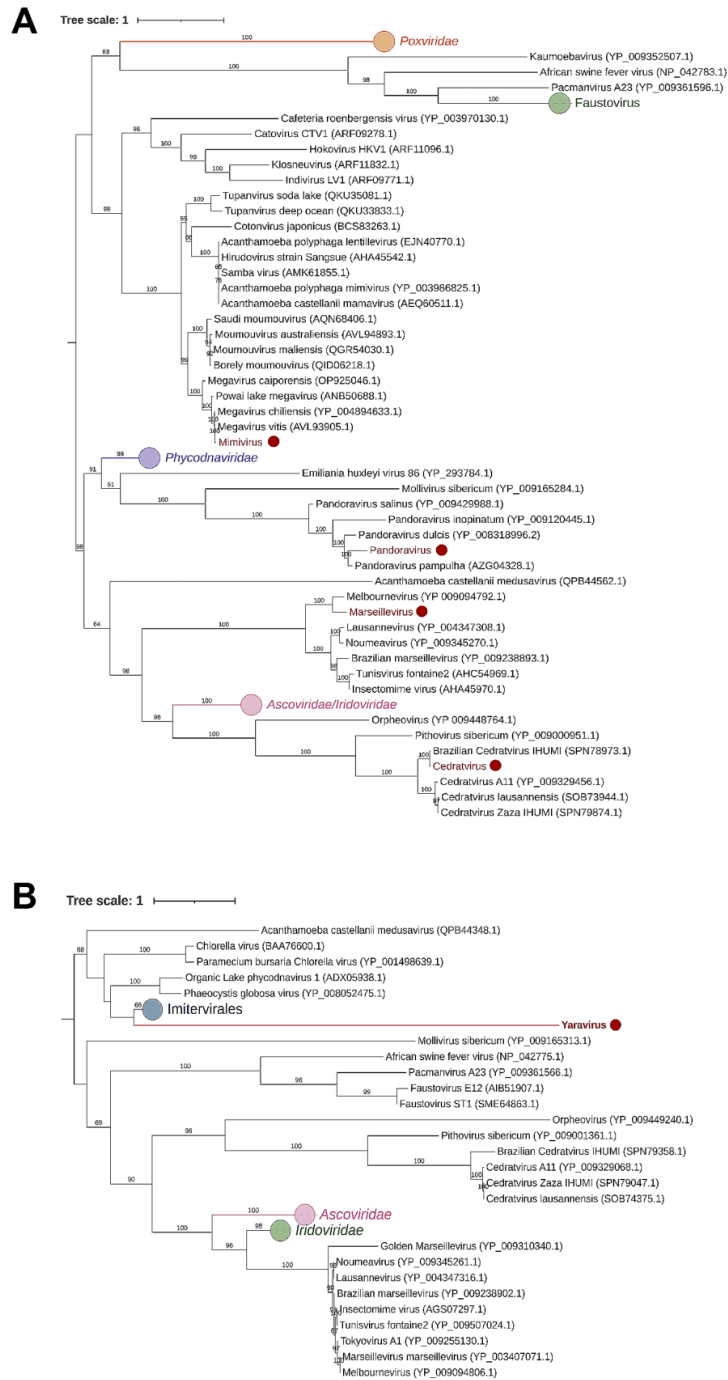


Fig. 6 Maximum likelihood phylogenetic trees constructed with amino acid sequences from the DNA polymerase subunit B (mimivirus, Pandoravirus, Marseillevirus and cedratvirus) and the major capsid protein (Yaravirus). The new isolates described here are red highlighted. The scale bar indicates the genetic distance

explore the ecological factors driving the distribution and diversity of giant viruses in Brazil and beyond.

Importantly, to an extended overview of such remarkable viral entities, our results suggest that morphological identification by TEM was effective in distinguishing between different viral groups. However, distinguishing between cedratviruses and pithoviruses proved challenging due to their strikingly similar characteristics. Therefore, additional PCR analysis or genome sequencing proved necessary to resolve identification ambiguities for these viruses. Last, phylogenetic analysis of representative viruses from each group further validated their taxonomic classification and evolutionary relationships. In conclusion, by combining such approaches we have expanded our understanding of the distribution of the giant viruses in Brazilian biomes. It is important to mention that some of the viral isolates described here have already undergone genomic and biological characterization [15, 21, 22]. This underscores the significance of prospecting studies as the initial step in knowledge construction.

Supplementary Information

The online version contains supplementary material available at <https://doi.org/10.1186/s12985-024-02404-z>.

Supplementary Material 1
Supplementary Material 2
Supplementary Material 3

Acknowledgements

We thank the Virus Laboratory of the Federal University of Minas Gerais for all the support provided. We also thank the UFMG Microscopy Center, especially the technicians Denilson Cunha, Rodrigo Ferreira, Altair Mendes, Thalita Arantes, Marilene Oliveira and Breno Moreira, who collaborated from the preparation to the sample observation session. We are also grateful to each of the people who contributed to this work by donating samples: Adriana, Betânia, Edney, Natalia, Paula, Paulo, Poliana, Ivan, Isabela, Juliana, Severino, Silvana, Thalita. The text was revised using artificial intelligence (OpenAI - ChatGPT). All authors approved the final manuscript.

Author contributions

JSA and ACSA designed and supervised the work. LSU and JPAJ sequenced the viral genomes. TBM, ILMA, BLA, MSS, MGB, performed experiments. AOC provided cells and assist on quality control. TBM, JSA, ER and LHR collected environmental samples. All authors reviewed the manuscript.

Funding

We would like to thank the Conselho Nacional de Desenvolvimento Científico e Tecnológico (CNPq), Coordenação de Aperfeiçoamento de Pessoal de Nível Superior (CAPES), Fundação de Amparo à Pesquisa do Estado de Minas Gerais (FAPEMIG), and Pró-Reitorias de Pesquisa e Pós-Graduação da UFMG (PRPG-UFMG) for the financial support. JPAJ, LHR and JSA are CNPq researchers.

Data availability

Viral sequences are available at Genbank under the accession numbers MT293574, OR343515, OR991738, MK131393.

Declarations

Ethical approval

The collections were carried out with authorization from the Biodiversity Authorization and Information System (SISBIO) under the identification numbers: 33326-2 and 34293-2; and SISGEN: A2291C9.

Sequencing data

Viral sequences are available at Genbank under the accession numbers MT293574, OR343515, OR991738, MK131393.

Competing interests

The authors declare no competing interests.

Received: 14 May 2024 / Accepted: 3 June 2024

Published online: 10 June 2024

References

- Scola BL, Audic S, Robert C, Jungang L, de Lamballerie X, Drancourt M, Birtles R, Claverie J-M, Raoult D. A giant virus in Amoebae. *Science*. 2003;299:2033–2033. <https://doi.org/10.1126/science.1081867>
- Dornas FP, Khalil JYB, Pagnier I, Raoult D, Abrahão J, La Scola B. Isolation of New Brazilian giant viruses from environmental samples using a Panel of Protozoa. *Front Microbiol*. 2015;6. <https://doi.org/10.3389/fmicb.2015.01086>
- Andrade AC, dos Arantes SP, Rodrigues TS, Machado RAL, Dornas TB, Landell FP, Furst MF, Borges C, Dutra LGA, Almeida LAL. Ubiquitous giants: a plethora of giant viruses found in Brazil and Antarctica. *Virology*. 2018;15. <https://doi.org/10.1186/s12985-018-0930-x>
- Mihara T, Koyano H, Hingamp P, Grimsley N, Goto S, Ogata H. Taxon Richness of Megaviridae exceeds those of Bacteria and Archaea in the Ocean. *Microbes Environ*. 2018;33:162–71. <https://doi.org/10.1264/jsm2.ME17203>
- Silva LKDS, Andrade ACDS, Dornas FP, Rodrigues RAL, Arantes T, Kroon EG, Bonjardim CA, Abrahão JS. Cedratvirus getuliensis replication cycle: an in-depth morphological analysis. *Sci Rep*. 2018;8(1):4000. <https://doi.org/10.1038/s41598-018-22398-3>. PMID: 29507337; PMCID: PMC5838162.
- Kerepesi C, Grolmusz V. Giant viruses of the Kutch Desert. *Arch Virol*. 2016;161:721–4. <https://doi.org/10.1007/s00705-015-2720-8>
- Kerepesi C, Grolmusz V. The Giant Virus Finder discovers an abundance of Giant viruses in the Antarctic Dry Valleys. *Arch Virol*. 2017;162:1671–6. <https://doi.org/10.1007/s00705-017-3286-4>
- Schulz F, Alteio L, Goudeau D, Ryan EM, Yu FB, Malmstrom RR, Blanchard J, Woyke T. Hidden diversity of Soil Giant viruses. *Nat Commun*. 2018;9:4881. <https://doi.org/10.1038/s41467-018-07335-2>
- Campos RK, Boratto PV, Assis FL, Aguiar ER, Silva LC, Albarnaz JD, Dornas FP, Trindade GS, Ferreira PP, Marques JT, Robert C, Raoult D, Kroon EG, La Scola B, Abrahão JS. Samba virus: a novel mimivirus from a giant rain forest, the Brazilian Amazon. *Virology*. 2014. <https://doi.org/10.1186/1743-422X-11-95>. PMID: 24886672; PMCID: PMC4113263.
- Legendre M, Lartigue A, Bertaux L, Jeudy S, Bartoli J, Lescot M, Alempic J-M, Ramus C, Bruley C, Labadie K, et al. In-Depth study of Mollivirus Sibericum, a New 30,000-y-Old giant virus infecting Acanthamoeba. *Proc Natl Acad Sci*. 2015;112:E5327–35. <https://doi.org/10.1073/pnas.1510795112>
- Abrahão J, Silva L, Silva LS, Khalil JYB, Rodrigues R, Arantes T, Assis F, Boratto P, Andrade M, Kroon EG, et al. Tailed giant Tupanvirus possesses the most complete translational apparatus of the known Virophere. *Nat Commun*. 2018;9. <https://doi.org/10.1038/s41467-018-03168-1>
- Yoshikawa G, Blanc-Mathieu R, Song C, Kayama Y, Mochizuki T, Murata K, Ogata H, Takemura M. Medusavirus, a Novel large DNA virus discovered from Hot Spring Water. *J Virol*. 2019;93. <https://doi.org/10.1128/jvi.02130-18>
- Boratto PVM, Serafim MSM, Witt ASA, Crispim APC, Azevedo BL. A brief history of giant viruses' studies in Brazilian biomes. *Viruses*. 2022;14:191. <https://doi.org/10.3390/v14020191>. MachadoTB.deQueiroz, V.F.; Rodrigues, R.A.L.; et al.
- Azevedo ALM, dos S. April. IBGE - Educa | Jovens Available online: <https://educalibge.gov.br/jovens/conheca-o-brasil/territorio/18307-biomas-brasileiros.html> (accessed on 11 2024).
- Boratto PVM, Oliveira GP, Machado TB, Andrade ACSP, Baudoin J-P, Klose T, Schulz F, Aza S, Decloquement P, Chabrière E, et al. Yaravirus: a novel 80-Nm virus infecting Acanthamoeba Castellani. *Proc Natl Acad Sci*. 2020;117:16579–86. <https://doi.org/10.1073/pnas.2001637117>

16. Machado TB, de Aquino ILM, Abrahão JS. Isolation of Giant viruses of *Acanthamoeba Castellani*. *Curr Protoc*. 2022;2:e455. <https://doi.org/10.1002/cpz1.455>
17. Bankevich A, Nurk S, Antipov D, Gurevich AA, Dvorkin M, Kulikov AS, Lesin VM, Nikolenko SI, Pham S, Prjibelski AD, et al. SPAdes: a New Genome Assembly Algorithm and its applications to single-cell sequencing. *J Comput Biol*. 2012;19:455–77. <https://doi.org/10.1089/cmb.2012.0021>
18. Minh BQ, Schmidt HA, Chernomor O, Schrempf D, Woodhams MD, von Haeseler A, Lanfear R. IQ-TREE 2: New models and efficient methods for phylogenetic inference in the genomic era. *Mol Biol Evol*. 2020;37:1530–4. <https://doi.org/10.1093/molbev/msaa015>
19. Benson DA, Cavanaugh M, Clark K, Karsch-Mizrachi I, Lipman DJ, Ostell J, Sayers EW, GenBank. *Nucleic Acids Res*. 2013;41:D36–42. <https://doi.org/10.1093/nar/gks1195>
20. Edgar RC, MUSCLE. Multiple sequence alignment with high accuracy and high throughput. *Nucleic Acids Res*. 2004;32:1792–7. <https://doi.org/10.1093/nar/gkh340>
21. Machado TB, Picorelli ACR, de Azevedo BL, de Aquino ILM, Queiroz VF, Rodrigues RAL, Araújo JP Jr, Ullmann LS, Dos Santos TM, Marques RE, Guimarães SL, Andrade ACSP, Gularte JS, Demoliner M, Filippi M, Pereira VMAG, Spilki FR, Krupovic M, Aylward FO, Del-Bem L-E, Abrahão JS. Gene duplication as a major force driving the genome expansion in some giant viruses. *J Virol*. 2023 Dec 21;97(12):e0130923. <https://doi.org/10.1128/jvi.01309-23>
22. Pereira Andrade ACDS, Victor de Miranda Boratto P, Rodrigues RAL, Bastos TM, Azevedo BL, Dornas FP, Oliveira DB, Drummond BP, Kroon EG, Abrahão JS. New isolates of pandoraviruses: Contribution to the study of replication cycle steps. *J Virol* 2019 Feb 19;93(5):e01942–18. <https://doi.org/10.1128/JVI.01942-18>

Publisher's Note

Springer Nature remains neutral with regard to jurisdictional claims in published maps and institutional affiliations.

Isolation of Giant Viruses of *Acanthamoeba castellanii*

Talita Bastos Machado,¹ Isabella Luiza Martins de Aquino,¹
and Jônatas Santos Abrahão^{1,2}

¹Instituto de Ciências Biológicas, Departamento de Microbiologia, Laboratório de Vírus,
Universidade Federal de Minas Gerais, Belo Horizonte, Minas Gerais, Brazil

²Corresponding author: jonatas.abrahao@gmail.com

This article describes a practical method for prospecting and isolating giant viruses based on direct inoculation of environmental samples into amoeba cultures of *Acanthamoeba castellanii*. The giant viruses that infect amoebas have already been isolated from various environmental samples in several countries worldwide, including in extreme environments. Here we describe the methodologic procedures regarding the prospecting of giant viruses in *A. castellanii*, including the preparation of environmental samples, the culture of amoebas, and the observation of cytopathic effects that can indicate the presence and potential isolation of giant viruses. © 2022 Wiley Periodicals LLC.

Basic Protocol 1: Sample collection

Support Protocol: Propagation of *Acanthamoeba castellanii*

Basic Protocol 2: Prospecting of giant viruses in environmental samples by cytopathic effect analysis

Keywords: *Acanthamoeba castellanii* • cytopathic effect • giant viruses • virus prospecting

How to cite this article:

Machado, T. B., de Aquino, I. L. M., & Abrahão, J. S. (2022). Isolation of giant viruses of *Acanthamoeba castellanii*. *Current Protocols*, 2, e455. doi: 10.1002/cpz1.455

INTRODUCTION

Since the discovery of *Acanthamoeba polyphaga* mimivirus (APMV) in 2003 (La Scola et al., 2003), several other groups of giant viruses that infect amoebas have been isolated: marseillevirus, pandoravirus, pithovirus, faustovirus, mollivirus, cedratvirus, kaumoebavirus, pacmanvirus, orpheovirus, and medusavirus (Andreani et al., 2016, 2017, 2018; Bajrai et al., 2016; Boyer et al., 2009; Legendre et al., 2014, 2015; Philippe et al., 2013; Reteno et al., 2015; Yoshikawa et al., 2019). These findings have contributed to the expansion of our knowledge regarding the so-called nucleocytoplasmic large DNA viruses. This group includes several virus families (e.g., *Poxviridae* and *Phycodnaviridae*) in addition to these giant amoebal viruses. The giant viruses of amoebas have already been isolated from different types of samples, such as soil, mud, sewage, spring water, seawater, ocean sediments, and even clinical samples. They have been isolated in several countries worldwide from different environments, including extreme ones such as the ocean floor, saline lagoons, and even Antarctica (Abrahão et al., 2018; Andrade et al., 2018). The abundant presence of giant virus sequences in metagenomics databases may indicate that these viral entities, as well as their hosts, are ubiquitous (Kerepesi & Grolmusz., 2016, 2017; Mihara et al., 2018; Schulz et al., 2017, 2018; Wu et al., 2020).

Machado et al.

1 of 9

Overall, giant viruses present a particularly narrow host range. Most of them were isolated from amoebas of the genus *Acanthamoeba*, mostly *A. castellanii*, including marseillevirus, pandoravirus, pithovirus, mollivirus, cedratvirus, pacmanvirus, and medusavirus. Giant viruses have also been isolated from the amoeba species *Vermamoeba vermiformis*, which is known to be permissive to the replication of faustovirus, kaumobavirus, and orpheovirus. Although members of the family *Mimiviridae* also have a narrow host range, notable known exceptions are the tupanviruses, which are able to infect different genera of protists including *Acanthamoeba*, *Vermamoeba*, *Willartia*, and *Dictyostelium* (Abrahão et al., 2018). Nevertheless, *A. castellanii* has been the most popular platform to isolate giant viruses, since this organism can be easily propagated and is permissive to a great diversity of giant viruses.

Here we describe how to isolate giant viruses of *A. castellanii*. This species was chosen because it is the most generalist host for giant viruses among amoeba species. The protocol for maintaining these amoebas is described, as is the protocol for preparing 96-well microplates for viral prospecting. We also describe how each type of environmental sample must be prepared before processing and preventive measures to avoid contamination with other microorganisms such as fungi and bacteria.

**BASIC
PROTOCOL 1**

SAMPLE COLLECTION

Samples can be collected from different environments, including soil, sewage, mud, and fresh and marine water.

Materials

- Sample of interest
- 15- and 50-ml conical centrifuge tubes

NOTE: All materials must be sterile. Gloves must be used to collect the samples.

Water and sewage samples (without sediment)

- 1a. Immerse tubes in liquid until collecting ≥ 10 ml.

Better results have been obtained when water samples were collected at the surface of creeks and shallow polluted lagoons.

Mud samples (water with sediment)

- 1b. Collect sediment along with the liquid until ≥ 10 ml liquid is collected.

Soil samples (sediment only)

- 1c. Collect soft and humid soil pushing the borders of the sterile tube onto the surface of the ground.

For soil samples, 1 g is sufficient.

2. Transport samples at room temperature, and store at 4°C for up to 1 month until the next step.

**SUPPORT
PROTOCOL**

PROPAGATION OF *Acanthamoeba castellanii*

In this protocol, amoebas of the species *A. castellanii* are presented and used as an isolation platform owing to its permissivity to a substantial number of known giant viruses.

Materials

- A. castellanii* cells (e.g., ATCC #30234)
- Peptone-yeast extract with glucose (PYG) medium (see recipe)

- 25-, 75-, and 175-cm² tissue culture flasks
- Inverted microscope

Machado et al.

2 of 9

50-ml conical centrifuge tubes
 Neubauer chamber and glass cover (for cell counting)
 1.5-ml microcentrifuge tubes
 30°C incubator

NOTE: This procedure must be performed in a biosafety level 2 (BSL-2) cabinet. All solutions and materials must be sterile.

1. Split fresh *A. castellanii* cells in 75-cm² tissue culture flasks containing 15 ml PYG medium at 30°C. First, under an inverted microscope, observe if the number of amoebas is adequate to undergo cell splitting (about 90% to 100% cell confluence).

When the tissue culture flask is too full of amoebas, cells begin to detach from the monolayer, so it is best to split closer to 90% cell confluence. After 2 or 3 days, the split can be performed again, according to the number of cells inoculated previously.

2. Discard medium from the tissue culture flask, and add 10 ml fresh PYG medium.

Cell splitting occurs only with amoebas that are attached to the culture flask.

3. To detach cells, gently hit the flask with the palm of the hand. Subsequently, gently homogenize cells with a pipette.

Unlike other cells, amoebas detach from the monolayer mechanically; trypsin is not required. Therefore, the tissue culture flasks must be handled carefully.

4. Transfer cells to 50-ml conical centrifuge tubes, and perform cell counting using a Neubauer chamber. For counting, prepare a 1:10 dilution of cells in a 1.5-ml microcentrifuge tube. Homogenize solution thoroughly with a micropipette before counting. Load Neubauer chamber with 10 µl dilution using a micropipette.

5. Subculture cells in a new tissue culture flask adding 500,000; 1,000,000; and 2,500,000 cells to 25-, 75-, and 150-cm² tissue culture flasks containing a final volume of 5, 15, and 25 ml PYG medium, respectively.

6. Incubate at 30°C until cell confluence (about 90% to 100%) is reached.

Perform cell splitting weekly, at least three times.

PROSPECTING OF GIANT VIRUSES IN ENVIRONMENTAL SAMPLES BY CYTOPATHIC EFFECT ANALYSIS

It is necessary to realize different preparations for each type of sample, according to its nature (water, mud, or soil). For all samples, up to 10 aliquots of 1 ml should be made. In order to prospect giant viruses in this protocol, 96-well microplates are used, which allows for the processing of several samples at the same time. This prospecting technique consists of a coculture method using 100 µl *A. castellanii* (4×10^4 cells) and 100 µl of each environmental sample per well.

Materials

Sample of interest (see Basic Protocol 1)
 Sterile water
 PYG medium (see recipe)
 Vancomycin
 Ciprofloxacin
 Doxycycline
 75-cm² tissue culture flasks containing *A. castellanii* (see Support Protocol)
 1 × phosphate-buffered saline (PBS) (see recipe)

 1.5-ml microcentrifuge tubes, sterile
 Inverted microscope

**BASIC
 PROTOCOL 2**

Machado et al.

3 of 9

50-ml conical centrifuge tubes
 Neubauer chamber and glass cover (for cell counting)
 96-well microplate
 Tape (to seal microplate)
 30°C incubator
 25-cm² tissue culture flask

NOTE: This procedure must be performed in a BSL-2 cabinet. All solutions and materials must be sterile.

Sample preparation

Water and sewage samples (without sediment)

- 1a. Aliquot contents collected in conical centrifuge tubes into 1.5-ml microcentrifuge tubes (1 ml per tube), and perform a 1:10 dilution of each aliquot in sterile water.

Mud samples (water with sediment)

- 1b. Refrigerate collected material for 24 hr to allow any sediment to settle. Subsequently, prepare 1-ml aliquots with the supernatant in 1.5-ml microcentrifuge tubes. Finally, prepare a 1:10 dilution with each aliquot in sterile water.

Soil samples (sediment only)

- 1c. Dilute collected soil in sterile water (1:10) and homogenize thoroughly. Subsequently, store solution at 4°C for 24 hr to allow for sedimentation. Then, aliquot supernatant into 1.5-ml microcentrifuge tubes (1 ml per tube).

All aliquots must undergo three freeze-thaw cycles prior to processing (in order to avoid contamination by fungi and bacteria). Store aliquots in freezer boxes at -20°C.

96-well microplate preparation

2. Supplement PYG medium with additional antibiotics (0.004 mg/ml vancomycin, 0.004 mg/ml ciprofloxacin, and 0.02 mg/ml doxycycline) to reduce potential contamination from environmental samples to be prospected.
3. Observe culture flasks under an inverted microscope to check cell confluence (ideally about 90% to 100%).
4. Discard medium from the tissue culture flask, and add 10 ml fresh PYG medium supplemented with additional antibiotics.

The procedure is carried out only with amoebas that are attached to the culture flasks.

5. To detach cells, gently hit the flask with the palm of the hand (as described in Support Protocol step 3).
6. Transfer cells to 50-ml conical centrifuge tubes, and perform cell counting using a Neubauer chamber. For counting, prepare a 1:10 dilution of cells in 1.5-ml microcentrifuge tubes and homogenize thoroughly. Load Neubauer chamber with 10 µl dilution using a micropipette.
7. In 96-well microplates, add 40,000 cells per well with a final volume of 100 µl per well.
8. Seal edges of the microplates with masking tape, and incubate at 30°C until inoculation of samples.

Sample inoculation

A total of three passages is performed.

9. Passage cells using sample and appropriate control. For each sample, include wells with the original sample (not diluted) and another with the sample diluted. Use the

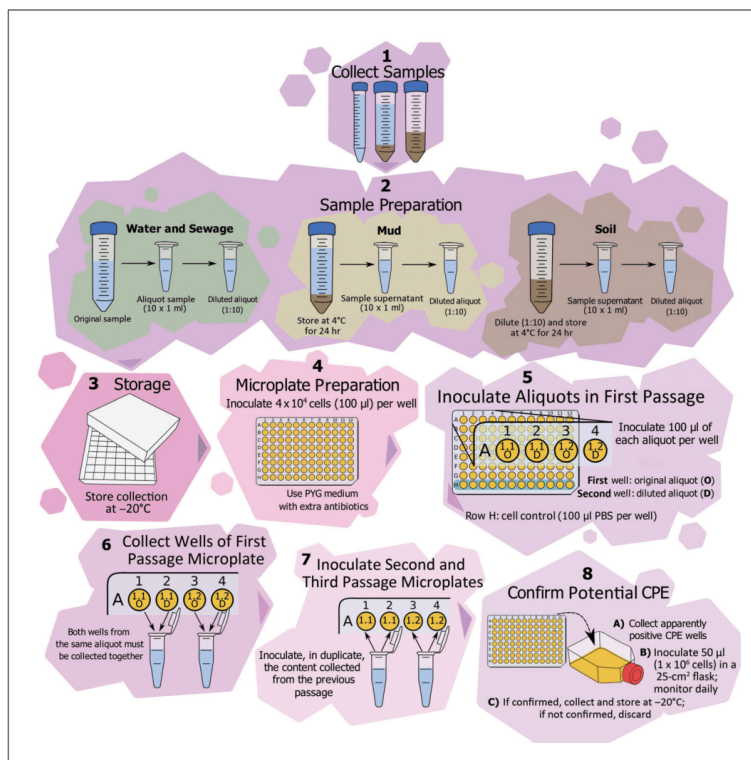


Figure 1 Complete pipeline of the prospecting processes. The process starts with the collection of samples (1). Different preparations are needed according to the nature of the sample (2). Collections are then organized in freezer boxes (3). The 96-well microplates must be prepared (4) to perform the three prospecting passages (5, 6, and 7). Finally, if CPE are observed in any well, they must be confirmed (8). CPE, cytopathic effects; PBS, phosphate-buffered saline; PGY, peptone-yeast extract with glucose.

entire row H (see Fig. 1, item 5) for a cell-only control, which consists of 100 μ l *A. castellanii* (4×10^4 cells) and 100 μ l PBS.

10. At the end of the first passage, collect original (not diluted) and diluted aliquots of each sample, and transfer to a single 1.5-ml microcentrifuge tube (see Fig. 1, item 6). Use this mixture in the next passage, and keep at -20°C until inoculation on a new microplate.
11. Perform the second and third passages with no further dilutions. Use the mixture of the two aliquots (from the same sample) collected from the previous passage in the next passage.

For each passage, the microplate must be sealed with tape to prevent the lid from opening and incubated at 30°C for 7 days, being visually inspected daily for cytopathic effects (CPE).

12. If any of the aliquots among the three passages presents CPE, collect contents of the wells, and store at -20°C for further identification.

This procedure must be performed in a BSL-2 cabinet, and all materials must be sterile.

Machado et al.

5 of 9

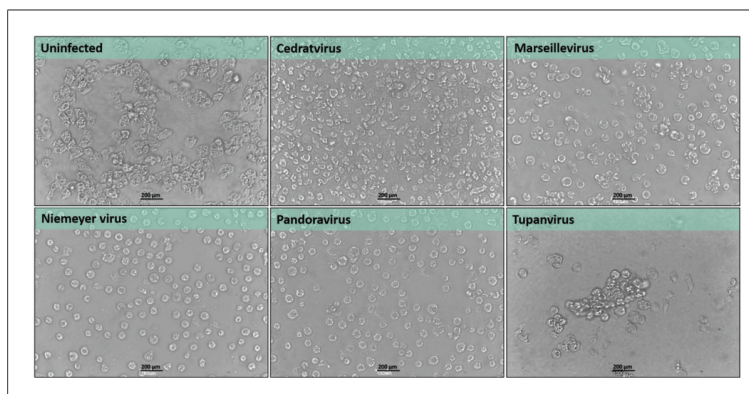


Figure 2 Cytopathic effects caused by different viral groups in *Acanthamoeba castellanii*. Most giant viruses cause cell rounding, detaching of the cell monolayer, and ultimately cell lysis. The formation of clusters or bunches is observed in cells infected by tupanviruses. Adapted and reprinted from de Souza et al. (2020) under Creative Commons Attribution 4.0 International License.

CPE may vary slightly between viral groups. However, the most common effect is cell rounding and detachment of the monolayer, followed by cell lysis. Tupanvirus induces a different CPE, which is the formation of clusters or bunches of rounded cells (Fig. 2). To date, this CPE has only been observed for the two tupanvirus isolates.

Confirmation of cytopathic effects

13. Add 1×10^6 *A. castellanii* cells to a 25-cm² tissue culture flask containing 5 ml PYG medium. Wait for cell attachment.
14. Inoculate 50 μ l of the previously collected well contents into the cell culture flask.
15. Incubate at 30°C for up to 7 days. Visually inspect cells daily to monitor for the appearance of CPE.
16. If CPE is confirmed, collect flask material, and store at –20°C for further identification. If CPE is not confirmed after 7 days, discard contents of the tissue culture flask.

Occasionally, false-positive results are observed. This is due to a cytotoxic effect (caused by some substance present in the sample that is toxic to cells), which causes nonspecific CPE. Because of this, the CPE confirmation procedure is important after collecting the well contents.

This procedure must be performed in a BSL-2 cabinet, and all materials must be sterile.

REAGENTS AND SOLUTIONS

PBS, 10 \times

Dissolve the following in 700 ml ultrapure water:

87.68 g NaCl

5.68 g Na₂HPO₄

2.72 g KH₂PO₄

Bring to 1 L with ultrapure water

Adjust pH to 7.2, if necessary, using 10 M NaOH or 4 M HCl

Autoclave in 1-L bottles for 30 min at 121°C, allowing bottles to cool at room temperature

Store at 4°C for up to 6 months

To make 1× PBS from 10× PBS, take 100 ml of 10× PBS and bring volume to 1 L with ultrapure water.

PYG medium

Combine PYG medium solutions 1 and 2 (see recipes) and mix thoroughly. Add ultrapure water to a final volume of 1 L. Adjust pH to 6.5, if necessary, using 10 M NaOH or 4 M HCl. Filter medium and then sterilize by autoclaving in 500-ml bottles for 20 min at 121°C. Allow bottles to cool at room temperature. In a BSL-2 cabinet, supplement medium with antibiotics and fungicides using 0.25 µg/ml amphotericin B, 100 U/ml penicillin, and 0.1 mg/ml streptomycin. Store at 4°C for up to 6 months.

PYG medium, solution 1

Dissolve the following in 300 ml ultrapure water:

0.98 g MgSO₄·7H₂O
 0.06 g CaCl₂
 9.0 g glucose (C₆H₁₂O₆)
 0.02 g ammonium iron (II) sulfate hexahydrate (Fe(NH₄)₂(SO₄)₆·6H₂O)
 0.40 g Na₂HPO₄·7H₂O
 0.34 g KH₂PO₄
 1.00 g sodium citrate tribasic dihydrate (C₆H₅Na₃O₇·2H₂O)

PYG medium, solution 2

Dissolve the following in 300 ml ultrapure water:

20.0 g Bacto-peptone extract in 200 ml ultrapure water
 2.0 g yeast extract in 200 ml ultrapure water

COMMENTARY

Background Information

Since the isolation of APMV, different techniques have been tested for the isolation of this virus that infects amoebas. In 2011, a technique was assessed that included filtering samples through a 1.2-µm filter (Arslan, Legendre, Seltzer, Abergel, & Claverie, 2011). Currently we know that this technique is not suitable for isolating giant viruses, as it only results in the isolation of viruses that manage to pass through these filters. Larger viruses, such as cedratvirus and pandoravirus, would still be retained on the filter and therefore not isolated.

In another technique, petri dishes containing agar were used. Amoebas were split on an agar surface forming a monolayer, and then samples were inoculated onto this cell monolayer. The objective of this technique was to identify the isolation of a virus from the observation of formation of lysis plaques (Gaia et al., 2013). However, this method frequently presents fungal contamination and needs to be validated with several viral groups.

In contrast, the direct inoculation technique presented here has proven to be efficient for the isolation of different giant viral groups. Furthermore, use of a 96-well microplate allows the processing of several samples at the same time. It is important to mention that this

technique is better suited for low-mobility protists and must be adapted for high-mobility protists. There is also a potential for culture contamination, depending on the nature of the samples. Nonetheless, some preventive measures are considered to reduce or prevent these contaminations, including the use of antibiotics as described in Basic Protocol 2.

Critical Parameters and Troubleshooting

Due to the nature of the samples, contamination with fungi and bacteria may occur. Contamination is more likely to occur within the first passage; therefore, the measures below were established to minimize or avoid these contaminations:

1. Supplement PYG medium with other antibiotics, in addition to those commonly used (herein referred as “additional antibiotics”).
2. Establish a dilution of the samples (1:10), which lowers the probability of contamination. On the other hand, the chance of isolating a virus in an aliquot that was not diluted is higher. Considering this, in the first passage for prospection, the original aliquot is inoculated in one well and the diluted aliquot in another well.

Machado et al.

7 of 9

3. Perform three freeze-thaw cycles of the aliquots prior to processing in an attempt to promote lysis of the cells in the environmental samples. As giant virus particles are very stable, they can resist and remain viable after this procedure.

Despite all precautions taken, contamination can still occur. In this scenario, other alternatives can be established. When contamination of only one of the wells of the same aliquot occurs, the next passage must proceed with only the aliquot that was not contaminated. When contamination of two wells of the same aliquot occurs, it is necessary to freeze and thaw the original aliquot three more times, perform a new dilution (1:10), and further dilute to 1:100. Thus, for the next passage, only the 1:10 and 1:100 dilutions will be inoculated in order to avoid further contamination.

Understanding Results

This protocol enables the isolation of giant viruses that have *A. castellanii* as a natural host or at least as a permissive host. As these viruses generally cause similar CPE, it is important to check the cells daily for roundness and cell lysis while passaging. In addition, it is important to be aware of other cellular changes. It is more common for CPE to appear on the second or third passage.

Last, even when observing CPE in the well, it is necessary to carry out the confirmation process, as it may be a cytotoxic effect caused by some other component of the sample itself.

Time Considerations

There is no specific period of time to collect environmental samples, and it may vary with the purpose of the study, the amount of sample available, or the type of sample to be collected (see Basic Protocol 1).

The time required for sample preparation (Basic Protocol step 12) might vary depending on the type and number of samples that will be processed. Typically, it takes 15 to 30 min to aliquot and dilute each sample. Mud and soil samples require an additional 24 hr for initial sediment settling.

The amoeba cultivation process is continuous and should be done at least three times a week. It usually takes 40 to 60 min for cell splitting and preparation of the 96-well microplates for prospecting (Basic Protocol 2 steps 2 through 8).

Inoculation of the original and diluted aliquots into the 96-well microplates (Basic Protocol 2 steps 9 through 12) usually takes 30 min to be completed. Plaque observation

for CPE should be done daily. Three passages must be carried out, with each passage lasting 7 days. For confirmation of CPE, it may take up to 7 days if there is no confirmation before these 7 days.

Acknowledgments

The authors thank the Laboratório de Vírus of Universidade Federal de Minas Gerais for the support provided. The authors also thank Conselho Nacional de Desenvolvimento Científico e Tecnológico (CNPq), Coordenação de Aperfeiçoamento de Pessoal de Nível Superior (CAPES), Pró-Reitoria de Pesquisa and Pró-Reitoria de Pós-Graduação of UFMG, and Fundação de Amparo à Pesquisa do Estado de Minas Gerais (FAPEMIG) for the financial support, which were fundamental for the development of these protocols. JSA is a CNPq researcher.

Author Contributions

Talita Bastos Machado: formal analysis, investigation, methodology, writing—original draft; **Isabella Luiza Martins de Aquino:** formal analysis, writing—original draft; **Jônatas Santos Abrahão:** conceptualization, formal analysis, funding acquisition, writing—review and editing.

Conflict of Interest

The authors declare no conflict of interest.

Data Availability Statement

Data sharing is not applicable to this article as no datasets were generated or analyzed during the current study.

Literature Cited

- Abrahão, J., Silva, L., Silva, L. S., Khalil, J. Y. B., Rodrigues, R., Arantes, T., ... La Scola, B. (2018). Tailed giant Tupanvirus possesses the most complete translational apparatus of the known virosphere. *Nature Communications*, 9, 749. doi: 10.1038/s41467-018-03168-1.
- Andrade, A. C., Arantes, T. S., Rodrigues, R. A., Machado, T. B., Dornas, F. P., Landell, M. F., ... Abrahão, J. S. (2018). Ubiquitous giants: A plethora of giant viruses found in Brazil and Antarctica. *Virology Journal*, 15, 22. doi: 10.1186/s12985-018-0930-x.
- Andreani, J., Aherfi, S., Bou Khalil, J. Y., Di Pinto, F., Bitam, I., Raoult, D., ... La Scola, B. (2016). Cedratvirus, a double-cork structured giant virus, is a distant relative of pithoviruses. *Viruses*, 8(11), 300. doi: 10.3390/v8110300.
- Andreani, J., Khalil, J. Y. B., Sevvana, M., Benamar, S., Di Pinto, F., Bitam, I., ... La Scola, B. (2017). Pacmanvirus, a new giant icosahedral virus at the crossroads between Asfarviridae and Faustoviruses. *Journal of Virology*, 91(14), e00212–17. doi: 10.1128/JVI.00212-17.

- Andreani, J., Khalil, J. Y., Baptiste, E., Hasni, I., Michelle, C., Raoult, D., ... La Scola, B. (2018). Orpheovirus IHUMI-LCC2: A new virus among the giant viruses. *Frontiers in Microbiology*, 8, 2643. doi: 10.3389/fmicb.2017.02643.
- Arslan, D., Legendre, M., Seltzer, V., Abergel, C., & Claverie, J. M. (2011). Distant Mimivirus relative with a larger genome highlights the fundamental features of Megaviridae. *Proceedings of the National Academy of Sciences of the United States of America*, 108(42), 17486–17491. doi: 10.1073/pnas.1110889108.
- Bajrai, L. H., Benamar, S., Azhar, E. I., Robert, C., Levasseur, A., Raoult, D., & La Scola, B. (2016). Kaumobavirus, a new virus that clusters with Faustoviruses and Asfarviridae. *Viruses*, 8(11), 278. doi: 10.3390/v8110278.
- Boyer, M., Yutin, N., Pagnier, I., Barrassi, L., Fournous, G., Espinosa, L., ... Raoult, D. (2009). Giant Marseillevirus highlights the role of amoebae as a melting pot in emergence of chimeric microorganisms. *Proceedings of the National Academy of Sciences of the United States of America*, 106(51), 21848–21853. doi: 10.1073/pnas.0911354106.
- de Souza, G. A. P., Queiroz, V. F., Lima, M. T., de Sousa Reis, E. V., Coelho, L. F. L., & Abrahão, J. S. (2020). Virus goes viral: An educational kit for virology classes. *Virology Journal*, 17(1), 13. doi: 10.1186/s12985-020-1291-9.
- Gaia, M., Pagnier, I., Campocasso, A., Fournous, G., Raoult, D., & La Scola, B. (2013). Broad spectrum of mimiviridae virophage allows its isolation using a mimivirus reporter. *PLoS One*, 8(4), e61912. doi: 10.1371/journal.pone.0061912.
- Kerepesi, C., & Grolmusz, V. (2016). Giant viruses of the Kutch Desert. *Archives of Virology*, 161(3), 721–724. doi: 10.1007/s00705-015-2720-8.
- Kerepesi, C., & Grolmusz, V. (2017). The “Giant Virus Finder” discovers an abundance of giant viruses in the Antarctic dry valleys. *Archives of Virology*, 162(6), 1671–1676. doi: 10.1007/s00705-017-3286-4.
- La Scola, B., Audic, S., Robert, C., Jungang, L., de Lamballerie, X., Drancourt, M., ... Raoult, D. (2003). A giant virus in amoebae. *Science*, 299(5615), 2033–2033. doi: 10.1126/science.1081867.
- Legendre, M., Bartoli, J., Shmakova, L., Jeudy, S., Labadie, K., Adrait, A., ... Claverie, J. M. (2014). Thirty-thousand-year-old distant relative of giant icosahedral DNA viruses with a pandoravirus morphology. *Proceedings of the National Academy of Sciences of the United States of America*, 111(11), 4274–4279. doi: 10.1073/pnas.1320670111.
- Legendre, M., Lartigue, A., Bertaux, L., Jeudy, S., Bartoli, J., Lescot, M., ... Claverie, J. M. (2015). In-depth study of Mollivirus sibiricum, a new 30,000-y-old giant virus infecting *Acanthamoeba*. *Proceedings of the National Academy of Sciences of the United States of America*, 112(38), E5327–E5335. doi: 10.1073/pnas.1510795112.
- Mihara, T., Koyano, H., Hingamp, P., Grimsley, N., Goto, S., & Ogata, H. (2018). Taxon richness of “Megaviridae” exceeds those of bacteria and archaea in the ocean. *Microbes and Environments*, 33(2), 162–171. doi: 10.1264/jsm2.ME17203.
- Philippe, N., Legendre, M., Doutre, G., Couté, Y., Poirot, O., Lescot, M., ... Abergel, C. (2013). Pandoraviruses: Amoeba viruses with genomes up to 2.5 Mb reaching that of parasitic eukaryotes. *Science*, 341(6143), 281–286. doi: 10.1126/science.1239181.
- Reteno, D. G., Benamar, S., Khalil, J. B., Andreani, J., Armstrong, N., Klose, T., ... La Scola, B. (2015). Faustovirus, an Asfarvirus-related new lineage of giant viruses infecting amoebae. *Journal of Virology*, 89(13), 6585–6594. doi: 10.1128/JVI.00115-15.
- Schulz, F., Yutin, N., Ivanova, N. N., Ortega, D. R., Lee, T. K., Vierheilig, J., ... Woyke, T. (2017). Giant viruses with an expanded complement of translation system components. *Science*, 356(6333), 82–85. doi: 10.1126/science.aal4657.
- Schulz, F., Alteio, L., Goudeau, D., Ryan, E. M., Yu, F. B., Malmstrom, R. R., ... Woyke, T. (2018). Hidden diversity of soil giant viruses. *Nature Communications*, 9(1), 4881. doi: 10.1038/s41467-018-07335-2.
- Wu, S., Zhou, L., Zhou, Y., Wang, H., Xiao, J., Yan, S., & Wang, Y. (2020). Diverse and unique viruses discovered in the surface water of the East China Sea. *BMC Genomics*, 21(1), 441. doi: 10.1186/s12864-020-06861-y.
- Yoshikawa, G., Blanc-Mathieu, R., Song, C., Kayama, Y., Mochizuki, T., Murata, K., ... Takemura, M. (2019). Medusavirus, a novel large DNA virus discovered from hot spring water. *Journal of Virology*, 93(8), e02130–18. doi: 10.1128/JVI.02130-18.

Review

A Brief History of Giant Viruses' Studies in Brazilian Biomes

Paulo Victor M. Boratto ¹, Mateus Sá M. Serafim ¹, Amanda Stéphanie A. Witt ¹, Ana Paula C. Crispim ¹, Bruna Luiza de Azevedo ¹, Gabriel Augusto P. de Souza ¹, Isabella Luiza M. de Aquino ¹, Talita B. Machado ¹, Victória F. Queiroz ¹, Rodrigo A. L. Rodrigues ¹, Ivan Bergier ², Juliana Reis Cortines ³, Savio Torres de Farias ⁴, Raíssa Nunes dos Santos ⁵, Fabrício Souza Campos ⁵, Ana Cláudia Franco ⁵ and Jônatas S. Abrahão ^{1,*}

- ¹ Laboratório de Vírus, Departamento de Microbiologia, Universidade Federal de Minas Gerais, Belo Horizonte 31270-901, Minas Gerais, Brazil; pvboratto@gmail.com (P.V.M.B.); mateusmserafim@gmail.com (M.S.M.S.); asawitt1997@gmail.com (A.S.A.W.); anapbio2@gmail.com (A.P.C.C.); azvdobruna@gmail.com (B.L.d.A.); neogaps@gmail.com (G.A.P.d.S.); isabellaaquino92@gmail.com (I.L.M.d.A.); bastostalita04@gmail.com (T.B.M.); victoriadf18@gmail.com (V.F.Q.); rodriguesral07@gmail.com (R.A.L.R.)
- ² Embrapa Pantanal, Corumbá 79320-900, Mato Grosso do Sul, Brazil; bergiercpap@gmail.com
- ³ Departamento de Virologia, Instituto de Microbiologia Paulo de Góes, Universidade Federal do Rio de Janeiro, Rio de Janeiro 21941-590, Rio de Janeiro, Brazil; cortines@micro.ufrj.br
- ⁴ Laboratório de Genética Evolutiva Paulo Leminsk, Departamento de Biologia Molecular, Universidade Federal da Paraíba, João Pessoa 58050-085, Paraíba, Brazil; stfarias@yahoo.com.br
- ⁵ Laboratório de Virologia, Departamento de Microbiologia, Imunologia e Parasitologia, Instituto de Ciências Básicas da Saúde, Universidade Federal do Rio Grande do Sul, Porto Alegre 90.050-170, Rio Grande do Sul, Brazil; engraisanunes@gmail.com (R.N.d.S.); camposvet@gmail.com (F.S.C.); anafanco.ufrgs@gmail.com (A.C.F.)
- * Correspondence: jonatas.abrahao@gmail.com



Citation: Boratto, P.V.M.; Serafim, M.S.M.; Witt, A.S.A.; Crispim, A.P.C.; Azevedo, B.L.d.; Souza, G.A.P.d.; Aquino, I.L.M.d.; Machado, T.B.; Queiroz, V.F.; Rodrigues, R.A.L.; et al. A Brief History of Giant Viruses' Studies in Brazilian Biomes. *Viruses* **2022**, *14*, 191. <https://doi.org/10.3390/v14020191>

Academic Editor: K. Andrew White

Received: 18 November 2021

Accepted: 15 January 2022

Published: 19 January 2022

Publisher's Note: MDPI stays neutral with regard to jurisdictional claims in published maps and institutional affiliations.



Copyright: © 2022 by the authors. Licensee MDPI, Basel, Switzerland. This article is an open access article distributed under the terms and conditions of the Creative Commons Attribution (CC BY) license (<https://creativecommons.org/licenses/by/4.0/>).

Abstract: Almost two decades after the isolation of the first amoebal giant viruses, indubitably the discovery of these entities has deeply affected the current scientific knowledge on the virosphere. Much has been uncovered since then: viruses can now acknowledge complex genomes and huge particle sizes, integrating remarkable evolutionary relationships that date as early as the emergence of life on the planet. This year, a decade has passed since the first studies on giant viruses in the Brazilian territory, and since then biomes of rare beauty and biodiversity (Amazon, Atlantic forest, Pantanal wetlands, Cerrado savannas) have been explored in the search for giant viruses. From those unique biomes, novel viral entities were found, revealing never before seen genomes and virion structures. To celebrate this, here we bring together the context, inspirations, and the major contributions of independent Brazilian research groups to summarize the accumulated knowledge about the diversity and the exceptionality of some of the giant viruses found in Brazil.

Keywords: amoebae viruses; Brazilian isolates; giant virus; NCLDV; virosphere; virus diversity

1. Introduction

The description and characterization of the first amoebal giant virus (GV) in 2003, *Acanthamoeba polyphaga mimivirus* (APMV), raised important questions regarding the limits of the virosphere. These first findings revealed viral particles of about 700 nm, non-filterable through 0.2 µm pore size filters [1]. Although not the first described nucleocytoplasmic large DNA virus (NCLDV) (phylum *Nucleocytoviricota*), which includes other families such as *Poxviridae* [2], the original discovered member of the family *Mimiviridae* motivated new interpretations of crucial features in an organism recognized as a virus, advancing both knowledge of, and perspectives on, the most abundant group of organisms on Earth [3].

Much of the subsequent work on GVs has been driven by curiosity and the possibility of isolating novel groups of amoebal viruses and finding intriguing new characteristics. For instance, in 2008 La Scola et al. had previously isolated a distinct strain of APMV, the

acanthamoeba castellanii mamavirus, together with the first ever described virophage, the Sputnik virus (SNV), both found in a water-cooling tower of a hospital in France [4]. Here, the interest in describing more GVs contributed by influencing the consolidation of “virophages” as new satellite-like viruses, which are dependent on the mimivirus factory for their replication by putatively hijacking some key features (e.g., the viral RNA polymerase) [5].

Similarly, in 2009, Boyer et al. reported the isolation of the marseillevirus, a novel GV for which analysis of its core genes suggested a previously uncharacterized family of NCLDV. In addition, by unveiling some of the main features of the genome’s repertoire for this new GV, the authors have proposed amoebas as potential “melting pots” of microbial evolution, given the convenient intracellular environment for gene transfer among parasites, including complex genomes that could advent from different GVs’ viral sources [6]. Some of the GVs’ hosts (different amoeba genus, e.g., *Acanthamoeba*) are indeed considered ubiquitous, found in almost all latitudes [7,8], as well as in a wide-range of environments, including wastewater [9], terrestrial and (deep) marine water [7,10], thermal springs [11], permafrost [12], ventilation and air conditioning systems, and even in hospital settings [13,14]. Notwithstanding, GVs can be found in a large set of different native hosts or host-associated organisms, from other various species of amoebas [8,15] to filtering feeding organisms such as oysters [16]. Recently, metagenomics studies have also indicated that GVs are even more abundant in marine environments than prokaryotes, suggesting that these viruses may play a fundamental role in nature as biological control agents, regulating biogeochemical cycles, and potentially acting as evolutionary driving forces [17–19]. Ultimately, hijacking or utilizing cellular components and translational machinery may indicate a common origin, regarding information on life’s evolution, and the presence of translation proteins may open new hypotheses about GVs’ origin and phylogenetic relationships with other domains of life [20].

The broad-spectrum environmental profile of GVs made Brazil an interesting field to search and study these microorganisms, especially considering the wide range and diversity of environments and biological dispersion throughout biomes, settings and native habitats around the country, such as the Amazon forest and Cerrado savannas, as well as the Pantanal wetlands, including the soda lakes of Nhecolândia in the middle of the woods, which hide rich organic sediments [7,10,21–23]. These characteristics were reflected in the findings and discoveries of several GV isolates in the Brazilian territory, such as: (i) tupanvirus soda lake, isolated from the Brazilian Pantanal (Nhecolândia lakes) and tupanvirus deep ocean, isolated from sediment at 3000 m below the water surface line at ‘Bacia de Campos’, in Rio de Janeiro [10]; (ii) samba virus (SMBV), isolated from the Brazilian Amazon [22]; (iii) cedratvirus getuliensis, from sewage samples in Minas Gerais state [24]; (iv) niemeyer virus [25], faustovirus mariensis [26] and yaravirus [27], all of them isolated from the Pampulha urban lagoon; (v) a number of *Mimivirus* isolates [7,21]; and many others (Figure 1A,B), some of which we will further discuss in this review.

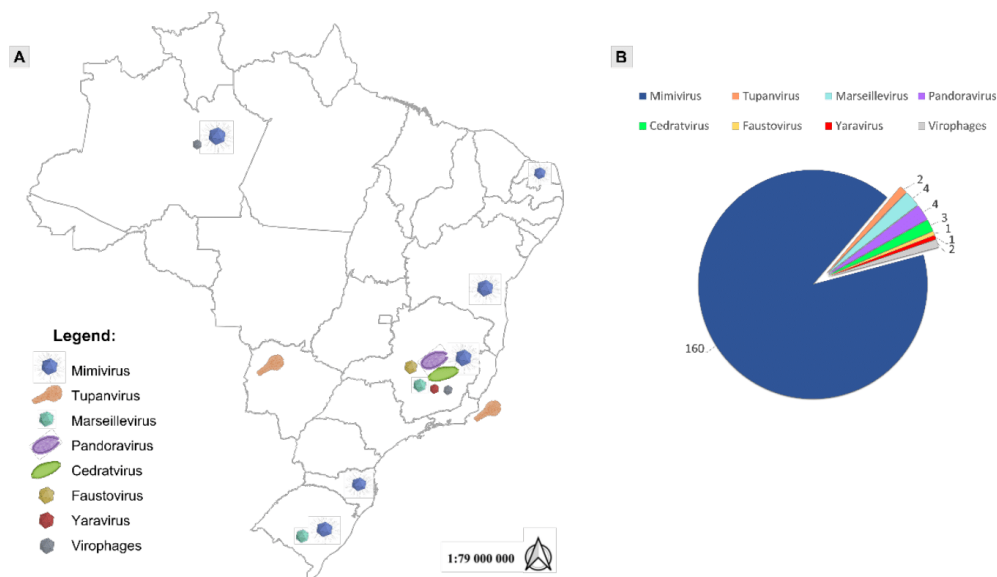


Figure 1. Location and numbers of giant viruses isolated in Brazil. (A) Schematic map showing the sites of isolation for the major groups of giant viruses discovered in Brazil. (B) Number of isolates discovered for each of these groups.

2. Giant Viruses Discovery and Isolation

2.1. *Mimiviruses Boosted Amoebal Giant Viruses' Research*

The first amoebal GV isolated in Brazil dates from 2011. During a field trip to the Brazilian Amazon, aiming to search for GVs, water samples were collected from the Negro River, in Manaus city. These samples were then assessed for prospection using *Acanthamoeba castellanii* cells as an isolation platform, which allowed the discovery of the first Brazilian GV, named samba virus (SMBV) [22].

Samba viruses have mimivirus-like particles, showing capsids with an average diameter of 527 nm, surrounded by fibrils of 155 nm [28]. The SMBV genome is composed of about 1.2 Mb, and the phylogenetic analysis clustered it within the lineage A of the mimiviruses (Table 1). Analysis of the SMBV replication cycle using a set of electron microscopy images showed several similarities with the APMV replication cycle. Moreover, these images also revealed the presence of smaller viral particles that were further confirmed as the first Brazilian virophage named Rio Negro virophage (RNV) [22]. A few years later, RNV genome was sequenced and assembled presenting 18,145 bp, very similar to the sputnik 2 virophage genome [29].

Later, a new sputnik-like virophage named guarani virophage was also isolated from water samples obtained in the Pampulha Lagoon, Belo Horizonte city, Minas Gerais state. A deep characterization of its genome (18,967 bp) was performed, and its replication is described as rather slow (replication at 4 h.p.i. and particles morphogenesis at 16 h.p.i.) when compared to the cycle of its associated GV [30].

After SMBV discovery, several mimiviruses belonging to the three currently known lineages (A, B and C) were isolated from different Brazilian environmental samples, such as the so-called "Br-mimiC", mimivirus golden (MVGd), isolated from golden mussels (*Limnoperna fortunei*) from Guaíba Lake, Rio Grande do Sul, in 2014 [31] and mimivirus gilmour (MVGm), isolated from water collected at the Pampulha Lagoon, in 2015 [21]. In this same work, the isolation of another 64 mimiviruses were described from water samples

collected at the Pampulha Lagoon. They were obtained from three different *Acanthamoeba* species (*A. castellanii*, *A. polyphaga* and *A. griffini*), and had representatives in the three lineages of mimiviruses [21]. Also in 2015, 20 mimiviruses belonging to the lineage A were obtained from oyster-related samples of three different coastal regions of Brazil [16]. Considering their water-filtering capacity, these bivalves were tagged as excellent sources for the isolation of new GV's because their body allows the accumulation of both viruses and amoebas [16].

Table 1. General features of Brazilian giant viruses with complete sequenced-genomes.

Group of Virus	Virus	Type of Sample	Location (Year of Isolation)	Genome Size (bp)	ORFs	ORFans	GC %	Reference
<i>Mimiviridae</i> (lineage A mimivirus)	Samba virus	Fresh water	Negro River (2011)	1,181,380	971	0	27	Campos et al., 2014
	Amazonia virus	Fresh water	Negro River (2011)	1,179,119	979	1 (0.1%)	27	Assis et al., 2015
	Kroon virus	Urban lake water	Lagoa Santa city (2012)	1,221,932	944	3 (0.3%)	27	Assis et al., 2015
	Oyster virus	Oysters	Santa Catarina state (2013)	1,200,220	948	1 (0.1%)	27	Assis et al., 2015
	Niemeyer virus	Urban lake water	Pampulha Lagoon (2011)	1,299,140	1003	0	28	Boratto et al., 2015
<i>Mimiviridae</i> (lineage B mimivirus)	Borely moutmouvirus	Fresh Water	Serra do Cipó (2018)	1,038,187	947	3 (0.3%)	25.2	Silva et al., 2020
<i>Mimiviridae</i> (lineage C mimivirus)	Mimivirus gilmour	Urban lake water	Pampulha Lagoon (2014)	1,258,663	1135	28 (2.4%)	26	Assis et al., 2017
	Mimivirus golden	Golden mussels	Guaiba Lake (2014)	1,248,960	1127	19 (1.6%)	26	Assis et al., 2017
<i>Mimiviridae</i>	Tupanvirus deep ocean	Deep Ocean sediments	Campos dos Goytacazes city (2018)	1,439,508	1276	378 (29.6%)	28	Abrahão et al., 2018
	Tupanvirus soda lake	Soda Lake	Nhecolândia, Pantanal biome (2018)	1,516,267	1359	375 (27.6%)	28	Abrahão et al., 2018
<i>Marseilleviridae</i>	Brazilian marseillevirus	Sewage	Pampulha Lagoon (2014)	362,276	491	29 (5.9%)	43.3	Dornas et al., 2016
	Golden marseillevirus	Golden mussels	Guaiba Lake (2014)	360,610	483	43 (8.9%)	43.1	Santos et al., 2016
Cedratviruses	Brazilian cedratvirus	Water supplemented with biofloc	Belo Horizonte city (2018)	460,038	533	11 (2.1%)	42.9	Rodrigues et al., 2018
Faustovirus	Faustovirus mariensis	Urban lake water	Pampulha Lagoon (2019)	466,080	483	0	36	Borges et al., 2019
Yaravirus	Yaravirus brasiliensis	Muddy water	Pampulha Lagoon (2020)	44,924	74	68 (91.9%)	57.9	Boratto et al., 2020

In another study, a mimivirus-related isolate called Niemeyer virus (NYMV) was discovered, once again from water samples obtained from the Pampulha Lagoon [25]. NYMV has a genome of approximately 1,299,140 bp, harboring a set of duplicated aminoacyl-tRNA synthetases, which suggests that such duplications may be important for the evolutionary history of mimiviruses (Table 1). In 2017, another lineage A mimivirus was described, this time from water samples collected from an urban lake at the Lagoa Santa city, also in the Minas Gerais state, and it was named kroon virus (KV) (Figure 2A) [32]. The study of KV (1,221,932 bp genome [33]) has established an interesting view of the distinct ways by

which the major capsid protein (MCP) mRNA can be differentially processed, depending on the lineages of mimiviruses (Table 1) [32]. Apparently, for each of these mimiviruses' lineages there is a genetic layout concerning how the MCP gene is organized in terms of its exons/introns and how they are arranged. As an example, in the KV study the nucleotide sequences of the third exon of the MCP (observed in the genome of all mimi-viruses) was described to be an alternative marker to disentangle each of the three lineages. In addition, a different form of mature mRNA was also described in transcripts of the MCP for mimiviruses of a given lineage (e.g., APMV and KV) [32]. Subsequently, in 2018, 64 giant viruses of the *Mimiviridae* family (26 from lineage A, 13 from lineage B, two from lineage C and 23 from unidentified lineages) were described from various types of samples, including marine water from Antarctica, which was the first time to our knowledge that mimiviruses were isolated in this continent [7].

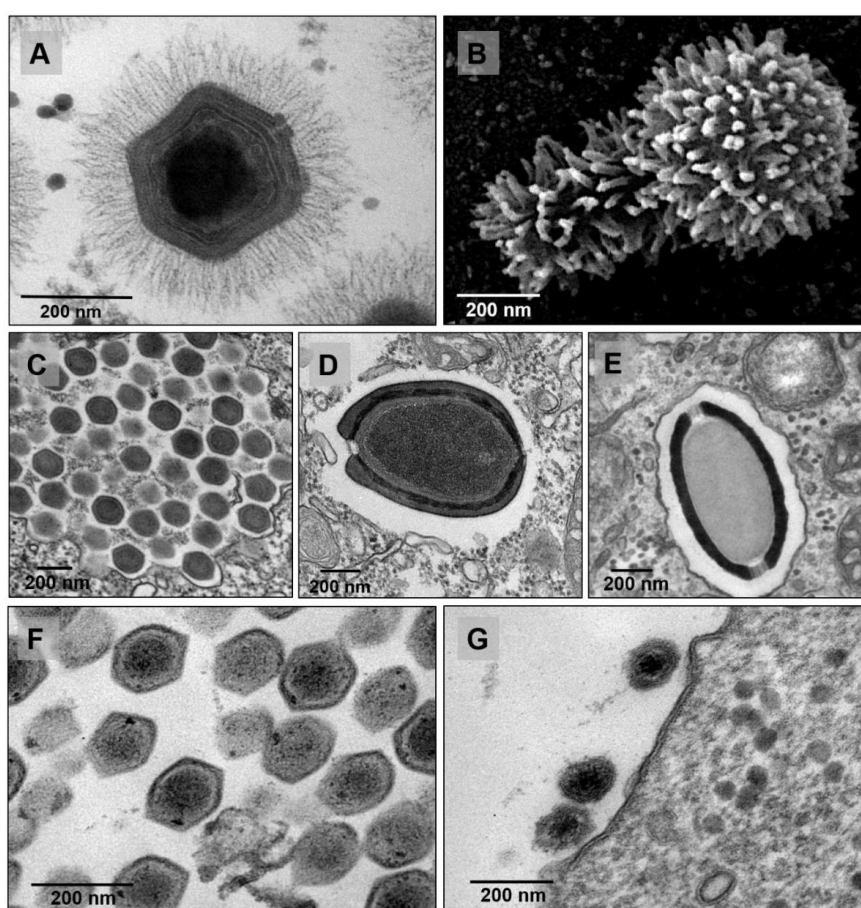


Figure 2. Panel with TEM images for the major groups of amoebal viruses isolated in Brazil. (A) mimivirus, (B) tupanvirus (source: 10.1038/s41598-018-36552-4), (C) marseillevirus, (D) pandoravirus, (E) cedratvirus, (F) faustovirus, and (G) yaravirus.

The year 2018 has also been marked by the description of one of the longest and most complex viruses described to date, obtained from a set of samples collected from

extreme aquatic environments. The tupanvirus soda lake was isolated from samples collected from an alkaline salty lake (Nhacolândia, Pantanal, Brazil) while the deep ocean tupanvirus was obtained from 3000 m depth sediment samples below the Atlantic Ocean at ‘Campos dos Goytacazes’ (Figure 2B) [10]. In contrast to other giant viruses previously isolated, these GVs are able to infect and establish a productive cycle in many species of amoebas, including *Acanthamoeba* spp., *Vermamoeba verniformis*, *Dictyostelium discoideum* and *Willartia magna* [10]. The tupanviruses’ capsid is similar to that of other mimiviruses already described in this review, around 450 nm in diameter, with a pseudo-icosahedral symmetry, covered by a layer of fibrils. They also present a “stargate” vertex, that is, a noticeable star-shaped opening at one capsid vertex. Interestingly, however, these viruses have a tail attached to the capsid, which is also covered with fibrils, a feature never seen before for amoebal viruses (Figure 2B). Due to the plasticity of this tail, the particles can vary from 1.2–2.3 µm in length, making it the longest virus ever described [10].

The genomes of the tupanviruses are complex and composed of double-stranded DNA of 1.44–1.51 Mb, encoding 1276–1425 predicted proteins (Table 1) [10]. Phylogenetic analysis using the DNA polymerase B family gene and other unique features exhibited by these viruses suggested that the tupanviruses group together with other mimiviruses form a distinct clade, which supported the proposal to form a new genus called “*Tupanvirus*” [10,34]. These viruses have been shown to be even more surprising, as deep genome analysis detected the largest translational apparatus ever described in the virosphere, with 20 aminoacyl-tRNA synthetases (aaRS), 67–70 tRNAs, in addition to other proteins in the translation process, such as translation factors (initiation, elongation and release) and proteins related to tRNA and mRNA maturation [10,34,35]. In addition, 20% of their genome is similar to genes originating from cellular organisms, with 9% from eukaryotes (of these, 3% originate from amoebas), 3% from archaea and 8% from bacteria [35].

These findings support data that demonstrate how other groups of organisms are relevant in studying the evolution of NCLDV genomes (Table 1). The fact that they have these genes shared with members of other cellular domains suggests that tupanviruses could also be found in non-extreme environments [35]. Altogether, the genetic arsenal of these and other mimiviruses within the virosphere add new levels of complexity to the understanding of the tree (or rhizome [36]) of life [20,37].

2.2. The Second Family Arises: The Discovery of Marseilleviruses

After the discovery of the first mimiviruses, the search for GVs intensified. In 2009, a virus named *Marseillevirus marseillevirus* was isolated in a biofilm from a water cooling tower in Paris, France [6], which gave rise to the family *Marseilleviridae*, officially recognized by the International Committee on Taxonomy of Viruses (ICTV) in 2013 (Figure 2C) [38]. Since then, other marseilleviruses have been isolated from different sources: (i) Lausannevirus, was discovered in water samples collected from the Seine river, in 2011 [39]; (ii) Cannes 8 virus was isolated from water in a cooling tower in Cannes, in 2013 [40]; (iii) tunisvirus and Fontaine Saint-Charles virus were isolated from freshwater collected in decorative fountains in Ariana, Tunisia, and in France, respectively [41,42]; (iv) insectomime virus was isolated from the internal organs and digestive tract of a dipteran drone fly’s larvae [43]; (v) Senegalvirus was discovered during metagenomic analysis of the bacterial diversity in the human gut microbiota from a apparently healthy African individual, in 2012 [44,45]; (vi) In 2014, the genomic characterization of Melbournevirus was reported, isolated from a freshwater pond in Melbourne, Australia [46]; and (vii) Port-Miou virus, isolated from a sample from a brackish submarine spring, in the Cassis Port-Miou Calanque, France, in 2015 [47].

Furthermore, different phylogenetic lineages of marseillevirus have been described. Initially, the phylogenetic analysis suggested the existence of three distinct lineages: Lineage A, consisting of *Marseillevirus*, Cannes 8 virus, Senegalvirus and Melbournevirus; Lineage B, consisting solely of Lausannevirus; and Lineage C, consisting of tunisvirus and insectomime virus [42]. That was based on phylogenetic reconstructions carried out with core genes

including the NA polymerase B family, the VV A18 helicase, the D5 primase–helicase, the very late transcription factor 2B and the MCP [42].

However, the discovery of the first marseillevirus in America resulted in the creation of a new lineage in the family. The Brazilian Marseillevirus (BrMV) was described in 2014 from a sewage sample from a treatment station in the Pampulha lagoon [47]. The new lineage is supported by comparative genomic analyses highlighting several divergences between BrMV and other marseilleviruses (Figure 3) [47].

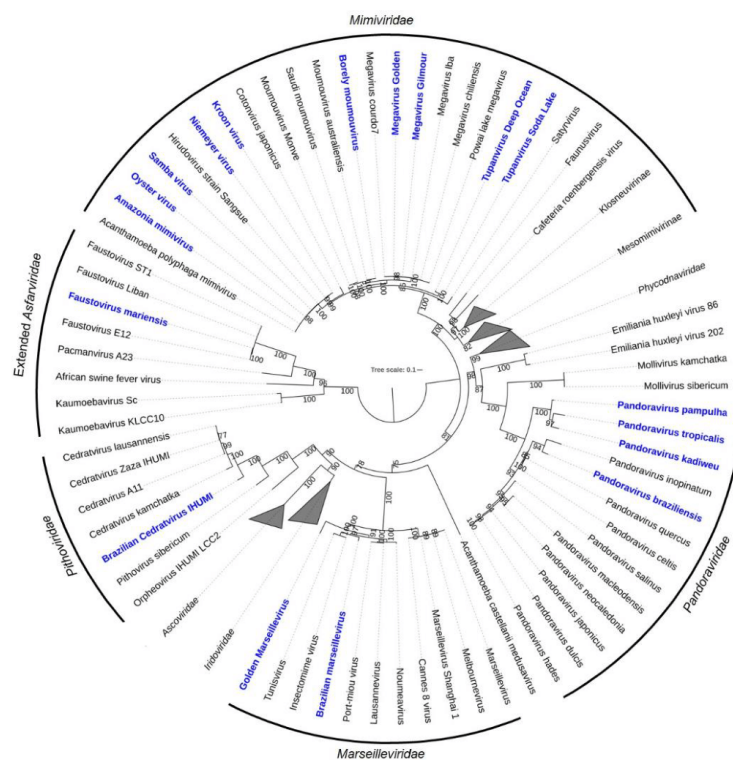


Figure 3. Maximum likelihood phylogenetic tree based on amino acid sequences of DNA polymerase B family of *Nucleocytoviricota*. Brazilian isolates are bold and highlighted in blue. Sequences were aligned using Muscle [48] and low conserved regions were removed using trimAl [49]. The tree was built using IQ-TREE [50] with 1000 ultrafast bootstrap replicates and the VT+F+R7 model chosen by ModelTest according to Bayesian Information Criterion. The tree was visualized in iTOL [51]. The tree scale indicates the substitution rate.

A few years later, in 2016, the golden marseillevirus (GMar) was described as a new member isolated from golden mussels collected in southern Brazil [52]. The structure of the virus particles strongly resembled other marseilleviruses, with particles of approximately 200 nm, obtained from a coculture with *A. polyphaga*. The genome is composed of a circular dsDNA with 360,610 bp, comparable in size to the genomes of other members of the family *Marseilleviridae*, which range from 346,754 bp to 386,631 bp for lausannevirus and insectomime virus, respectively (Table 1) [52]. A total of 483 ORFs were characterized. Curiously, despite this genome size similarity, the GMar genes' content harbors 48.03% uncharacterized proteins. Many of these uncharacterized proteins can be considered as orphan genes (ORFans), also reported in other GVs such as Pandoravirus with

93% ORFans [53]. In addition, comparatively to the 212 genes shared among Brazilian marseillevirus, marseillevirus, lausannevirus, tunisvirus and golden marseillevirus, there are fourteen non-shared genes, of which seven are among the GMar genes [52].

2.3. Opening the GVs' Box: The Discovery of Pandoraviruses

Ten years after the discovery of the first GVs, the description of a brand-new group of amoebal viruses has led virologists to become again surprised, as a series of new paradigms started to be challenged and the study of modern virology advanced. At the time, the discovery and characterization of the pandoraviruses established for the first-time a group with viral particles with sizes as great as 1 μm in length and genomes that exceeded the mark of 2.5 Mb, with an astonishing number of 93% of genes without recognizable homologs in available databases (e.g., GenBank) (Figure 2D) [53].

Before the investigations in Brazil, it is important to mention the initial studies regarding the first representatives of this group. Starting from 2013, these discoveries were made: (i) *Pandoravirus salinus*, isolated from a superficial sediment layer collected at the mouth of the Tunquen river in Chile; and (ii) *Pandoravirus dulcis*, isolated from a mud taken at the bottom of a freshwater pond near Melbourne, Australia [53]. A couple of years later, a study led to the reinvestigation of an endosymbiont isolated from an *Acanthamoeba* strain and concluded, by whole genome sequencing, that this organism was in fact a pandoravirus isolate, named *Pandoravirus inopinatum* [54,55]. In another work, a newly characterized isolate called *Pandoravirus celtis* was used to investigate a putative scenario in which the genetic divergence among the different isolates of pandoraviruses was caused by an ability of these viruses to perform the creation of genes through a de novo microevolution process [56].

During the years 2018 to 2019, two different studies carried out a series of in-depth approaches focusing on establishing a detailed view of the diversity of pandoraviruses, their evolution processes and aspects of their replication cycle [57,58]. In the first study, three samples of pandoravirus were first isolated and named as pandoravirus quercus, pandoravirus neocaledonia and pandoravirus macleodensis. Their replication cycles were independently investigated and interestingly, for the first time, the mature particles of pandoraviruses were filmed while being exocytosed by vesicles which were full of viruses [57]. The genomes of these isolates were fully sequenced and a new stringent reannotation protocol was established. With this new methodology, the genetic analysis of different isolates suggested a still open pan-genome for GVs, in which each novel isolate is predicted to be responsible for contributing more than 50 additional genes [57].

For the second study, three novel Brazilian isolates were used: (i) pandoravirus kadiweu, coming from samples of water collected in the city of Bonito, Mato Grosso do Sul; (ii) pandoravirus pampulha, and (iii) pandoravirus tropicalis, both coming from samples of water from an artificial lake located at the city of Belo Horizonte, Minas Gerais [58]. Here, the microscopy analysis was an important tool, not only to reinforce some already established data but also to reveal new features of the virus replication. As for other GVs, within 30 min of infection the pandoravirus virions were phagocytosed and engulfed inside a host vesicle called the phagosome [57]. This structure quickly fuses with lysosome-like organelles and triggers the next stage of replication, which is the start of viral uncoating [53,57]. The next step involves an intense manipulation of the host cell and deep modification of the cytoplasm environment in order to make the region of viral morphogenesis, known as the viral factory. The loss of the cell nucleus and an intense recruitment of the host membranes and mitochondria are necessary for this. The beginning of viral morphogenesis does not seem to have a polarization, as thought earlier [53]. Finally, the viral cycle ends with the host cell lysis [53,57].

Interestingly, however, it was observed in some microscopy images that several pandoravirus particles were packaged inside vesicles and transported to the periphery of the host cell before amoebal disintegration. Additionally, one-step-growth curves have shown the beginning of viral release around 6 to 9 h post-infection, before the onset of

the amoebas' lysis [58]. These results, together with data that show a negative impact on pandoravirus release by cells treated with brefeldin (a membrane traffic inhibitor), suggest an important role of exocytosis for early liberation of pandoravirus particles in an amoeba infection [58]. Such observations are commonplace to other GV's with analogous replication cycles, including, for example, the cedratviruses described in the next section.

2.4. A Double-Corked GV: Isolation and Characterization of the Cedratviruses

Viruses belonging to the cedratvirus group were first detected in 2016, with the isolation of Cedratvirus A11, a viral representative coming from diverse environmental samples collected in Algeria [59]. Their structure is constructed by a $\sim 1 \mu\text{m}$ ovoid-shaped particle, resembling some morphological features of the pithovirus virions, though with a notable difference: the presence of two corked regions (instead of a single one) at the extremities of the particle [59]. Their genome is composed of a circular dsDNA with about 590 kbp, and it has been found to share a close relationship with the genomes of the two currently known pithoviruses (both in size and in genome content), pithovirus sibericum and pithovirus massiliensis [59].

The second cedratvirus isolate, called cedratvirus lausannensis, was obtained in an attempt to look for amoeba-resisting bacteria inside a drinking water plant located at the Morsang-sur-Seine commune, in France [60]. Four other isolates have been discovered since then: (i) cedratvirus zaza IHUMI, deriving from samples of sterile distilled water collected near Toulon city, in France; (ii) Brazilian cedratvirus IHUMI, collected from water samples supplemented with bio-floc in Belo Horizonte city, Brazil; (iii) cedratvirus Kamchatka, obtained from a muddy grit soil collected next to a volcano area in Russia; and (iv) cedratvirus getuliensis (Figure 2E), collected from sewage samples from the Itaúna city, Brazil [24,61,62]. Interestingly, the isolate Brazilian cedratvirus IHUMI is a representative of the group which harbors both particle and genome sizes with remarkable differences in comparison with the other cedratviruses discovered so far. The virion is approximately 910 nm in length, with some of the particles reaching around 696 nm, and the genome is also smaller, with a DNA molecule of 460,038 bp (Table 1) [63]. Comparative genomic analysis also indicated that this Brazilian isolate is the founding member of a new lineage of cedratviruses (Figure 3) [63].

In 2018, through the analysis of a series of electron microscopy images and by performing biological assays, an interesting study has helped to reveal most of the steps in the replication of cedratviruses. As expected for an amoeba virus with large-sized virions, the viral cycle starts by the particles getting into the infected cell through the exploration of a phagocytic pathway that is physiologically presented by the host [24]. Corroborating this observation, lower titers of the cedratvirus virions are observed when the infected amoeba cells are pre-treated with cytochalasin D, an inhibitor of phagocytosis. The cycle then progresses to the formation of an electron-lucent viral factory (as large as the cellular nucleus) in the cytoplasm of the infected amoeba and, differently from observed during infection of most giant viruses, the cellular nucleus seems to remain intact [24].

However, some typical cellular alterations are still observed, such as the recruitment of mitochondria around the viral factory region, the polarization of lysosomal vesicles in the infected cell and an intense traffic of membranes which were seen to be important during the morphogenesis of cedratvirus virions [24]. This step is described as very complex and relies on the formation of several membrane precursors (or crescents) which later assume the correct conformation of a mature viral particle. Finally, the viral cycle ends with the mature particles released via cell lysis or exocytosis [24]. Cedratviruses also present structural similarities and infection features to other GV's, such as the orpheoviruses, as discussed below.

2.5. Another Amoeba, Another Virus: Discovery and Characterization of Orpheovirus

By implementing amoebas of the *Vermamoeba vermiformis* species as a platform of isolation, new groups of viruses were discovered from different samples. Among them, an

Orpheovirus was isolated in Marseille, France, from samples of rat stool [62]. Nevertheless, Souza et al. observed that, differently to previous findings of viruses infecting amoeba, CPE caused by Orpheovirus could be split into an early stage (3 to 12 h.p.i.), when cells stretch into a branched fusiform shape, and a late stage (starting at 24 h.p.i.), when cells become rounded [64].

The in-depth characterization of the replication cycle demonstrates that it takes approximately 30 h to be completed. It is suggested that one or more particles of Orpheovirus, which are around 1.1 μm , are phagocytized by the host cell within 1 h.p.i. [62,64]. After entry, the particle's internal content is released when the membrane that surrounds the viral core fuses with the endosomal membrane through a structure called ostiole, located at the apex of the particle. Subsequently, the formation of the large electron lucent viral factory is observed, concomitantly with the recruitment of mitochondria and membranes [64]. Membrane recruitment and bleb formation also seems to be important for the viral factory formation and particle morphogenesis since they are affected by treatment with a membrane trafficking inhibitor at the middle stage of infection (8 h.p.i.), which is also observed for cedratviruses [24]. Similarly, as described for other viruses, the particle morphogenesis initiates with the formation of electron-dense semicircular structures, which are filled with their internal content until the formation of the complete closed particle [64].

The complete particle presents smaller fibrils, when compared to mimiviruses, and at least two layers between the fibril layer and the inner membrane [62,64]. Finally, the infectious particles start to be released by exocytosis, detected in the supernatant at 12 h.p.i. Moreover, it is observed that cell lysis also plays a role in viral particle release, mostly at late timepoints of infection. Along with the infectious particles, the formation of defective particles is also observed [64].

2.6. The Isolation and Characterization of Faustoviruses

The faustoviruses are a group of giant viruses first detected in 2015 from samples of sewage from different regions in France and in Dakar, Senegal [65]. In Brazil, the first representative of this group was isolated and described in 2019, from prospecting studies of water samples from the Pampulha lagoon. Faustovirus mariensis, as it was called, is a virus with icosahedral particles reaching approximately 190 nm in diameter and inducing cytopathic effects on amoebas of the *Vermamoeba vermiformis* species (Figure 2F) [26]. Their genome is composed of a circular, double-stranded DNA molecule of about 466,080 bp (Table 1). Like other GVs, the *f. mariensis* replication cycle starts with the infection of the amoeba in its trophozoite form. This infection progresses to the formation of a large electron-lucent viral factory and the recruitment of mitochondria to its periphery [26]. The morphogenesis of *f. mariensis* is similar to that of other faustoviruses previously described in the literature, with new mature particles being formed in small honeycomb structures within the cytoplasm of the host cell. Lysis of the infected cell is the most important means of releasing the *f. mariensis* progeny described so far [26].

In a rare antiviral strategy described for GVs and their amoebal hosts, Borges et al. have observed that the infection of *Vermamoeba vermiformis* cultures is able to trigger a process of encystation of the neighboring cells, trapping the particles of *f. mariensis* inside their host and preventing further infection in the population of amoebas [26]. This event, considered to be observed for the first time in these viruses, was directly influenced by *f. mariensis* infection at a multiplicity of infection (MOI) dependent rates. When cysts were derived from cells infected at high MOIs, they were permanently incapable of excysting, therefore becoming trapped inside the particles of *f. mariensis*. However, when these amoebal cells came from infections at lower MOIs, only the cells with neither viral particles nor factories were able of excysting [26].

Faustoviruses are also phylogenetically related to kaumobaviruses and asfarviruses, with the hypothesis that a common ancestor is shared between these viruses (Figure 3) [62]. After analysis considering this evolutionary proximity, motifs that play the role of promoter sequence in asfarvirus have been identified within the faustovirus genome, leading to the

conclusion that rich A-T (TATTT and TATATA) regions may also have an important role in the gene expression of both kaumobavirus and faustovirus. These findings shed new light for a better understanding of giant virus's gene expression [66]. As aforementioned, intriguing information regarding the GVs' discovery and characteristics are quite common, and some unique factors have attracted attention in the field, such as the recent discovery of the yaravirus in 2020 [27].

2.7. Yaravirus, a Small Virus among the Giants

In late 2020, the discovery of a new lineage of dsDNA virus would enhance our knowledge on the diversity and evolution of viruses in amoeba. The yaravirus brasiliensis, as it was called, has been described as a novel virus of *Acanthamoeba castellanii*, harboring a genome of ~45 kbp enclosed in an icosahedral particle of about 80 nm in diameter [27]. Differently from any other virus isolated from acanthamoeba so far, this virus does not seem to share many of the features which are thought to represent the NCLDV, as it has neither a large particle nor a complex genome (Figure 4) [27]. This may indicate one of the following: (i) yaraviruses either belong to an extremely reduced group of amoebal viruses which are part of the NCLDVs; or (ii) these viruses represent the first discovered lineage of amoebal viruses that are not part of this complex group [27].

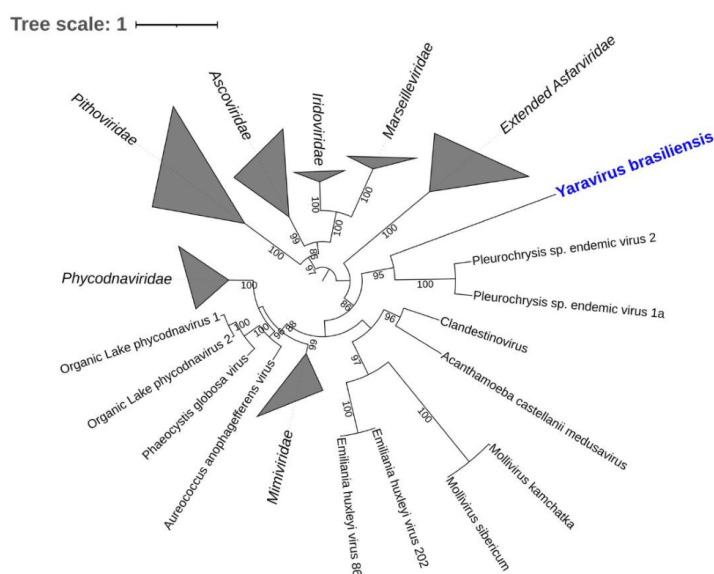


Figure 4. Maximum likelihood phylogenetic tree based on amino acid sequences of major capsid protein of Nucleocytoviricota. Yaravirus brasiliensis is bold and highlighted in blue. Sequences were aligned using Muscle [48] and low conserved regions were removed using trimAl [49]. The tree was built using IQ-TREE [50] with 1000 ultrafast bootstrap replicates and the VT+R3 model chosen by ModelTest according to Bayesian Information Criterion. The tree was visualized in iTOL [51]. The tree scale indicates the substitution rate.

The genome of yaraviruses is composed mainly of ORFans, with an astonishing percentage of ~90% of their genes with functions never described before [27]. The search for yaravirus sequences in a huge dataset consisting of more than 8500 publicly available metagenomes from the most diverse habitats around the globe has also shown hits with distant homologs for the ATPase gene (NCVOG0249), with amino acid similarities that represented a number lower than 33% [27]. The discovery of yaravirus demonstrates

how important are studies focusing on isolating new viruses from the environment [27]. Although metagenomics analyses have an important role in describing new viral species by using their standard methods [67–69], microorganisms like yaraviruses would be very difficult to discover, as these protocols mostly involve recognition of genes already described [27]. This finding could also be seen as a marking point to revamp expositions in the virology field, from intriguing or persuading scientists to stimulating novel research and future researchers.

3. A Fight for Supremacy: Peculiar Features of GVs and Their Interaction with Amoeba Hosts

Much of the biology and particularities of mimivirus interactions with their hosts were discovered during early investigations of GVs. In this regard, both imaging and genomic techniques (e.g., electron microscopy, atomic force microscopy, sequencing, etc.) were of pivotal importance in uncovering many peculiar features of mimiviruses. APMV, for example, was observed to attach to the host cell through glycoside interactions between the long fibrils and surface glycans, with such adhesion also occurring with other unrelated organisms (e.g., arthropods and fungi), potentially facilitating the dispersion of these viruses in the environment [70].

Once they reach their hosts, differently from most non-giant viruses, mimiviruses (and most of the described GVs) enter the host cell through phagocytosis [71]. This was initially observed by transmission electron microscopy (TEM) analysis and further corroborated by biological assays, especially in cells treated with phagocytosis and endocytosis inhibitors [72]. At the apex of the mimivirus capsid there is a starfish-shaped protein complex that acts as a seal for the stargate, until the phagosome's internal environment promotes a new protein arrangement, unleashing the opening of the stargate and the release of the genome [73,74]. The acidification of the phagosome is suggested to be a factor that leads to capsid disassembly and membrane fusion [72,74,75].

In this regard, in 2011, the isolation of SMBV paved the way for further studies performed by other Brazilian research groups, enriching knowledge of mimiviruses' structure and biology. These studies included analysis of different Gs particles using distinct imaging techniques, such as cryo-electron microscopy (cryo-EM) and tomography, as well as fluorescence microscopy [28,76]. In a structural study developed by Schrad et al. (2020), for example, the viral particles of SMBV, tupanvirus, antarctica virus and mimivirus M4 were used to investigate the process of genome release in mimivirus-like particles [77]. Taking this work as an example, the authors have corroborated the importance of conditions such as temperature and pH for the opening of the vertex in these GVs. Here, new additional information on the viral uncoating was settled, as liberation of the viral seed (extra membrane sac) and the complete release of the viral genome were both manifested by experiments using specific conditions of these GVs' replication cycle (e.g., pH = 2 and/or 100 °C) [73]. Even though these conditions are non-biological, the authors suggest that they mimic GVs' replication cycle steps. It may also suggest that during the replication cycle other factors may play a role in capsid opening. In the same study, during the steps of viral genomic release and by adopting different imaging techniques such as cryo-EM, cryo-electron tomography and scanning electron microscopy (SEM), the authors have observed the formation of pockets devoid of DNA within the nucleocapsids of these GVs. Likewise, the analyses led to the identification of a set of proteins released from capsids during the early stages of infection within this whole complex [73]. Looking into another study, with analyses involving SEM and TEM, the authors have observed that for different mimiviruses the density of the fibrils on the surface of their capsid was variable and that this could be acquired simultaneously to genome acquisition throughout the process of morphogenesis in the large viral factories [72]. These techniques were also important in revealing key aspects of the replication cycle of different giant viruses. As already mentioned above, an antiviral strategy was beautifully described in a TEM study showing faustovirus mariensis particles trapped inside the cysts of the *Vermamoeba vermiformis* host

(Figure 5A) [26]. An in-depth description of the replication cycle of orpheovirus and cedratvirus was also established, mostly by imaging methods. For orpheovirus, we started to understand that viral exocytosis was as important as the cell lysis to the final step of this giant virus cycle (Figure 5B) [64]. For cedratvirus getuliensis, the contribution of these techniques has helped to describe a unique and complex sequential organization of the viral particle morphogenesis, including different steps of the formation of horseshoe and rectangular compartments, the incorporation of the second cork and thickening of the capsid well, and finally the formation of the ovoid-shaped virion (Figure 5C) [24]. Considering some intriguing observed features after the mimiviruses' release, another interesting study was proposed by Oliveira et al. (2019) and observed an aggregation of released tupanvirus particles with uninfected amoeba, promoting viral dissemination by the formation of host cell bunches (Figure 5D) [78]. This study revealed that this amoeba-bunch formation is correlated with the mannose-binding protein (MBP) gene expression, either induced by tupanviruses or between amoebas, through interactions among their receptor, both factors that may be important for the optimization of this process [78]. However, when we talk about the genome of tupanviruses, we observe that a great number of their genes are not present in many other mimiviruses' genomes [10], which may still hide some important information about these GVs' cycle. In view of how life has evolved on Earth, the complexity of this genome has also recently been used as an argument to suggest that viruses come from an ancestral strategy of life. According to the authors, in the period comprising the First to the Last Universal Common Ancestor (FUCA to LUCA), an intermediate ancestral (Transitional-LUCA) may have been arisen as an undifferentiated subsystem resembling a virus-like structure, from which most of the currently known viruses came [79]. Besides, aside from the already mentioned unique structural tail, and the formation of bunches [78], tupanviruses exhibited for the first time a cytotoxic phenotype to non-host cells [10]. These intriguing aspects metaphorically resemble a constant fight for supremacy [80] and help unravel the evolutionary history of GVs.

In addition to these distinct characteristics, it is worth mentioning that, as expected, the host cell does not remain indifferent to mimivirus infection. The encystment process is understood as a mechanism used by *Acanthamoeba* populations to become protected against several kinds of stressful conditions, such as dehydration, lack of nutrients, UV light, and viral infections, including against mimiviruses [26,81,82]. As observed in a study developed by Boratto et al. (2015), mimivirus infection is hampered even if those amoebas are not yet morphologically encysted but had already received the stimulus to turn into their resistant form (Figure 5E) [81]. Nonetheless, if the stimulus to become a cyst is triggered before the infection, mimiviruses as APMV are able to evade this protective status of the *Acanthamoeba* cyst, by preventing the expression of an encystment-mediating subtilisin-like serine protease and thus proceeding with the infection (Figure 5E) [81]. These studies demonstrate how complex are processes involving GVs' replication cycle and what an intricate interaction these viruses have with their amoeba hosts.

In addition to isolation studies already mentioned above, other works developed in Brazil have contributed to add knowledge of genomics and important relationships between marseilleviruses and their host. One of these studies has helped to bring light to pivotal processes in the replication cycle of marseilleviruses, specifically related to the viral entry and release. As extensively described in the literature, phagocytosis is a general route used by most GVs to enter amoeba cells [1,6,53,80]. This process is triggered only after recognition of particles larger than 500 nm [83]. However, viruses with particle sizes between 200 to 250 nm, as is the case for marseilleviruses, do not have the minimum size required to trigger this process [84].

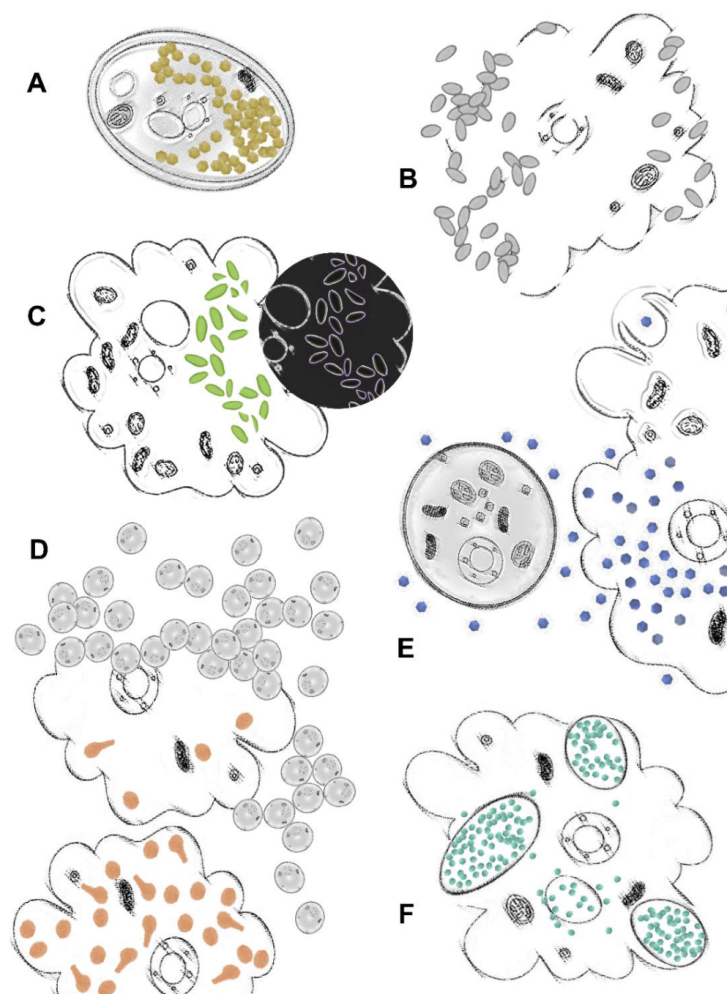


Figure 5. Unique features of giant viruses' (GVs) replication cycles unraveled in Brazil. (A) faus-tovirus dissemination is circumvented by amoebas with the enclosing of viral progeny inside the host's cysts [26]; (B) orpheovirus particles are released from the host by exocytosis or cell lysis [64]; (C) cedratvirus particles' morphogenesis follows a unique and complex sequential organization, including horseshoe and rectangular compartments, the incorporation of the second cork and thickening of the capsid well, and finally the formation of the ovoid-shaped virion [24]; (D) amoebas infected with tupanvirus are induced to aggregate with uninfected cells, forming giant host cell bunches [78]; (E) mimiviruses are able to infect amoebal trophozoites and prevent encystment, while cysts are resistant to infection [81]; (F) MsV are able to form giant vesicles with numerous viral particles derived from amoebal endoplasmic reticulum [84]. Amoeba images were generated from free vectors available online at Vecteezy: <https://www.vecteezy.com> (accessed on 22 September 2021).

By performing an in-depth investigation of the marseillevirus replication cycle and using a different set of virological assays (e.g., TEM, SEM, immunofluorescence, immunoblot-

ting), Arantes et al. have shown that during marseillevirus assembly the viral particles are organized inside large vesicles (some reaching about 3 μm in size) which are originated from the endoplasmic reticulum of the infected cells (Figure 5F) [84]. After viral release, those particles are then ready to infect another cell by exploring the phagocytosis of these vesicles that contain dozens to thousands of viral particles in their interior. In addition, viral release also seems to occur by individual virions. In this case, marseilleviruses exploit the endocytosis route to enter the cell by a mechanism which is dependent on acidification [84].

The *Marseilleviridae* family is also well known for its genomic mosaicism, which consists of the ability to incorporate foreign genes from other organisms that have *Acanthamoeba* as a common host [6]. Genomic studies of several strains of marseillevirus showed the presence of an A-T-rich promoter motif (AAATATTT) that is associated with 55% of the viral genes and that is conserved among all lineages. In addition, biological assays showed that the alteration of the promoter sequence negatively impacts the genes' transcription, showing a possible link of these sequences to the increased expression of some genes [85]. The presence of multiple copies of these motifs in the intergenic regions suggests that they may favor the fixation of newly acquired genes [85].

More recently, in 2020, analysis of the marseillevirus transcriptome revealed a temporal gene expression profile, indicating the existence of three categories: early, intermediate and late [86]. Genes belonging to different functional groups exhibited distinct expression levels throughout the infection cycle and marseillevirus infection causes significant changes in the host's transcription machinery, downregulating many genes [86].

Finally, it is worth mentioning that much of the features above described for GVs and their hosts have an influence directly affected by the intracellular environment of the amoebas. This environment has already been seen as an ecological site that comprehends a number of different and phylogenetic distant microorganisms, which not only inhabit the same location but are also observed to be in a strong process of coevolution. Even if not genetically related, an important portion of the genomic signatures (described as "the total net response to selective pressures") of the coevolving microorganisms are found to be incredibly conserved. This makes the intracellular environment of the amoebal host a sanctuary for interactions among several species of ecological and biomedical relevance [87].

4. Giant Viruses As a Tool to Update and Inspire: From the Research Fields to the Classroom

Since the known virosphere is notably anthropocentric, virology classes usually present viruses as pathogenic organisms, strongly associated with human diseases [3,88]. Instead of presenting these organisms as important tools of natural selection, ecological balance and the Earth's biogeochemical cycles, the commonly used material for teaching virology leads to a biased misconception of viruses as strictly bad, generating a certain fear in the students [89]. Besides this, other problems are the high cost of ensuring biosafety for practical virology classes, and motivation and mastery of the subject by the teachers (especially at the elementary school level) [90]. A further point is that viruses are typically very abstract for students, mainly due to their size, which limits their visualization to schematic figures, illustrations, and electron microscopy images [88].

The expansion of the perception of the virosphere by the giant viruses has unleashed a new way of understanding and teaching virology. Due to their colossal particles, the size limitation has been considered obsolete, turning these viruses into excellent learning tools [88,91]. Therefore, GVs can be visualized by optical microscopy, like bacteria and fungi, which are traditionally presented to students through common microscopes. Moreover, since they infect free-living amoebae, they represent a safe and low-cost instrument for practical virology classes [88,91].

In 2020, our group developed an educational kit to update the content typically taught in virology classes and align it to recent breakthroughs in virus research. Using slides, staining materials, viruses from the laboratory stock, and cell lineages, a microscope

slides kit called “Virus Goes Viral” was created (Figure 6A) [91]. This allows students to observe giant viruses’ particles (Figure 6B–D), viral factories, and different lysis plaques in important viruses that infect animals [91]. As basic research regarding GVs in the Brazilian territory may enrich the knowledge of these microorganisms in the virology field, this kit may also aim to foster an inspiring learning environment, as well as ignite more interest in these fascinating organisms in the future.

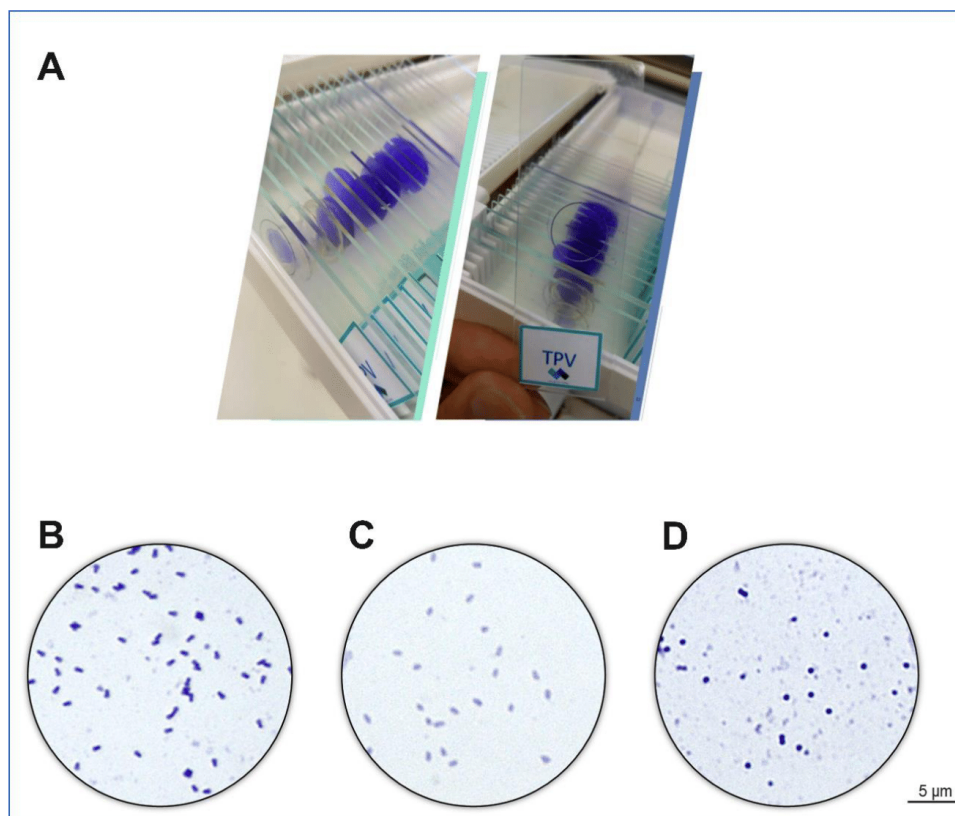


Figure 6. Optical microscopy images. (A) Source: Reference [91]. Visualization under 1000 times magnification of the stained purified particles of (B) tupanvirus, (C) cedratvirus and (D) Niemeyer virus, respectively.

5. Conclusions

The serendipitous discovery of APMV in 2003 changed the concept of viruses and expanded the limits of the virosphere [1]. Over the last two decades, different groups of large and giant viruses of amoebae have been described throughout the world, revealing many unusual particles’ shapes and genome length and content. Culture-independent studies have proved the ubiquity and the astonishing diversity of giant viruses on Earth [18,68]. Now, we must go deeper into the characterization of these viruses, by using different isolates as models. Several new viruses isolated from distinct viral families (e.g., *Mimiviridae* and *Marseilleviridae*) are now under in-depth investigation to better understand their biology and evolution, and these outstanding discoveries may even change our perception of

life itself (e.g., *Mimiviridae* as a new branch derived from a population that gave origin to the modern Eukarya [20]).

Brazil is the fifth largest country in terms of territory and harbors different biomes, making the country an important global hub of tropical biodiversity. Over the past 10 years, the diversity of amoebal viruses in Brazilian environments has been uncovered, with hundreds of isolates belonging to distinct groups, including members of *Mimiviridae*, *Marseilleviridae*, *Pandoraviridae*, *Pithoviridae*, *Faustoviridae*, *Lavidaviridae*, among others, as discussed in previous sections. Interestingly, the most complex giant viruses described to date were isolated from two distinct areas in Brazil [10]. Furthermore, the recent discovery of the small mysterious yaravirus in the country highlighted the importance of continuing the search for new isolates, which could reveal completely new entities on Earth [27]. Brazilian groups, working alongside other experts in the field, have contributed to uncovering this unusual and exciting side of the virosphere. The study of amoebal viruses has already changed our perception of basic virology. Furthermore, giant viruses have recently been proposed as tools to improve virology learning at different educational levels [91]. Surely, other potential applications for these viruses are waiting to be revealed as new data emerges. This is an open field for remarkable discoveries, and we can expect great innovations as new amoebal viruses are isolated and characterized. In this context, the preservation of Brazilian biomes is a sine qua non condition, not only for the discovery of novel biological entities (including giant viruses), but also because of climatic, philosophical, political and economic reasons. Finally, we would like to reinforce that, although this review is a celebration of the 10th anniversary of giant virus studies in Brazilian biomes, we do not support any kind of excessive scientific nationalism. We are aware that studies of giant viruses in Brazil represent a modest contribution to the giant viruses' universe. This field has been constructed by remarkable worldwide research groups, and we are very grateful for their efforts and inspiring work.

Author Contributions: Conceptualization, P.V.M.B., M.S.M.S., A.S.A.W., A.P.C.C., B.L.d.A., G.A.P.d.S., I.L.M.d.A., T.B.M., V.F.Q., R.A.L.R. Writing—original draft preparation, P.V.M.B., M.S.M.S., A.S.A.W., A.P.C.C., B.L.d.A., G.A.P.d.S., I.L.M.d.A., T.B.M., V.F.Q., R.A.L.R. Writing—review and editing, P.V.M.B., M.S.M.S., I.B., J.R.C., S.T.d.F., R.N.d.S., F.S.C., A.C.F., J.S.A. Supervision and funding acquisition, J.S.A. All authors have read and agreed to the published version of the manuscript.

Funding: JSA is a CNPq researcher (302081/2018-6).

Institutional Review Board Statement: The data here presented was partially or fully registered at SISGEN—numbers AA3B21E, A702EB8, A25764F, AC31840, A473BD3, A3DAB3F, AC3045D, A96431C, ABF23CC, A2F8816, A580BBD, AEC3EAA. Collection authorization -SISBIO numbers 33326, 34293 and 80252.

Informed Consent Statement: Not applicable.

Data Availability Statement: Genomic data can be found at genbank (<https://www.ncbi.nlm.nih.gov/genbank/>, accessed on 11 January 2022).

Acknowledgments: We would like to thank all colleagues that contributed to studies on giant viruses in Brazil and worldwide. It has been a long, hard, challenging but pleasant journey. We are grateful to Bernard La Scola (Aix Marseille Université, France) for those years of fruitful collaboration. We also thank the institutes that provided support in the last 10 years, including the CNPq, CAPES, FAPEMIG, Ministério da Saúde, Ministério de Meio Ambiente, Ministério da Educação and Pró-Reitoria de Pesquisa e de Pós-Graduação da UFMG and Centro de Microscopia da UFMG.

Conflicts of Interest: The authors declare no conflict of interest.

References

1. Scola, B.L.; Audic, S.; Robert, C.; Jungang, L.; de Lamballerie, X.; Drancourt, M.; Birtles, R.; Claverie, J.-M.; Raoult, D. A Giant Virus in Amoebae. *Science* **2003**, *299*, 2033. [[CrossRef](#)]
2. Iyer, L.M.; Aravind, L.; Koonin, E.V. Common Origin of Four Diverse Families of Large Eukaryotic DNA Viruses. *J. Virol.* **2001**, *75*, 11720–11734. [[CrossRef](#)] [[PubMed](#)]

3. Rodrigues, R.A.; Andrade, A.C.; Boratto, P.V.d.M.; Trindade, G.d.S.; Kroon, E.G.; Abrahão, J.S. An Anthropocentric View of the Virophere-Host Relationship. *Front. Microbiol.* **2017**, *8*, 1673. [[CrossRef](#)] [[PubMed](#)]
4. La Scola, B.; Desnues, C.; Pagnier, I.; Robert, C.; Barrassi, L.; Fournous, G.; Merchat, M.; Suzan-Monti, M.; Forterre, P.; Koonin, E.; et al. The Virophage as a Unique Parasite of the Giant Mimivirus. *Nature* **2008**, *455*, 100–104. [[CrossRef](#)] [[PubMed](#)]
5. Koonin, E.V.; Yutin, N. Origin and Evolution of Eukaryotic Large Nucleo-Cytoplasmic DNA Viruses. *Intervirology* **2010**, *53*, 284–292. [[CrossRef](#)]
6. Boyer, M.; Yutin, N.; Pagnier, I.; Barrassi, L.; Fournous, G.; Espinosa, L.; Robert, C.; Azza, S.; Sun, S.; Rossmann, M.G.; et al. Giant Marseillevirus Highlights the Role of Amoebae as a Melting Pot in Emergence of Chimeric Microorganisms. *Proc. Natl. Acad. Sci. USA* **2009**, *106*, 21848–21853. [[CrossRef](#)] [[PubMed](#)]
7. Andrade, A.C.D.S.P.; Arantes, T.S.; Rodrigues, R.A.L.; Machado, T.B.; Dornas, F.P.; Landell, M.F.; Furst, C.; Borges, L.G.A.; Dutra, L.A.L.; Almeida, G.; et al. Ubiquitous Giants: A Plethora of Giant Viruses Found in Brazil and Antarctica. *Virol. J.* **2018**, *15*, 22. [[CrossRef](#)]
8. Aherfi, S.; Colson, P.; La Scola, B.; Raoult, D. Giant Viruses of Amoebas: An Update. *Front. Microbiol.* **2016**, *7*, 349. [[CrossRef](#)]
9. Schulz, F.; Yutin, N.; Ivanova, N.N.; Ortega, D.R.; Lee, T.K.; Vierheilig, J.; Daims, H.; Horn, M.; Wagner, M.; Jensen, G.J.; et al. Giant Viruses with an Expanded Complement of Translation System Components. *Science* **2017**, *356*, 82–85. [[CrossRef](#)]
10. Abrahão, J.; Silva, L.; Silva, L.S.; Khalil, J.Y.B.; Rodrigues, R.; Arantes, T.; Assis, F.; Boratto, P.; Andrade, M.; Kroon, E.G.; et al. Tailed Giant Tupanvirus Possesses the Most Complete Translational Apparatus of the Known Virophere. *Nat. Commun.* **2018**, *9*, 749. [[CrossRef](#)] [[PubMed](#)]
11. Yoshikawa, G.; Blanc-Mathieu, R.; Song, C.; Kayama, Y.; Mochizuki, T.; Murata, K.; Ogata, H.; Takemura, M. Medusavirus, a Novel Large DNA Virus Discovered from Hot Spring Water. *J. Virol.* **2019**, *93*, e02130-18. [[CrossRef](#)] [[PubMed](#)]
12. Legendre, M.; Lartigue, A.; Bertaux, L.; Jeudy, S.; Bartoli, J.; Lescot, M.; Alempic, J.-M.; Ramus, C.; Bruley, C.; Labadie, K.; et al. In-Depth Study of Mollivirus Sibericum, a New 30,000-y-Old Giant Virus Infecting Acanthamoeba. *Proc. Natl. Acad. Sci. USA* **2015**, *112*, E5327–E5335. [[CrossRef](#)] [[PubMed](#)]
13. Abrahão, J.S.; Dornas, F.P.; Silva, L.C.; Almeida, G.M.; Boratto, P.V.; Colson, P.; La Scola, B.; Kroon, E.G. Acanthamoeba Polyphaga Mimivirus and Other Giant Viruses: An Open Field to Outstanding Discoveries. *Virol. J.* **2014**, *11*, 120. [[CrossRef](#)] [[PubMed](#)]
14. Marciano-Cabral, F.; Cabral, G. *Acanthamoeba* spp. as Agents of Disease in Humans. *Clin. Microbiol. Rev.* **2003**, *16*, 273–307. [[CrossRef](#)] [[PubMed](#)]
15. Colson, P.; La Scola, B.; Raoult, D. Giant Viruses of Amoebae: A Journey through Innovative Research and Paradigm Changes. *Annu. Rev. Virol.* **2017**, *4*, 61–85. [[CrossRef](#)]
16. Andrade, K.R.; Boratto, P.P.V.M.; Rodrigues, F.P.; Silva, L.C.F.; Dornas, F.P.; Pilotto, M.R.; La Scola, B.; Almeida, G.M.F.; Kroon, E.G.; Abrahão, J.S. Oysters as Hot Spots for Mimivirus Isolation. *Arch. Virol.* **2015**, *160*, 477–482. [[CrossRef](#)]
17. Mihara, T.; Koyano, H.; Hingamp, P.; Grimsley, N.; Goto, S.; Ogata, H. Taxon Richness of “Megaviridae” Exceeds Those of Bacteria and Archaea in the Ocean. *Microbes Environ.* **2018**, *33*, 162–171. [[CrossRef](#)] [[PubMed](#)]
18. Moniruzzaman, M.; Martinez-Gutierrez, C.A.; Weinheimer, A.R.; Aylward, F.O. Dynamic Genome Evolution and Complex Virocell Metabolism of Globally-Distributed Giant Viruses. *Nat. Commun.* **2020**, *11*, 1710. [[CrossRef](#)]
19. Moniruzzaman, M.; Weinheimer, A.R.; Martinez-Gutierrez, C.A.; Aylward, F.O. Widespread Endogenization of Giant Viruses Shapes Genomes of Green Algae. *Nature* **2020**, *588*, 141–145. [[CrossRef](#)]
20. Marcelino, V.M.; Espinola, M.V.P.C.; Serrano-Solis, V.; Farias, S.T. Evolution of the Genus Mimivirus Based on Translation Protein Homology and Its Implication in the Tree of Life. *Genet. Mol. Res.* **2017**, *16*, 1–7. [[CrossRef](#)]
21. Dornas, F.P.; Khalil, J.Y.B.; Pagnier, I.; Raoult, D.; Abrahão, J.; La Scola, B. Isolation of New Brazilian Giant Viruses from Environmental Samples Using a Panel of Protozoa. *Front. Microbiol.* **2015**, *6*, 1086. [[CrossRef](#)] [[PubMed](#)]
22. Campos, R.K.; Boratto, P.V.; Assis, F.L.; Aguiar, E.R.; Silva, L.C.; Albarnaz, J.D.; Dornas, F.P.; Trindade, G.S.; Ferreira, P.P.; Marques, J.T.; et al. Samba Virus: A Novel Mimivirus from a Giant Rain Forest, the Brazilian Amazon. *Virol. J.* **2014**, *11*, 95. [[CrossRef](#)]
23. Guerreiro, R.L.; Bergier, I.; McGlue, M.M.; Warren, L.V.; de Abreu, U.G.P.; Abrahão, J.; Assine, M.L. The Soda Lakes of Nhecolândia: A Conservation Opportunity for the Pantanal Wetlands. *Perspect. Ecol. Conserv.* **2019**, *17*, 9–18. [[CrossRef](#)]
24. Dos Santos Silva, L.K.; Andrade, A.C.S.P.; Dornas, F.P.; Rodrigues, R.A.L.; Arantes, T.; Kroon, E.G.; Bonjardim, C.A.; Abrahão, J.S. Cedrativirus Getuliensis Replication Cycle: An in-Depth Morphological Analysis. *Sci. Rep.* **2018**, *8*, 4000. [[CrossRef](#)]
25. Boratto, P.V.M.; Arantes, T.S.; Silva, L.C.F.; Assis, F.L.; Kroon, E.G.; La Scola, B.; Abrahão, J.S. Niemeyer Virus: A New Mimivirus Group A Isolate Harboring a Set of Duplicated Aminoacyl-TRNA Synthetase Genes. *Front. Microbiol.* **2015**, *6*, 1256. [[CrossRef](#)]
26. Borges, I.; Rodrigues, R.A.L.; Dornas, F.P.; Almeida, G.; Aquino, I.; Bonjardim, C.A.; Kroon, E.G.; La Scola, B.; Abrahão, J.S. Trapping the Enemy: *Vermamoeba vermiformis* Circumvents Faustovirus Mariensis Dissemination by Enclosing Viral Progeny inside Cysts. *J. Virol.* **2019**, *93*, e00312-19. [[CrossRef](#)]
27. Boratto, P.V.M.; Oliveira, G.P.; Machado, T.B.; Andrade, A.C.S.P.; Baudoin, J.-P.; Klose, T.; Schulz, F.; Azza, S.; Decloquement, P.; Chabrière, E.; et al. Yaravirus: A Novel 80-Nm Virus Infecting Acanthamoeba Castellani. *Proc. Natl. Acad. Sci. USA* **2020**, *117*, 16579–16586. [[CrossRef](#)]
28. Schrad, J.R.; Young, E.J.; Abrahão, J.S.; Cortines, J.R.; Parent, K.N. Microscopic Characterization of the Brazilian Giant Samba Virus. *Viruses* **2017**, *9*, 30. [[CrossRef](#)] [[PubMed](#)]

29. Borges, I.A.; de Assis, F.L.; Silva, L.K.D.S.; Abrahão, J. Rio Negro Virophage: Sequencing of the near Complete Genome and Transmission Electron Microscopy of Viral Factories and Particles. *Braz. J. Microbiol.* **2018**, *49* (Suppl. S1), 260–261. [[CrossRef](#)] [[PubMed](#)]
30. Mougari, S.; Bekliz, M.; Abrahao, J.; Di Pinto, F.; Levasseur, A.; La Scola, B. Guarani Virophage, a New Sputnik-Like Isolate From a Brazilian Lake. *Front. Microbiol.* **2019**, *10*, 1003. [[CrossRef](#)]
31. Assis, F.L.; Franco-Luiz, A.P.M.; Dos Santos, R.N.; Campos, F.S.; Dornas, F.P.; Boratto, P.V.M.; Franco, A.C.; Abrahao, J.S.; Colson, P.; Scola, B.L. Genome Characterization of the First Mimiviruses of Lineage C Isolated in Brazil. *Front. Microbiol.* **2017**, *8*, 2562. [[CrossRef](#)] [[PubMed](#)]
32. Boratto, P.V.M.; Dornas, F.P.; da Silva, L.C.F.; Rodrigues, R.A.L.; Oliveira, G.P.; Cortines, J.R.; Drumond, B.P.; Abrahão, J.S. Analyses of the Kroon Virus Major Capsid Gene and Its Transcript Highlight a Distinct Pattern of Gene Evolution and Splicing among Mimiviruses. *J. Virol.* **2018**, *92*, e01782-17. [[CrossRef](#)]
33. Assis, F.L.; Bajrai, L.; Abrahao, J.S.; Kroon, E.G.; Dornas, F.P.; Andrade, K.R.; Boratto, P.V.M.; Pilotto, M.R.; Robert, C.; Benamar, S.; et al. Pan-Genome Analysis of Brazilian Lineage A Amoebal Mimiviruses. *Viruses* **2015**, *7*, 3483–3499. [[CrossRef](#)] [[PubMed](#)]
34. Rodrigues, R.A.L.; Mougari, S.; Colson, P.; La Scola, B.; Abrahão, J.S. “Tupanvirus”, a New Genus in the Family Mimiviridae. *Arch. Virol.* **2019**, *164*, 325–331. [[CrossRef](#)]
35. De Miranda Boratto, P.V.; Dos Santos Pereira Andrade, A.C.; Araújo Lima Rodrigues, R.; La Scola, B.; Santos Abrahão, J. The Multiple Origins of Proteins Present in Tupanvirus Particles. *Curr. Opin. Virol.* **2019**, *36*, 25–31. [[CrossRef](#)] [[PubMed](#)]
36. Raoult, D. The Post-Darwinist Rhizome of Life. *Lancet* **2010**, *375*, 104–105. [[CrossRef](#)]
37. Abrahão, J.S.; Araújo, R.; Colson, P.; Scola, B.L. The Analysis of Translation-Related Gene Set Boosts Debates around Origin and Evolution of Mimiviruses. *PLoS Genet.* **2017**, *13*, e1006532. [[CrossRef](#)]
38. Aherfi, S.; La Scola, B.; Pagnier, I.; Raoult, D.; Colson, P. The Expanding Family Marseilleviridae. *Virology* **2014**, *466–467*, 27–37. [[CrossRef](#)]
39. Thomas, V.; Bertelli, C.; Collyn, F.; Casson, N.; Telenti, A.; Goesmann, A.; Croxatto, A.; Greub, G. Lausannevirus, a Giant Amoebal Virus Encoding Histone Doublets. *Environ. Microbiol.* **2011**, *13*, 1454–1466. [[CrossRef](#)]
40. Aherfi, S.; Pagnier, I.; Fournous, G.; Raoult, D.; La Scola, B.; Colson, P. Complete Genome Sequence of Cannes 8 Virus, a New Member of the Proposed Family “Marseilleviridae”. *Virus Genes* **2013**, *47*, 550–555. [[CrossRef](#)]
41. Pagnier, I.; Reteno, D.-G.L.; Saadi, H.; Boughalmi, M.; Gaia, M.; Slimani, M.; Ngounga, T.; Bekliz, M.; Colson, P.; Raoult, D.; et al. A Decade of Improvements in Mimiviridae and Marseilleviridae Isolation from Amoeba. *Intervirology* **2013**, *56*, 354–363. [[CrossRef](#)]
42. Aherfi, S.; Boughalmi, M.; Pagnier, I.; Fournous, G.; La Scola, B.; Raoult, D.; Colson, P. Complete Genome Sequence of Tunisvirus, a New Member of the Proposed Family Marseilleviridae. *Arch. Virol.* **2014**, *159*, 2349–2358. [[CrossRef](#)] [[PubMed](#)]
43. Boughalmi, M.; Pagnier, I.; Aherfi, S.; Colson, P.; Raoult, D.; La Scola, B. First Isolation of a Marseillevirus in the Diptera Syrphidae *Eristalis Tenax*. *Intervirology* **2013**, *56*, 386–394. [[CrossRef](#)]
44. Lagier, J.-C.; Armougom, F.; Million, M.; Hugon, P.; Pagnier, I.; Robert, C.; Bittar, F.; Fournous, G.; Gimenez, G.; Maraninchi, M.; et al. Microbial Culturomics: Paradigm Shift in the Human Gut Microbiome Study. *Clin. Microbiol. Infect.* **2012**, *18*, 1185–1193. [[CrossRef](#)]
45. Colson, P.; Fancello, L.; Gimenez, G.; Armougom, F.; Desnues, C.; Fournous, G.; Yoosuf, N.; Million, M.; La Scola, B.; Raoult, D. Evidence of the Megavirome in Humans. *J. Clin. Virol.* **2013**, *57*, 191–200. [[CrossRef](#)] [[PubMed](#)]
46. Doutre, G.; Philippe, N.; Abergel, C.; Claverie, J.-M. Genome Analysis of the First Marseilleviridae Representative from Australia Indicates That Most of Its Genes Contribute to Virus Fitness. *J. Virol.* **2014**, *88*, 14340–14349. [[CrossRef](#)]
47. Dornas, F.P.; Assis, F.L.; Aherfi, S.; Arantes, T.; Abrahão, J.S.; Colson, P.; La Scola, B. A Brazilian Marseillevirus Is the Founding Member of a Lineage in Family Marseilleviridae. *Viruses* **2016**, *8*, 76. [[CrossRef](#)] [[PubMed](#)]
48. Edgar, R.C. MUSCLE: A Multiple Sequence Alignment Method with Reduced Time and Space Complexity. *BMC Bioinform.* **2004**, *5*, 113. [[CrossRef](#)] [[PubMed](#)]
49. Capella-Gutiérrez, S.; Silla-Martínez, J.M.; Gabaldón, T. TrimAl: A Tool for Automated Alignment Trimming in Large-Scale Phylogenetic Analyses. *Bioinformatics* **2009**, *25*, 1972–1973. [[CrossRef](#)]
50. Nguyen, L.-T.; Schmidt, H.A.; von Haeseler, A.; Minh, B.Q. IQ-TREE: A Fast and Effective Stochastic Algorithm for Estimating Maximum-Likelihood Phylogenies. *Mol. Biol. Evol.* **2015**, *32*, 268–274. [[CrossRef](#)]
51. Letunic, I.; Bork, P. Interactive Tree of Life (ITOL) v5: An Online Tool for Phylogenetic Tree Display and Annotation. *Nucleic Acids Res.* **2021**, *49*, W293–W296. [[CrossRef](#)]
52. Dos Santos, R.N.; Campos, F.S.; Medeiros de Albuquerque, N.R.; Finoketti, F.; Córrea, R.A.; Cano-Ortiz, L.; Assis, F.L.; Arantes, T.S.; Roehe, P.M.; Franco, A.C. A New Marseillevirus Isolated in Southern Brazil from *Limnoperna Fortunei*. *Sci. Rep.* **2016**, *6*, 35237. [[CrossRef](#)]
53. Philippe, N.; Legendre, M.; Doutre, G.; Couté, Y.; Poirot, O.; Lescot, M.; Arslan, D.; Seltzer, V.; Bertaux, L.; Bruley, C.; et al. Pandoraviruses: Amoeba Viruses with Genomes up to 2.5 Mb Reaching That of Parasitic Eukaryotes. *Science* **2013**, *341*, 281–286. [[CrossRef](#)]
54. Scheid, P.; Balczun, C.; Schaub, G.A. Some Secrets Are Revealed: Parasitic Keratitis Amoebae as Vectors of the Scarcely Described Pandoraviruses to Humans. *Parasitol. Res.* **2014**, *113*, 3759–3764. [[CrossRef](#)] [[PubMed](#)]

55. Antwerpen, M.H.; Georgi, E.; Zoeller, L.; Woelfel, R.; Stoecker, K.; Scheid, P. Whole-Genome Sequencing of a Pandoravirus Isolated from Keratitis-Inducing Acanthamoeba. *Genome Announc.* **2015**, *3*, e00136-15. [[CrossRef](#)]
56. Legendre, M.; Alempic, J.-M.; Philippe, N.; Lartigue, A.; Jeudy, S.; Poirot, O.; Ta, N.T.; Nin, S.; Couté, Y.; Abergel, C.; et al. Pandoravirus Celtis Illustrates the Microevolution Processes at Work in the Giant Pandoraviridae Genomes. *Front. Microbiol.* **2019**, *10*, 430. [[CrossRef](#)]
57. Legendre, M.; Fabre, E.; Poirot, O.; Jeudy, S.; Lartigue, A.; Alempic, J.-M.; Beucher, L.; Philippe, N.; Bertaux, L.; Christo-Foroux, E.; et al. Diversity and Evolution of the Emerging Pandoraviridae Family. *Nat. Commun.* **2018**, *9*, 2285. [[CrossRef](#)]
58. Pereira Andrade, A.C.D.S.; Victor de Miranda Boratto, P.; Rodrigues, R.A.L.; Bastos, T.M.; Azevedo, B.L.; Dornas, F.P.; Oliveira, D.B.; Drumond, B.P.; Kroon, E.G.; Abrahão, J.S. New Isolates of Pandoraviruses: Contribution to the Study of Replication Cycle Steps. *J. Virol.* **2019**, *93*, e01942-18. [[CrossRef](#)] [[PubMed](#)]
59. Andreani, J.; Aherfi, S.; Bou Khalil, J.Y.; Di Pinto, F.; Bitam, I.; Raoult, D.; Colson, P.; La Scola, B. Cedratvirus, a Double-Cork Structured Giant Virus, Is a Distant Relative of Pithoviruses. *Viruses* **2016**, *8*, 300. [[CrossRef](#)]
60. Bertelli, C.; Mueller, L.; Thomas, V.; Pillonel, T.; Jacquier, N.; Greub, G. Cedratvirus Lausannensis—Digging into Pithoviridae Diversity. *Environ. Microbiol.* **2017**, *19*, 4022–4034. [[CrossRef](#)]
61. Jeudy, S.; Rigou, S.; Alempic, J.-M.; Claverie, J.-M.; Abergel, C.; Legendre, M. The DNA Methylation Landscape of Giant Viruses. *Nat. Commun.* **2020**, *11*, 2657. [[CrossRef](#)]
62. Andreani, J.; Khalil, J.Y.B.; Baptiste, E.; Hasni, I.; Michelle, C.; Raoult, D.; Levasseur, A.; La Scola, B. Orpheovirus IHUMI-LCC2: A New Virus among the Giant Viruses. *Front. Microbiol.* **2018**, *8*, 2643. [[CrossRef](#)]
63. Rodrigues, R.A.L.; Andreani, J.; Andrade, A.C.D.S.P.; Machado, T.B.; Abdi, S.; Levasseur, A.; Abrahão, J.S.; La Scola, B. Morphologic and Genomic Analyses of New Isolates Reveal a Second Lineage of Cedratviruses. *J. Virol.* **2018**, *92*, e00372-18. [[CrossRef](#)]
64. Souza, F.; Rodrigues, R.; Reis, E.; Lima, M.; La Scola, B.; Abrahão, J. In-Depth Analysis of the Replication Cycle of Orpheovirus. *Virol. J.* **2019**, *16*, 158. [[CrossRef](#)]
65. Reteno, D.G.; Benamar, S.; Khalil, J.B.; Andreani, J.; Armstrong, N.; Klose, T.; Rossmann, M.; Colson, P.; Raoult, D.; La Scola, B. Faustovirus, an Asfarvirus-Related New Lineage of Giant Viruses Infecting Amoebae. *J. Virol.* **2015**, *89*, 6585–6594. [[CrossRef](#)] [[PubMed](#)]
66. Oliveira, G.P.; de Aquino, I.L.M.; Luiz, A.P.M.F.; Abrahão, J.S. Putative Promoter Motif Analyses Reinforce the Evolutionary Relationships Among Faustoviruses, Kaumoebavirus, and Asfarvirus. *Front. Microbiol.* **2018**, *9*, 1041. [[CrossRef](#)] [[PubMed](#)]
67. Tully, B.J.; Graham, E.D.; Heidelberg, J.F. The Reconstruction of 2,631 Draft Metagenome-Assembled Genomes from the Global Oceans. *Sci. Data* **2018**, *5*, 170203. [[CrossRef](#)]
68. Schulz, F.; Roux, S.; Paez-Espino, D.; Jungbluth, S.; Walsh, D.A.; Deneff, V.J.; McMahon, K.D.; Constantinidis, K.T.; Eloë-Fadrosh, E.A.; Kyrpides, N.C.; et al. Giant Virus Diversity and Host Interactions through Global Metagenomics. *Nature* **2020**, *578*, 432–436. [[CrossRef](#)]
69. Hingamp, P.; Grimsley, N.; Acinas, S.G.; Clerissi, C.; Subirana, L.; Poulain, J.; Ferrera, I.; Sarmiento, H.; Villar, E.; Lima-Mendez, G.; et al. Exploring Nucleo-Cytoplasmic Large DNA Viruses in Tara Oceans Microbial Metagenomes. *ISME J.* **2013**, *7*, 1678–1695. [[CrossRef](#)] [[PubMed](#)]
70. Rodrigues, R.A.L.; dos Santos Silva, L.K.; Dornas, F.P.; de Oliveira, D.B.; Magalhães, T.F.F.; Santos, D.A.; Costa, A.O.; de Macêdo Farias, L.; Magalhães, P.P.; Bonjardim, C.A.; et al. Mimivirus Fibrils Are Important for Viral Attachment to the Microbial World by a Diverse Glycoside Interaction Repertoire. *J. Virol.* **2015**, *89*, 11812–11819. [[CrossRef](#)]
71. Ghigo, E.; Kartenbeck, J.; Lien, P.; Pelkmans, L.; Capo, C.; Mege, J.-L.; Raoult, D. Ameobal Pathogen Mimivirus Infects Macrophages through Phagocytosis. *PLoS Pathog.* **2008**, *4*, e1000087. [[CrossRef](#)]
72. Andrade, A.C.D.S.P.; Rodrigues, R.A.L.; Oliveira, G.P.; Andrade, K.R.; Bonjardim, C.A.; La Scola, B.; Kroon, E.G.; Abrahão, J.S. Filling Knowledge Gaps for Mimivirus Entry, Uncoating, and Morphogenesis. *J. Virol.* **2017**, *91*, e01335-17. [[CrossRef](#)] [[PubMed](#)]
73. Schrad, J.R.; Abrahão, J.S.; Cortines, J.R.; Parent, K.N. Structural and Proteomic Characterization of the Initiation of Giant Virus Infection. *Cell* **2020**, *181*, 1046–1061.e6. [[CrossRef](#)] [[PubMed](#)]
74. De Souza, G.A.P.; Queiroz, V.F.; Coelho, L.F.L.; Abrahão, J.S. Alohomora! What the Entry Mechanisms Tell Us about the Evolution and Diversification of Giant Viruses and Their Hosts. *Curr. Opin. Virol.* **2021**, *47*, 79–85. [[CrossRef](#)] [[PubMed](#)]
75. Quemin, E.R.; Corroyer-Dulmont, S.; Krijnse-Locker, J. Entry and Disassembly of Large DNA Viruses: Electron Microscopy Leads the Way. *J. Mol. Biol.* **2018**, *430*, 1714–1724. [[CrossRef](#)]
76. Parent, K.N.; Schrad, J.R.; Young, E.J.; Abrahão, J.S.; Cortines, J.R. A Gateway into Understanding the Unique Vertex of Samba Virus. *Microsc. Microanal.* **2018**, *24*, 1438–1439. [[CrossRef](#)]
77. Zauberman, N.; Mutsafi, Y.; Halevy, D.B.; Shimoni, E.; Klein, E.; Xiao, C.; Sun, S.; Minsky, A. Distinct DNA Exit and Packaging Portals in the Virus Acanthamoeba Polyphaga Mimivirus. *PLoS Biol.* **2008**, *6*, e114. [[CrossRef](#)] [[PubMed](#)]
78. Oliveira, G.; Silva, L.; Leão, T.; Mougari, S.; da Fonseca, F.G.; Kroon, E.G.; La Scola, B.; Abrahão, J.S. Tupanvirus-Infected Amoebas Are Induced to Aggregate with Uninfected Cells Promoting Viral Dissemination. *Sci. Rep.* **2019**, *9*, 183. [[CrossRef](#)] [[PubMed](#)]
79. De Farias, S.T.; Jheeta, S.; Prosdociimi, F. Viruses as a Survival Strategy in the Armory of Life. *Hist. Philos. Life Sci.* **2019**, *41*, 45. [[CrossRef](#)] [[PubMed](#)]
80. Oliveira, G.; La Scola, B.; Abrahão, J. Giant Virus vs Amoeba: Fight for Supremacy. *Virol. J.* **2019**, *16*, 126. [[CrossRef](#)]

81. Boratto, P.; Albarnaz, J.D.; Almeida, G.M.; Botelho, L.; Fontes, A.C.L.; Costa, A.O.; Santos, D.d.A.; Bonjardim, C.A.; La Scola, B.; Kroon, E.G.; et al. Acanthamoeba Polyphaga Mimivirus Prevents Amoebal Encystment-Mediating Serine Proteinase Expression and Circumvents Cell Encystment. *J. Virol.* **2015**, *89*, 2962–2965. [[CrossRef](#)]
82. Silva, L.K.D.S.; Boratto, P.V.M.; La Scola, B.; Bonjardim, C.A.; Abrahão, J.S. Acanthamoeba and Mimivirus Interactions: The Role of Amoebal Encystment and the Expansion of the “Cheshire Cat” Theory. *Curr. Opin. Microbiol.* **2016**, *31*, 9–15. [[CrossRef](#)] [[PubMed](#)]
83. Korn, E.D.; Weisman, R.A. Phagocytosis of Latex Beads by Acanthamoeba. II. Electron Microscopic Study of the Initial Events. *J. Cell Biol.* **1967**, *34*, 219–227. [[CrossRef](#)] [[PubMed](#)]
84. Arantes, T.S.; Rodrigues, R.A.L.; Dos Santos Silva, L.K.; Oliveira, G.P.; de Souza, H.L.; Khalil, J.Y.B.; de Oliveira, D.B.; Torres, A.A.; da Silva, L.L.; Colson, P.; et al. The Large Marseillevirus Explores Different Entry Pathways by Forming Giant Infectious Vesicles. *J. Virol.* **2016**, *90*, 5246–5255. [[CrossRef](#)]
85. Oliveira, G.P.; Lima, M.T.; Arantes, T.S.; Assis, F.L.; Rodrigues, R.A.L.; da Fonseca, F.G.; Bonjardim, C.A.; Kroon, E.G.; Colson, P.; La Scola, B.; et al. The Investigation of Promoter Sequences of Marseilleviruses Highlights a Remarkable Abundance of the AAATATTT Motif in Intergenic Regions. *J. Virol.* **2017**, *91*, e01088-17. [[CrossRef](#)] [[PubMed](#)]
86. Rodrigues, R.A.L.; Louazani, A.C.; Picorelli, A.; Oliveira, G.P.; Lobo, F.P.; Colson, P.; La Scola, B.; Abrahão, J.S. Analysis of a Marseillevirus Transcriptome Reveals Temporal Gene Expression Profile and Host Transcriptional Shift. *Front. Microbiol.* **2020**, *11*, 651. [[CrossRef](#)]
87. Serrano-Solís, V.; Toscano Soares, P.E.; de Fariás, S.T. Genomic Signatures Among Acanthamoeba Polyphaga Entoorganisms Unveil Evidence of Coevolution. *J. Mol. Evol.* **2019**, *87*, 7–15. [[CrossRef](#)]
88. Akashi, M.; Fukaya, S.; Uchiyama, C.; Aoki, K.; Takemura, M. Visualization of Giant Virus Particles and Development of “VIRAMOS” for High School and University Biology Course. *Biochem. Mol. Biol. Educ.* **2019**, *47*, 426–431. [[CrossRef](#)]
89. Paez-Espino, D.; Eloé-Fadros, E.A.; Pavlopoulos, G.A.; Thomas, A.D.; Huntemann, M.; Mikhailova, N.; Rubin, E.; Ivanova, N.N.; Kyrpidis, N.C. Uncovering Earth’s Virome. *Nature* **2016**, *536*, 425–430. [[CrossRef](#)]
90. Matza-Porges, S.; Nathan, D. A Biosafety Level 2 Virology Lab for Biotechnology Undergraduates. *Biochem. Mol. Biol. Educ.* **2017**, *45*, 537–543. [[CrossRef](#)]
91. De Souza, G.A.P.; Queiroz, V.F.; Lima, M.T.; de Sousa Reis, E.V.; Coelho, L.F.L.; Abrahão, J.S. Virus Goes Viral: An Educational Kit for Virology Classes. *Virol. J.* **2020**, *17*, 13. [[CrossRef](#)] [[PubMed](#)]